# UNIVERSITY OF LONDON THESIS

Degree PhD Year 2007 Name of Author VINEETH SUKUMAR RAJKUMAR

# The role of microvascular pericytes in systemic sclerosis

**Vineeth Sukumar Rajkumar**

**A thesis submitted for the degree of Doctor of Philosophy at University College London**

**August 2006**

**Centre for Rheumatology & Connective Tissue Diseases**
**Department of Medicine**
**Royal Free and University College Medical School**
**University College London**





ProQuest LLC
789 East Eisenhower Parkway
P.O. Box 1346
Ann Arbor, MI 48106-1346

## ABSTRACT

Systemic sclerosis (SSc) represents a spectrum of fibrotic connective tissue disorders. Endothelial cell damage preceding fibrosis is thought to be a key component of the pathological cascade that ultimately results in fibrosis. However, the cell and molecular mechanism(s) linking microvascular damage to the subsequent fibrogenic response are poorly understood. Microvessels consist of two cell types, endothelial cells and pericytes and while recent studies have demonstrated that pericytes play a critical role in the progression of a number of fibrotic conditions, hitherto, nothing is known about their role in SSc. The aim of my thesis was to determine whether microvasuclar pericytes can be implicated in the pathogenesis of SSc.

Pericyte activation and proliferation was found to be an early and prevalent feature in SSc and was accompanied by an upregulation of PDGF-β receptor expression by pericytes ($p<0.01$). Pericytes in SSc lesions phenotypically resembled myofibroblasts with regards to the expression of α-SMA, ED-A FN and Thy-1. When cultured *in vitro*, microvascular pericytes spontaneously changed to a myofibroblastic phenotype maintaining expression of α-SMA and increasing their expression of ED-A FN and vinculin within fibronexus adhesion junctions. The use of the PDGF-β receptor inhibitor imatinib mesylate inhibited fibroblast and pericyte migration and proliferation *in vitro* ($p<0.01$), but did not block TGF-β-mediated differentiation of fibroblasts into myofibroblasts. *In vivo*, PDGF-β receptor inhibition during tissue repair severely disrupted microvascular architecture, delayed wound healing and reduced collagen deposition in healing wounds.

The data presented in this thesis provide the first evidence that pericytes may play an important role in the pathogenesis of SSc as precursors for myofibroblasts. Pericytes are also demonstrated to be a target of endogenous PDGF–β receptor blockade during cutaneous tissue repair and should thus be considered a candidate cell when considering therapeutic targets in SSc and fibrosis.

# TABLE OF CONTENTS

# LIST OF FIGURES

## CHAPTER 1



## CHAPTER 2



## CHAPTER 3



## CHAPTER 4

**CHAPTER 5**

**CHAPTER 6**



**CHAPTER 7**

# LIST OF TABLES

## CHAPTER 1



## CHAPTER 2



## CHAPTER 3



## CHAPTER 4

# ABBREVIATIONS

| | |
|---|---|
| ACA | Anti-centromere antibodies |
| ACEA | Anti-endothelial cell antibodies |
| ACE | Angiotensin-converting enzyme |
| APS | Ammonium persulphate |
| ARP | Autoimmune Raynaud's phenomenon |
| ATA | Anti-toposisomerase antibodies |
| ATP | Adenosine triphosphate |
| α-SMA | alpha-smooth muscle actin |
| BAL | Bronchoalveolar lavage |
| BMDF | Bone marrow-derived fibroblast |
| BMP | Bone morphogenic protein |
| BRDU | Bromodeoxyuridine |
| BSA | Bovine serum albumin |
| CD | Cluster determinant |
| CTGF | Connective tissue growth factor |
| DAPI | 4,6-diamidino-2-phenylindole |
| DLCO | Transfer factor for carbon monoxide |
| DMEM | Dulbecco's modified Eagle's medium |
| DNA | Deoxyribonucleic acid |
| dcSSc | Diffuse cutaneous systemic sclerosis |
| ECL | Enhanced chemiluminescence |
| ECM | Extracellular matrix |
| ED-A FN | ED-A splice variant of fibronectin |
| EMT | Epithelial-mesenchymal transition |
| EDTA | Ethylene-diamine-tetra-acetic acid |
| EGTA | Ethylene-glycol-tetra-acetic acid |
| ET-1 | Endothelin-1 |
| ETAR | Endothelin-A receptors |
| ETBR | Endothelin-B receptors |
| FASSc | Scleroderma associated fibrosing alveolitis |
| FBN-1 | Fibrillin-1 |
| FCS | Foetal calf serum |

| | |
|---|---|
| FGM | Fibroblast growth medium |
| FITC | Fluorescein isothiocyanate |
| GAP | GTPase activating protein |
| GTP | Guanidine triphosphate |
| GVHD | Graft versus host disease |
| HEPES | N-2-hydroxyethylpiperazine-N'-2ethanesulphonic acid |
| HIF | Hypoxia inducible factor |
| HLA | Human leukocyte antigen |
| HMW-MAA | High molecular weight melanoma associated antigen |
| HRP | Horseradish peroxidase |
| ICAM | Intracellular adhesion molecule |
| ID | Inhibitor of differentiation |
| IL | Interleukin |
| IPAH | Isolated PAH |
| lcSSc | Limited cutaneous systemic sclerosis |
| LOX | Lysyl Oxidase |
| MAPK | p38 Mitogen activated protein kinase |
| MCP | Monocyte chemoattractant protein |
| MHC | Major histocompatibilty complex |
| MIP | Macrophage inflammatory protein |
| MMP | Matrix metalloproteinase |
| mRNA | Messenger ribonucleic acid |
| MRSS | Modified Rodnan skin score |
| NO | Nitric oxide |
| NSIP | Non-specific interstitial pneumonia |
| PAH | Pulmonary arterial hypertension |
| PARC | Pulmonary and activation-regulated chemokine |
| PBS | Phosphate buffered saline |
| PBST | PBS/Tween |
| PCNA | Proliferating cell nuclear antigen |
| PDGF | Platelet-derived growth factor |
| PDGFRβ | Platelet-derived growth factor receptor-beta |
| $PI_3$-kinase | Phosphatidylinositol 3 kinase |

| | |
|---|---|
| PFT | Pulmonary function test |
| PLC-γ | Phospholipase C-γ |
| PMSF | Phenylmethylsulphonylfluoride |
| PRP | Primary Raynaud's phenomenon |
| $PO_2$ | Oxygen pressure |
| RANTES | Regulated upon activation, normal T cell expressed and secreted |
| RP | Raynaud's phenomenon |
| RNAP | RNA Polymerase |
| RNP | Ribonuclear protein |
| ROS | Reactive oxygen species |
| SDS | Sodium dodecyl sulphate |
| SDS-PAGE | Sodium dodecyl sulphate polyacrylamide gel electrophoresis |
| SLE | Systemic lupus erythematosus |
| SMC | Smooth muscle cell |
| SNP | Single nucleotide polymorphism |
| SRF | Serum replacement factor |
| SSc | Systemic sclerosis |
| SScRC | Scleroderma renal crisis |
| TCR | T cell receptor |
| TdT | Terminal deoxynucleotidyl transferase |
| TEMED | N,N,N',N'-tetramethyl-ethylenediamine |
| TIMP | Tissue inhibitor of metalloproteinase |
| TNF | Tumour necrosis factor |
| TGF-β | Transforming growth factor-β |
| TSK | Tight skin mouse |
| UCD | University California at Davies |
| UIP | Usual interstitial pneumonia |
| VEGF | Vascular endothelial growth factor |
| VEGF-R | Vascular endothelial growth factor-receptor |
| VSMC | Vascular smooth muscle cell |
| X-GAL | 5-bromo-4-chloro-3-indolyo-B-D-galactoside |

## ACKNOWLEDGEMENTS

I would like to express my gratitude to my supervisors, Professors Carol Black and David Abraham, for providing me the opportunity to study for a PhD and for their help and support throughout my time in the Centre for Rheumatology. I would like to thank Professor Chris Denton for proof-reading the clinical sections of my thesis. I would also like to thank members of the lab both past and present, particularly Patricia and Markella for critically reading my thesis, Alan for helpful and often pleasantly distracting discussions, Gisela for being an excellent roommate and Xu for his assistance in all things cell culture. I would also like to thank Kevin Howell for his help in analysing countless videos of nailfold capillaroscopy. I am also grateful to the staff of the CBU for their help. I would like to thank our collaborators, Kristofer Rubin and Christian Sundberg for their assistance with confocal microscopy and image analysis, Mikael Ivarsson, Bengt Gerdin and Marja Bostrom for their help in the isolation and culturing of pericytes and John Muddle for his help in navigating KS300 software. To my family and friends, I have appreciated your support and encouragement over the years. Finally, I would like to thank my Silke, for your endless proofreading, always being available when I needed your help and putting up with my frustrations.

# CHAPTER 1: INTRODUCTION

## 1.1 Overview

Systemic sclerosis (SSc) encompasses a spectrum of connective tissue disorders of unknown aetiology. These are classified into subsets that can be distinguished both clinically and serologically (Table 1.1). Most major organ systems can be affected, most noticeably the skin, but more clinically significant, the lungs, kidneys, gastrointestinal tract and heart (34).

Pathologically, SSc is characterised by four processes; chronic microvascular injury, inflammation and autoantibody production, increased synthesis of extracellular matrix (ECM) macromolecules and tissue atrophy. The near universal occurrence of microvascular dysfunction often preceding fibrosis suggests that changes in vascular integrity are an early and pivotal event in the pathogenesis of scleroderma. Microvessels are comprised of two principal cell types, luminal endothelial cells and abluminal pericytes (Figure 1). The function and role of endothelial cells has been extensively studied in SSc, however, little is known about the function of pericytes. It has become increasingly apparent that endothelial function is regulated by physical and molecular interactions with pericytes (146). The work described in this thesis focuses on the contribution of microvascular pericytes to SSc pathogenesis.

## 1.2 Classification of systemic sclerosis

### 1.2.1 Epidemiology

SSc has a worldwide distribution and affects both males and females. Incidence rates, from retrospective studies, vary from 2-19 cases per million population per year and a US prevalence has been reported of between 19 and 75 per 100,000 (293). A recent study put the UK prevalence at 10 per 100,000 (10). The native North American Indian Choctaw tribe from Oklahoma shows an increased prevalence of scleroderma-like disease of 469 per 100,000 population. The Choctaw Indian adults have a particularly homogenous clinical phenotype with prominent lung involvement and anti-topoisomerase I autoantibodies (17).

**Table 1.1: Spectrum of SSc and SSc-like diseases**

| Disease | Subtype |
|---|---|
| I - Raynaud's phenomenon | Raynaud's disease (primary) |
| | Raynaud's syndrome (secondary) |
| II - Scleroderma | |
| 1) Systemic | Limited cutaneous systemic sclerosis (lcSSc) |
| | Diffuse cutaneous systemic sclerosis (dcSSc) |
| | Scleroderma sine scleroderma |
| 2) Localised | Morphea |
| | Linear |
| | En coup de sabre |
| 3) Juvenile | Localised forms |
| | Systemic forms |
| 4) Chemically induced | Environmental/occupational |
| | Drugs |
| III- Scleroderma-like diseases | Metabolic |
| | Immunological/inflammatory |
| | Eosinophilic fascitiis |
| | Eosinomyalgic syndrome |
| | Mixed connective tissue disease (MTCD) |
| | Overlap syndromes |

Modified from Black and Denton, 1998.

In the general population, the peak incidence of the disease occurs between the fourth and sixth decades, although it can occur much earlier, even in childhood. The overall survival rate of SSc patients is 60-83% at 5 years and 40-75% at 10 years after disease onset (211;322). The major causes of mortality within the diffuse disease subset are renal crisis in the first five years of onset and pulmonary complications (lung fibrosis and secondary pulmonary arterial hypertension) after 6 years of disease progression (431). In contrast, pulmonary arterial hypertension (PAH) represents the leading cause of mortality in patients with the limited form of the disease (311).

### 1.2.2 Classification criteria and subgroups

The original criteria for the classification of SSc were proposed by a committee of the American Rheumatism Association (ARA) (1) (Table 1.2). They are based on the presence of proximal scleroderma defined as symmetric thickening, tightening and induration of the skin of the fingers and the skin proximal to the metacarpophalangeal or metatarsophalangeal joints. Minor criteria are the presence of sclerodactyly, digital pitting scars and pulmonary fibrosis. For purposes of classifying patients in clinical trials, population surveys and other studies, a person is considered to have SSc if one major or two or more minor criteria are present. Localised forms of scleroderma, eosinophilic fasciitis, and forms of pseudosclerodema are excluded form these criteria.

In order to include those patients that have SSc characteristics but do not fulfil the original ARA criteria, LeRoy and Medsger proposed a new set of criteria defining a 'pre-SSc' subgroup. These patients have Raynaud's phenomenon (RP), at least one SSc-specific autoantibody and an SSc pattern of nailfold capillaries but no detectable fibrosis (272).

The most commonly adopted classification for SSc subgroups is based upon skin involvement and specific clinical, laboratory and natural history associations (Table 1.3) (270). It divides the systemic disease into limited cutaneous systemic sclerosis (lcSSc) and diffuse cutaneous systemic sclerosis (dcSSc). LcSSc tends to be associated with late involvement of internal organs in the evolution of the disease and is usually preceded by a lengthy period of RP. The dcSSc subtype tends to have a rapid onset, with organ failure present within the first 5 years of the disease (35).

**Table 1.2: ARA criteria for the classification of SSc**

| Criteria | Characteristic | Definition |
|---|---|---|
| A. Major criterion | Proximal Scleroderma | Symmetric thickening, tightening and induration of the skin of the fingers and the skin proximal to the metacarpophalangeal or metatarsophalangeal joints. The changes may affect the entire extremity, face, neck, and trunk. |
| B. Minor criteria | 1. Sclerodactyly | Above-indicated changes limited to the fingers. |
| | 2. Digital pitting scars | Depressed areas at tips of fingers or loss of digital pad tissues as a result of ischemia. |
| | 3. Bibasilar pulmonary fibrosis | Bilateral reticular pattern of linear or lineo-nodular densities most pronounced in basilar portions of the lungs on standard chest roentgenogram; may assume appearance of diffuse mottling or honeycomb lung. These changes should not be attributable to primary lung disease. Depressed areas at tips of fingers or loss of digital pad tissues as a result of ischaemia. |

**Table 1.3: SSc subsets classification according to Leroy *et al.*, 1988**

| Subset | Characteristics |
|---|---|
| 1. "Pre-scleroderma" | Raynaud's phenomenon plus nailfold capillary changes, disease specific circulating antibodies (anti-Topoisomerase I, anti-Centromere, nucleolar), digital ischaemic changes. |
| 2. Diffuse cutaneous SSc (dcSSc) | Onset of skin changes within 1 year of onset of Raynaud's.<br>Truncal or acral involvement.<br>Presence of tendon friction rubs.<br>Early and significant incidence of interstitial lung disease, oliguric renal failure, diffuse gastrointestinal disease and myocardial involvement.<br>Nailfold capillary dilatation and drop out.<br>Anti-Topoisomerase1 antibodies ~30% of patients. |
| 3. Limited cutaneous SSc (lcSSc) | Raynaud's phenomenon for years.<br>Skin sclerosis restricted to extremities, face and neck.<br>Significant involvement of pulmonary hypertension, skin calcification, telangiectasiae and gastrointestinal involvement.<br>High incidence of anti-centromere antibodies (70-80%) |
| 4. Scleroderma sine scleroderma | With or without Raynaud's phenomenon-<br>No skin involvement.<br>Pulmonary fibrosis, scleroderma renal crisis, cardiac or gastrointestinal disease.<br>Antinuclear antibodies may be present. |

Modified from Black and Denton, 1998.

### 1.3 Clinical features of SSc

#### 1.3.1 Raynaud's phenomenon

Raynaud's phenomenon (RP) is defined as the episodic vasoconstriction of small arteries and arterioles of the extremities. The vasospastic events may be brought on by cold exposure, vibration or emotional stress. Patients experience pallor and/or cyanosis followed by rubor during re-warming. It affects 3-5% of the general population and 95% of patients are classified as primary Raynaud's phenomenon (PRP). Generally, RP will remain a benign if sometimes painful condition. Approximately 95% of SSc patients present with underlying RP (481). RP may precede skin changes by several months or years and together with skin thickening is the most frequent clinical feature of SSc (481). Patients with isolated RP who have abnormal nailfold capillaries and anti-nuclear antibodies have a 10-15% likelihood of developing a connective tissue disorder (425). Usually, these include SSc, systemic lupus erythematosus (SLE) or an overlap syndrome with features of both these conditions plus inflammatory muscle or joint disease (425).

#### 1.3.2. Skin disease

Involvement of the skin is the most visible pathological characteristic of scleroderma. There are considered to be three phases of skin involvement; oedematous, indurative and atrophic (34).

In the early oedematous phase, fingers and hands become puffy and often stiff. Swelling may be apparent on the extremities and the face. This phase can last from few weeks to several years. The skin changes usually begin distally in the extremities and advance proximally. Subsequently, the skin becomes firm, thickens and eventually becomes tightly bound to underlying subcutaneous tissue. This constitutes the indurative phase. In patients with dcSSc, skin changes become widespread, including all the extremities, face, trunk and abdomen, however, the lower back is often spared (270). Rapid progression of these changes over a relatively short period of time is usually associated with internal organ involvement, especially lungs, kidneys and heart (34). The skin changes observed in dcSSc usually peak around 3-5 years after onset and can then show improvement. After many years, the skin may soften and return to the normal thickness or become thin and atrophic. In the localised subset, the skin changes tend to be more gradual and are restricted to fingers, distal extremities and face (35).

Biopsies obtained during the active indurative phase display a marked increase in matrix deposition accompanied by a transient but significant infiltration of mononuclear cells particularly in perivascular locations (188). In the atrophic phase, loss of rete pegs and atrophy of epidermal appendages is evident accompanied by a reduction in overall cell numbers and vascularity (35).

The near-universal occurrence of dermal fibrosis has ensured that assessment of SSc traditionally focuses on the extent of skin involvement as a measure of disease activity. Findings from several studies suggest that the extent and rate of skin progression is associated with mortality and organ involvement (270;430;467). Therefore, skin score has been developed as a widely used assessment marker. The modified Rodnan skin score (MRSS) is the most commonly used scoring system and allows analysis of 17 different anatomical sites. Each site is scored from 0 to 3, giving a theoretical maximum of 51 (83).

### 1.3.3 Lung disease

Lung disease is a frequent manifestation in SSc with approximately 30% of patients exhibiting some pulmonary involvement (100). Since the emergence of effective treatment for renal involvement, lung disease is now considered as the primary cause of mortality in patients with SSc (429). The course of lung disease in SSc patients is highly variable. Lung function tends to decline early before stabilising and often improving. However, in a small subset of patients (~15%) the pulmonary function test decline is faster in the 3 first years of the disease with a median survival of 50% at 5 years (431). There are 2 major types of pulmonary disease affecting SSc patients: fibrosing alveolitis (FASSc, also known as interstitial lung disease, ILD) and PAH (37).

#### a) Fibrosing alveolitis

FASSc usually develops insidiously and tends to remain silent until later stages of the disease, when it may become a major cause of mortality. Lung biopsy allows the pattern of lung disease to be determined. The non-specific interstitial pneumonia pattern (NSIP) predominates in SSc as opposed to the usual interstitial pneumonia pattern (UIP), which is rarely associated with SSc (45). NSIP tends to be more responsive to treatment and have a better prognosis than UIP (95;320). However, in FASSc, the overall outcome is linked to disease severity at presentation and serial DLCO (transfer factor for carbon monoxide) trends

rather than histological findings (45). FASSc tends to be more frequent and more severe in patients with dcSSc and with those expressing anti-topoisomerase I antibodies (26;110).

**b) Pulmonary arterial hypertension**

PAH defined as a median pulmonary artery pressure higher than 30 mmHg at rest by echocardiography has a reported incidence of approximately 10% in patients with SSc (311). Isolated PAH (IPAH) is more frequent in patients with lcSSc and is associated with the presence of anti-centromere antibodies (ACA). The secondary form of PAH occurs in patients with either dcSSc or lcSSc but always in association with pulmonary or cardiac fibrosis (84;491). The presence of PAH represents an adverse prognostic factor and is a major cause of mortality, irrespective of whether it occurs in isolation or in association with pulmonary fibrosis, with a median survival rate of 12-20 months (286). The detection of PAH is difficult as the symptoms may appear late in the evolution of the disease. The most common abnormality in pulmonary function test (PFT) is the decrease of the DLCO. Echocardiography with Doppler provides a non-invasive measure of pulmonary artery pressure (101). Right heart catheterisation, although a more invasive technique, is considered a more reliable method for measurement and evaluation of the pulmonary artery pressure in SSc (311).

### 1.3.4 Renal disease

The most important clinical manifestation of renal disease in SSc is the scleroderma renal crisis (SScRC). Reported in 12% of dcSSc patients and up to 2% of cases of lcSSc, SScRC is characterised by accelerated hypertension and/or progressive renal failure (100). Identified risk factors include diffuse disease, use of corticosteroids and the presence of anti-RNA polymerase III antibody (428;431). The mortality of this complication has been dramatically reduced by the use of angiotensin-converting enzyme (ACE) inhibitors in the past 10 years, with survival rates improving from less than 10% at five years to 70% after the use of ACE inhibitors was introduced (431).

### 1.3.5 Cardiac disease

Clinically significant cardiac involvement is reported in up to 10% of SSc cases and is associated with an adverse prognosis (100). Several studies have indicated widespread subclinical cardiac involvement in SSc. However controversy exists as to their prognostic significance (84). The two principle mechanisms thought to be involved in SSc-related heart disease are; a fibrotic process secondary to myocardial Raynaud's phenomenon or an immune-mediated myocarditis. The total number of observations regarding cardiac involvement remains small and further studies are required to understand the pathophysiological basis of SSc related cardiac disease.

### 1.3.6 Gastrointestinal disease

Gastrointestinal manifestations in SSc are prevalent in up to 90% of the patients and represent the most common visceral complication (100). They include oesophageal, small bowel and colon alterations. Dysphagia and heartburn secondary to oesophageal hypo-motility are frequent complaints. Small bowel hypo-motility can lead to diarrhoea, weight loss and malabsorption with bacterial overgrowth as a recurrent problem. Large bowel involvement is also common with patients often experiencing ano-rectal disease (100). Vascular lesions in the gut mucosa are a recognised cause of anaemia in SSc patients and can be treated successfully by laser treatment if blood loss is significant (60;477).

### 1.3.7 Macrovascular disease

While microvascular disease is a pathological hall mark of SSc, there is also evidence of macrovascular disease in SSc (203;469). Prevalence of carotid artery disease and peripheral arterial disease have been reported to be elevated in SSc (203), while increased ulnar artery thickening has been demonstrated in SSc patients (427). The relationship between macrovascular disease and SSc pathophysiology is unclear.

## 1.4 Autoantibodies in SSc

Antibodies against nuclear antigens (ANA) have been described in up to 95% of patients with SSc (57). There are 3 main autoantibodies associations and a number of minor mutually exclusive serologic subgroups in SSc. The major autoantibody specificities are usually associated with distinctive clinical profiles. Therefore, they can be and used as diagnostic and prognostic factors (Table 1.4) (57;132;261).

### 1.4.1 Anti-topoisomerase I antibodies

Anti-topoisomerase I antibodies (ATA), also termed Scl-70, are found exclusively in patients with SSc and particularly within the dcSSc subset (35). Scl-70 antibodies are associated with heart disease and pulmonary fibrosis (133;216). Titres of ATA were thought to remain relatively constant over time (468), however, a subset of dcSSc patients were recently identified in which the ATA titre declined to undetectable levels during the course of the disease. These patients were reported to have a more favourable disease outcome (260).

### 1.4.2 Anti-centromere antibodies

Anti-centromere antibodies (ACA) are the most common autoantibodies occurring in approximately 25% of SSc patients (35). These antibodies recognise one or more centromere proteins (CENP-A, -B, or -C) (58). ACA are found more frequently in patients within the lcSSc subgroup and in a retrospective analysis have been identified as a positive predictive factor for digital ischemic loss (482).

### 1.4.3 Anti-RNA polymerase antibodies

Autoantibodies to RNA polymerase I and III (RNAP I and III) are highly specific for SSc, although they occur in only approximately 20% of patients (57). Anti-RNA polymerase II (RNAP II) autoantibodies have also been described in patients with SSc (384), however, they are more readily associated with SLE and overlap syndromes (383). Anti-RNAP antibodies are associated with dcSSc and particularly SSc renal crisis (428;431), as well as with greater mortality (216). Previous studies have reported no statistically significant associations between the presence of anti-RNAP I/III antibodies and HLA class II alleles in SSc patients (131;133).

### 1.4.4 Other autoantibodies

Anti-fibrillarin antibodies (AFA) have a prevalence in SSc of 4%. They are more frequently detected in the Afro-Caribbean population and have been associated with an increased risk of internal organ involvement, especially IPAH (373;456). Anti-PM-Scl antibodies are present in 2% of SSc patients but are found in 24% of patients with polymyositis/scleroderma overlap (327). Between 43% and 88% of the patients positive for anti-PM-Scl antibodies are diagnosed with myositis/scleroderma overlap syndrome (291;327). Anti-Th/To antibodies recognise a 40 kD protein component of the Th ribonucleoprotein, which is located in the nucleolus (503). Antibodies to Th/To ribonucleoprotein are detected in 4% of SSc patients and reported to be associated with reduced survival (330). The anti-Ku antibodies are found in a wide spectrum of connective tissue diseases including overlap syndromes. Raynaud's phenomenon and muscular and joint involvement are the most frequent clinical features associated with anti-Ku antibodies (148).

### 1.4.5 Antibodies against extractable nuclear antigens

Anti-RNP antibodies react with the nuclear RNA splicing particle U1 snRNP (357). High titers of anti-U1RNP antibodies are most often found in association with what was previously designated "mixed connective tissue disease" with a frequency of more than 90% (400). This serotype is found in approximately 10% of SSc patients and has been associated with a low frequency of renal disease, arthritis and pulmonary arterial hypertension (210;261). Anti-Ro antibodies have also been detected in the sera of SSc patients (28) and a strong association between SSc and Sjogren's syndrome has been reported in Japanese SSc patients with anti-Ro antibodies (152).

**Table 1.4: Main serologic groups in SSc**

| Antibodies | Prevalence (%) | Autoantigens recognised | Clinical associations |
|---|---|---|---|
| Anti-centromere | 20-26 | CENPs -A, -B, -C | 70-80% lcSSc<br>Peripheral vascular occlusive disease. |
| Anti-topoisomerase I (Scl-70) | 22-25 | Topoisomerase I | 40% dcSSc 10-15% lcSSc<br>Pulmonary fibrosis |
| Anti-RNA polymerase I, II, III | 18-23 | RNA polymerase I, II, III. | 23 % dcSSc, renal crisis |
| Anti-Pm-Scl | 4 | Pm-Scl | Scleroderma/polymyositis overlap |
| U1-RNP | 10 | U1 snRNP | Overlap features |
| Th/To | 4 | Th RNP particle | Poor outcome lcSSc |
| Anti-fibrillarin | 4-6 | U3 RNP | IPAH and renal crisis |

Modified from Black and Denton, 1998 and Harvey and McHugh, 2000.

### 1.5 Aetiology of SSc

Whilst a significant number of risk factors have been associated with SSc, the basic aetiology of the disease remains unknown. Several environmental agents have been linked to the development of SSc, including toxins, epoxy resins and chemicals (321). This has led to studies investigating whether SSc is associated with particular vocations. A recent study identified construction workers as being at a significantly higher risk of developing SSc (288). Exposure to elemental silicon has been associated with SSc particularly within coalminers and stonemasons (412), however, no association was found between silicone gel breast implants and SSc (205). A number of other agents have been put forward, including epoxy resins, toxic oil and organic solvents such as vinyl chloride, but to date the evidence is inconclusive (321).

A novel hypothesis investigated in recent years is that the presence of foetal cells in maternal tissue that is human leukocyte antigen (HLA) class II incompatible produces a graft-versus-host reaction, which leads to clinical SSc (microchimerism) (220). As the exchange of cells at

birth can be two-way, the concept of microchimerism can be expanded to explain SSc in males. Both HLA and Y-chromosome sequences have been investigated, but from the results to date, no definitive conclusions can be drawn (220).

### 1.5.1 Genetic Factors

The strongest genetic association in SSc is gender with females being 3 to 8 times more likely to develop the disease (411). Recent large cohort studies from Australia and the USA reported that SSc occurred in one or more first-degree relatives with a frequency of 1.4% and 1.6% respectively in the families of patients with SSc (16;127). The estimated prevalence of SSc in the USA is 2.6 cases/10,000 (0.026%) (16). Therefore, while the absolute risk for each family member is less than 1%, a positive family history is the strongest risk factor yet identified for SSc. Comparative studies of monozygotic and dizygotic twins, which could define the relative contributions from genetic and environmental factors, have been limited by the rarity of the disease, but they suggest that the majority of monozygotic pairs are discordant for clinical disease (258;305). A Belgian study reported 2 female identical twin pairs concordant for scleroderma. The first twin pair was diagnosed with SSc, the second pair with the localised form (98). Recently Zhou *et al.* published a study, in which fibroblast-derived RNA from 10 monozygotic discordant twin pairs was subjected to microarray analysis. They found that dermal fibroblasts from SSc patients and from 40-50% of their genetically identical but clinically unaffected monozygotic twins exhibited a similar gene expression pattern, which could be induced in normal fibroblasts by sera from both twins (513). This data implies a strong genetic pre-disposition at the molecular level and suggests that development of the full clinical phenotype may depend on additional non-genetic factors such as environmental triggers or stochastic genetic factors.

### 1.5.2 Immunogenetics

A number of candidate genes have been analysed for associations with SSc. Numerous studies have focused on the major histocompatibilty complex (MHC) for associations with disease susceptibility. While there is a lack of definitive evidence that MHC genes are associated with susceptibility, there is increasing evidence that certain HLA-II alleles are associated with the presence of specific autoantibodies (Table 1.5) (259;449). On the basis of several studies, it has been argued that defining disease subsets by their autoantibody profile would provide closer linkage disequilibrium between the disease gene, marker, or haplotype and disease subgroup. Weak associations between SSc and different ethnic groups have been

reported. DR5 (DRB1*1101 and *1104, DQA*0501, DQB1*0301) and DR3 haplotypes (DRB1*0301, DQA1*0501, DQB1*0301) have been associated with the North American and European population. The DRB1*08 haplotype was reported to be more common in African Americans than ethnically matched controls (223).

**Table 1.5: Main HLA-autoantibody associations in SSc**

| Autoantibody | DRB1 | DQA1 | DQB1 | Ethnicity | Reference |
|---|---|---|---|---|---|
| ATA | *1101 | *0501 | *0301 | White, Black | Reveille et al., 2001 |
| | *1104 | | | | |
| | *1502 | *0102 | *0601 | Japanese | Kuwana et al., 1999 |
| | *0802 | | *0301 | | |
| | *1602 | *0501 | *0301 | Choctaw | Arnett et al., 1996 |
| ACA | *0101 | | *0501 | Japanese | Kuwana et al., 1999 |
| | | *0301 | | | Falkner et al., 1998 |
| U1-RNP | *0104/*0802 | | | Japanese | Kuwana et al., 1999 |
| | *0302 | | | | |
| PM-Scl | *0301 | *0501 | *0201 | White | Marguerie et al., 1992 |
| U3-RNP | *1302 | | *0601 | | Arnett et al., 1996 |
| (fibrillin) | | | | | |
| Th/To | *1104 | | | White | Falkner et al., 1998 |
| RNA | | | | White | Falkner et al., 2000 |
| polymerase | | | | | |
| I, II, III | | | | | |

Modified from Tan and Arnett, 2000.

### 1.5.3 Candidate gene analysis

The complexity of SSc pathophysiology implicates a number of genes as potential candidates that are key to driving the disease process either singly or more likely in combination. Genes related to ECM formation, vascular structure and function, and autoimmunity have been investigated. A number of genes encoding fibrogenic cytokines have been analysed, pre-eminent amongst these is transforming growth factor-β (TGF-β), which is known to be increased at the message and protein level in SSc skin (352). Analyses of microsatellite and intragenic markers in and around genes encoding TGF-β1 and platelet-derived growth factors- A and B (PDGF-A, B) and their respective receptors in Choctaw Native Americans revealed no association with SSc (512). A lack of association with TGF-β1 has also been found in European and Japanese populations (329;437;442), however, one study has shown a significant association between a single-nucleotide polymorphism (SNP) in the TGF-β1 gene and SSc (89). Significant associations between SNPs in the TGF-β2 and β3 genes and SSc have also been detected (442).

While no association with TGF-β and PDGF was found in the SSc Choctaw population, a significant association with a SNP in the 5'-untranslated region of the fibrillin-1 (FBN1) gene was detected. The two haplotypes in Choctaws containing this polymorphism were also shown to be associated with SSc in Japanese patients (451;452). Fibrillin-1 is a major component of microfibrils and interestingly, duplications in the FBN1 gene are thought underlie the fibrotic phenotype of the tight skin mouse (Tsk/+) model of SSc (see 1.7.1) (241). Although a molecular abnormality in FBN1 has not been identified in SSc, functional studies in fibroblasts from patients have revealed microfibril abnormalities and reduced incorporation of FBN-1 into microfibrils (475). Furthermore, autoantibodies to several epitopes on FBN-1 have been detected in the majority of patients with SSc with the exception of Caucasians (450). In a further study of the SSc Choctaw population, SNPs in the matrix modifying protein SPARC (secreted protein, acidic and rich in cysteine) gene were associated with susceptibility to and clinical manifestations of SSc (511). However, these results could not be repeated in subsequent analyses of European Caucasians (262). A number of studies associating SNPs within the tumour necrosis factor (TNF) gene family and SSc have been reported (334;446;454). In a recent study, a functionally relevant NF-kappaB binding site polymorphism in the promoter of the tumour necrosis factor-α gene (TNF-α) was associated with the presence of ACA in SSc patients (378). Although significant associations between a

number of SNPs and SSc have been reported, a functional relationship between these SNPs and SSc has yet to be demonstrated. Genetic studies of potentially important candidate genes are summarised in table 1.6.

**Table 1.6: Reported polymorphisms in potentially significant candidate genes and their clinical associations**

| Polymorphism | Clinical Association | Reference |
|---|---|---|
| CXCR2 | SSc | (356) |
| TNF-863A | ACA | (378) |
| IL-10 | ACA | (206) |
| SPARC | SSc | (511) |
| SPARC | No association | (262) |
| MCP-1 | SSc | (233) |
| TGF-β1 | SSc | (89) |
| TGF-β1 | No association | (329) |
| TGF-β1 | No association | (437) |
| ACE | SSc | (136) |
| NO | No association | (9) |
| Fibrillin 1 | SSc | (452) |
| Collagen 1α2 | SSc | (184) |

## 1.6 The Pathogenesis of SSc

The pathology of SSc consists of four distinct yet overlapping and interactive phases. The initial stimuli triggering the disease are unknown. Endothelial cell damage and activation are among the earliest events in SSc pathogenesis. The vascular damage is universal and clinically manifests as RP (179;350). Inflammation, another major component of the disease pathology is often contemporaneous with the vascular phase. Initially, this is composed of a perivascular monocytic/macrophage infiltrate, but a variety of inflammatory cell types such as T and B cells are present in the latter stages. The third and final phase and the pathological hallmark of the disease is tissue fibrosis. This is characterised by an increased synthesis and deposition of ECM components, such as collagen (222), fibronectin (139) and proteoglycans (54), resulting in the destruction of normal tissue architecture and ultimately in organ

dysfunction and failure. While the four phases of SSc pathology are well delineated, the cellular and molecular mechanisms that link them are poorly understood.

### 1.6.1 SSc Pathophysiology I-The immune response and antibodies

Activation of the immune system is an early event in SSc pathophysiology. Autoantibodies and increased numbers of activated immune cells are found in SSc tissue. These cells are capable of modifying fibroblast and endothelial cell functions through the production of soluble mediators. Although immune activation occurs across the disease spectrum, anti-inflammatory agents have little or no affect on disease progression. Therefore, it is unclear whether SSc represents an autoimmune disorder or whether the immune response is secondary to the underlying disease process.

#### 1.6.1.1 T cells

T cells dominate the early inflammatory infiltrates of SSc tissue. In the skin, CD4+ T cells are the predominant population (350), whereas in the lungs, increased levels of CD8+ T cells have been reported in the presence of alveolitis (505). Clonal T cells, which are commonly encountered in T cell disorders such as T cell leukemias, have been found with greater frequency in the blood of SSc patients than controls (151;294). The Th2 response (IL-4+, interferon-γ+) is generally considered to be predominant in SSc (301;459) although Th1 (interferon-γ+, IL-2+) polarisation may occur under specific conditions (165;460). There is also evidence that the Th2 cytokine response is more common in patients with aggressive disease (23;289). Th1 and Th2 cytokines induce different patterns of chemokine synthesis by cultured fibroblasts, which may in turn modulate the inflammatory response (76).

The majority of T lymphocytes express a heterodimeric T cell receptor (TCR) consisting of α and β chains (500). However, a restricted population (1-5%) of T cells express the γ and δ chains, which differ with respect to their HLA expression, the recognition of self-antigens (234) and the synthesis of soluble mediators (165). In SSc patients, accumulation of γ/δ T cells has been noted in skin and lung (166;480) where they enhance interaction and cytotoxicity towards endothelial cells (228). It also has been reported that the expansion of specific γ/δ subpopulations in SSc tissue may be antigen driven (504). Whether T cells directly induce fibrosis in SSc through the synthesis of pro-fibrotic cytokines is unknown. However, SSc fibroblasts have been shown to be resistant to the down-regulation of type I

collagen synthesis, which normally occurs in healthy tissues upon contact with cell membranes derived from activated T cells (78).

### 1.6.1.2 B cells and autoantibodies

Several theories have been proposed to explain the mechanisms responsible for the loss of self-tolerance and autoantibody formation in SSc.

**a) Molecular mimicry between infectious agents and normal host cell component**

Autoreactive lymphocytes are present in all individuals and benign unless activated. Molecular mimicry is one of the mechanisms thought to be responsible for such activation (338). In this case, an antigenic determinant on a protein expressed by an infectious agent is sufficiently different to be recognised as foreign by the host's immune system yet is structurally similar to a determinant on one of the host proteins. Consequently, both humoral and cellular immune responses to this exogenous determinant cross-react with the host tissue and lead to autoimmunity. In SSc, autoimmunity and human cytomegalovirus (CMV) infections have been linked. Increased levels of antibodies against CMV are present in the sera of SSc patients while monoclonal antibodies against topoisomerase-I recognise a pentapeptide of the autoantigen sharing homology with the CMV derived UL70 protein (312;318). In a follow-up study, sera from SSc patients were found to contain antibodies against an epitope contained within the CMV-derived protein UL94 (283). This epitope has homology to the NAG-2 protein expressed by endothelial cells and incubation with anti-UL94 antibodies was found to induce apoptosis of endothelial cells upon engagement of the NAG-2 complex, thereby linking CMV infection, autoantibody production and endothelial cell damage. NAG-2 is also expressed by fibroblasts (444) and the binding of anti-UL94 antibodies to fibroblasts promotes a 'SSc-like' phenotype as determined by gene microarray analysis (284). Taken together these studies suggest that anti-human CMV antibodies may be associated with the pathogenesis of SSc by inducing endothelial cell and fibroblast activation.

A number of alternative mechanisms linking infection and autoimmunity have been proposed, including activation of T cells by superantigens and the induction of cytokines and co-stimulatory molecules by microbial products. A primary inflammatory process may also cause tissue damage such that sequestered protein components that are normally 'hidden' from the immune system are exposed to auto-reactive T cells and evoke a secondary

autoimmune response (465). This phenomenon is termed epitope spreading and has been implicated in a number of autoimmune disorders (68) including SSc (50;471;495).

**c) Non-infection mediated cryptic epitope exposition**

A number of processes have been identified by which immunocryptic epitopes on cellular proteins are exposed to the immune system that has not developed self-tolerance for them. Several autoantigens targeted in dcSSc are susceptible to cleavage by reactive oxygen species (ROS) and it has been suggested that ROS-mediated protein fragmentation reveals cryptic epitopes that provoke an autoimmune response (65).

### 1.6.1.3 The role of autoantibodies in SSc pathophysiology

While there is compelling evidence that autoantibodies are associated with specific clinical phenotypes in SSc, whether they themselves play a direct pathogenic role remains unknown. Peripheral blood B cells in Tsk/+ mice and SSc patients have been shown to express higher levels of CD19 (221;374;380). Subsequent studies of Tsk/+ mice that do not express CD19 (Tsk/+/CD19-/-) mice demonstrated that these mice have reduced B cell activity, serum autoantibody titers and fibrotic skin changes (374). While loss of CD19 signalling reduces the degree of skin thickening, skin fibrosis still develops in Tsk/+/CD19-/- mice, suggesting that B cells play a role in disease amplification, perhaps by promoting epitope spreading.

SSc-derived autoantibodies are known to induce phenotypic changes in target cells *in vitro*. For example, addition of FBN-1 autoantibodies to normal fibroblasts *in vitro* induces a fibrotic phenotype via a TGFβ-dependent mechanism (510). Anti-endothelial cell antibodies (AECA) can induce pathogenic changes in endothelial cells *in vitro* including increased leukocyte adhesion, increased secretion of inflammatory cytokines such as IL-1 and inducing endothelial cell apoptosis (39;64;396). AECA also induce upregulation of the adhesion molecule ICAM-1 and increased transcription of the genes encoding for cytokines IL-1α, Il-1β, and IL-6 (77). Anti-fibroblast autoantibodies have been detected in the sera of SSc patients (48;198) and in the sera of patients with SSc-associated and idiopathic PAH (448), however, their pathological significance, if any, is unclear. Autoantibodies against matrix-metalloproteinases-1 and 3 (MMP-1, 3) have been found in sera of up to 75% of patients with dcSSc and appear to correlate with disease severity (323;381). Serum immunoglobulin fractions were shown to significantly inhibit MMP-1 collagenase activity, potentially

disrupting the balance between collagen synthesis and degradation (381). Another recent study showed that the immunoglobulin fractions from sera of SSc patients could inhibit M3-muscarinic receptor-mediated contractions in mouse colon longitudinal muscle (171). This result is of interest as gastrointestinal dysmotility is commonly associated with SSc. The specific molecular targets of SSc-derived autoantibodies, the cell type-specific expression of these molecules, and the *in vivo* effects of such antibodies in SSc remain unknown.

#### 1.6.1.4 The role of other immune cells in SSc

Other immune cells have also been implicated in SSc pathophysiology. Reports regarding numbers of mast cells detected in SSc tissue have been contradictory. They have been reported as increased (393), decreased (212) or normal (144). Evidence for increased mast cell degranulation has been found in SSc skin (212;393) and it has been argued that the differentiation of fibroblasts into myofibroblasts, a key step in the development of fibrosis, is regulated by mediators derived from de-granulated mast cells (157). Lung biopsies from scleroderma patients with lung inflammation and pulmonary fibrosis show increased numbers of mast cells in close contact with interstitial fibroblasts (69). The increase in mast cells is associated with elevated levels of histamine in BAL fluids (69). Experimental evidence suggests that mast cells stimulate collagen production through production of MCP-1, and that fibroblasts in turn release stem cell factor, which further upregulates the production of MCP-1 from mast cells (488). Histamine, a product of mast cells, is elevated in the plasma of scleroderma patients (130) and promotes the synthesis of collagen (185). Macrophages are a major source of wound growth factors and as such are crucial coordinators of the tissue repair process and the development of fibrosis. PU.1 null mice, which lack macrophages, heal wounds without scarring (297), while SMAD3 (an intracellular effector of TGF-β signalling) null mice show a reduction in myofibroblast frequency and diminished scarring during wound healing due to impaired recruitment of macrophages (138). In SSc, infiltrating macrophages have been identified as a source of soluble mediators including TGF-β, TNF-α and IL-8, thought to be key players in disease progression (182;336;337). Alveolar macrophages are the most frequent cell type seen in the inflammatory infiltrate in active scleroderma lung disease. Macrophages in scleroderma lung disease have undergone 'alternative', rather than 'classical', activation (22). Macrophages activated by lipopolysaccharide, TNF-α and interferon-γ, produce elevated levels of the pro-inflammatory cytokines but little TGF-β (169;432). Activation by these stimuli induces "classically

activated macrophages" that are efficient at antigen presentation and inhibit collagen production by fibroblasts (419;432). In contrast, macrophages activated by IL-4 and TGF-β have an anti-inflammatory and pro-fibrotic phenotype (129;432). Alternatively activated macrophages make large amounts of TGF-β, PDGF and CC chemokines such as monocyte chemotactic protein (MCP)-1 (285). They also stimulate collagen production by fibroblasts (419). Thus, alternatively activated macrophages appear to be key players in pathologic processes that are associated with fibrosis. Degranulation of eosinophils occurs in the fibrotic tissues in scleroderma patients, with eosinophil-derived major basic protein accumulating in the lungs of these patients (88). Levels of major basic protein negatively correlate with pulmonary function (88). Eosinophils adhere to fibroblasts and directly activate fibroblast proliferation and collagen production through production of TGF-β (274).

### 1.6.1.5 Chemokines in SSc

More recently, it has become apparent that chemokines may be essential contributors to tissue damage in SSc. Chemokines are a group of cytokines that share sequence homology and similar tertiary structures. Chemokines are classified on the basis of the first two cysteine residues as CC (in which the first two cysteine residues are immediately adjacent in the primary structure), CXC (the first two cysteine residues are separated by an amino acid), and CX3C (the separation involves three amino acids) and C chemokines (one cysteine residue is missing). In addition to chemoattraction of T cells and nonspecific inflammatory cells into tissues, chemokines have other functions. Among these are the regulation of angiogenesis, vascular proliferation, and fibrosis: functions that may contribute to manifestations of SSc (70).

#### a) Monocyte chemoattractant protein-1

One of the best studied of the CC chemokines in SSc is monocyte chemoattractant protein-1 (MCP-1). MCP-1 is predominantly a monocyte chemoattractant, however, it also stimulates collagen production by fibroblasts in part by promoting the autocrine synthesis of TGF-β (163). MCP-1 mRNA and protein are increased in the skin and BAL fluid of dcSSc patients, with expression by fibroblasts, keratinocytes, perivascular inflammatory mononuclear cell infiltrates and vascular endothelial cells throughout the skin (113;181). SSc fibroblasts also display increased expression of MCP-1 mRNA and protein, compared with normal fibroblasts (158) and exogenously administered MCP-1 stimulates autocrine synthesis of MCP-1 mRNA by SSc, but not normal dermal fibroblasts (158). Increased MCP-1 production by scleroderma dermal fibroblast lines promotes recruitment of monocytic cells (158), suggesting that MCP-1 may directly contribute to dermal fibrosis by stimulating collagen production and indirectly by promoting the synthesis of more MCP-1 and the recruitment of monocytes to the skin.

#### b) Interleukin-8

Interleukin-8 (IL-8), a CXC chemokine, is primarily a neutrophil chemoattractant factor. Levels of IL-8 protein are elevated in SSc skin and more commonly in skin from patients with disease of less than one year's duration (251). Cultured SSc dermal fibroblasts express more IL-8 than normal fibroblasts (225). Interleukin-8 is also increased in BAL fluids from patients with SSc (36) and is produced by macrophages and fibroblasts in patients with lung

fibrosis (337). Interestingly two SNPs in the CXCR-2 (an IL-8 receptor) gene have been associated with scleroderma (356). Reduction of IL-8 levels by neutralising antibodies resulted in a significant decrease in angiogenesis, suggesting that IL-8 may also contribute to new vessel formation (238).

**c) Pulmonary and activation regulated chemokine**

Recent data has shown that Pulmonary and activation-regulated chemokine (PARC) stimulates collagen mRNA and protein synthesis by skin and lung fibroblasts (21). In SSc patients with lung inflammation, PARC protein levels are elevated in the BAL fluids in comparison with patients without lung inflammation and normal BAL fluid (285). Alternatively activated macrophages that are prevalent in SSc lung (22), synthesise PARC protein (169), which may be a significant activating ligand for resident fibroblasts.

**d) Other chemokines**

Regulated upon activation, normal T cell expressed and secreted (RANTES) and macrophage inflammatory protein-1α (MIP-1α) are increased in the BAL fluid from scleroderma patients (36). T-cells derived from SSc sera also produce elevated amounts of these chemokines (385). Increased expression of RANTES and MIP-1α is an early phenomenon precedes the development of dermal and pulmonary fibrosis in a murine model of scleroderma (509). While the levels of these chemokines are clearly elevated in SSc, their precise contributions to the disease phenotype are currently unknown.

### 1.6.2 SSc Pathophysiology II-Microvascular abnormalities

A unifying feature across the disease spectrum, microvascular disease is believed to be a significant pathogenic factor in SSc. Amongst the first clinical manifestations of vessel abnormalities are the failure to re-warm after cold challenge and an abnormal peripheral nailfold capillary pattern, with enlarged loops and capillary dropout (292). RP associated with SSc results in irreversible structural damage to the digital microvasculature while in primary RP, the associated digital ischaemia is reversible, without apparent tissue damage (197). It is thought that the pattern of microvascular damage as detected by nailfold capillaroscopy may change with disease progression (92). Early and advanced patterns of microvasculopathy are characterised by the appearance of giant capillaries and hemorrhages and are more frequent in the active phase of the disease. Loss of capillaries, architectural disorganisation and the

presence of ramified/bushy capillaries represent the late pattern of SSc microvascular damage and are associated with atrophic disease (92). It has been suggested that these patterns of microvascular damage show a degree of correlation with autoantibodies. The presence of ATA appears to be related to earlier expression of the active and late patterns of SSc microvascular damage while the presence of ACA seems to be related to delayed expression of the late nailfold capillary pattern (91). Interestingly, patterns of capillary damage do not appear to correlate with skin score and disease duration (353). Despite the reduced capillary density, there is paradoxically no counteracting angiogenic response in the skin of patients with SSc (268). Recently the pro-angiogenic factor vascular endothelial growth factor (VEGF) together with its receptors VEGF-R1 and VEGF-*R* were demonstrated to be markedly upregulated in SSc skin samples (112). This was paradoxically accompanied by reduced expression of hypoxia-induced HIF-1$\alpha$ despite reduced oxygen pressure ($PO_2$) levels in SSc skin (112). Further studies are required to clarify whether VEGF over-expression can lead to the vascular abnormalities that characterise SSc.

Microvascular damage appears to be systemic as affected internal organs can display significantly perturbed blood flow (237). At the ultrastructural level, the most prevalent microvascular abnormality in SSc patients is broadening and splitting of the basement lamina accompanied by perivascular edema, fibroblast activation and an increased number of mast cells (474). Basement membrane changes may underlie increased vascular permeability, which is well described in SSc (172). Changes in vessel function and/or endothelium integrity are amongst the earliest features of SSc pathogenesis (350). The first discernable changes that occur in the endothelium include concentric proliferation of the intimae and perivascular oedema (61). The described ultrastructural alterations in early SSc adversely affect endothelial cell vacuolisation, leading to necrosis and increased inter-endothelial cell permeability (143). Increased permeability allows increased passage of plasma and mononuclear cells with the consequent formation of oedema and perivascular infiltrates.

Serum and plasma levels of markers indicating endothelial activation such as von Willebrand factor, adhesion molecules and endothelin-1 (ET-1) are all increased in SSc patients (12;257;290;435). Furthermore, *in situ* analyses of SSc skin and other affected organs have demonstrated increased expression of ET-1, adhesion molecules, PDGF-B, TGF-$\beta$ and chemokines and their receptors by endothelial cells (156;160;180;463).

There is also evidence for impaired vasodilatation in SSc, which in the presence of potent vasoconstrictors such as ET-1 results in sustained vasoconstriction and reduced microcirculatory flow (13;227). Therefore, one of the initial stimuli mediating endothelial cell activation in SSc is likely to be ischaemia associated hypoxia. The synthesis of adhesion molecules and key mediators such as ET-1, PDGF-B and VEGF by cultured endothelial cells is rapidly induced by hypoxia (168;253;254;307;314). Cycles of ischaemia and reperfusion lead to the formation and accumulation of ROS, which can result in oxidative stress, inducing endothelial cell injury and death by apoptosis and necrosis (213). ROS also promote the synthesis of vasoactive mediators such as ET-1, which can in turn lead to further vasoconstriction and oxidative stress (44). Establishment of these feedbacks may be an important factor in the perpetuation of the vasomotor instability. There is circumstantial evidence that oxidative stress is a complication of SSc. Low density lipoproteins from SSc patients have been shown to be susceptible to oxidation (51). In addition, monocytes from SSc patients release increased amounts of the superoxide anion when cultured *in vitro* (375) while increased nitric oxide (NO) synthesis in SSc patients is thought to derive from activated endothelium (12).

Other putative mediators of endothelial cell activation are AECA, which are detectable in the sera of SSc patients with a prevalence up to 50% (208;345;345). The antigens they bind to are heterogeneous within and between sera of different patients (208). While AECA can induce pathogenic changes in endothelial cells *in vitro* (section 1.6.1.3) the pathogenicity of AECA *in vivo* has yet to be demonstrated. Observations in an animal model of SSc, University of California at Davies Line (UCD) 200 chickens (see 1.7.1) have linked endothelial cell apoptosis and AECA. These chickens spontaneously develop an inherited scleroderma-like disease, with immune, vascular and fibrotic characteristics similar to the human symptoms. Histochemical analysis of UCD 200 chicken showed that apoptosis of endothelial cells is an early event in the pathogenesis preceding the mononuclear perivascular infiltration observed in the skin and internal organs (319;396). The UCD chicken have circulating AECA, which induce endothelial cell apoptosis when transferred to control animals (483). Further analysis of SSc tissue is necessary to clarify whether this is also an active mechanism of the human disease.

### 1.6.2.1 Structure and formation of microvessels

Microvessels consist of an endothelial cell lined lumen surrounded by extramural cells; pericytes in medium-sized and smooth muscle cells (SMC) in large vessels (Figure 1) (146). Vascular formation in the embryo consists of two phases, vasculogenesis and angiogenesis. Vasculogenesis refers to the formation of large blood vessels by endothelial progenitors termed angioblasts while angiogenesis refers to the sprouting and subsequent stabilisation of these vessels by extramural cells (146). At the onset of angiogenesis, pericytes dissociate from the endothelial cell layer and migrate into the surrounding interstitial space where they attain a fibroblastic phenotype (106). The balance between adhesion and dissociation of endothelial cells and pericytes is regulated by the soluble mediators angiopoeitin-1 and 2, which bind the tie2 receptor tyrosine kinase (287). After maturation of new vessels, perivascular fibroblast-like cells are recruited by endothelial-derived PDGF-BB and attach to the endothelium (194).

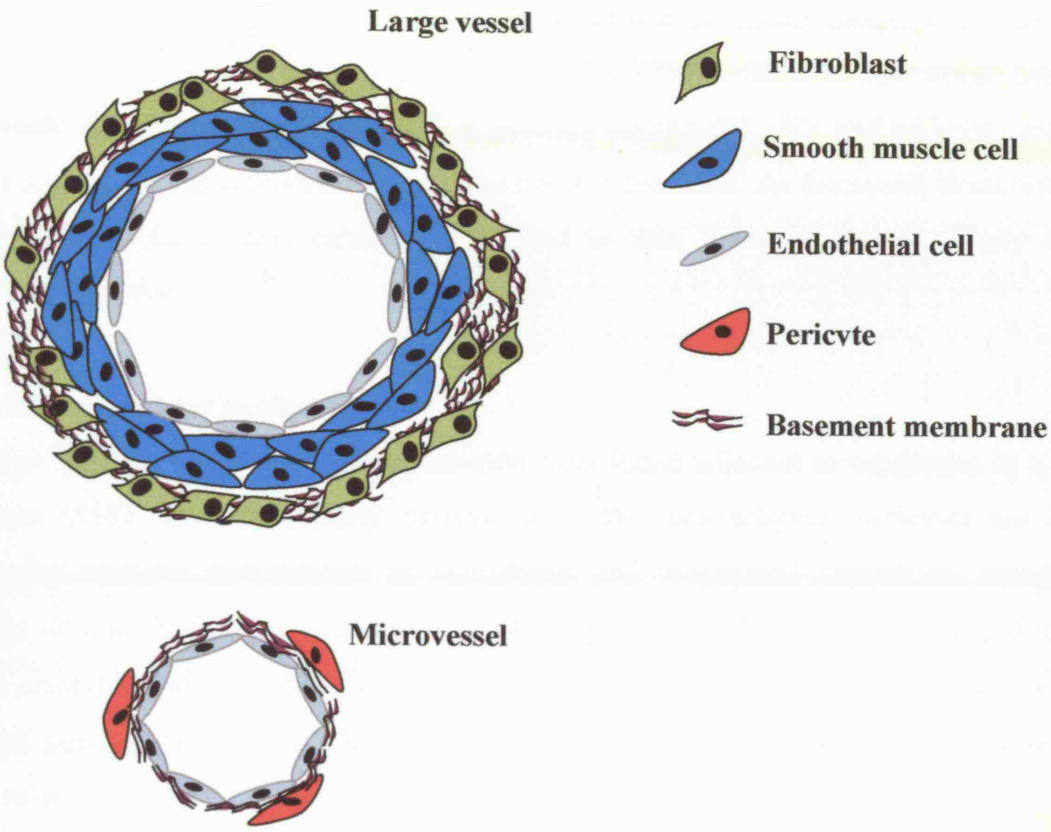


**Figure 1.1.**

**Structure of large blood vessels and microvessels.**

Large blood vessels are characterised by an endothelial cell lumen surrounded by concentric layers of vascular smooth muscle cells. By contrast, microvessels consist of an endothelial cell lumen enveloped by pericytes. Both endothelial cells and pericytes are embedded within a mutually synthesised basement membrane.

The pericyte coverage of new vessels arises from a combination of resident pericyte proliferation and recruitment and differentiation of circulating bone marrow-derived progenitor cells into pericytes (420). *De novo* synthesis of basement membrane components by both endothelial cells and pericytes then cements the cells together to complete vascular assembly (106). Once formed, microvessels remain in a state of dynamic equilibrium that is homeostatically maintained by physical and molecular interactions between endothelial cells and pericytes. During tissue repair and the development of human diseases such as cancer and SSc, there is a reprogramming of microvascular cells resulting in new vessel formation and growth. Alterations in the relationship between endothelial cells and pericytes are at the heart of microvascular activation and angiogenesis in the adult. As discussed in section 1.6.2, endothelial cells have been extensively studied in SSc, however, comparatively little is known about pericytes.

### 1.6.2.2 Microvascular pericytes

The word 'pericyte' was first used to describe cells found adjacent to capillaries in a variety of tissues (516). Developmentally derived from the mesenchyme, pericytes are located outside the vascular endothelium in continuous and fenestrated capillaries, venules and arterioles of less that 30μm in diameter (359) (Figure 1.2). They surround the endothelium and are embedded within a basement membrane, that is mutually synthesised by endothelial cells and pericytes (Figure 1) (85). Pericytes usually exhibit an elongated cell body from which arises a system of primarily longitudinal branches enveloping the endothelial tube (107). Both pericytes and endothelial cells are associated with each other through interruptions in the basement membrane. These contacts can be classified into three types; peg and socket arrangements, in which pericyte processes interdigitate into endothelial cell membranes; adherence plaques that are ultrastructurally similar to desmesomes and gap junctions (107). The number of pericytes varies between different tissues and among blood vessels of different sizes. In the retina, the pericyte:endothelial cell is ratio is almost 1:1, in the skin it is 1:3 (359). Pericytes and smooth muscle cells are structurally and functionally similar and share the expression of a number of cytoskeletal proteins such as α-smooth muscle actin (α-SMA) and desmin (401). However, there are a number of proteins that distinguish both cell types. For instance, the high-molecular weight-melanoma associated antigen (HMW-MAA) identifies pericytes in activated tissues such as wound healing and tumours (389). Furthermore, the mouse homologue of HMW-MAA, NG2 is elevated by

pericytes but not smooth muscle cells in pathological tissue (333). The GTPase-activating protein RGS5 has also been shown to be selectively expressed by pericytes in developing mouse embryo (79), while the expression of annexin A5 was recently reported to be specific to microvascular pericytes *in vivo* (46).

### 1.6.2.3 Pericyte Function

Pericytes have been implicated in a broad range of functions. Their phenotypic similarity to smooth muscle cells has led to the hypothesis that pericytes have a contractile role analogous to that of smooth muscle cells in larger vessels (317). It has also been suggested that the contraction of pericytes plays a role in regulating microvascular permeability by modulating the size of inter-endothelial cell junctions (360). Pericytes express receptors for the vasoconstrictor ET-1 (445) and contractile proteins such as α-SMA (316). While the contractile ability of pericytes has been demonstrated *in vitro* (239), there is no evidence that pericytes regulate microvascular contraction *in vivo*.

Developmental studies in mice have demonstrated a critical role for pericytes in maintaining vascular integrity. During vessel formation in the embryo, the bi-directional release of soluble mediators between endothelial cells and smooth muscle cell/pericyte precursor cells results in the recruitment of pericytes to nascent capillaries (146). PDGF and the angiopoietins play a major role in this process (146). Studies of knockout mice that lack the β receptor for PDGF (PDGFRβ) (422), the PDGF-B chain (273) or angiopoetin-1 (441) have demonstrated that failure to recruit pericytes to the developing vasculature results in impaired vascular morphogenesis and embryonic lethality as a result of severe hemorrhaging.

**Figure 1.2.**

**Scanning electro micrograph of microvascular pericytes.**

Pericytes (white arrows) envelope the underlying endothelial cells lining a microvessel (black arrowhead) with long cytoplasmic processes (black arrows). Image courtesy of Dr. Michael Pepper.

In contrast to systemic knockout models, endothelium-specific PDGF-B chain knockout mice (PDGF-B -/-) are viable and have been particularly useful in elucidating the role of pericytes in the maintenance of vascular integrity (33). In these animals, gene inactivation is incomplete, resulting in a chimeric situation where stretches of vessels with normal pericyte coverage adjoin stretches of vessels without associated pericytes. Whereas pericyte-covered stretches have normal diameter and lack signs of leakage or hemorrhage, neighbouring pericyte-deficient stretches display microaneurysms, leakage and micro-hemorrhage (33), implying that pericytes exert a local effect on vessel diameter and function. A key component of this regulatory function is the ability of pericytes to control endothelial cell number. Lack of pericytes *in vivo* leads to endothelial hyperplasia (193), while *in vitro* studies have shown that pericytes inhibit endothelial cell proliferation via the actions of TGF-β (14;202). An absence of pericytes also leads to a number of ultra-structural changes in the endothelial cells. These include changes in inter-endothelial junctions and signs of increased trans-cellular transport, suggesting that pericytes are essential for the control of endothelial cell differentiation and function (193). The capillary luminal surface, which is normally flat and smooth, displays numerous membrane folds in PDGF-B-/- mice (193). This may in turn affect the curvature of the endothelial cell, and hence the diameter of the microvessel. Morphometric analyses of pericyte-deficient microvessels have shown that their diameters are abnormally variable, with focal sites of abnormal distension or narrowing. Thus, one of the most essential roles of pericytes may be to provide necessary cues for the formation of endothelial tubes with uniform diameter (193). Taken together, these studies clearly demonstrate that pericytes provide essential physical and molecular cues that maintain endothelial and microvascular integrity.

Another key function of pericytes is that of mesenchymal progenitor cells. In vitro studies have demonstrated that pericytes undergo a phenotypic transition to other mesenchymal cell types (201). The transition of pericytes to osteoblasts has been particularly well documented both *in vivo* and *in vitro* (115). Several key genes are involved in this differentiation process, including the matrix Gla protein, osteopontin and osteonectin (116). Similarly, the transition of pericytes to adipocytes and chondrocytes has been demonstrated *in vitro* and *in vivo* (135). The local microenvironment is key in influencing the ultimate cellular phenotype of differentiating pericytes (135). In a number of fibrotic conditions pericytes have also been shown to differentiate into fibroblasts and myofibroblasts. During excessive dermal scarring,

microvascular pericytes leave the microvascular wall and differentiate into collagen-synthesising fibroblasts (439) while in the placenta, fibroblasts have been shown to be derived from microvascular pericytes (214). In dcSSc skin and fibrotic liver, it has been shown that pericytes are precursors for myofibroblasts (353;391). Annexin A5 was recently identified as a generic marker of pericytes with progenitor capacity, however, it is not yet clear whether it has a functional role in the differentiation process (46).

### 1.6.2.4 Pericytes and platelet-derived growth factor

Over the last few years it has become apparent that the PDGF family and particularly the PDGF-B isoform are central to pericyte biology and function. Since its first description 30 years ago (365;478), members of the PDGF family have been established as potent mitogens and motogens for connective tissue cells such as fibroblasts and smooth muscle cells (191). The PDGF family consists of five different dimeric isoforms, PDGF-AA, AB, BB and the two recently discovered isoforms PDGF-CC and DD. All five dimers exert their functional effects via activation of two structurally similar receptors, PDGF-α receptors (PDGFRα) and PDGFRβ. The five PDGF dimers exhibit distinct binding affinities for the PDGF receptors (PDGFRs). PDGF-AA, AB, BB and CC bind to and activate PDGFRα, while PDGF-BB and DD bind to and activate PDGFRβ (Figure 1.3). Heterodimers of PDGFRαβ have also been described, which can be stimulated by PDGF-AB, BB and CC (150). Ligand-binding leads to receptor dimerisation, resulting in autophosphorylation of specific tyrosine residues. These phosphorylated sites create docking sites for a number of downstream signalling molecules that contain SH2 domains, leading to the initiation of signalling cascades such as the phosphatidylinositol 3 kinase ($PI_3$-kinase), the P38 mitogen activated protein kinase (MAPK) or the phospholipase C-γ (PLC-γ) pathway (Figure 1.4) (447).

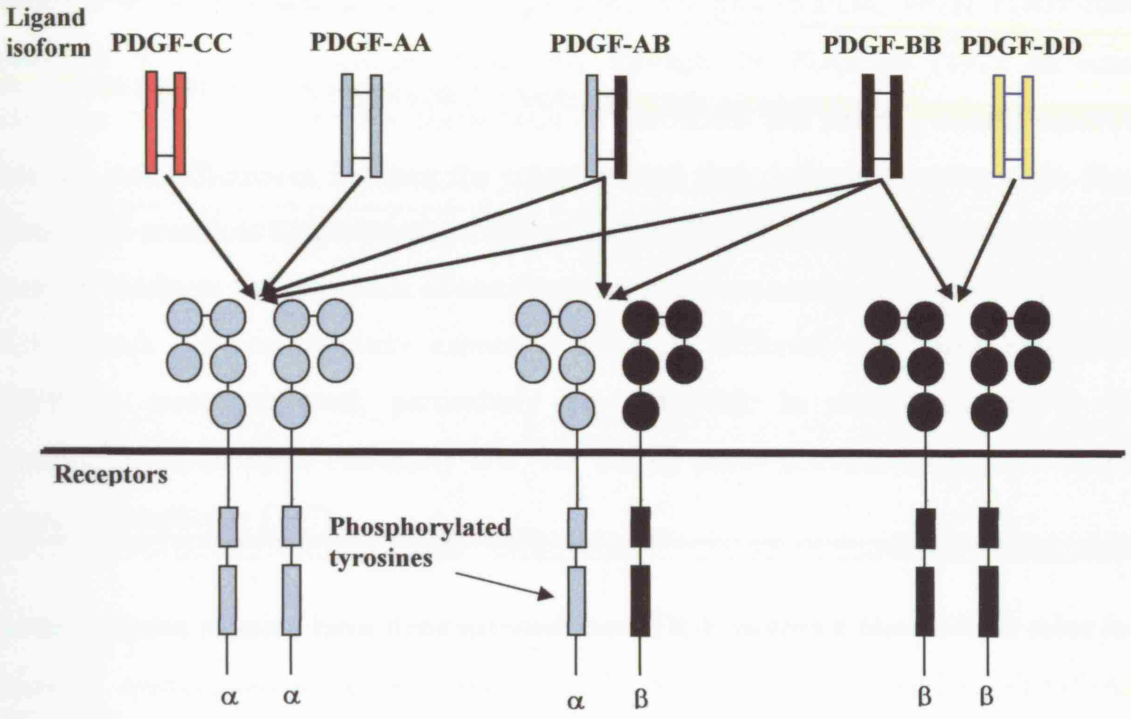


**Figure 1.3.**

**Binding affinities of the five PDGF dimeric isoforms.**

Different PDGF isoforms bind to and dimerise α and β receptors with different specificities. Receptors are drawn to illustrate that extracellular parts consist of 5 Ig-like domains. Intracellular parts of receptors contain tyrosine residues which become phosphorylated upon ligand binding. Modified from Heldin and Westermark, 1999.

*In vitro* systems have revealed that the signal transduction pathways evoked by PDGFRα and β are similar but differ subtly with respect to interactions with specific SH2 domain proteins, which may explain their differential effects on target cells (128). Studies have suggested a distinct requirement for specific pathways to initiate certain PDGFRβ-mediated cellular functions. For example, the $PI_3$-kinase and phospholipase C-γ (PLCγ) pathways are necessary for mitosis and migration, while RasGAP activity inhibits migration (256;461). Activation of both α and β receptors stimulate cell proliferation, while PDGF-induced chemotaxis *in vitro* is mediated exclusively through the PDGFRβ (191). In contrast, stimulation of PDGFRα inhibits chemotaxis of fibroblasts and smooth muscle cells (410). There are also differences between the receptors and their influence on the actin filament system. Both receptors stimulate edge ruffling and the loss of stress fibres, however, only the β-receptor mediates the formation of circular actin structures on the cell surface (128).Whilst PDGF ligands are constitutively expressed by many different cell types, expression of PDGFRs is more restricted, particularly the PDGFRβ. In normal connective tissue, expression of PDGFRβ is extremely low, but during tissue activation, receptor expression increases dramatically (367).

Genetic analyses in mice have demonstrated that PDGF isoforms play critical roles in key aspects of mammalian embryogenesis (30;204). Studies using PDGFRα, PDGF-A and PDGF-C null mutants have demonstrated that PDGFRα signalling is essential for palatogenesis and patterning of somites and mesodermal tissue (109;421). PDGF-B and PDGFRβ null mutants die *in utero* from widespread haemorrhaging due to impaired recruitment of mural pericytes and smooth muscle cells to nascent blood vessels (194).

Both *in vitro* and *in vivo* analyses have revealed a particular importance of PDGF-BB to pericyte biology (31;204). Genetic disruption in mice of either the PDGF-B chain or PDGFRβ results in extensive haemorrhaging caused by a failure to recruit pericytes to developing blood vessels (273;422).

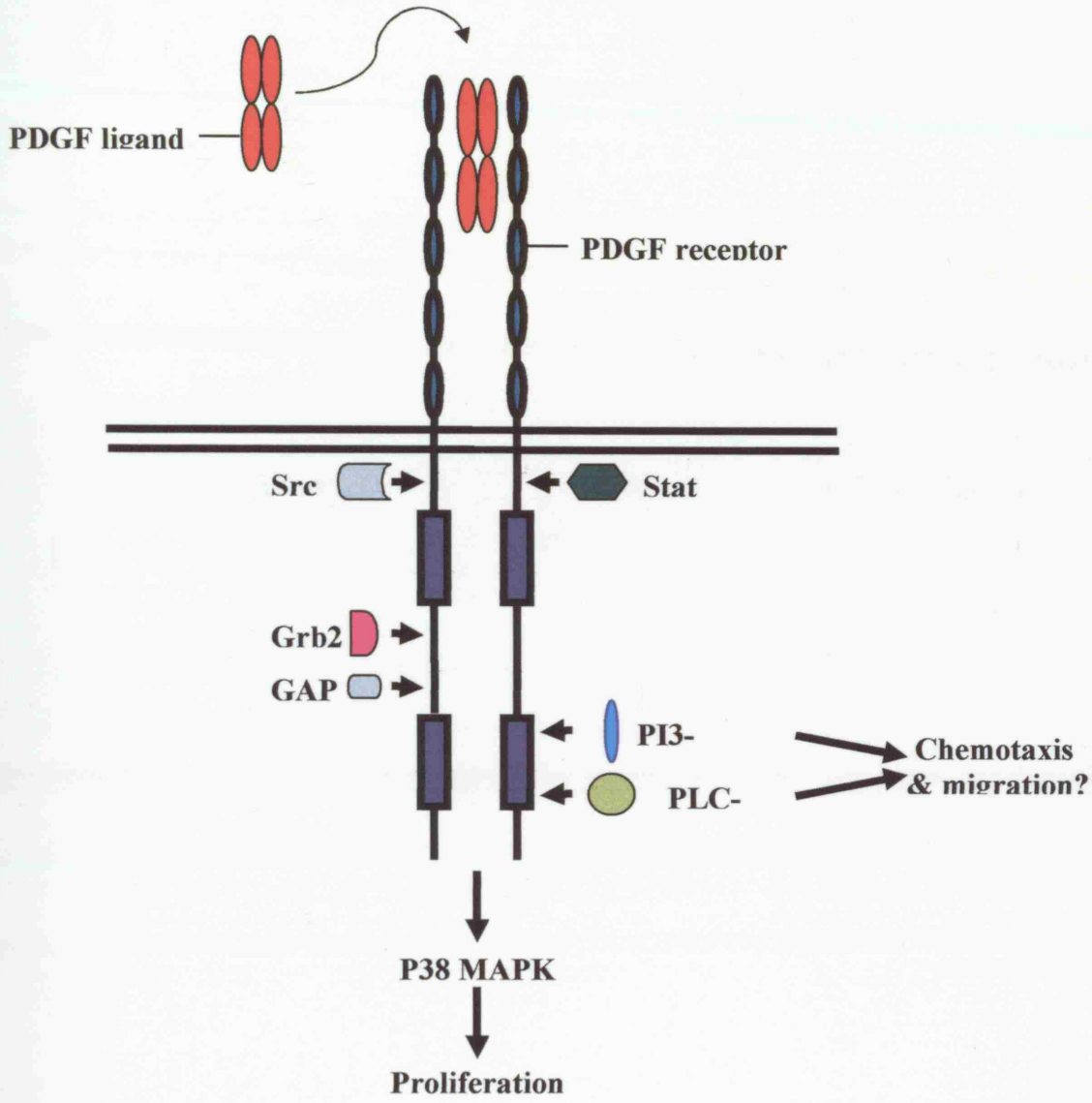


**Figure 1.4.**

**Binding of different signalling molecules to the PDGFRβ.**

Ligand induced receptor activation leads to the binding of signalling molecules such as Src and Grb2 to phosphorylated tyrosine residues in the intracellular domain of the PDGF receptor (blue boxes). In vitro studies suggest that specific signalling cascades mediate different functions. For example, activation of the P38 MAPK pathway leads to a proliferative response while PI3-K and PLC-γ activate chemotaxis.

The primary role of PDGFRβ-mediated signalling during embryogenesis appears to be the induction of chemotaxis and proliferation of PDGFRβ-expressing smooth muscle cells and pericytes in response to endothelial-derived PDGF-B chain ligands (194).

PDGFRβ-mediated signalling also appears to play an important role in pericyte activation during adult pathologies. The over-expression of PDGFRβ by microvascular pericytes has been reported in a number of diverse conditions, including wound healing, tumours, dcSSc and dermal scarring (354;439;440). This is supported by autoradiographic studies identifying pericytes as one of the first cell types to undergo mitosis during tumour development and wound healing (24;106). Furthermore, the blockade of PDGFRβ signalling by imatinib mesylate results in pericyte loss around microvessels and a subsequent reduction in tumour growth (29). In hypoxia-induced angiogenesis, pericyte proliferation was shown to be activated by VEGF in both an autocrine and paracrine manner (325;486;499). The same group also demonstrated that the differentiation of pericytes from circulating precursors during tumour formation is PDGFRβ dependent (420). The loss of retinal pericytes that characterises diabetic retinopathy is recapitulated identically in the endothelial cell specific PDGF-B-/- mouse (126;414). Pericytes have also been implicated in the progression of hypertension, liver cirrhosis and atherosclerosis (108;183;196).

### 1.6.2.5 Pericytes and Fibrosis

It has been proposed that pericytes contribute directly to the development of fibrosis by acting as progenitor cells to collagen-synthesising fibroblasts and myofibroblasts (391;439). Morphological analysis of tissue actively undergoing angiogenesis has revealed that pericytes migrate from the microvascular wall into the interstitium and acquire a fibroblast-like morphology (90;106). In hypertrophic scars and SSc skin, collagen-synthesising cells are located predominantly in the perivascular area (245;386;386). The differentiation of pericytes into collagen-synthesising fibroblasts has been demonstrated in dermal scarring tissue and human placenta (214;439). Similar findings have been reported in fibrotic liver and kidney, in which pericytes have been shown to express PDGFRβ and synthesise extracellular matrix components during experimentally induced fibrosis (27;145;248;299). The differentiation of pericytes into myofibroblasts has also been demonstrated in fibrotic kidney (186), liver (391) and dcSSc skin (353).

### 1.6.3 SSc Pathophysiology III-Connective tissue fibrosis

The pathological hallmark of SSc is increased synthesis of ECM macromolecules, resulting in connective tissue fibrosis. Histological examination of affected SSc tissue has revealed that the normal interstitium is gradually replaced with a dense ECM. In patients with early dcSSc, collagen type III is predominant, particularly in the lower reticular dermis (140). Interestingly, increased expression of total fibronectin and the ED-A splice variant of fibronectin (ED-A FN) has also been demonstrated in the reticular dermis (139;353). The significance of this is unknown. As the disease progresses, collagen type I levels increase until it becomes the dominant ECM constituent, however, the final relative proportion of type I: type III is similar to that of normal skin (140;282). Elevated expression of collagens type VI and XVI have also been reported in affected SSc skin (8;369).

The regulated turnover of ECM macromolecules is essential to a variety of biological processes. Matrix metalloproteinases (MMPs), of which 23 have been identified, are responsible for ECM degradation (473). They are regulated by specific tissue inhibitors of metalloproteinases (TIMPs) (49). Evidence for the dysregulated expression of several members of the MMP and TIMP family has been reported in SSc. Elevated expression of TIMP-1 and TIMP-3 has been demonstrated in cultured SSc fibroblasts (43;300), while increasing concentrations of TIMP-1 in SSc serum have been associated with adverse disease severity (458;501). Increased Serum levels of TIMP-2 have been detected in SSc sera and associated with an increased risk of cardiac fibrosis (123;497). In addition, reduced expression of MMP-3 has been reported in SSc fibroblasts and MMP-3 autoantibodies have also been reported in SSc sera (43;323).

While the majority of SSc related studies have focussed on the relationship between increased collagen biosynthesis and fibrosis, the levels of several other matrix components are also elevated in affected SSc tissue. For example, increased expression of total fibronectin and the ED-A splice variant have been demonstrated in SSc skin, notably in the deep reticular layers (87;353). Interestingly, SNPs in the fibronectin gene have been associated with an increased risk of developing FASSc (25), however, it is unknown whether these polymorphisms underlie the elevated expression of the protein. The case for elastin is more contentious. Expression of elastin in SSc has been reported as both elevated (351) and normal (141) in SSc skin. Circumstantial evidence indicates increased cross-linking and degradation of elastin in SSc, however, to date there is a lack of corroborative *in situ* data (97;433).

Increased expression of glycosaminoglycans has also been reported in SSc skin and cultured SSc fibroblasts (54;142).

### 1.6.3.1 Fibroblasts

Fibroblasts are mesenchymally derived cells that form the major cell type within soft connective tissue. These cells are responsible for the synthesis of ECM macromolecules and the assembly and maintenance of connective tissues. During tissue repair following injury, fibroblasts adopt a central role in the remodelling process culminating in the synthesis, deposition and assembly of new ECM. While the development of SSc is dependent upon a complex cascade of events and cell types, fibroblasts are considered the key effector cell of SSc pathology as they are directly responsible for its ultimate phenotype. A number of studies have examined the role of the fibroblast in SSc. The early studies of note were carried out by LeRoy *et al.*, who demonstrated that skin fibroblasts from SSc patients, when cultured *in vitro*, produce increased amounts of type I collagen compared with fibroblasts from normal controls (269). Subsequent studies have revealed that the production of several ECM components, including collagens type III, VI, VII, fibronectin, decorin and glycosaminoglycans is elevated in cultured SSc fibroblasts (436). The increased production of matrix components is maintained for several passages *in vitro* in the absence of exogenous stimuli, suggesting that fundamental alterations in the regulatory pathways controlling ECM synthesis have occurred in these cells.

### 1.6.3.2 The origins and heterogeneity of fibroblasts

It has been proposed that connective tissue fibrosis arises due to the expansion of a particular sub-population or clone of fibroblasts with a pro-fibrotic phenotype (218;224). Fibroblasts are quite diverse with respect to proliferation, cell surface receptors and production of ECM macromolecules (103;224;457). Heterogeneity of fibroblasts has been demonstrated in SSc, *in vivo* and *in vitro* (87;218;229;353). It has been suggested that fibroblast heterogeneity is a result of the differentiation of fibroblasts from diverse cellular sources (Figure 1.5). During the development of scarring and fibrosis, circulating blood cells, epithelial cells and resident non-fibroblastic cells can differentiate into matrix synthesising fibroblasts and myofibroblasts. These are summarised below.

#### a) Fibrocytes

Fibrocytes are bone marrow-derived, circulating fibroblastic cells that are recruited to sites of

injury (73). They express collagen type I, CD11b, CD13, CD34, CD45 RO and CD86 but are negative for α-SMA (74;75). It has been reported that TGF-β can induce fibrocytes to assume a myofibroblast phenotype, expressing α-SMA and mediating collagen gel contraction (3). *In vitro*, fibrocytes and fibroblasts appear to be responsive to separate repertoires of cytokines. However, whether this translates into functional differences during tissue repair *in vivo* is unknown (75;348).

**b) Bone marrow-derived fibroblasts**

Hashimoto *et al.* identified a population of bone marrow-derived cells in fibrotic lung (183). Preliminary analysis indicated that they are collagen-synthesising cells phenotypically distinct to fibrocytes (183). They were shown to constitute the overwhelming majority (>80%) of collagen-synthesising cells in bleomycin-induced lung fibrosis. However, these collagen-synthesising cells did not express α-SMA and treatment of these fibroblasts *in vitro* with TGF-β failed to induce myofibroblast differentiation. A significant proportion of myofibroblasts in fibrotic liver (147) and collagen rich tumour stroma (111) are also derived from the bone marrow and express both collagen and α-SMA. These studies indicate that the identity of cells responsible for collagen biosynthesis and tissue contraction may vary between tissue beds and reveals an unexpected degree of tissue specificity.

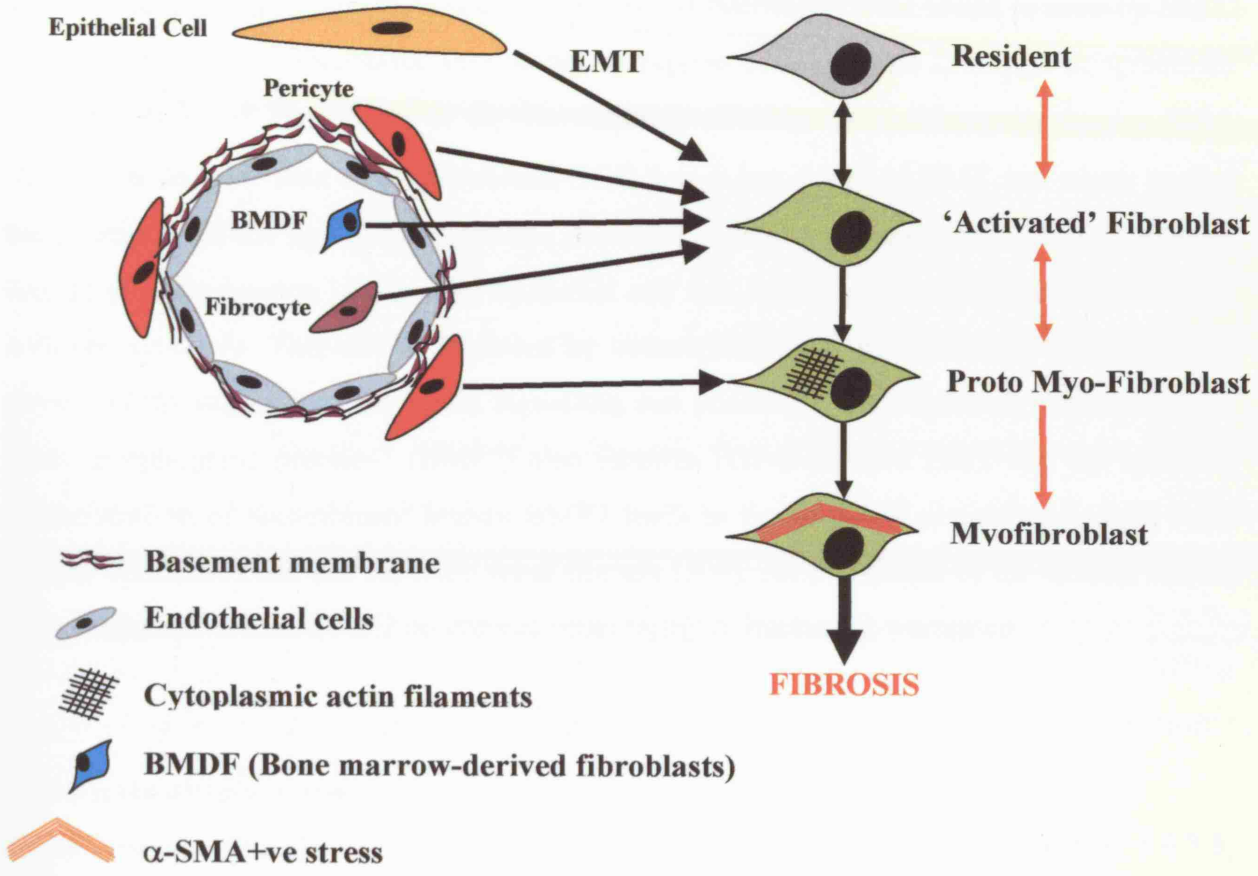


**Figure 1.5.**

**Cell lineages that are involved in connective tissue fibrosis.**

In the development of fibrosis, fibroblasts are derived from a number of diverse sources. In addition to the activation and differentiation of resident fibroblasts into myofibroblasts, an epithelial-mesenchymal transition (EMT) of epithelial cells and the differentiation of pericytes add to the fibroblastic pool. Circulating cells such as fibrocytes and bone marrow-derived fibroblasts (BMDF) extravasate into interstitial tissue and synthesise collagen during wound healing and may play a key role in the development of pathological fibrosis.

**c) Epithelial-Mesenchymal Transition**

Epithelial-mesenchymal transition (EMT) has been relatively well studied with regards to tumour metastases (177) and been particularly well studied as a mechanism by which collagen-synthesising fibroblasts are generated during renal fibrosis (215). Using bone marrow chimeras and transgenic reporter mice, interstitial kidney fibroblasts were shown to be derived from two sources. A small number of fibroblasts migrate to normal interstitial spaces from the bone marrow, while the majority of fibroblasts were found to arise by EMT. Both populations of fibroblasts were found to express collagen type I, though in agreement with the study of Hashimoto et al, the majority of these cells did not express α-SMA (183;215). *In vitro* data have established TGF-β as a key factor in EMT and many studies have focused on the signalling pathways involved in TGF-β induced EMT. TGF-β induces Smad2 phosphorylation in a tubular epithelial cell line, which markedly promotes EMT and collagen synthesis. This can be inhibited by overexpression of the inhibitory Smad protein, Smad7 (276) suggesting that Smad signalling can positively and negatively regulate EMT. Bone morphogenic protein-7 (BMP7) also inhibits TGF-β-induced EMT and the systemic administration of recombinant human BMP7 leads to the repair of severely damaged renal tubular epithelial cells and reversed renal fibrosis (506). An evaluation of the clinical effects of recombinant human BMP7 on chronic renal injury in humans is warranted.

**d) Pericyte differentiation**

Fibroblasts can also derive from microvascular pericytes. As described in section 1.6.2.5, during the progression of fibrosis both collagen-synthesising fibroblasts and myofibroblasts in a variety of organs are believed to be derived from local tissue pericytes (186;353;391;439). These studies raise interesting questions. For example, do different modes of fibroblast differentiation predominate in different tissues and different diseases? Equally important is the question of whether fibroblasts derived from different anatomical sites perform different functions in fibrotic tissue.

### 1.6.3.3 Fibroblast progenitors and SSc

The involvement of fibroblast progenitors in SSc has not been extensively studied, however, there is increasing interest as to their potential association with the disease. While the presence of fibrocytes has yet to be demonstrated in SSc tissue, sera from patients with SSc were less able to inhibit fibrocyte differentiation in vitro than control sera, possibly as a result of decreased serum amyloid protein levels (346). Peripheral blood monocytes from patients with SSc when cultured on type I collagen generate more fibroblast-like cells than control monocytes (349). The activation and phenotypic convergence of pericytes into a myofibroblast phenotype has been reported in SSc skin (353).

### 1.6.3.4 Myofibroblasts

Essential in the development of fibrosis, myofibroblasts were initially described in granulation tissue of healing wounds as modified fibroblasts, exhibiting features of smooth muscle cells, including bundles of microfilaments and gap junctions (155). Myofibroblasts generate the force required to contract tissues and have been identified in many fibrotic conditions (455). Morphologically, myofibroblasts are characterised by a contractile apparatus that contains bundles of actin microfilaments which are analogous to stress fibres and are associated with contractile proteins such as non-muscle myosin (255). *In vivo* connective tissue fibroblasts lack the contractile microfilamentous apparatus or stress fibres that are observed in myofibroblasts; rather, actin microfilaments are organised predominantly into a cortical meshwork. Thus, in connective tissues *in vivo*, myofibroblasts are both morphologically and functionally different from fibroblasts. Myofibroblasts, in addition to expressing the β- and γ-cytoplasmic actins that are found in fibroblasts, express α-SMA (96;417). There are, however, several locations *in vivo,* in which cells show the morphological characteristics of myofibroblasts, such as stress fibres, but do not express α-SMA, for example, in the lung alveolar septa and the early phases of granulation-tissue formation (200;232). This has led to the hypothesis that there are two types of myofibroblasts, those that do not express α-SMA, termed 'proto-myofibroblasts' and those that do express α-SMA, termed 'differentiated myofibroblasts' (455). Differentiated myofibroblasts can be distinguished from normal fibroblasts by the expression of α-SMA and the ED-A splice variant of fibronectin, ED-A FN.

The ontogeny of myofibroblasts is an area of controversy. The established hypothesis that myofibroblasts are solely derived from resident fibroblasts has been superseded with the finding that in certain conditions, myofibroblasts can also be derived from pericytes (186) and bone marrow-derived stem cells (111;147). Therefore, the origin of myofibroblasts is highly tissue-specific. A factor implicated in the differentiation of myofibroblasts is Thy-1, a cell surface glycoprotein, that is differentially expressed by fibroblasts (41). Thy-$1^{+ve}$ and Thy-$1^{-ve}$ populations of fibroblasts are known to be functionally distinct with regards to the production of cytokines and extracellular matrix (103;413). In a study of myometrial fibroblasts, only Thy-$1^{+ve}$ fibroblasts were found to be capable of differentiating into myofibroblasts after treatment with TGF-β (252), suggesting that Thy-1 is a marker of cells with myofibroblastic potential in the myometrium. However, another study of lung fibroblasts demonstrated that myofibroblasts were derived from Thy-$1^{-ve}$ fibroblasts (514). Further studies are necessary to clarify the role of Thy-1 in myofibroblast differentiation and whether these differences can be attributed tissue-specificity.

It is now accepted that the transition from fibroblast to myofibroblast begins with the appearance of the proto-myofibroblast. The formation of myofibroblasts from proto-myofibroblasts is not well understood, however, mechanical tension, TGF-β and ED-A FN are thought to play key roles. Inhibiting the interaction between ED-A FN and the cell surface blocks TGF-β induced myofibroblast differentiation and α-SMA expression (394). Thus, the *de novo* synthesis of ED-A FN is a pre-requisite to α-SMA expression and the differentiation of myofibroblasts. This was recently supported by *in vivo* wound healing studies showing that ED-A FN expression precedes the appearance of α-SMA positive myofibroblasts (200). Increased expression of ED-A FN has been reported in fibrotic conditions such as liver fibrosis and graft versus host disease (GVHD) (328;462), however, not in dcSSc. In the presence of both factors, the myofibroblast phenotype is lost when mechanical tension is removed, however, increased mechanical tension in splinted wounds increases ED-A FN and α-SMA expression without changing the expression levels of TGF-β (200).

Little is known about the signalling pathways that govern myofibroblast differentiation. In bleomycin induced lung fibrosis, FIZZ1 has been identified using microarray analysis as promoting myofibroblast differentiation (280). In a separate study, again utilising cDNA

microarrays, the inhibitor of differentiation (ID) family members, ID1 and ID3, were identified as potential mediators of myofibroblast differentiation during lung fibrosis (67).

Myofibroblasts appear in granulation tissue at the time of wound contraction and disappear during the transition towards scar tissue (96), as a result of apoptosis (105). This observation has led to the hypothesis that the development of pathological fibrosis may be a consequence of failed myofibroblast apoptosis. Myofibroblasts have been identified dcSSc tissue (219;353;377), however, little is known about their role in the disease. Moreover, it is unclear whether myofibroblasts also contribute to the excessive deposition of ECM during fibrosis. While it is known that myofibroblasts produce ED-A FN, the question of whether they are the principal collagen-synthesising cell in fibrotic tissue is more controversial. Collagen biosynthesis by myofibroblasts has been demonstrated predominantly by *in vitro* analysis (244). *In vivo* data suggest that the production of collagen by myofibroblasts is tissue specific. In fibrotic liver, for example, a significant correlation between myofibroblasts and collagen type I mRNA has been observed (134). However, during dermal tissue repair the synthesis of collagen type I continues after the apoptotic removal of myofibroblasts (200). Analyses of renal (215) and lung fibrosis (183) has revealed that the majority of collagen-synthesising cells do not express markers of myofibroblasts. While increased collagen biosynthesis by myofibroblasts derived from SSc skin has been reported *in vitro*, analyses of affected dcSSc skin has shown no correlation between the presence of myofibroblasts and collagen biosynthesis (219;353).

#### 1.6.3.5 Cytokines and growth factors

Biosynthesis of ECM macromolecules by fibroblasts is the culmination of a coordinated sequence of events requiring the collaborative efforts of different cell types. The orchestration of these events is regulated by a large number of soluble mediators. A variety of cytokines, chemokines and growth factors have been associated with the pathophysiology of SSc.

**a) Transforming growth factor-β**

Due to its multi-functional role in tissue repair and scarring, TGF-β is one of the most extensively studied fibrogenic growth factors. In mammals, the age of onset of scarring correlates with an inflammatory response and increased expression of TGF-β (479). In the

embryo, characterised by scarless tissue repair, TGF-β is only expressed transiently and at low levels after injury (298). Conversely in the adult wound site it is present at high levels for the duration of healing and beyond (149). TGF-β has been implicated in a number of fibrotic conditions in kidney, liver, and lung (264). Neutralisation of TGF-β in experimental models almost universally results in reduced collagen biosynthesis and fibrosis (379;496). As previously discussed, TGF-β also plays a central role in promoting the formation of myofibroblasts from fibroblasts (394). To date three TGF-β isoforms have been identified, TGF-β1, 2 and 3. Their distinct functions have yet to be clearly delineated, however, TGF-β1 and 2 promote fibrosis while TGF-β3 reduces fibrosis (326). Delivery of neutralising antibodies against TGF-β1 and -β2 at the time of wounding reduces scarring (397), as does exogenous application of TGF-β3. The anti-fibrotic effects of TGF-β3 are thought to be a result of its down-regulation of TGF-β1 (326;398). These findings suggest that a balance among the TGF-β isoforms is critical for the regulation of efficient tissue repair. The critical role for TGF-β in the fibrotic process has led to its being widely studied in SSc. Increased expression of TGF-β1 and -β2 has been reported in the affected skin of SSc patients (352). Increased expression of TGF-β type I and II receptors stimulates collagen synthesis in cultured SSc fibroblasts in an autocrine pathway (236). Recent studies suggest that expression of type I receptors is increased on SSc fibroblasts whilst type II receptor levels are slightly decreased (335). Blockade of endogenous TGF-β signalling *via* neutralising antibodies or antisense TGF-β oligonucleotides prevents increased collagen synthesis by SSc fibroblasts (209). The forced expression of TGF-β type I receptor but not type II in normal fibroblasts results in elevated collagen synthesis suggesting that upregulation of collagen synthesis by SSc fibroblasts may primarily depend on the signalling downstream from the TGF-β type I receptor (335). Dermal and pulmonary fibrosis develops in transgenic mice with fibroblast-specific expression of a kinase-deficient TGF-β type II receptor. Therefore, perturbations of specific aspects of the TGF-β signalling pathway in fibroblasts can induce fibrosis *in vivo* (102). Of note is a study demonstrating increased expression of the TGF-β co-receptor, endoglin on SSc fibroblasts (265). Expression increased with disease severity and forced over-expression of endoglin into normal fibroblasts was found to inhibit the TGF-β mediated increase in CTGF promoter activity, suggesting that it acts as a negative regulator of CTGF expression. The authors concluded that lesional SSc fibroblasts may overexpress

endoglin as a negative feedback mechanism in an attempt to block further induction of profibrotic genes by TGF-β (265).

Smads are the primary transducers of TGF-β signalling. Three families of Smad proteins have been identified; the receptor–regulated Smad (Smad 2 and Smad 3); common partner Smad (Smad 4); and inhibitory Smad (Smad 7) (403). Increased phosphorylation of Smad 2 and increased nuclear localisation of Smad 2 and 3 has been reported in SSc fibroblasts (310). Interestingly, the nuclear localisation of Smads in SSc fibroblasts is insensitive to the blockade of TGF-β signalling using neutralising TGF-β antibodies or overexpression of kinase-deficient TGF-β type II receptor (309). However, other groups have reported increased levels of phosphorylated Smad2 and Smad3 in cultured SSc fibroblasts coupled with decreased expression of the inhibitory Smad 7 (19), suggesting a combination of these factors gives rise to increased TGF-β signalling in SSc fibroblasts. Interestingly, Smad 7 deficiency has also been reported in lesional dcSSc skin (117). A recent study showed that treatment with a pharmacologic inhibitor of PI-3 kinase abrogated constitutive Smad3 phosphorylation in SSc fibroblasts (18). Inhibitors of the PI-3 kinase pathway also reduce the expression of TGF-β type II receptor in SSc fibroblasts (492) suggesting that interactions between diverse signalling networks regulate the TGF-β response in SSc. Evidence that inhibition of MMP-1 by TGF-β is mediated through Smad 3 and Smad 4 suggests that stimulation of the TGF-β pathway in fibroblast results in collagen synthesis whilst simultaneously inhibiting matrix degradation (502).

**b) Platelet-derived growth factor**

As a potent mitogen and chemoattractant for fibroblasts, PDGF has been implicated in the pathophysiology of SSc. Expression of both PDGFRα and β is increased in SSc tissue, specifically on fibroblasts and pericytes (246;354;487). Endothelial cells and macrophages appear to be the primary sources of PDGF ligand in SSc skin (160;354). PDGF induces the expression of monocyte chemoattractant protein 1 (MCP-1) by cultured SSc fibroblasts (113). MCP-1 has been shown to stimulate collagen biosynthesis in cultured fibroblasts (489), suggesting that some of the pro-fibrotic effects of PDGF may be regulated by secondary mediators.

**c) Connective tissue growth factor**

Connective tissue growth factor (CTGF) is a heparin-binding growth factor that is secreted by fibroblasts after activation by TGF-β. Also known as CCN2, CTGF belongs to an early gene response family known as CCN, that includes CTGF, Cyr61 and Nov (339). Since its initial identification in endothelial cells (47), several other cell types, including fibroblast, smooth muscle cells, tumour cells and chondrocytes have also been shown to express the protein (266). In fibroblasts, CTGF is robustly induced by TGF-β and based on a number of studies, it has been suggested that the pro-fibrotic properties of TGF-β can be attributed to CTGF (407). The overexpression of CTGF in normal fibroblasts leads to an increase in the synthesis of collagen and fibronectin (406), whilst the inhibitory effect of prostacyclin derivates on collagen biosynthesis is thought to be mediated by a downregulation of CTGF production (434). Moreover, the injection of both TGF-β and CTGF into murine skin results in persistent fibrosis while addition of either factor alone results in an acute granuloma formation but not fibrosis (308). Therefore, TGF-β/CTGF synergy may be critical in the development of fibrosis. In SSc, elevated CTGF serum levels have been detected (382), while increased CTGF tissue expression appears to correlate with the degree of fibrosis in SSc skin (207). Increased autocrine CTGF production has been argued to be responsible for the maintained fibrotic phenotype of SSc fibroblasts in culture (406). N-terminal cleavage products of CTGF are elevated in the plasma and dermal interstitial fluid of scleroderma patients, compared to healthy controls. Their levels correlate positively with the severity of skin disease and negatively with disease duration, suggesting the utility of N-terminal CTGF as a marker of fibrosis (122).

**d) Endothelin-1**

ET-1 is a member of the endothelin family of which there are 3 isoforms, ET-1, -2 and -3. Originally identified as a potent vasoconstrictor, a growing body of evidence has implicated ET-1 as a mediator of organ-based fibrosis. ET-1 exhibits a wide range of biological properties on normal cells, including mitosis (4) and inducing the biosynthesis of extracellular matrix macromolecules (275;405). Exogenous ET-1 enhances the synthesis of collagen types I and III and inhibits the production of MMP-1 in normal fibroblast culture (484). ET-1 is also able to induce matrix contraction of normal fibroblasts within three-dimensional collagen lattices and to promote the formation of myofibroblasts (404). In SSc, elevated levels of circulating ET-1 have been detected in patients with skin and lung fibrosis, which correlated with disease severity (493;494). The increase in circulating ET-1 is paralleled by

an increase in ET-1 expression *in vivo* (5). In the skin, ET-1 is predominantly located in the superficial papillary microvessels and to a lesser extent in the deeper dermal vessels. Increased staining of ET-1 has also been identified on fibroblasts, endothelial and smooth muscle cells (463). In addition, dermal fibroblasts cultured from SSc patients showed increased cytoplasmic ET-1 expression and increased secretion into the supernatant when compared to normal fibroblasts (235).

The biological effects of ET-1 are mediated by at least two different receptors; the endothelin receptor type A (ETAR) and the endothelin receptor type B (ETBR). The presence of both receptor types has been demonstrated in normal and SSc fibroblasts, however, ETAR expression is reduced on SSc fibroblasts when compared to normal fibroblasts (484). Immunohistochemical analyses from lung biopsies of patients have demonstrated increased expression of total ET-1 receptors mainly in the sclerotic tissue localised in the alveolar epithelium and the pulmonary interstitium (5). Endothelin-1 has also been associated with the development of SSc-associated PAH. Endothelin plasma levels are raised in the bronchoalveolar lavage (BAL) fluid of patients with SSc-associated PAH. (167;493). To date the endothelin receptor antagonist bosentan is the only licensed drug available for the treatment of PAH (368).

## 1.7 Animal models of Scleroderma

There are several models of SSc that have been used to study the basic mechanisms of the disease process. Each model exhibits a specific aspect of scleroderma pathogenesis, however, none of the available animal models presents a full range of the human SSc characteristics (vascular injury, inflammation, immunologic changes and tissue fibrosis). Nonetheless, these models constitute a valuable resource for the investigation of the SSc pathogenesis and testing potential treatments. Table 1.7 summarises the major characteristics of SSc animal models.

### 1.7.1 Naturally occurring animal models

Two natural occurring animal models have been described; the tight skin mouse (Tsk/+ mouse) models and the UCD 200 chicken (162;173).

Tight skin mice (Tsk/+) harbour a duplication in exon 17 of the fibrillin gene. Mice homozygous for this duplication die *in utero*, however, heterozygote mice spontaneously develop a marked and progressive skin fibrosis from 2 weeks of age. Whilst the mechanisms underlying this fibrosis are unknown, IL-4 and TGF-β have both been implicated (304). There are several differences to the human disease. In particular, there is no evidence for vascular damage in the murine model. Moreover, the pulmonary presentation resembles more an emphysema-type process rather than fibrosing alveolitis and there are no inflammatory infiltrates in the affected tissues (6).

The UCD 200 chicken share many features of human SSc, including skin and visceral fibrosis, vascular occlusion, lymphocyte infiltration in involved organs, elevated rheumatoid factor, antinuclear antibodies and polyarthritis. Unlike Tsk/+ mice, there is pronounced vascular damage in UCD chicken with accompanying endothelial apoptosis and AECA. This model differs from the human counterpart in the acute onset. In addition, smooth muscle proliferation is seen during the vascular disease in UCD chicken, which is absent in the human disease (395).

### 1.7.2 Induced animal models

Bleomycin is an antibiotic derived from *Streptomyces verticullus* that is used for the treatment of cancer. Pulmonary fibrosis is an adverse side effect of the treatment and

consequently bleomycin can be used to induce lung fibrosis in mouse. The fibrogenic effects of this drug may be secondary to a free radical injury. Unlike FASSc, bleomycin-induced pulmonary fibrosis is reversible, however there, are common features such as immune dysregulation, including positive antinuclear antibodies and the development of both dermal and pulmonary fibrosis (7;490).

Patients that undergo an heterologous bone marrow transplantation sometimes develop a chronic graft versus host disease (GvHD) with skin and visceral fibrosis resembling scleroderma. Bone marrow transplantation into irradiated recipients can lead to a similar GvHD response in specific strains of mice and rats (508). The phenotype is characterised by the presence of infiltrating immune cells, upregulation of TGF-β and increased synthesis of collagen type I in the skin.

**Table 1.7: Animal models of SSc**

| Parameters | Human SSc | Tsk/+1 mouse | Murine Bleomycin-induced | Murine SSc GvHD | UCD 200 chicken |
|---|---|---|---|---|---|
| Skin fibrosis | + | + | + | + | + |
| Visceral fibrosis | + | + | + | + | + |
| Pulmonary | + | - | + | + | + |
| Renal | + | - | - | - | + |
| Cardiac | + | + | - | - | + |
| Inflammation | + | - | + | + | + |
| Vascular injury | + | - | + | - | + |
| Autoantibodies | + | + | + | - | + |

SSc GvHD (Sclerodermatous graft vs. host disease). Modified from (508).

## 1.8 Work presented in this thesis

Microvessels are comprised of two intimately associated cell types; endothelial cells and pericytes and interactions between these two cell types govern the phenotype of microvessels in health and disease. PDGFRβ-expressing pericytes have been demonstrated to contribute to the development of several fibrotic disorders such as liver fibrosis and excessive dermal scarring. Yet although microvascular damage is regarded as a key component of SSc pathogenesis and is known to result in a fundamental reprogramming of endothelial cell phenotype, the potential role of pericytes in SSc has yet to be investigated. The work presented in this thesis examines the phenotype of pericytes in SSc tissue with the aim of determining whether they play a role in SSc disease development. In chapter 3, the expression levels of PDGFRβ by pericytes in SSc tissue is examined. In chapters 4 and 5 the potential of pericytes to act as precursors for myofibroblasts *in vivo* and *in vitro* is investigated. Lastly in chapter 6, the effects of PDGFRβ inhibition on pericyte function during dermal wound repair is presented. The findings presented in chapters 3 and 4 have been published and the papers are presented in Appendix 1.

# CHAPTER 2: MATERIALS AND METHODS

## 2.1 Clinical samples

### 2.1.1 Patient samples

Clinical details of patients are provided in tables 3.1 and 4.1. Dermal punch biopsies were taken from primary and autoimmune Raynaud's patients, fibrotic and atrophic dcSSc patients. Fibrotic dcSSc patients were biopsied within 18 months of disease onset which was defined as the first non-Raynaud's symptom. In the case of fibrotic patients, paired biopsies were taken. Lesional skin was taken from areas of progressive fibrosis while non-lesional skin, which was clinically defined as having a modified rodnan skin score of zero, was taken from the lower back region. Patients with atrophic disease had at least a three year history of disease. All patients in the study met the American College of Rheumatology's classification for SSc (1) and were diagnosed as having dcSSc using the classification established by LeRoy (270). Primary Raynaud's patients were diagnosed on the basis of the biphasic/triphasic digital colour changes characteristic of Raynaud's phenomenon (271). Autoimmune Raynaud's patients were identified as having Raynaud's phenomenon plus a positive titre of circulating antinuclear autoantibodies detected by indirect immunofluorescence on Hep2 cells (303) and abnormal nailfold capillaries determined by nailfold capillary microscopy. They do not have any other features of a connective tissue disease. Site-matched normal skin samples were obtained from sex and age matched volunteers.

The biopsies were embedded in OCT and immediately snap frozen in isopentane cooled by liquid nitrogen and subsequently stored at -70$^{o}$C prior to cryosectioning. Disease severity and internal organ involvement was assessed according to the recently published consensus for SSc studies (38). Skin involvement was assessed using the modified Rodnan skin score, gastrointestinal involvement was defined symptomatically. A restrictive pattern of pulmonary function abnormalities with reduction in forced vital capacity (FVC) and carbon monoxide diffusion capacity (DLCO) below 80% of predicted value (based on age, sex, height and ethnic origin) was used to assess interstitial lung involvement. This was confirmed by high resolution computed tomography of the chest. Pulmonary arterial hypertension was assessed by right heart catheterisation diagnosed if pulmonary arterial pressure (PAP) was >25mmHg at rest and 30mmHg after exertion with pulmonary capillary wedge pressure <15mmHg. Cardiac involvement was considered present if any significant conduction defects were found

on electrocardiogram or impaired left or right ventricular (systolic and diastolic) function or haemodynamically significant pericardial effusion were detected by echocardiography. A greater than four-fold elevation of creatinine kinase accompanied by the clinical finding of proximal weakness defined muscular involvement, whilst renal involvement was determined by history of scleroderma renal crisis or significant impairment in creatinine clearance (<65ml/minute) without alternative explanation.

### 2.1.2 Nailfold capillaroscopy

Nailfold capillaroscopy was performed using a Nikon optical system illuminated by a fibre optic light source. Images were analysed and recorded with a Hitachi CCD digital camera. Microvascular damage was analysed and quantified using the criteria recently established by Cutolo *et al* (92), which involves the grading of dcSSc patients as having an early (E), active (A) or late (L) pattern of capillary damage.

## 2.2 Cell culture

### 2.2.1 Explant culture of fibroblasts in a monolayer

Tissue samples from placenta and skin were cut into 1-2mm$^3$ pieces and placed in sterile 10cm dishes or tissue culture flasks (25cm$^2$) (Invitrogen, UK). After 15 minutes drying at room temperature, the adherent tissue samples were bathed with growth medium (GM) consisting of Dulbecco's modified Eagle's medium (DMEM) containing 10% foetal calf serum (FCS), 2mM L-glutamine, 1mM sodium pyruvate, 100 units per ml penicillin and 100mg per ml streptomycin (Invitrogen, UK). After 2 weeks of incubation in a humidified atmosphere of 5% $CO_2$ in air, fibroblast outgrowths were detached by brief trypsin treatment and sub-cultured. For serum starvation and to study the effects of growth factors in serum-free medium, cells were incubated in medium containing sodium pyruvate, glutamine and serum replacement factor (SRF) (Sigma, UK). All fibroblasts were used between passages 2 to 8.

### 2.2.2 Culture of pericytes in a monolayer

Human full term placenta, which is a highly vascularised organ, was used as a source of microvascular pericytes in accordance with the protocol established by Ivarsson *et al.* (214). In order to obtain highly purified microvessels, perivascular connective tissue was removed. Approximately 20grams of placental tissue was incubated with a mixture of collagenase (1mg/ml in serum-free DMEM) with strong agitation in a Wheaton flask (Invitrogen, UK) at

37°C. Resulting tissue fragments were passed through a 125μm nylon mesh to further select for microvessels. The filtrate was then centrifuged in a 10% Percoll solution (Amersham Biosciences, UK) for 10 minutes at 200g. The pellet was resuspended in 4mls of supernatant and incubated with 25mls/20grams tissue of 0.25% pronase with strong agitation in a Wheaton flask for 15 minutes at 37°C. Single cells and tissue debris were then removed using a Percoll discontinuous gradient (60%, 10% and 0%). After centrifugation for 30 minutes at x1400g, single cells including red blood cells were pelleted. Residual tissue debris and dead cells were retained at the top of the pellet while small microvascular fragments were recovered from the middle portion of the gradient. These fragments were resuspended in sterile phosphate buffered saline (PBS) and pelleted by centrifugation. After centrifugation, pellets were washed 3 times in serum-free DMEM, resuspended in 50mls of ice cold serum-free DMEM and allowed to stand for 30 minutes at 4°C. After 30 minutes, the heavier microvascular fragments settled to the bottom of the tube while single cells remained in suspension in the supernatant. The supernatant was gently discarded and the procedure was repeated two further times. After the final wash, microvascular fragments were resuspended in 20mls of DMEM containing 10%FCS.

For primary culture of microvascular fragments flasks were coated with a mixture of fibronectin and collagen. Collagen (Vitrogen 100, Invitrogen, UK) was used at 3.2mgs/ml and fibronectin (Sigma, UK) was used at 1mg/ml. After 5 to 7 days of culture, cell that migrated from the microvascular fragments were lifted from the surface with ice cold 0.05M ethylene-diamine-tetra-acetic acid (EDTA) in PBS, leaving the larger microvascular fragments attached to the growth surface. The cell suspension was centrifuged and resuspended in growth medium and plated onto tissue culture plastic favouring the growth of pericytes over endothelial cells (214).

### 2.2.3 Characterisation of pericytes

Microvascular pericytes were characterised by their expression of α-SMA and 3G5 in accordance with previous studies (214;316;416). Immunofluorescence staining was carried out as described in section 2.3.9.

### 2.2.4 Culture of cells in free-floating collagen lattices

In order to allow uniform contraction of collagen gels, 24-well tissue culture plates were pre-coated with sterile 2% (w/v) bovine serum albumin (BSA) in PBS (2ml/well) and incubated at 37°C overnight. The plates were then washed 3 times with sterile PBS. A collagen gel solution was then made, consisting of 1 part 0.2 M N-2-hydroxyethylpiperazine-N'-2ethanesulphonic acid (HEPES), pH 8.0, 4 parts collagen (Vitrogen-100, 3mgs/ml) and 5 parts DMEM. A cell/collagen suspension was made, yielding a final concentration of 80,000 cells per ml and 1.2mg/ml collagen. 1ml of the cell/collagen suspension was added to each well, after which the plates were immediately incubated at 37°C to allow the collagen to polymerise. After 1 hour, 1ml of DMEM was gently added to each well resulting in detachment of the collagen gels from the tissue culture plastic.

### 2.2.5 Force measurement during tethered collagen gel contraction

In cell-populated tethered collagen lattices, the gels are tethered to the underlying plastic tissue culture dish. During the first phase of gel contraction fibroblasts reorganise the collagen fibrils through tractional forces that are parallel to the underlying plastic dish (Figure 2.1). In the second phase, mechanical stress begins to develop and the cells align along the lines of stress. The mechanical stress induces fibroblasts to become proto-myofibroblasts and acquire their characteristic features, including stress fibres, fibronexus adhesion complexes and fibronectin fibres (455). As mechanical tension increases, this leads to the formation of differentiated myofibroblasts (455). The addition of TGF-β accelerates the differentiation of proto-myofibroblasts to differentiated myofibroblasts (455).

Measurements of tension across a three-dimensional, cell-populated collagen lattice were performed as described previously (124). 1 x $10^6$ cells/ml were seeded into a collagen gel (made as described in section 2.2.4), which was then floated in DMEM. The collagen gel was tethered to two flotation bars at either end with one bar attached to an anchor point and the other bar connected to a force transducer. Cell-generated tensional forces in the collagen gel were detected by the force transducer and logged into a computer. Graphical readings were produced every 10 minutes, averaged from 600 readings (1/s), providing a continuous output of the force (Dynes) generated.

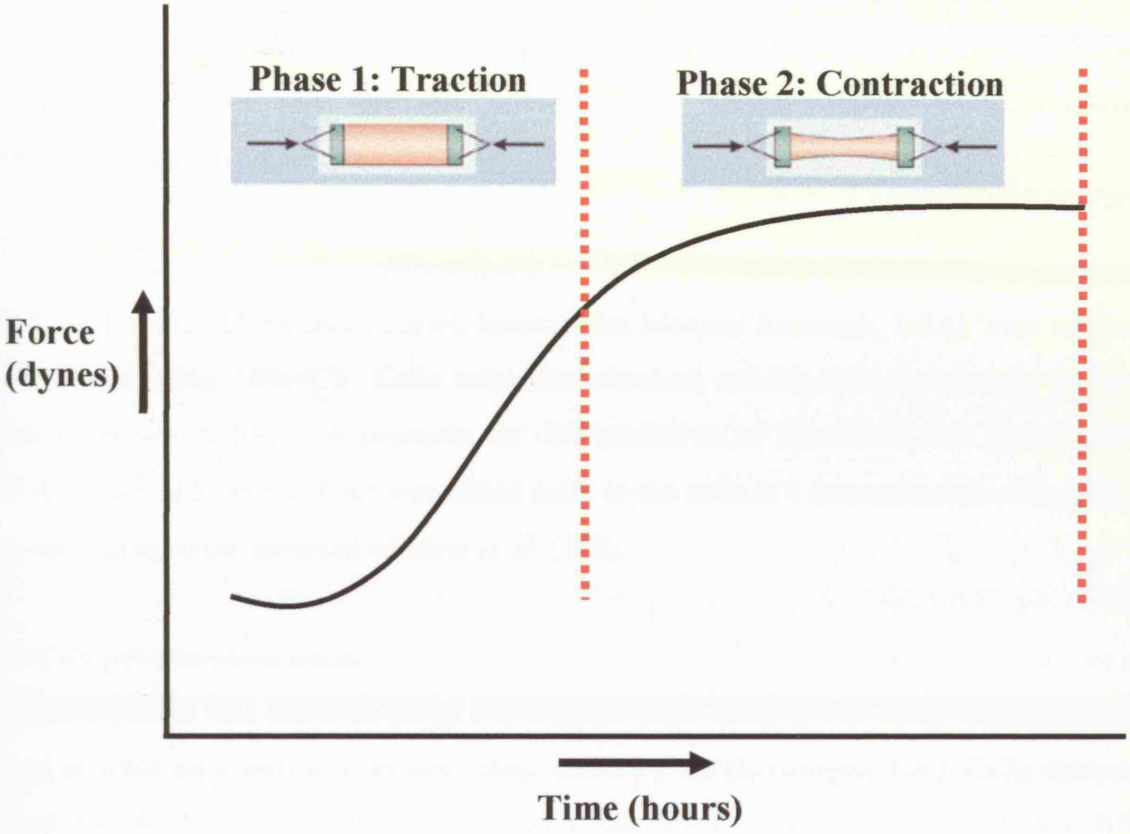


**Figure 2.1.**

**Measurement of force generation in uniaxially tethered collagen lattices.**

The culture force monitor allows force measurement of cell populations in uniaxially tethered collagen lattices. The force–time plot indicates how force increases linearly as fibroblasts exert tractional forces on the collagen matrix.

### 2.2.6 *In vitro* scratch wound assay

*In vitro* wound closure assays were performed by creating clear lines in a confluent cell monolayer with a sterile plastic pipette tip. The migration of the cells into the cleared spaces was monitored over time and photographed. PDGF-BB (R and D Systems, UK) was used at a concentration of 10ng/ml for *in vitro* closure assays. For PDGFRβ inhibition, cells were preincubated with imatinib mesylate (2μm) for 30 minutes before initiation of the assay. Comparison was performed by using Student's t-test with a p-value of $<0.05$ considered as statistically significant.

### 2.2.7 *In vitro* formation of myofibroblasts

AG01518 foreskin fibroblasts (Coriell Institute for Medical Research, USA) were cultured in DMEM containing 10%FCS. Cells were then washed and incubated overnight in DMEM supplemented with SRF. To promote the differentiation of fibroblasts into myofibroblasts, TGF-β (R and D Systems, UK) was added daily to the cells at a concentration of 2ng/ml for 4 days according to the protocol of Hinz *et al.* (199).

### 2.2.8 Cell proliferation assay

Cell proliferation was assessed using a methylene blue assay (331). Cells were counted and seeded at 1000 cells/well in a 96 well tissue culture plate (Invitrogen, UK). Cells were serum starved for 48 hours and then treated with increasing concentrations of PDGF-BB (1-100ng/ml) for 48 hours in order to determine the optimal concentration. For PDGFRβ inhibition, cells were preincubated with imatinib at a concentration of 2μM for 30 minutes prior to addition of PDGF-BB in accordance with the protocol established by Daniels *et al* (94). At the end of the incubation period, cells were washed in PBS and fixed with 4% (w/v) formaldehyde in PBS for 30 minutes at room temperature. Plates were incubated with 100μl of methylene blue solution for 30 minutes at room temperature and then washed in 4 changes of 0.01M sodium borate. 100μl of ethanol:0.1M HCl (1:1) was pipetted into each well and the absorbance was measured at 650nm on a Mithras LB 940 plate reader (Berthold Technologies, UK). Comparison was performed by using Student's t-test with a p-value of $<0.05$ considered as statistically significant.

### 2.2.9 Assessment of apoptosis *in vitro*

The effect of imatinib on apoptosis was assessed in cultured fibroblasts and pericytes. Cells were seeded at equal densities in DMEM containing 10% FCS and grown to 70% confluence. To induce apoptosis, cells were treated with the DNA topoisomerase inhibitor, etoposide at a concentration of 100μM for 48 hours as previously described (302). Etoposide was freshly prepared as a 100 fold stock solution in dimethyl sulphoxide. Cells were also treated with imatinib (2μM) for 48 hours. Apoptosis was then assessed by TUNEL staining as described in section 2.3.10.

## 2.3 Histological staining techniques

### 2.3.1 Haematoxylin and eosin

Specimens for haematoxylin and eosin were fixed for at least 24 hours in 10% neutral buffered formalin (38% formaldehyde in PBS) after which they were embedded in paraffin. Paraffin-embedded sections were cut (3μm) on a Leica RM 2135 microtome. Sections were dewaxed by immersion in xylene for 10 minutes and then rehydrated through a series of ethanol solutions from 100%, to 90%, 70% and finally in tap water. Sections were stained in haematoxylin for 1 minute and blued in 0.5M sodium tetraborate for 15 seconds. Sections were stained in eosin for 1 minute, washed in water and dehydrated through the ethanol solutions, cleared in xylene and mounted using DPX mounting medium. The magnification of figures has been expressed as the objective magnification.

### 2.3.2 Massons trichrome

Paraffin-embedded sections were dewaxed and taken to water as described above. Sections were stained with celestine blue for 2 minutes, washed in running water and stained with Lillie-Mayer's haematoxylin for 2 minutes and then blued in running tap-water for 5 minutes. Sections were then stained with 0.5% (v/v) Ponceau-acid fuchsin for 3 minutes, washed in water and differentiated in 1% (v/v) phosphomolybdic acid for 15 minutes. Sections were checked microscopically to ensure that interstitial tissue was colourless and muscle was stained red. Sections were washed with distilled water and counterstained with 0.1% (v/v) aqueous light green solution for 1 minute. Sections were then washed in distilled water, dehydrated through ethanol and xylene and mounted with DPX mounting medium.

### 2.3.3 Antibodies

The antibodies used for immunostaining are summarised in table 2.1. Optimal concentrations were determined after serial titration of antibodies.

### 2.3.4 Immunohistochemical staining of cryosections

Serial frozen sections (5μm) were cut on a Bright cryostat at -25°C and air-dried for at least 1 hour. Sections were fixed in ice cold acetone for 10 minutes at 4°C and then washed in PBS. Endogenous peroxidase was then quenched by incubation with 0.3% (v/v) hydrogen peroxide in methanol at room temperature for 15 minutes in the dark. Sections were then washed in PBS and non-specific binding of immunoglobulins was blocked by treatment with 2.5% (v/v) normal serum (Vector Laboratories, UK) for 30 minutes after which sections were incubated with primary antibodies for 1 hour at room temperature or overnight at 4°C. After washing in PBS, sections were incubated with a species-specific biotinylated secondary antibody (Vector Laboratories, UK) for 30 minutes, rinsed in PBS and incubated with Vectastain ABC reagent (Vector Laboratories, UK) for 30 minutes. After washing in PBS, sections were visualised using 3-amino-9-ethylcarbazole (AEC) (Vector Laboratories, UK). Sections were then washed in tap water, counterstained with haematoxylin and mounted with aqueous media (Crystalmount, Biomeda, UK). Sections were viewed and photographed on a Zeiss Axioskop 2 mot plus microscope. All incubations were carried out at room temperature. Controls included an exchange of primary antibodies with irrelevant isotype matched antibodies and primary antibodies omission.

**Table 2.1: Antibodies and dilutions used for immunostaining**

| Antibody | Antigen/Cell | Dilution | Origin | Reference |
|---|---|---|---|---|
| PDGFR-B2 | PDGFRβ (Human) | 1/1000 | Donated by K. Rubin, Sweden | (190;364) |
| Anti-PDGFRβ | PDGFRβ (Murine) | 1/200 | Santa Cruz (UK) | (94) |
| 225.28 | HMW-MAA | 1/16 | Donated by S. Ferrone, NY | (515) |
| PDGF007 | PDGF-B chain | 1/100 | Mochida (Japan) | (279;408) |
| PAL-E | Endothelium | 1/100 | Monosan, Holland | (388) |
| EBM11 | CD68 | 1/50 | Dakocytomation, UK | (306) |
| 1A4 | α-SMA | 1/400 | Sigma, UK | (96;416) |
| AS02 | Thy-1 | 1/400 | Oncogene, UK | (370) |
| 3E2 | ED-A FN | 1/400 | Sigma, UK | (340) |
| Anti-LOX | Lysyl Oxidase | 1/100 | Donated by K. Csiszar, USA | (187) |
| Anti-PCNA | PCNA | 1/100 | Abcam, UK | (240) |
| BU 1/75 | BRDU | 1/250 | Abcam, UK | (464) |
| MEC13.3 | CD31 | 1/200 | BD Pharmingen | (470) |
| Anti-NG2 | NG2 | 1/100 | Chemicon | (333) |
| Anti-Collagen | Collagen type I | 1/200 | Chemicon | (281) |
| Phalloidin | F-Actin | 1/50 | Molecular probes | (200) |
| 3G5 | O-acetylated disialoganglioside | Neat | Donated by Dr. Anne Canfield, UK | (315) |

### 2.3.5 Immunohistochemical staining of paraffin sections

Paraffin-embedded sections were dewaxed and taken to water as described in section 2.3.1. Where appropriate, antigen retrieval was performed by microwaving sections in pre-heated 0.01M citric acid, pH 6.0 for 10 minutes, allowed to cool and washed in PBS. Endogenous peroxidase was quenched by incubation with 3% (v/v) hydrogen peroxide in PBS at room temperature for 15 minutes in the dark. Immunostaining was carried out as described in section 2.3.4. Sections were washed in PBS, dehydrated through ethanol and xylene and mounted with DPX mounting medium.

### 2.3.6 Single immunofluorescence staining of cryosections

Serial frozen sections (5μm) were cut on a Bright cryostat at -25°C and air-dried for 1 hour. Sections were fixed in ice cold acetone after which non-specific binding of immunoglobulins was blocked by treatment with 2.5% (v/v) normal serum for 30 minutes. Sections were incubated with primary antibodies for 1 hour at room temperature. For the three-layer procedure, sections were incubated with the appropriate biotinylated secondary antibody for 30 minutes and then avidin conjugated to either Alexa Fluor$^{488}$ (Molecular Probes, UK) or Texas Red (Vector Laboratories, UK) for 30 minutes. For the two-layer procedure, sections were incubated with Texas Red/Alexa Fluor$^{488}$ species specific secondary antibodies for 30 minutes at room temperature. Sections were counterstained with 4,6-diamidino-2-phenylindole (DAPI) (Molecular Probes, UK) to visualise cell nuclei. The sections were then mounted using Gel-Mount anti-fade medium (Biomeda, UK).

### 2.3.7 Double immunofluorescence staining of cryosections

To investigate colocalisation between cell specific antigens, double immunofluorescence labelling was carried out as previously described (354;438-440). Briefly, cryosections were blocked with 2.5% (v/v) normal species-specific serum for 30 minutes and incubated with the first primary antibody for 1 hour, rinsed in PBS and incubated with the appropriate biotinylated secondary antibody for 30 minutes. Sections were rinsed in PBS and incubated with avidin-Texas Red for 30 minutes. After blocking with 2.5% (v/v) normal goat serum for 30 minutes, the sections were then incubated with the second primary antibody for 1 hour, rinsed and incubated an Alexa Fluor$^{488}$-conjugated species specific for 30 minutes. Sections were finally counterstained with DAPI and mounted using Gel-Mount anti-fade medium as described above. All incubations were carried out at room temperature. Controls included

single labelling experiments, primary and secondary antibody omission and exchange of primary antibody with irrelevant isotype-matched control. All sections were viewed on an Axioskop Mot Plus microscope with an Axiocam digital camera in combination with Axiovision software and KS300 (Carl Zeiss, UK).

### 2.3.8 TUNEL staining of tissue sections

Paraffin-embedded sections were dewaxed and taken to water as described in section 2.3.1. Sections were then treated with freshly prepared Proteinase K (20μg/ml) (Sigma, UK) for 15 minutes at room temperature. After 3 x 5 minute washes in PBS, the sections were incubated with a mixture of terminal deoxynucleotidyl transferase (TdT) and digoxigenin-labelled nucleotide triphosphates (Chemicon, UK) for 1 hour at 37°C according to the manufacturer's instructions. The sections were then washed in PBS and incubated with a Texas-Red conjugated anti-digoxigenin antibody for 30 minutes at room temperature. The sections were washed in PBS and counterstained with DAPI and mounted as above.

### 2.3.9 Immunofluorescence staining of cells in a monolayer

Cells were sub-cultured onto 8-chamber well slides (Invitrogen, UK) and grown to 70% confluence. Cells were initially fixed and permeabilised with a solution containing 4% (w/v) formaldehyde, 0.1% (v/v) Triton in PBS for 5 minutes at room temperature. Cells were washed 3 times in PBS and refixed in 4% (w/v) formaldehyde in PBS for 10 minutes at room temperature. After 3 washes in PBS, non-specific binding was blocked with 1% (w/v) BSA. Cells were incubated with the primary antibody for 1 hour at room temperature. For the three-layer procedure, sections were incubated with the appropriate biotinylated secondary antibody for 30 minutes and then avidin-conjugated to either fluorescein isothiocyanate (FITC) or Texas Red for 30 minutes (Vector Laboratories, UK). For the two-layer procedure, sections were incubated with Texas Red/Alexa Fluor$^{488}$-conjugated species specific secondary antibodies (Molecular Probes, UK) for 30 minutes at room temperature. Cells were counterstained with DAPI and mounted as previously described. All incubations were carried out at room temperature. Controls included an exchange of primary antibodies with irrelevant isotype matched antibodies and omission of primary antibodies. For double immunofluorescence labelling, cells were permeablised and fixed in the same way and immunofluorescence labelling was carried out as described in section 2.3.7.

### 2.3.10 TUNEL staining of cells in a monolayer

Cells were sub-cultured onto 8-chamber well slides (Invitrogen, UK), grown to 70% confluence and fixed in 1% (w/v) formaldehyde in PBS for 10 minutes at room temperature after which they were permeabilised in a mixture of ethanol:acetic acid (2:1) for 5 minutes at -20°C. The slides were then washed in PBS and incubated with TdT and digoxigenin-labelled nucleotide triphosphates (Chemicon, UK) for 1 hour at 37°C. Following another wash in PBS, the slides were incubated with a Texas-Red conjugated anti-digoxigenin antibody for 30 minutes at room temperature, washed again and counterstained with DAPI.

## 2.4 Quantification and image analysis

### 2.4.1 Determination of PDGFRβ, HMW-MAA and PCNA positive microvessels

In order to determine the proportion of microvessels expressing PDGFRβ, HMW-MAA and PCNA, mirror image cryostat sections were used. Briefly, cryostat sections were treated as previously described except that serial sections were cut with subsequent sections being juxtaposed so as only to be separated by a blade width. Serial sections were then stained with the following combinations;1. PAL-E/PDGFR, 2. PAL-E/HMW-MAA, 3. PAL-E/PCNA. Stained sections were analysed using the x40 objective lens on a Zeiss Axioskop 2 mot plus microscope. From each clinical subset, 40 to 48 fields of vision were analysed to determine the percentage of PAL-E positive microvessels expressing PDGFRβ, HMW-MAA and PCNA, respectively. The Mann-Whitney test was used to determine significance with p-values $<0.05$ representing significant differences. All comparisons were made using control skin.

### 2.4.2 Quantification of immunohistochemistry

Stained slides were analysed using a Zeiss Axioskop microscope. All images were viewed with a x40 objective lens (Carl Zeiss, UK) and captured using a medium resolution Axiocam digital colour camera and KS300 software (Carl Zeiss, UK). For each image, contrast levels were optimised to allow for correct colour segmentation. For each field of view, both the total number of cells present and the number of immunopositive cells was quantified by computer-aided analysis. False positive and negative results were corrected manually. The number of immunopositive cells was then expressed as a percentage of the total number of cells per field of view.

### 2.4.3 Quantification of immunofluorescence

Stained slides were analysed using a Zeiss Axiovert 35 microscope. Images were collected with a DAGE CCD 72 camera with a DAGE GenIIsys light amplifier and analysed with the IC 300 system (Inovision, UK). For combinations of monoclonal antibodies 7 fields were assessed from each patient. Images were digitised in 512 x 512 pixels of 8 bits (256 grey levels) and stored for further analysis. Reduction in resolution due to the GenIIsys light amplifier gives a net resolution of 350 x 350 pixels, which corresponds to a pixel size of 0.9μm x 0.9μm. Areas displaying obvious autofluorescence and structures not fully displayed at the periphery of the image were excluded from further analysis as were areas located outside areas of interest. A threshold level slightly higher than the grey value of the negative controls was introduced and all pixels with grey values below this threshold were excluded from analysis. The Texas Red image was aligned with the FITC image using the IC 300 system and digitised images were subjected to numerical analysis using previously described procedures (440). All pixels having FITC or Texas Red fluorescence exceeding background were assigned the value 1 and pixels having no fluorescence above background were assigned the value 0. The percentage of FITC-positive pixels that were also positive for Texas Red and *vice versa* were calculated. This percentage is a measurement of the degree of colocalisation between two different antigens recognised by the respective monoclonal antibodies on the same tissue section. The number of positive pixels does not depict the number of cells expressing a certain antigen nor do they depict the absolute quantity of an antigen. A background colocalisation varying between 20-30% between markers for cells not expected to colocalise was recorded in agreement with earlier studies using this technology (439;440). This background colocalisation is due to limitations in camera resolution, out of focus fluorescence and to close proximity of the investigated cell types in relation to each other.

### 2.4.4 Confocal Microscopy

Samples were examined with the Multiprobe confocal laser scanning microscope with a Nikon inverted microscope (Optics: Nikon fluor 40x/1.3 oil) and an argon/krypton laser. Texas Red and FITC images were registered separately in sections stained by double immunofluorescence digitised in 512 x 512 pixels and stored for further analysis. The 3D reconstructions were created using the volume workbench and the ray modelling program.

The 3D reconstructions were rotated 70° in order to depict the Z-axis in 3D. As confocal microscopy excludes out of focus fluorescence, background colocalisation was minimised.

## 2.5 Protein biochemistry techniques

### 2.5.1 Preparation of protein extracts

For all cell-associated proteins, cell monolayers were washed twice in ice cold PBS and lysed in the appropriate volume of cell lysis buffer (10mM Tris pH 7.2, 0.1% (w/v) SDS, 1% (v/v) Triton X-100, 1% (w/v) deoxycholate and 5mM ethylene-diamine-tetra-acetic acid (EDTA)) containing the protease inhibitors phenylmethylsulphonylfluoride (PMSF) (1mM) and 2μg/ml leupeptin) (Sigma, UK). Each cell lysate was collected with a cell scraper and DNA sheared by passing the sample repeatedly through a 23-gauge needle. The samples were centrifuged x 1,200g for 5 minutes and the supernatants stored at -80°C.

### 2.5.2 Cytosolic and cytoskeletal fractionation

Adherent cells were overlaid with ice-cold low-salt buffer (60 mM Pipes, 25 mM Hepes, 10 mM ethylene-glycol bis(2-aminoethyl ether)-N,N,N'N'-tetra-acetic acid (EGTA), 2 mM $MgCl_2$, 0.5% (v/v) Triton X-100 and 1 mM sodium orthovanadate, pH 6.9), supplemented with the cocktail of protease inhibitors Complete-EDTA (Boehringer Mannheim, UK) and extracted for 5 minutes. The supernatant was recovered as the cytosolic TritonX-100-soluble fraction. This operation was repeated twice and both fractions were pooled. The material remaining tightly bound to the surface corresponded to the cytoskeletal TritonX-100-insoluble fraction and was scraped and dissolved in 4x Laemmli buffer (0.2M Tris-HCl, pH 6.8, 8% (w/v) SDS, 40% (v/v) glycerol and 0.004% (w/v) bromophenol blue).

### 2.5.3 Measurement of protein concentration

The total protein content of cell lysates was determined using a bicinchoninic acid (BCA) protein assay (Pierce, UK). Standard concentrations of BSA diluted in lysis buffer were used to calibrate the assay and to confirm reliability in the concentration range being measured. The assay was performed according to the manufacturer's instructions (Pierce, UK). Briefly, protein standard was prepared by serial dilutions ranging from 1 to 25μg/ml BSA. 200 μl of standards and diluted samples were added to replicate wells of a

96 well flat bottomed plate. Then, 50µl of dye reagent concentrate was added to each well. After mixing, the test plate was incubated for 30 minutes at room temperature. Absorbance was measured at 595nm on a Mithras LB 940 plate reader (Berthold Technologies, UK). The absorbance for standards was plotted against protein concentration to give a standard curve and linear regression analysis was used to determine the protein concentration of the test samples.

### 2.5.4 Sodium dodecyl sulphate polyacrylamide gel electrophoresis

Sodium dodecyl sulphate polyacrylamide gel electrophoresis (SDS-PAGE) was performed using the discontinuous buffer system. Mini gels (10 x8cms) with 10 or 12 wells and 1mm thick were used. Resolving and stacking gels were composed of 10% and 5% acrylamide respectively with 0.1% (w/v) SDS and an acrylamide:bisacrylamide ratio of 37.5:1 (Flowgen, UK). Gels were polymerised with 0.1% (w/v) ammonium persulphate and 0.1% (v/v) N,N,N',N'-tetramethyl-ethylenediamine (TEMED). Cell lysates were diluted in an appropriate volume of 4x Laemmli sample buffer (0.2M Tris-HCl, pH 6.8, 8% (w/v) SDS, 10% (v/v) glycerol, 0.004% (w/v) bromophenol blue) and 5% (v/v) β-mercaptoethanol. For molecular weight calibration, a 5-240Kd molecular weight marker was used (New England Biolabs, UK). The samples were then denatured at 90°C for 5 minutes. Gels were run for approximately 2 hours at 120 Volts in SDS-PAGE running buffer (25mM Tris-Cl pH8.3, 192mM glycine, 0.1% (w/v) SDS). Coomassie blue staining was used to visualise proteins. Gels were fixed and stained for 30 minutes in fixation buffer (30% (v/v) methanol, 10% (v/v) acetic acid) containing 0.25% (w/v) Coomassie brilliant blue R250. Gels were de-stained by extensive washing in fixation buffer and then dried onto 3M chromatography paper (Whatman) on a gel dryer for 1 hour at 80°C under vacuum.

### 2.5.5 Western blotting

Western blotting was performed using standard techniques. Proteins separated by SDS-PAGE were transferred onto Hybond-C membrane (Amersham Biosciences, UK) for 90 minutes at 30 Volts in transfer buffer (25mM Tris, 192mM glycine, 20% (v/v) methanol). Following transfer, membranes were stained for 1 minute with wash buffer (PBS/0.1% (v/v) Tween (PBST)) containing 0.1% (w/v) Ponceau S solution and 5% (v/v) acetic acid to confirm transfer of proteins and then washed in PBST. All antibodies were diluted in PBST containing 5% (w/v) non-fat milk powder. Primary antibodies were added at the

appropriate concentration (Table 2.2) for 2 hours at room temperature followed by 3 washes for 15 minutes with PBST. Horseradish-peroxidase (HRP) conjugated secondary antibodies (Pierce, UK) were diluted 1:5000 and incubated with membranes for 1 hour at room temperature, followed by 3x15 minute washes in PBST. HRP-conjugated antibodies were visualised using enhanced chemiluminescence (ECL) reagent (Amersham Biosciences, UK) on exposure to ECL Hyperfilm (Amersham Biosciences, UK).

### 2.5.6 Densitometry

Western blots were quantified by densitometry. X-ray films of Western blots were digitised using a UVP v1.0 digital camera and UVP Grab software (Synoptics, UK). Protein signal intensities were measured using Gelplate software (Synoptics, UK) and normalised against GAPDH levels.

**Table 2.2: Antibodies and dilutions used for Western blotting**

| Antibody | Antigen/Cell | Dilution | Origin | Reference |
|---|---|---|---|---|
| Anti α–SMA | α-smooth muscle actin | 1/5000 | Sigma, UK | (72) |
| Anti-vinculin | Vinculin | 1/1000 | Sigma, UK | (170) |
| 3E2 | ED-A Fibronectin | 1/1000 | Sigma, UK | (340) |
| Thy-1 | AS02 | 1/1000 | Oncogene, UK | (370) |
| Anti-GAPDH | Glyseraldehyde-3-phosphate dehydrogenase | 1/10000 | Abcam, UK | (72) |

## 2.6 Animal studies

A transgenic mouse was used that harbours a construct of the mouse collagen 1α2 promoter containing 17 kb 5′ of transcription start site, including the far upstream enhancer region fused to the minimal promoter and luciferase and β-galactosidase (LacZ) reporter genes (42). Previous studies have established that this transgene is activated during wound healing and that its expression and distribution recapitulates that of the endogenous gene (243;347).

### 2.6.1 Preparation of imatinib mesylate

For PDGFRβ blockade, imatinib was prepared as previously described (94). Briefly, imatinib was obtained from the Royal Free Hospital pharmacy in 100mgs capsules and solubilised in deionised $H_2O$. The particulate matter was removed by centrifugation at 2,500*g* and the supernatant recovered. Imatinib was administered intraperitoneally (i.p.) at 75mgs/kg per day as previously described (94;476). For *in vitro* experiments, imatinib was used at a concentration of 2μM as previously described (53;302).

### 2.6.2 Wound healing experiments

All animal protocols were approved by the local animal ethics committee at the Royal Free and University College Medical School. Female mice aged between 6 to 8 weeks were anesthetised with Avertin (500mgs/kg). A stock solution of Avertin (1 gram tribromoethanol in 1ml 2-methylbutan-2-ol) was made immediately prior to use. The dorsum was shaved and cleaned with alcohol. Four equidistant $4mm^3$ full-thickness excisional wounds were made on either side of the midline of the mouse. For PDGFRβ inhibition, mice were injected intraperitoneally (i.p.) just after wounding. Mice were sacrificed after 3, 7, 10 and 14 days. Immediately after sacrifice the wound diameter was measured and wounds were photographed before samples were collected for histology, immunohistochemistry and protein extraction.

### 2.6.3 Assessment of *in vivo* proliferation using bromodeoxyuridine labelling

Mice were injected i.p. with 2 ml bromodeoxyuridine (BRDU) labelling reagent per 100 grams mouse weight (Amersham Biosciences, UK) 2 hours prior to sacrifice. Upon sacrifice, wound samples were collected and fixed, paraffin-embedded and sectioned as previously described (see section 2.3.5). After dewaxing the sections were microwaved in 0.01 M citric acid, pH 6.0 for 10 minutes and then denatured in 4N HCl for 30 minutes at 37°C. Sections were stained with an anti-BRDU antibody as described in section 2.3.5.

### 2.6.4 β-galactosidase expression and distribution

Levels of the β-galactosidase transgene expression were assayed using a β-galactosidase chemiluminescent reporter gene assay system according to the manufacturer's instructions (Applied Biosystems, UK). Wound tissue was weighed and homogenised in lysis buffer. An aliquot was removed and measured for protein content using the BCA protein assay as described in section 2.5.3.To assess the spatial distribution of the β-galactosidase transgene, wound tissue sections were stained histochemically. One sample of wound tissue from each animal was fixed with 0.2% (w/v) glutaraldehyde, 0.8% (w/v) formaldehyde in 0.1M sodium phosphate buffer pH 7.3 containing 2 mM $MgCl_2$ and EGTA for 45 minutes. Samples were then washed three times for 30 minutes each in the phosphate buffer with 0.1% (w/v) sodium deoxycholate and 0.2% (v/v) Nonidet P-40 and stained overnight at room temperature in the dark with 1 mg/ml 5-bromo-4-chloro-3-indolyo-B-D-galactoside solution (X-gal) containing 5 mM potassium ferrocyanide and 5 mM potassium ferricyanide. For histological analysis, wound samples were then embedded in paraffin and 4μm sections were cut and counterstained with eosin.

## 2.7 Statistical analysis

### 2.7.1 Analysis of PDGFRβ expression in dcSSc skin

To test the overall hypothesis that activated pericytes expressing PDGFRβ are involved in the pathophysiology of dcSSc, the expression and colocalisation of PDGF AB/BB ligand and β receptors was examined within the microvasculature. The results of the colocalisation studies were compared and the Student's t-test was used to evaluate significance between values of colocalisation and p-values $<0.05$ considered significant. The following comparisons were made to answer the following questions.

**1) Do PDGFRβ colocalise with activated pericytes to a significantly higher degree than background colocalisation?** Comparison 1: PDGFRβ/HMW colocalisation against HMW/PAL-E colocalisation.

**2) Do PDGFRβ colocalise with activated pericytes to a significantly higher degree than with endothelial cells?** Comparison 2: PDGFRβ/HMW colocalisation against PDGFRβ/PAL-E colocalisation.

**3) Do PDGFRβ colocalise with endothelial cells to a significantly higher degree than background colocalisation?** Comparison 3: PDGFRβ/PAL-E colocalisation against HMW/PAL-E colocalisation.

In order to delineate the pattern of PDGF AB/BB ligand expression, similar comparisons were made with the colocalisation data derived from using the anti-PDGF AB/BB antibody.

**1) Does PDGF AB/BB colocalise with activated pericytes to a significantly higher degree than background colocalisation?** Comparison 1: PDGF AB/BB/HMW colocalisation against HMW/PAL-E.

**2) Does PDGF AB/BB colocalise with activated pericytes to a significantly higher degree than with endothelial cells?** Comparison 2: PDGF AB/BB/HMW colocalisation against PDGF AB/BB/PAL-E.

**3) Does PDGF AB/BB colocalise with endothelial cells to a significantly higher degree than background colocalisation?** Comparison 3: PDGF AB/BB/PAL-E colocalisation against HMW/PAL-E.

### 2.7.2 Correlation between myofibroblasts and clinical parameters in dcSSc

To correlate the presence of myofibroblasts with clinical features, immunohistochemical findings were assessed and grouped according to the following criteria:

**1. Evidence of myofibroblasts/ED-A FN only; 2. Evidence of collagen synthesis only**

**3. Evidence of myofibroblasts/ED-A FN and collagen synthesis; 4. No evidence of either myofibroblasts/ED-A FN or collagen synthesis.**

Patients from each of these groups were then assessed for disease duration, skin score and capillary damage (see Table 4.3). An ANOVA analysis was used to detect any association between defined immunohistochemical groups and clinical findings.

### 2.7.3 Patient samples and statistical limitations

Due to the difficulties in obtaining skin biopsy samples for purely research purposes and the generally low prevalence of the SSc in the general population, the overall numbers of patient samples while reasonable for the nature of the study and in keeping with previous analyses are not sufficient for powerful statistical analysis. For example, the frequency of PDGFRβ expression and pericyte activation (see section 3.3.3) was analysed in 29 different biopsies. The number of positive vessels in representative sections counted and p-values obtained using the Mann-Whitney test showed a significant increase in PDGFRβ and HMW-MAA expression in ARP and dcSSc. Therefore, while these findings are in agreement with analyses of PDGFRβ expression in colon cancer and wound healing (440), the differences shown between patient groups require careful follow up investigation with larger cohorts of patients.

# CHAPTER 3: EXPRESSION OF PDGFRβ BY ACTIVATED PERICYTES IN SYSTEMIC SCLEROSIS

## 3.1 INTRODUCTION

There is a considerable body of evidence to suggest that microvascular abnormalities are an aetiological factor in the pathogenesis of SSc, however, the cellular and molecular mechanisms linking microvascular damage and fibrosis remain unknown. While a number of studies have documented endothelial cell abnormalities in SSc biopsy tissue (described in 1.6.2), by comparison almost nothing is known regarding the role of pericytes in SSc. This is surprising, given that it is now accepted that microvascular physiology is primarily governed by the relationship between endothelial cells and the surrounding pericyte and that alterations in endothelial phenotype and function affect pericyte phenotype and function and *vice versa* (146). Pericyte activation, identified by the dual expression of PDGFRβ and the high molecular weight melanoma associated antigen (HMW-MAA) is a key step in the process of tissue repair, remodelling and scarring and is believed to precede a phenotypic transition of pericyte to fibroblast (439;440). The expression of PDGFRβ by pericytes is in fact a key feature of several human diseases characterised by replacement fibrosis, including liver cirrhosis (40) and kidney fibrosis (145;355). Therefore, a substantial body of evidence exists that pericyte expression of PDGFRβ is a key pathogenic characteristic of fibrotic tissue. Although PDGFRβ and PDGF-B chain expression have been reported in dcSSc, the cellular origin and the precise role of the PDGF-B/PDGFRβ axis in SSc pathophysiology remain unknown (160;246). The objective of the current study was to determine whether pericytes become activated and express PDGFRβ in SSc tissue.

## 3.2 EXPERIMENTAL DESIGN

To determine whether pericytes are activated in SSc tissue, an immunohistochemical study was carried out to analyse the distribution of activated pericytes and PDGFRβ in frozen tissue sections derived from different SSc clinical disease subsets. Patient details are provided in Table 3.1. Initial studies focused upon the distribution of PDGFRβ, HMW-MAA and PDGF-B chain across the disease spectrum. Subsequent analyses using double immunofluorescence labelling coupled with confocal microscopy and computer aided image analysis were carried out to determine whether the expression of PDGFRβ and PDGF-B chain localised to microvascular pericytes in dcSSc and autoimmune Raynaud's tissue. Details of antibody

concentrations are provided in Table 2.1 and staining procedures are described in Section 2.3.4.

## 3.3 RESULTS

### 3.3.1 PDGFRβ and PDGF AB/BB ligand expression in autoimmune Raynaud's and fibrotic dcSSc

In agreement with previous studies, little or no expression of PDGFRβ was detected in normal human skin (Figure 3.1a) (367). Similarly, in PRP skin, PDGFRβ expression was detectable, but at only low levels (Figure 3.1b). In contrast, in ARP skin, PDGFRβ was detected in association with the dermal vasculature, notably at the epidermal/dermal junction (Figure 3.1c). In both lesional and non-lesional dcSSc skin the expression of PDGFRβ was detected in vascular cells of dermal vessels and on isolated fibroblastic cells within the dermis (Figure 3.1d and 3.1e). PDGFRβ expressing cells were clearly detected on the abluminal side of microvessels, suggesting that the expression was not localised to endothelial cells (Figure 3.1e). In atrophic dcSSc skin, little or no expression of PDGFRβ could be detected (Figure 3.1f).

**Table 3.1: Clinical and serological characteristics of dcSSc patients**

| Characteristics | Normal (n=11) | Primary RP (n=7) | Autoimmune RP (n=6) | Fibrotic (n=7) | Atrophic (n=4) |
|---|---|---|---|---|---|
| Mean age (range) | 49 (22-62) | 46 (32-68) | 47 (36-56) | 50 (21-65) | 60 (57-69) |
| Mean disease duration, months (range) | n/a | 40 (21-74) | 28 (12-45) | 8 (4-12) | 93 (63-120) |
| Male/female | 3/8 | 2/5 | 2/4 | 2/5 | 1/3 |
| **Organ involvement** | | | | | |
| Mean skin score (range) | n/a | 0 | 0 | 30 (16-39) | 20 (11-27) |
| Oesophageal | n/a | 0/7 | 0/6 | 5/7 | 3/4 |
| Other gastrointestinal | n/a | 0/7 | 0/6 | 1/7 | 1/4 |
| Lung | n/a | 0/7 | 0/6 | 3/7 | 2/4 |
| Muscle | n/a | 0/7 | 0/6 | 3/7 | 1/4 |
| Renal | n/a | 0/7 | 0/6 | 1/7 | 0/4 |
| Cardiac | n/a | 0/7 | 0/6 | 0/7 | 0/4 |
| Pulmonary hypertension | n/a | 0/7 | 0/6 | 0/7 | 0/4 |
| **Serology** | | | | | |
| Antinuclear | n/a | 0/7 | 6/6 | 7/7 | 4/4 |
| Anti-topoisomerase 1 | n/a | 0/7 | 0/6 | 4/7 | 1/4 |
| Anti-RNA polymerase I/III | n/a | 0/7 | 0/6 | 1/7 | 1/4 |
| Anti-nuclear RNP | n/a | 0/7 | 0/6 | 0/7 | 1/4 |
| *** Microvascular damage** | | | | | |
| Structural capillary damage | n/a | 0/7 | 6/6 | 7/7 | 4/4 |

* Assessed by nailfold capillaroscopy

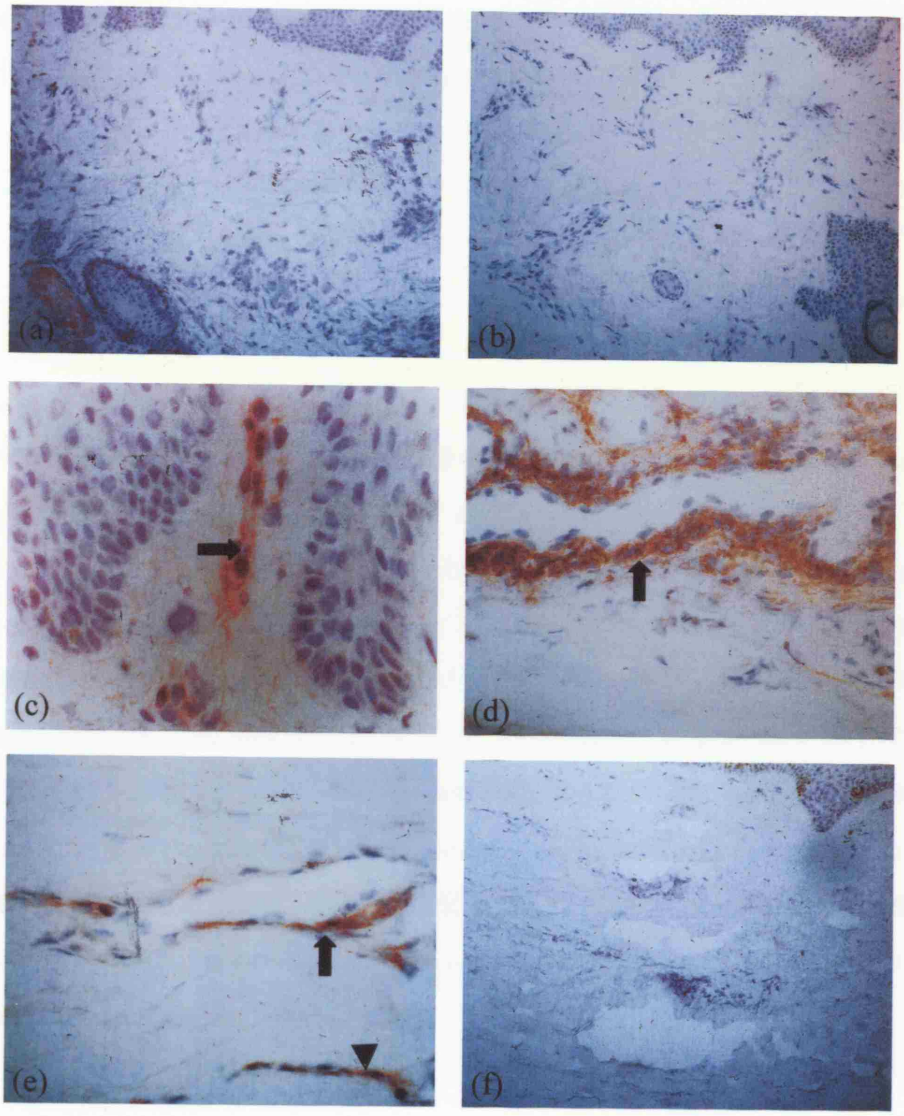


**Figure 3.1.**

**Expression of PDGFRβ in autoimmune Raynaud's and fibrotic dcSSc.**

Little or no expression of PDGFRβ was observed in normal (**a**) and primary Raynaud's skin (**b**). A granular pattern of immunostaining for PDGFRβ was observed around capillaries at the epidermal/dermal junction in autoimmune Raynaud's skin (arrow, **c**) and in interstitial dermal microvessels in fibrotic lesional (arrow, **d**) and non-lesional dcSSc skin (arrow, **e**). Staining in autoimmune Raynaud's and early scleroderma was restricted to the dermal microvasculature and isolated dermal cells (arrowhead, **e**). In atrophic disease, no expression of PDGFRβ was seen (**f**). Original magnification **a,b,f** x10, **d,e** x20 and **c** x40.

The expression of PDGF AB/BB was investigated using the monoclonal antibody PDGF 007. Using this antibody, PDGF AB/BB was readily detected in normal skin (Figure 3.2a) and PRP skin (Figure 3.2b). Staining was primarily found in cells within the epidermis and at the epidermal/dermal junction, but was also present in structures morphologically identified as peripheral nerve fibres. PDGF AB/BB immunostaining was also detected in ARP skin in microvessels (Figure 3.2c) and lesional dcSSc skin, notably in infiltrating mononuclear cells (Figure 3.2d). By staining mirror image sections with antibodies against PDGF-B and CD68, the mononuclear cells expressing PDGF AB/BB were characterised as dermal macrophages (Figure 3.2e and 3.2f).

### 3.3.2 Pericyte activation in autoimmune Raynaud's phenomenon and dcSSc

The monoclonal antibody 225.28 was used to analyse the distribution of HMW-MAA in the microvasculature of skin from ARP and lesional and non-lesional dcSSc. Little or no expression of HMW-MAA was observed in skin from normal adults, PRP patients (Figure 3.3a and 3.3b) or atrophic SSc skin (Figure 3.3e). In ARP and dcSSc skin, HMW-MAA expression was detected predominantly in microvessels throughout the dermis (Figures 3.3c and 3.3d). In order to confirm the presence of pericytes in normal, PRP and atrophic skin, sections were stained with the anti-α-SMA antibody. In normal, PRP and atrophic skin, microvascular expression of α-smooth muscle actin was clearly detected, confirming that pericytes are present around the microvessels. Therefore, while pericytes are present in normal, PRP and atrophic dcSSc skin they appear not to be activated.

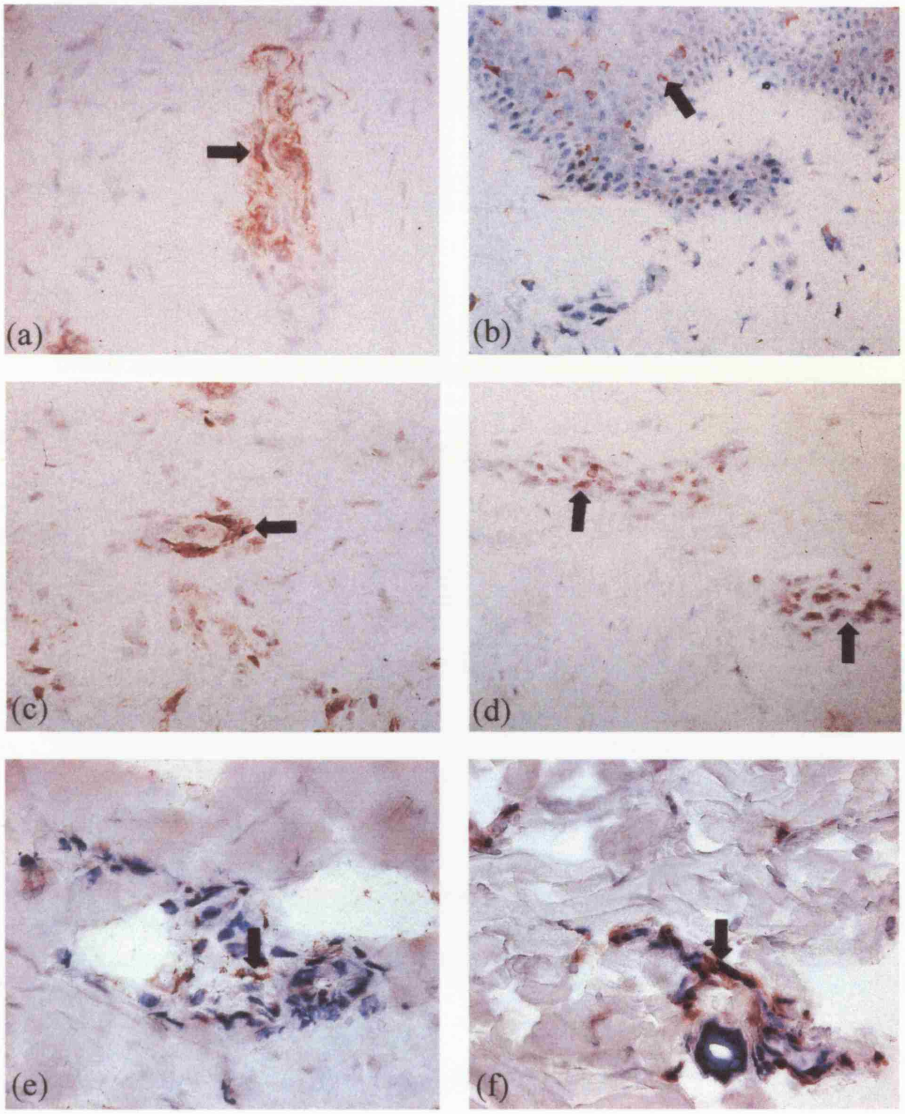


**Figure 3.2.**

**Expression of PDGF AB/BB ligand in normal, RP and dcSSc skin.**

Immunohistochemical staining using the PDGF 007 antibody showed that in normal and PRP skin, peripheral nerve fibres stained positively for the PDGF AB/BB ligand (arrow, **a**). PDGF AB/BB expression was also detected in cells within the epidermal layer (arrow, **b**). PDGF AB/BB was detected in autoimmune RP skin in microvessels (arrow, **c**) and in dcSSc skin, PDGF AB/BB expression was also observed in infiltrating mononuclear cells (arrows, **d**). Serial section analysis demonstrated that PDGF AB/BB expression (arrow, **e**) colocalised with CD68 positive macrophages (arrow, **f**). Original magnification **a-d** x20 and **e,f** x40.

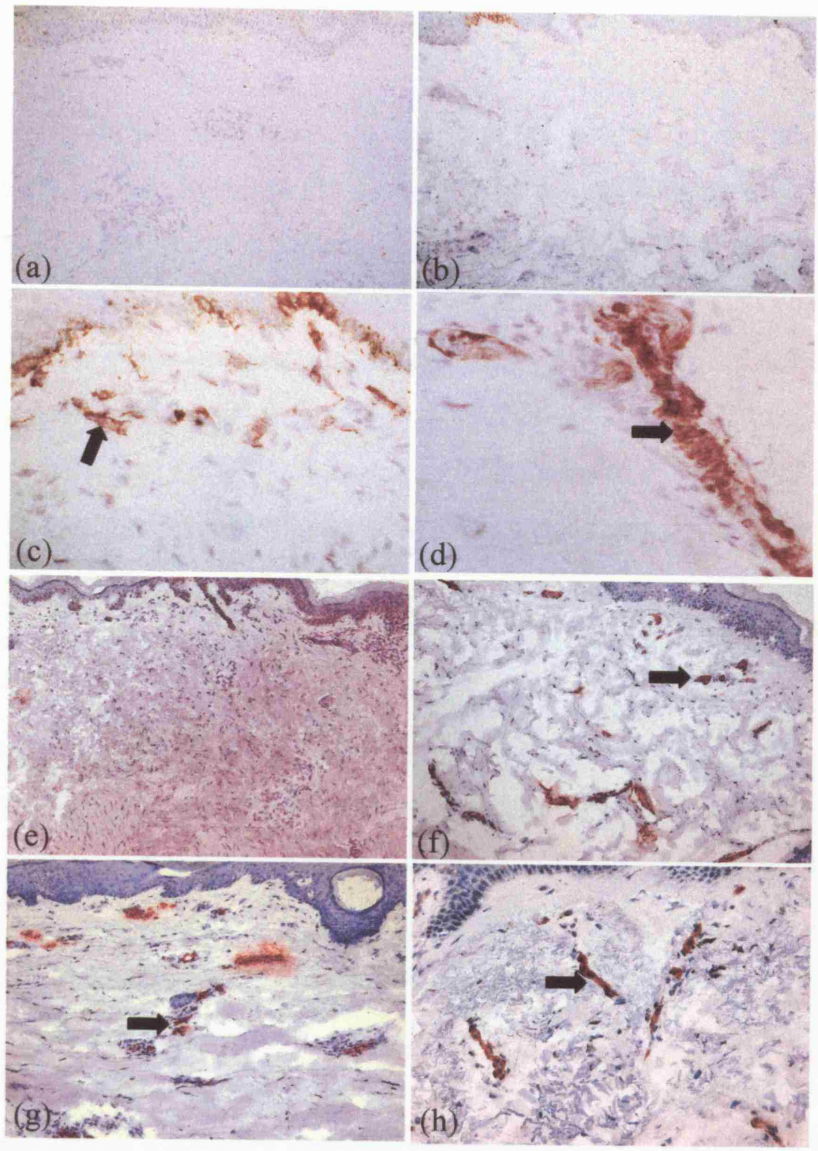


**Figure 3.3.**

**Pericyte activation in normal, RP and dcSSc skin.**

No expression of HMW-MAA was seen in normal or primary Raynaud's skin, respectively (**a,b**). However, immunostaining for HMW-MAA was observed in the microvasculature of autoimmune RP and dcSSc samples respectively (arrows, **c and d**). By contrast, little or no expression of HMW-MAA was observed in the dermis of atrophic disease (**e**). α-SMA expression was detected around capillaries in normal, PRP and atrophic skin, indicating the presence of pericytes (arrows, **f,g and h**). Original magnification **a,b,e,f,g,h** x10 and **c** and **d** x20.

expression and the number of activated pericytes in ARP and in fibrotic lesional or non-lesional dcSSc skin ($p<0.01$). In normal, PRP and atrophic dcSSc skin, less than 20% of microvessels expressed PDGFRβ or the activated pericyte marker.

### 3.3.4 Spatial relationship between PDGFRβ and activated pericytes in ARP and dcSSc

Initially, mirror image serial sections were used to analyse the spatial relationship between PDGFRβ and activated pericytes. As shown in Figure 3.5, markers for PDGFRβ and activated pericytes exhibited a very similar distribution in dcSSc tissue, colocalising predominantly to microvessels. Double immunofluorescence labelling was carried out to determine the spatial relationship between the markers. Figure 3.6 shows representative images from ARP skin of the expression of PDGFRβ and PDGF AB/BB between endothelial cells and activated pericytes. The optical images shown are from autoimmune Raynaud's analysed using confocal microscopy as described in the methods. The images have been rotated $70^{o}$ through two axes in order to provide a 3D representation. The PDGFRβ was found to be expressed on activated pericytes as shown by the yellow staining (Figure 3.6a-c). In contrast, the absence of colocalisation observed between PDGFRβ (green) and endothelial cells (red) indicated that PDGFRβ are not expressed by endothelial cells (Figure 3.6d-f). Similarly, the staining pattern for activated pericytes and endothelial cells was also found to be mutually exclusive (Figure 3.6g-i). Similar colocalisation patterns between PDGFRβ, endothelial cells and activated pericytes were observed in fibrotic lesional or non-lesional dcSSc skin. PDGF AB/BB ligand expression colocalised significantly to activated pericytes in ARP skin, but not in any of the other disease subsets (Figure 3.6j-l). In addition, there was no colocalisation between PDGF AB/BB and endothelial cells in any of the samples studied (Figure 3.6m-o).

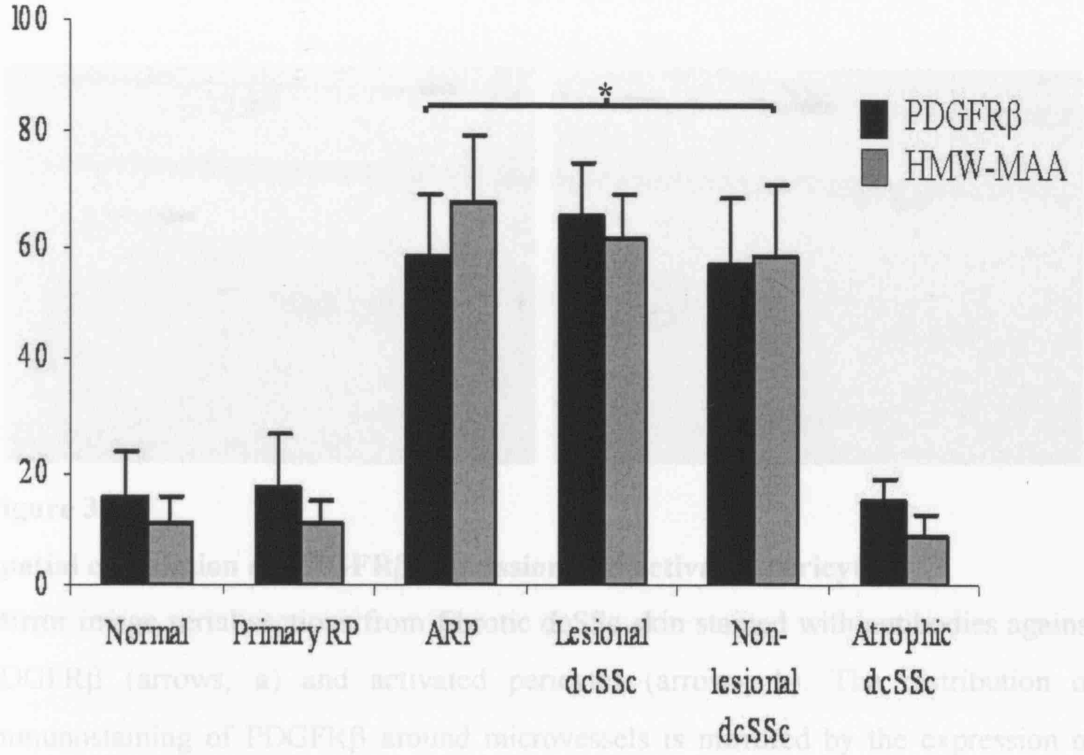


**Figure 3.4.**

**Percentage of microvessels expressing PDGFRβ and HMW-MAA in dcSSc subsets.** Mirror image serial sections from 5 samples of each clinical subset were analysed, except for atrophic stage disease, for which 4 samples were analysed (n=29). Less than 20% of microvessels were positive in normal, primary RP and atrophic dcSSc compared with approximately two thirds of microvessels in ARP and lesional dcSSc skin. Bars show mean values ±s.d. *=$p<0.01$.

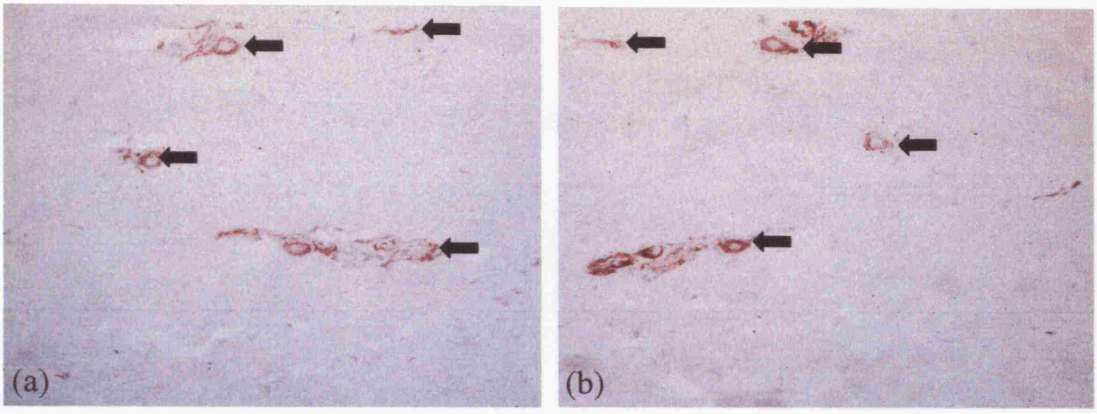


**Figure 3.5.**

**Spatial correlation of PDGFRβ expression and activated pericytes.**

Mirror image serial sections from fibrotic dcSSc skin stained with antibodies against PDGFRβ (arrows, **a**) and activated pericytes (arrows, **b**). The distribution of immunostaining of PDGFRβ around microvessels is mirrored by the expression of HMW-MAA demonstrating a strong co-localisation between activated pericyte and PDGFRβ expression. Original magnification x5.

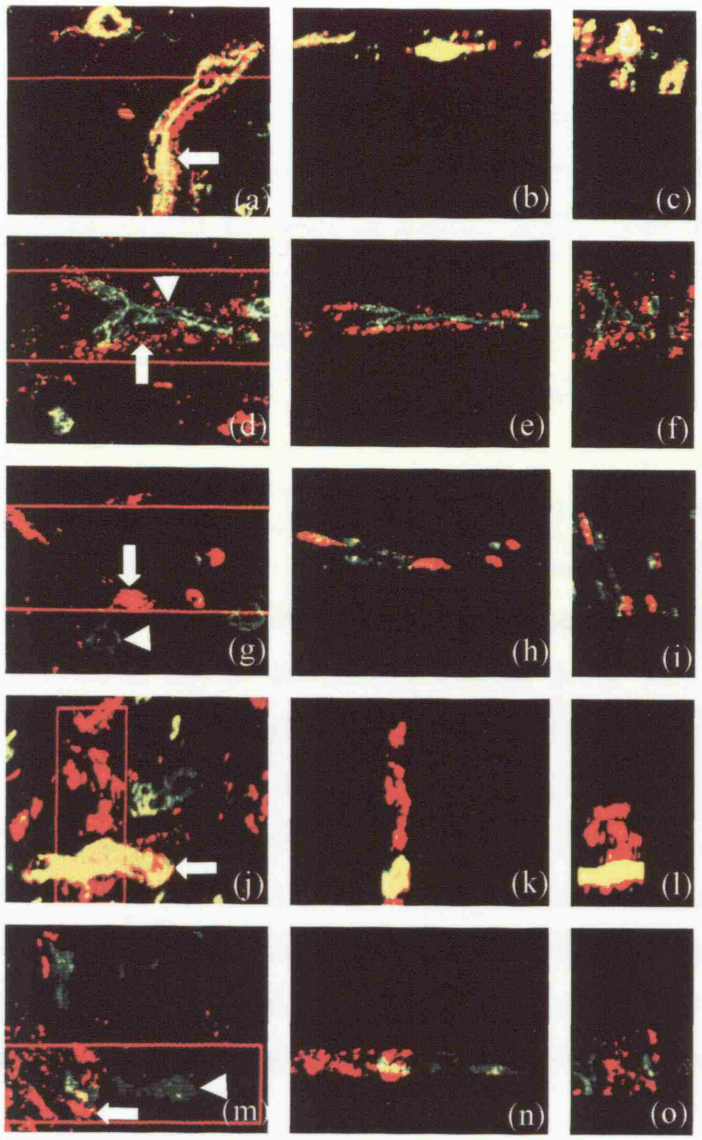


**Figure 3.6.**

**Cellular localisation of PDGFRβ using double immunofluorescence labelling.**

Representative optical sections from ARP tissue (**a,d,g,j,m**) and 3D reconstructions rotated 70° clockwise along the long axis of the red rectangle (**b,e,h,k,n**) and 3D reconstructions rotated 70° clockwise along the short axis of the red rectangle (**c,f,i,l,o**); Figures **a-c** shows PDGFRβ (red colour), HMW-MAA (green colour) and colocalisation (arrows, yellow colour). Figures **d-f** showing PDGFRβ (arrow, red colour), PAL-E (arrowhead, green colour) and co-localisation (yellow colour) showing no co-localisation between PDGFRβ and endothelium; Figures **g-i** showing HMW-MAA (arrow, red colour), PAL-E (arrowhead, green colour) and colocalisation (yellow colour) demonstrating no co-localisation between pericytes and endothelium; Figures **j-l** shows PDGF-B chain (red colour), HMW-MAA (green colour) and co-localisation (arrow, yellow colour), showing co-localisation between PDGF-B chain and pericytes in some microvessels but not others. Figures **m-o** shows PDGF-B chain (arrow, red colour), PAL-E (arrowhead, green colour) and co-localisation (yellow colour) demonstrating no co-localisation between PDGF-B chain and endothelium. Original magnification x20.

In order to quantify the degree of colocalisation between markers, labelled cryosections from dcSSc and ARP skin were analysed using computer-aided image analysis. The results of the colocalisation studies are presented in Table 3.2 and summarised in Figure 3.7. In all cases of fibrotic dcSSc, both lesional and non-lesional skin and ARP skin, PDGFRβ colocalised with activated pericytes significantly higher than background levels ($p<0.01$). Furthermore, the degree of colocalisation between PDGFRβ and activated pericytes was significantly higher than that observed between PDGFRβ, PDGF AB/BB and endothelial cells. (Figure 3.7a and 3.7b). However, in ARP, the degree of colocalisation of PDGF AB/BB with activated pericytes was significantly higher than background levels (Figure 3.7b). In contrast, no colocalisation above background levels was seen between PDGF AB/BB and activated pericytes in any of the fibrotic lesional dcSSc skin. In non-lesional dcSSc, colocalisation between PDGF AB/BB and activated pericytes was increased (37%), but this was not statistically significant (Figure 3.7b). In Table 3.3, the mean and median values of the number of pixels per field of vision for each marker are given for all cases studied. Table 3.3 also shows the variations in the size of the total area per field of vision that stained positively. Standard deviation values for all markers are high, however, the median values were close to the mean values, indicating a large but homogenous spread of recorded values compared to mean values.

**Table 3.2: Quantification of colocalisation in double immunofluorescence labelling**

| **DcSSc** | **CASE 1** | **CASE 2** | **CASE 3** | **CASE 4*** |
|---|---|---|---|---|
| Percentage colocalisation of **PDGF-β receptor** with: | | | | |
| HMW-MAA | 61 (0.01) | 79 (0.01) | 61 (0.01) | 78 (0.01) |
| PAL-E | 24 (0.92) | 24 (0.88) | 14 (0.91) | 8 (0.51) |
| Percentage colocalisation of **PDGF AB/BB** with: | | | | |
| HMW-MAA | 18 (0.38) | 12 (0.35) | ND | 37 (0.1) |
| PAL-E | 10 (0.01) | 16 (0.34) | ND | 18 (0.51) |
| Percentage colocalisation of **PAL-E** with: | | | | |
| PDGF-β receptors | 33 | 30 | 20 | 23 |
| PDGF AB/BB | 8 | 28 | ND | 26 |
| HMW-MAA | 18 | 14 | 14 | 14 |

| **ARP** | **CASE1** | **CASE2** | **CASE3** | **CASE4** |
|---|---|---|---|---|
| Percentage colocalisation of **PDGF-β receptor** with: | | | | |
| HMW-MAA | 68 (0.01) | 73 (0.01) | 84 (0.01) | 73 (0.01) |
| PAL-E | 17 (0.88) | 18 (0.17) | 9 (0.4) | 19 (0.7) |
| Percentage colocalisation of **PDGF AB/BB** with: | | | | |
| HMW-MAA | 52 (0.01) | 22 (0.3) | 51 (0.01) | 58 (0.02) |
| PAL-E | 12 (0.26) | 9 (0.98) | 17 (0.54) | 14 (0.7) |
| Percentage colocalisation of **PAL-E** with: | | | | |
| PDGF-β receptors | 19 | 13 | 18 | 26 |
| PDGF AB/BB | 16 | 17 | 22 | 15 |
| HMW–MAA | 28 | 9 | 27 | 22 |

Biopsies from three lesional and one non-lesional (*) dcSSc and four autoimmune Raynaud's phenomenon (ARP) patients were stained by double immunofluorescence labeling with various combinations of monoclonal antibodies. The percentage values represent the spatial distribution of two markers in relation to each other measured as percentage of pixels that colocalise. P-values are given in brackets.

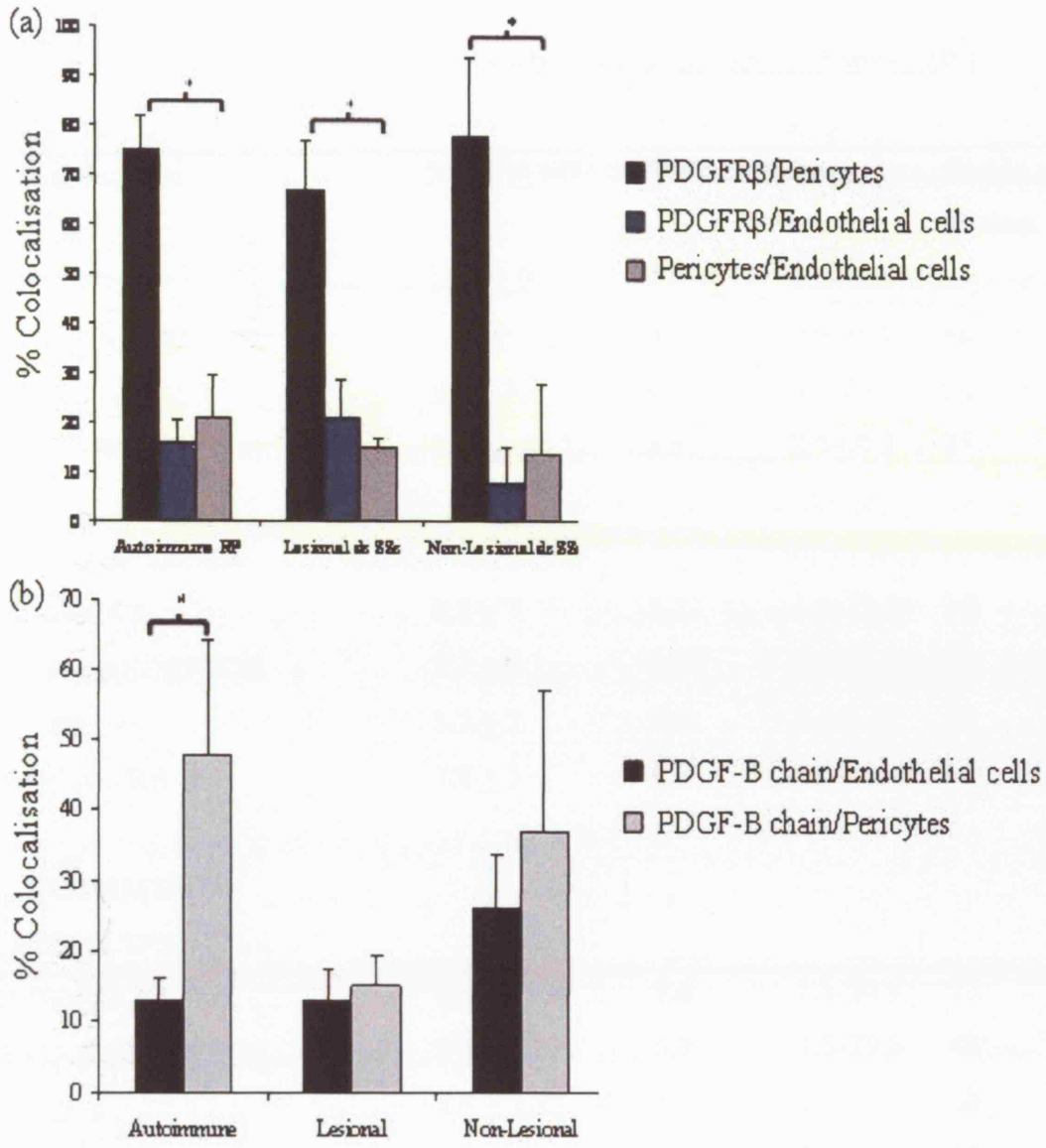


**Figure 3.7.**

**Quantification of colocalisation in double immunofluorescence labelling.**

Significant co-localisation between PDGFRβ and HMW-MAA was seen all clinical subsets (**a**). Co-localisation between PDGFRβ and PAL-E was similar to background levels as determined by HMW-MAA and PAL-E (**a**). Significant co-localisation between PDGF AB/BB and HMW-MAA was observed in ARP (**b**). In lesional and non-lesional dcSSc, no significant co-localisation between PDGF AB/BB and HMW-MAA was observed. No significant co-localisation was observed between PDGF AB/BB and PAL-E in any of the clinical subsets (**b**). *=$p<0.01$

**Table 3.3: Average and median number of pixels (1 Pixel=0.9 μm x 0.9 μm)**

| | Number of Pixels/Field of Vision ($10^3$) | | | |
|---|---|---|---|---|
| **Lesional dcSSc** | **Mean ± SD** | **Median** | **Range** | **Fields of Vision.** |
| HMW-MAA | 11.4 ± 9 | 8.8 | 1.2-46.8 | 55 |
| PDGF-β RECEPTOR | 11.1 ± 11.6 | 8.8 | 0.6-59.9 | 48 |
| PAL-E | 5.4 ± 3.7 | 4.6 | 0.9-20 | 54 |
| PDGF AB/BB | 11.7 ± 11.7 | 8.6 | 2.5-60.3 | 25 |
| **Non-lesional dcSSc** | | | | |
| HMW-MAA | 8.2 ± 7 | 5.2 | 1.5-23.1 | 18 |
| PDGF-β RECEPTOR | 9.2 ± 6.1 | 8.2 | 3.1-22.9 | 12 |
| PAL-E | 3.3 ± 2 | 2.6 | 0.4-8.1 | 18 |
| PDGF AB/BB | 7.8 ± 5 | 6.9 | 2.6-21.1 | 12 |
| **AUTOIMMUNE RAYNAUD'S** | | | | |
| HMW-MAA | 10.9 ± 7.9 | 9.6 | 1.1-36.4 | 73 |
| PDGF-β RECEPTOR | 9 ± 6.3 | 6.9 | 1.5-29.6 | 48 |
| PAL-E | 4.5 ± 2.8 | 3.5 | 1.1-17.6 | 68 |
| PDGF AB/BB | 7.9 ± 6.1 | 5.5 | 1.1-27.1 | 43 |

Average and median number of pixels present in each field of vision (300 μm x 300 μm) from biopsies of three lesional and one non-lesional dcSSc samples and four ARP samples for the different Mabs used in this study (n=8).

## 3.4 KEY FINDINGS AND CONCLUSIONS

### Pericyte activation and PDGFRβ expression are increased in dcSSc skin

The data presented demonstrated a significant increase in the expression of PDGFRβ within the dermal microvasculature of patients with ARP and fibrotic dcSSc compared with control skin. Increased PDGFRβ expression was not detected in PRP or atrophic dcSSc skin. A concomitant increase in the expression of HMW-MAA, indicating pericyte activation, was also detected in the dermis from ARP and fibrotic dcSSc patients. In agreement with previous studies, in normal skin, little or no expression of PDGFRβ (358;367;439) or HMW-MAA (389;440) was detected. In PRP and atrophic skin, increased HMW-MAA expression was not seen, however, the presence of pericytes surrounding microvessels was confirmed using an antibody against α-SMA. Therefore, the absence of HMW-MAA staining in PRP and atrophic skin is likely to be due to a loss of HMW-MAA expression rather than the absence of pericytes.

### Pericytes express PDGFRβ in dcSSc and ARP skin

A previous immunohistochemical study has reported increased microvascular expression of PDGFRβ in cryosections of dcSSc skin. In these experiments, single label immunostaining was carried out and the authors concluded that PDGFRβ expression localised to endothelial cells (246). However, due to the reduced resolution afforded by cryosections, localising the cellular source of receptor expression using single label immunostaining is difficult. To overcome this problem, I have applied double immunofluorescence labelling coupled with image analysis and confocal microscopy. Using this combined approach, I was able to show that in ARP and both lesional and non-lesional dcSSc skin, the microvascular expression of PDGFRβ was localised to HMW-MAA expressing pericytes rather than endothelial cells.

### Pericytes express PDGF AB/BB ligand in ARP but not in dcSSc skin

Using the same approach, PDGF AB/BB ligand was found to colocalise to activated pericytes in ARP but not in dcSSc skin. The PDGF007 antibody used in these experiments does not bind to either receptor bound ligand or the PDGF pro-peptide (408). Therefore, the detected immunoreactivity is due to the binding of the antibody to active PDGF-B chain located in the cytosol rather than internalised receptor-ligand

complexes. The data also shows that in ARP, pericytes express both the PDGFRβ and PDGF AB/BB ligand while in dcSSc, pericytes express the PDGFRβ but not the PDGF AB/BB ligand. It is noteworthy that this is the first report of PDGF AB/BB expression by pericytes *in vivo*. PDGF-B expression by immature capillary endothelial cells and the endothelium of growing arteries is a key signal in the recruitment of pericytes to nascent vessels (278) and the expression of PDGF AB/BB by dermal macrophages is thought to be a critical source of PDGF AB/BB during tissue repair (358). Further studies are required to elucidate the functional consequences of autocrine PDGF AB/BB expression by pericytes in ARP tissue.

In summary, the data presented in this chapter demonstrate that in ARP and dcSSc, microvascular pericytes are activated and express elevated levels of PDGFRβ. Furthermore, the activating ligand PDGF AB/BB is expressed by pericytes in ARP, whilst macrophages are the main source of PDGF AB/BB in dcSSc. Thus, microvascular pericytes may be mediators of the fibrotic response in dcSSc.

# CHAPTER 4: THE SPATIAL RELATIONSHIP BETWEEN PERICYTES, FIBROBLASTS AND MYOFIBROBLASTS IN dcSSc

## 4.1 INTRODUCTION

The capacity of pericytes to differentiate into other mesenchymal cell types, including osteoblasts (114), adipocytes and chondrocytes (135) has led to the suggestion that they may play a significant role in a variety of human diseases (485). In the previous chapter, it was demonstrated that microvascular pericytes become activated and express PDGFRβ in dcSSc. A number of studies have demonstrated that activation of pericytes often precedes their differentiation to another mesenchymal cell type. For example, in dermal scarring tissue, expression of PDGFRβ by pericytes is associated with a differentiation to collagen-synthesising fibroblasts (439), while in the liver, pericytes expressing PDGFRβ become activated and undergo a phenotypic transition to myofibroblasts during liver fibrosis (66).

Like pericytes, myofibroblasts express α-SMA and share phenotypic traits of both fibroblasts and smooth muscle cells. Under normal conditions, myofibroblasts are only found in highly specialised tissues such as alveolar septa and the bone marrow stroma (455), however, they are strongly associated with fibrotic tissue (104). While myofibroblasts have been reported as being present in dcSSc skin (219;377), key questions remain unanswered, particularly with regards to their ontogeny and precise role in the disease pathology. The finding that pericytes express PDGFRβ in dcSSc skin (354) supports the hypothesis that the differentiation of pericytes into fibroblasts and/or myofibroblasts may play a role in SSc disease pathogenesis. Such a differentiation process would provide a cellular mechanism by which microvascular damage gives rise to chronic fibrosis in dcSSc. Therefore, the focus in this chapter was to determine the spatial relationship between pericytes, myofibroblasts and fibroblasts in dcSSc tissue.

## 4.2 EXPERIMENTAL DESIGN

An immunohistochemical analysis was carried out to determine the spatial correlation between pericytes, myofibroblasts and collagen-synthesising fibroblasts in dcSSc skin. The clinical details of the patients are provided in Table 4.1. Double immunofluorescence labelling using combinations of cell-specific markers was carried out. The immunofluorescent labelling was analysed using con-focal

microscopy. Immunohistochemical findings were then correlated with specific disease parameters including skin score and disease duration. Pericytes were identified by means of α-SMA expression (416;439). Myofibroblasts were identified by using antibodies against α-SMA and ED-A FN as previously described (121;200). Collagen synthesis was determined by expression of lysyl oxidase (LOX). Due to a lack of suitable antibodies, identification of active collagen biosynthesis in fixed tissues was achieved by indirect measurement of enzymes that are needed for post-translational processing of collagen. LOX plays a central role in catalysing collagen cross-linking within the extracellular matrix (418) and has been established as a surrogate marker for collagen-synthesising cells (81;187;242). The expression of Thy-1 was also investigated to determine whether Thy-1 expression identified cells with myofibroblastic potential as reported for myometrial fibroblasts (252). Details of the antibody concentrations used are provided in Table 2.1 and staining procedures are described in Section 2.3.4.

## 4.3 RESULTS

### 4.3.1 Immunohistochemical analysis of myofibroblasts in dcSSc skin

In accordance with previous studies, myofibroblasts were identified as interstitial fibroblastic cells expressing α-SMA (121;200;341). In normal skin, α-SMA immunostaining was restricted to microvascular pericytes, sweat glands and smooth muscle cells of the erector pili muscles (Figure 4.1a). No α-SMA immunoreactivity was detected in interstitial fibroblasts (Figure 4.1a). The analysis of dcSSc samples revealed that six out of ten dcSSc cases were characterised by the presence of myofibroblasts (Figure 4.1b). In five of these cases, myofibroblasts were located almost exclusively in the lower reticular dermis. In these cases, α-SMA immunoreactivity in the upper papillary dermis, α-SMA was localised to microvessels (Figure 4.1c), while in the lower reticular dermis was localised to myofibroblasts (Figure 4.1c). In the remaining dcSSc case, myofibroblasts were detected in both the reticular and papillary dermis. The pattern of α-SMA expression in microvessels differed between the papillary and reticular dermis. In the papillary dermis, α-SMA expression was closely associated with the microvascular wall (Figure 4.1a), while in reticular dermal layers, α-SMA expressing cells appeared to be dissociated from the microvascular wall (Figure 4.1c and 4.1d). Myofibroblasts were not detected in any of

the non-lesional and atrophic dcSSc samples in which α-SMA expression was restricted to the vessel wall (Figure 4.1e and 4.1f).

**Table 4.1: Clinical and serological characteristics of dcSSc patients**

| Characteristics | Fibrotic (*n*=10) | Atrophic (*n*=6) |
|---|---|---|
| Mean age (range) | 54 (39-72) | 58 (37-69) |
| Mean disease duration, months (range) | 11 (4-18) | 96 (36-168) |
| Male/female | 2/8 | 0/6 |
| **Organ involvement** | | |
| Mean skin score (range) | 33 (19-41) | 17 (11-24) |
| Oesophageal | 7/10 | 3/6 |
| Other gastrointestinal | 4/10 | 1/6 |
| Lung | 4/10 | 2/6 |
| Muscle | 3/10 | 0/6 |
| Renal | 2/10 | 1/6 |
| Cardiac | 0/10 | 1/6 |
| Pulmonary hypertension | 2/10 | 0/6 |
| **Serology** | | |
| Antinuclear | 10/10 | 6/6 |
| Anti-topoisomerase 1 | 4/10 | 3/6 |
| Anti-RNA polymerase I/III | 2/10 | 1/6 |
| Anti-nuclear RNP | 1/10 | 1/6 |
| *** Microvascular damage** | | |
| Structural capillary damage | 10/10 | 6/6 |

* Assessed by nailfold capillaroscopy

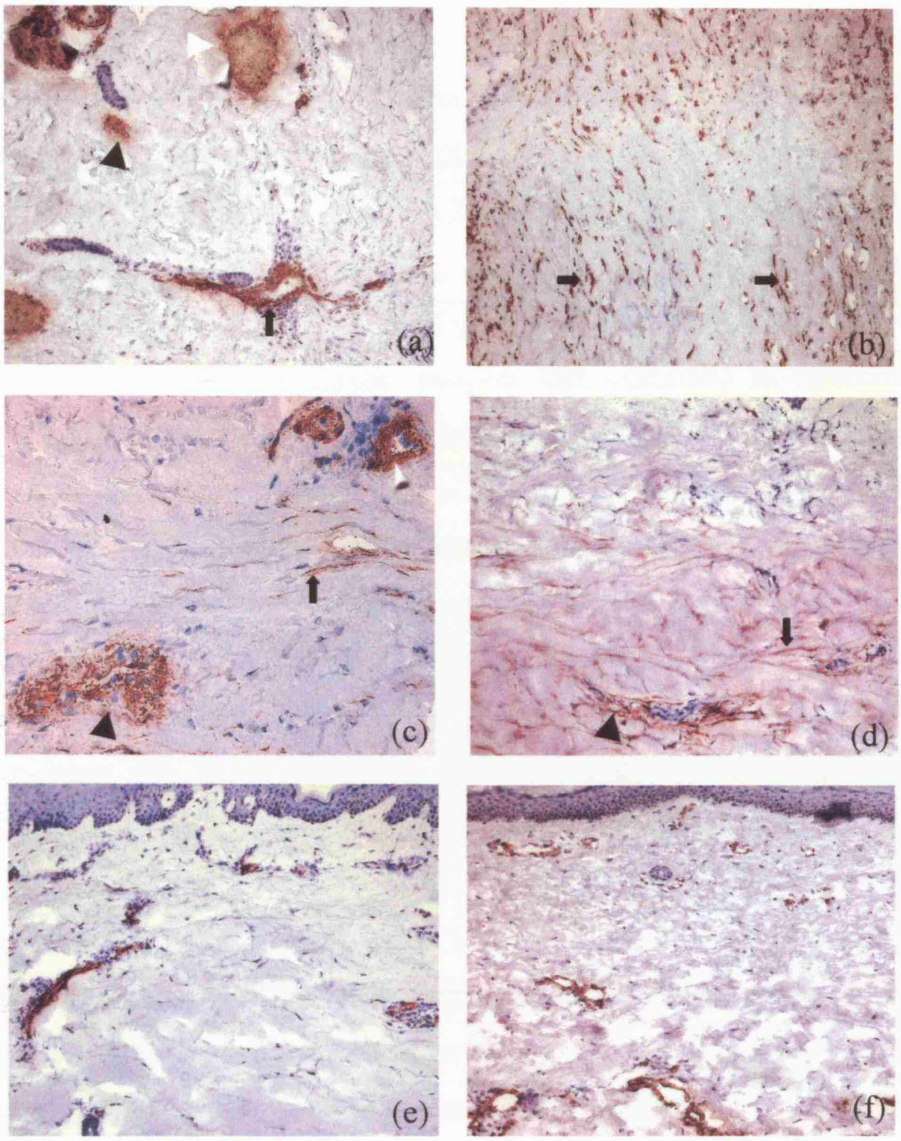


**Figure 4.1.**

**Presence of myofibroblasts in dcSSc skin.**

Cryosections from normal (**a**) and dcSSc (**b-f**) were stained with an antibody against α-SMA. In normal skin α-SMA staining was restricted primarily to microvascular pericytes enveloping capillaries (arrows, **a**), sweat glands (black arrowhead, **a**) and smooth muscle cells of erector pili muscles (white arrowhead, **a**). In dcSSc samples, α-SMA expressing myofibroblasts were detected in the dermis (arrows, **b, c and d**). In reticular dermal layers, α-SMA expressing cells appeared to be disassociated from the vessel wall (black arrowheads, **c and d**) while in the papillary dermal layers α-SMA expressing cells were closely associated with the vessel (white arrowhead, **c**). In non-lesional (**e**) and atrophic dcSSc (**f**), the expression of α-SMA was restricted to the microvascular wall. Original magnification **a,b,e,f** x10 and **c,d** x20.

### 4.3.2 Immunohistochemical analysis of ED-A FN and collagen in dcSSc skin

The expression of ED-A FN plays a key role in the differentiation and contractile function of myofibroblasts(455) and can be used to identify them in tissues in combination with α-SMA expression (200). Little or no immunostaining for ED-A FN was detected in normal skin (Figure 4.2b). However, in six dcSSc cases, there was a marked increase in ED-A FN staining, predominantly in fibroblastic cells and in small capillaries (Figure 4.2d and 4.2f). Significantly, increased ED-A FN expression was only observed in those dcSSc samples that contained myofibroblasts. The analysis of serial cryosections demonstrated that expression of ED-A FN and α-SMA colocalised to the same cellular structures. Increased immunostaining for ED-A FN was located predominantly in the reticular dermis and localised to areas of the dermis containing α-SMA expressing myofibroblasts (Figure 4.3a and 4.3b). Papillary dermal layers, which were negative for myofibroblasts, contained little or no ED-A FN expression (Figure 4.3a and 4.3b). In the lower reticular dermis in dcSSc, immunostaining for ED-A FN was also frequently observed associated with microvessels surrounded by α-SMA positive pericytes (Figure 4.3c and 4.3d).

Collagen-synthesising fibroblasts were identified using an antibody against the enzyme lysyl oxidase (LOX) as previously reported (189;249). Little or no expression of LOX was observed in the dermis of normal skin, atrophic and non-lesional dcSSc skin, indicating low levels of new collagen synthesis (Figure 4.2a). In four dcSSc cases, an increase in LOX immunostaining was observed when compared to normal skin. This elevated expression was found to be associated with fibroblastic cells throughout the dermis (Figure 4.2c) and with microvascular cells (Figure 4.2e). However, LOX expression in six out of ten dcSSc samples was similar to that seen in normal skin. Of all the dcSSc samples investigated, LOX-expressing cells and myofibroblasts were both present in two out of ten samples (Table 4.3).

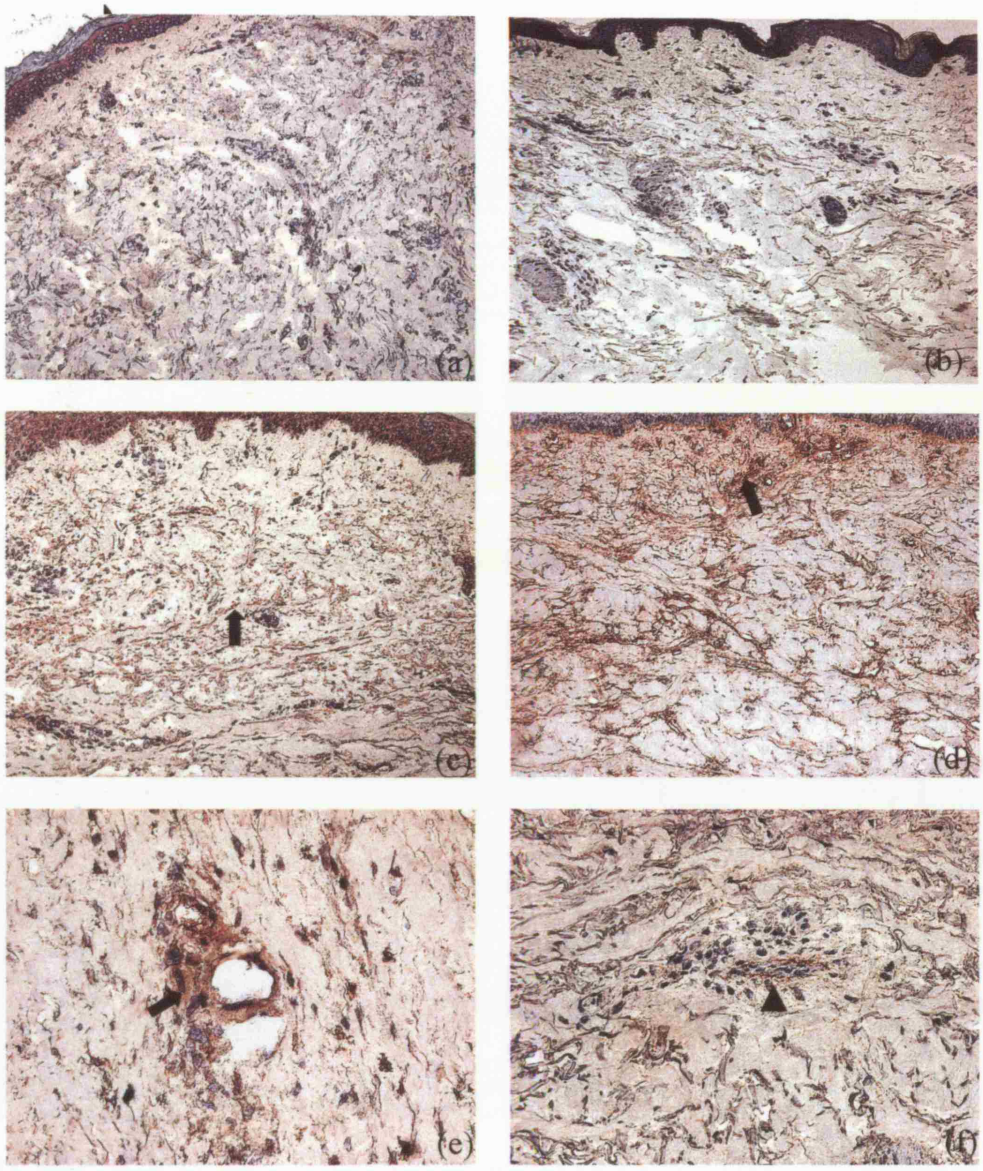


**Figure 4.2.**

**Increased expression of Lysyl Oxidase (LOX) and the ED-A splice variant of fibronectin in dcSSc skin.**

Cryosections of normal skin (**a and b**) were compared with dcSSc skin (**c-f**). Little or no immunostaining for LOX was detected in normal skin (arrow, **a**). In dcSSc skin, immunostaining for LOX was detected in fibroblast like cells throughout the dermis (arrows, **c and e)** and in cells of the microvascular wall (arrowhead, **e**). Little or no expression of ED-A FN was seen in normal skin (**b**), however, ED-A FN immunostaining was markedly increased in dcSSc skin (arrows, **d and f**). Immunostaining for ED-A FN was also detected in cells of the microvascular wall (arrowhead**, f**). Original magnification **a-d** x10 and **e,f** x20.

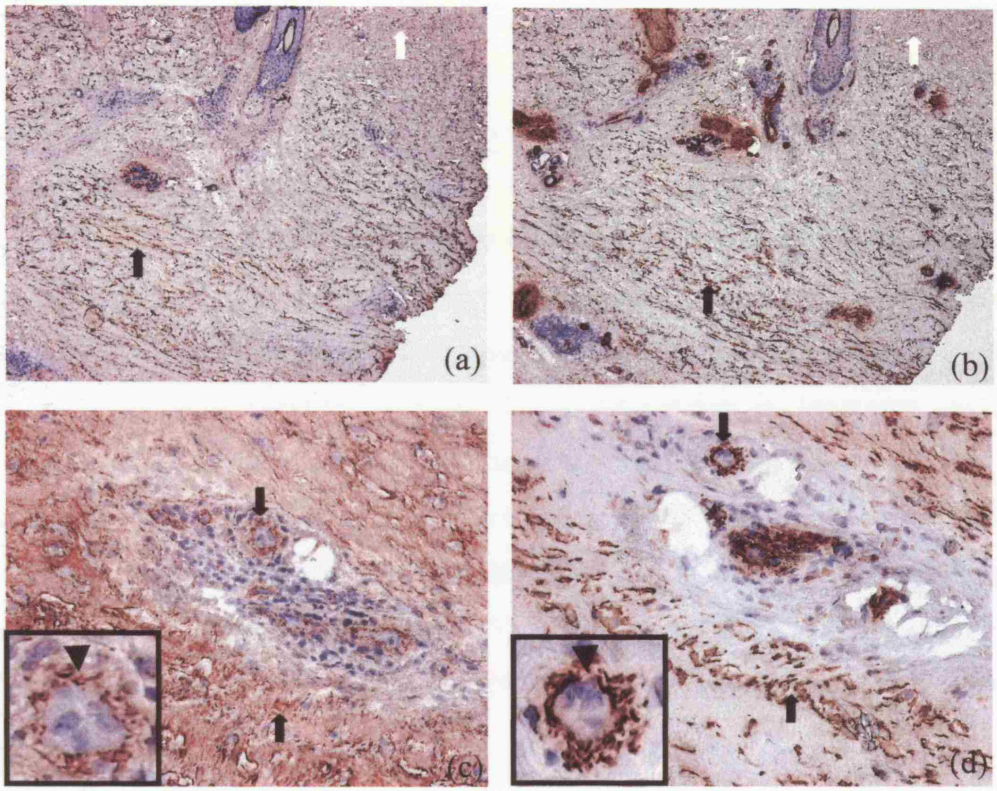


**Figure 4.3.**

**The expression of ED-A FN correlates with myofibroblasts in dcSSc skin.**

Serial cryosections were stained with antibodies against ED-A FN (**a and c**) and α-SMA (**b and d**). Both ED-A FN (arrows **a,c**) and α-SMA$^{+ve}$ myofibroblasts (arrow, **b,d**) were predominant in the lower reticular dermis of dcSSc skin. Note the absence of ED-A FN (white arrow, **a**) and α-SMA$^{+ve}$ myofibroblasts (white arrow, **b**) in the papillary dermis. In addition, immunostaining for ED-A FN was detected in the wall of microvessels (arrowheads, inset **c**) surrounded by α-SMA expressing pericytes (arrowheads, inset **d**). Original magnification **a,b** x10 and **c,d** x20, **inset c, d,** x40.

### 4.3.3 Analysis of Thy-1 expression in dcSSc skin

It was recently reported that myofibroblasts differentiate from Thy-$1^{+ve}$ fibroblasts (252). Therefore, to identify putative sources of myofibroblasts, Thy-1 expression was evaluated in normal and dcSSc skin. In normal skin, Thy-1 immunostaining was located mainly in the microvascular wall and the immediate perivascular region (Figure 4.4a and 4.4b). Occasional cells within the dermis were also stained in both the papillary and reticular dermal layers (Figure 4.4b). In agreement with previous studies, Thy-1 immunostaining was not detected in keratinocytes (370). In all samples of dcSSc skin, there was a marked increase in Thy-1 staining throughout the dermis (Figure 4.4c). In perivascular regions, Thy-1 immunostaining was frequently less pronounced than in normal skin (Figure 4.4d). In atrophic dcSSc and non-lesional dcSSc skin, Thy-1 expression was less pronounced than that seen in lesional dcSSc skin. Expression was detected predominantly in microvascular cells (Figure 4.4e and 4.4f). In order to determine whether Thy-1 expression is increased on dcSSc fibroblasts, cultured cell lysates were analysed by Western blot analysis. These experiments revealed no significant differences in Thy-1 expression levels between control and dcSSc fibroblast cell lysates ($p=0.48$) (Figure 4.5), suggesting that increased interstitial Thy-1 staining in dcSSc skin was due to an altered distribution of Thy-$1^{+ve}$ cells.

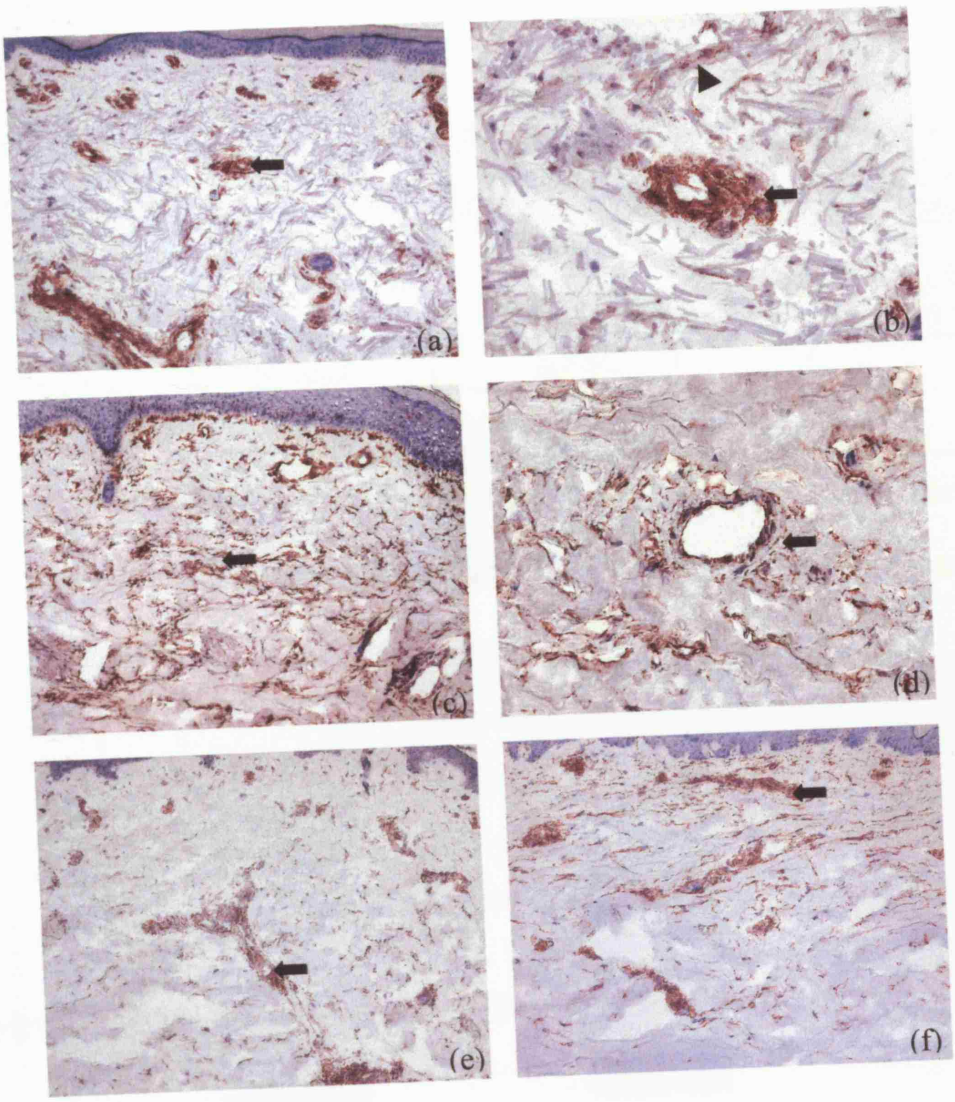


**Figure 4.4.**

**The expression of Thy-1 is increased in dcSSc skin.**

Cryosections from normal (**a and b**) and dcSSc (**c and d**) were stained for Thy-1 expression. In normal skin, immunostaining for Thy-1 was predominantly located within the microvascular wall and immediate perivascular region (arrows, **a and b**). Thy-1 staining of interstitial fibroblasts was also detected (arrowhead, **b**). In dcSSc skin, immunostaining of fibroblastic cells was considerably more pronounced throughout the interstitial dermis (arrows, **c**) while perivascular immunostaining in dcSSc skin (arrow, **d**) was less pronounced than that observed in normal skin (arrow, **b**). In atrophic (arrow, **e**) and non-lesional skin (arrow, **f**), Thy-1 expression was located primarily in microvessels. Original magnification **a,c** x10 and **b,d** x20.

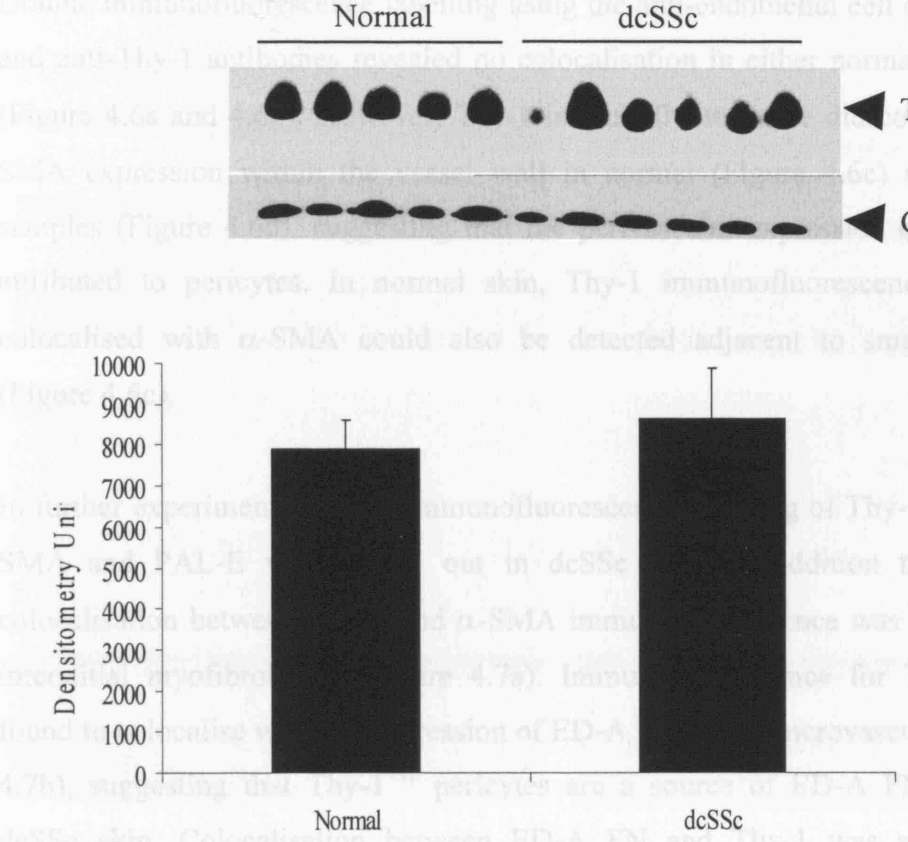


**Figure 4.5.**

**Expression of Thy-1 by fibroblasts derived from normal and dcSSc skin.** Comparison of Thy-1 expression between normal and dcSSc fibroblasts reveals no significant differences in expression levels ($p=0.48$). Samples were normalised against GAPDH expression and quantified by Gelplate$^{TM}$ image analysis. The significance was determined using the Student's t-test. The bars show the means +/- s.d.

### 4.3.4 Spatial correlation of cellular markers with matrix biosynthesis in dcSSc skin

Multiple labelling experiments using markers of specific cell lineages and matrix biosynthesis were performed on normal and dcSSc skin sections. The results are summarised in Table 4.2.

Double immunofluorescence labelling using the anti-endothelial cell antibody PAL-E and anti-Thy-1 antibodies revealed no colocalisation in either normal or dcSSc skin (Figure 4.6a and 4.6b). However, Thy-1 immunofluorescence did colocalise with α-SMA expression within the vessel wall in normal (Figure 4.6c) and dcSSc skin samples (Figure 4.6d), suggesting that the perivascular expression of Thy-1 can be attributed to pericytes. In normal skin, Thy-1 immunofluorescence that did not colocalised with α-SMA could also be detected adjacent to small microvessels (Figure 4.6c).

In further experiments, double immunofluorescence labelling of Thy-1, ED-A FN, α-SMA and PAL-E was carried out in dcSSc skin. In addition to microvessels, colocalisation between Thy-1 and α-SMA immunofluorescence was also detected in interstitial myofibroblasts (Figure 4.7a). Immunofluorescence for Thy-1 was also found to colocalise with the expression of ED-A FN in the microvascular wall (Figure 4.7b), suggesting that Thy-$1^{+ve}$ pericytes are a source of ED-A FN expression in dcSSc skin. Colocalisation between ED-A FN and Thy-1 was also detected in interstitial myofibroblasts (Figure 4.7c). ED-A FN expression was found to colocalise with α-SMA expression in the vessel wall (Figure 4.7d), supporting the idea that pericytes express ED-A FN in dcSSc. Immunofluorescence for ED-A FN also colocalised with α-$SMA^{+ve}$ cells in the dermis, confirming that myofibroblasts are a source of ED-A FN in dcSSc skin (Figure 4.7e). Immunofluorescence for ED-A FN did not colocalise with endothelial cells (Figure 4.7f).

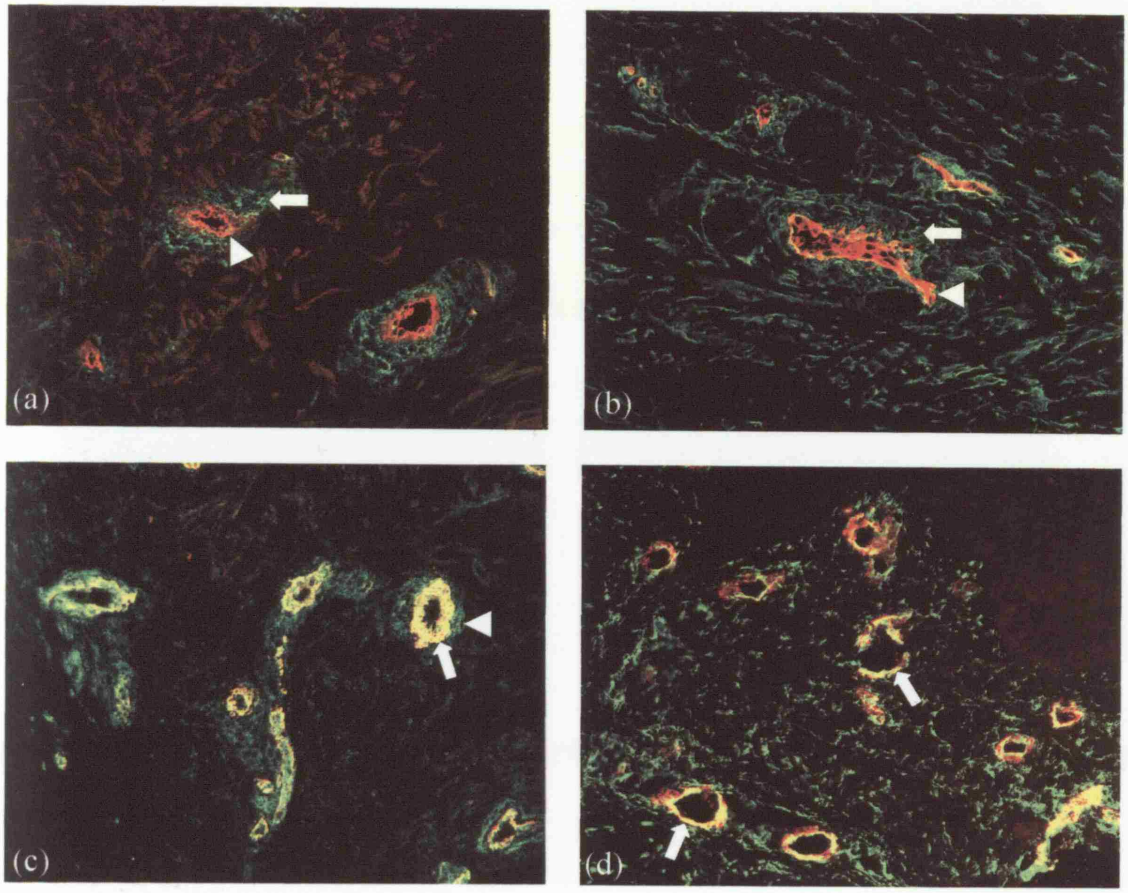


**Figure 4.6.**

**Cellular localisation of Thy-1 using double immunofluorescence labelling.** Cryosections from normal (**a and c**) and dcSSc (**b and d**) were double-stained for endothelial cells using the PAL-E antibody (red colour) and Thy-1 (green colour) (**a and b**) and for α-SMA (red colour) and Thy-1 (green colour) (**c and d**). In normal (**a**) and dcSSc (**b**), immunofluorescence for Thy-1 (arrow, green colour, **a and b**) and PAL-E (arrowhead, red colour, **a and b**) showed no colocalisation. In normal (**c**) and dcSSc (**d**), colocalisation between Thy-1 and α-SMA was evident (arrows, yellow colour, **c and d**). In normal skin, Thy-1 immunofluorescence that did not colocalise with α-SMA was detected immediately adjacent to microvessels (arrowhead, green colour, **c**). Original magnification **a-d** x20.

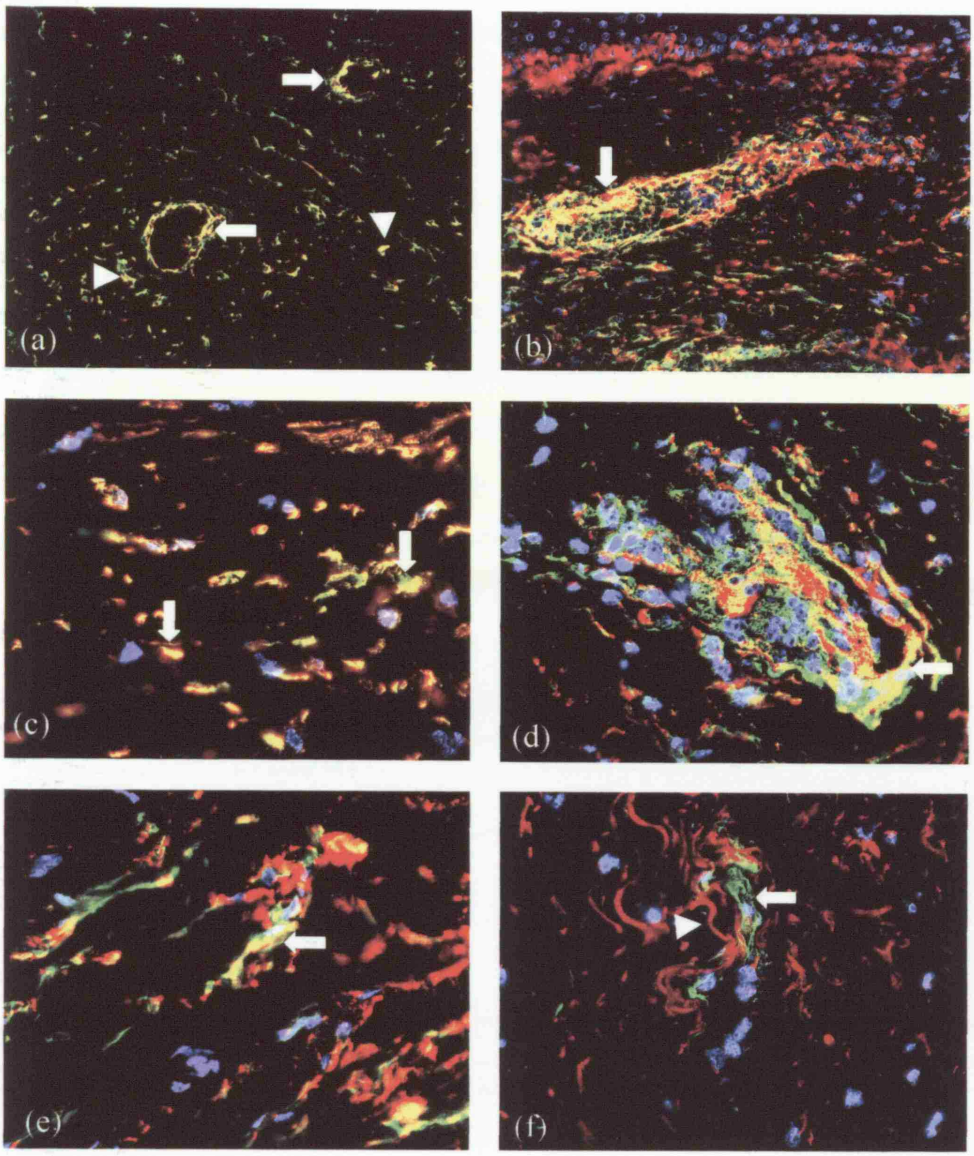


**Figure 4.7.**

**Cellular localisation of ED-A FN using double immunofluorescence labelling.**

Cryosections from dcSSc skin were labelled with antibodies against α-SMA, Thy-1, ED-A FN and PAL-E. Immunofluorescence for Thy-1 (green colour) colocalised with α-SMA (red colour) in the vessel wall (arrow, yellow colour, **a)** and in interstitial cells (arrowhead, yellow colour, **a**). Immunofluorescence for ED-A FN (red colour) colocalised with Thy-1 (green colour) in the microvascular wall (arrow, yellow colour, **b**) and in interstitial cells (arrows, yellow colour, **c**). Colocalisation between ED-A FN (red colour) and α-SMA (green colour) was detected in the vessel wall (arrow, yellow colour, **d**) and in interstitial cells (arrow, yellow colour, **e**). Immunofluorescence for ED-A FN (arrowhead, red colour, **f**) did not colocalise with PAL-E expressing endothelial cells (arrow, green colour, **f**). Original magnification **a, b** x20, **c-f** x40.

To identify collagen-synthesising cells in dcSSc skin, multiple labelling analyses were carried out with antibodies against LOX, α-SMA, ED-A FN and Thy-1. Within the microvascular wall, LOX and α-SMA immunofluorescence did not appear to colocalise (Figure 4.8a). Colocalisation between LOX and PAL-E expressing endothelial cells was detected in a proportion of microvessels (Figure 4.8b). Examination of dcSSc samples positive for both myofibroblasts and LOX expressing cells, revealed little colocalisation between α-SMA expressing myofibroblasts and collagen-synthesising cells (Figure 4.8c), suggesting that myofibroblasts and collagen-synthesising cells were distinct populations. However, colocalisation between LOX and Thy-1 immunofluorescence was observed in dcSSc skin indicating that LOX expressing cells express the Thy-1 antigen (Figure 4.8d).

**Table 4.2: Expression of markers in specific cell types in dcSSc tissue**

| | **Pericytes** | **Endothelial Cells** | **Myofibroblasts** |
|---|---|---|---|
| α-SMA | + | - | + |
| ED-A FN | + | - | + |
| Thy-1 | + | - | + |
| LOX | - | + | - |

+ denotes positive immunostaining and - denotes negative immunostaining.

### 4.3.5 Identification of proliferating cells in dcSSc

To determine whether the appearance of myofibroblasts was accompanied by cell proliferation, the expression of proliferating cell nuclear antigen (PCNA) was analysed. In normal skin, PCNA immunostaining was detected in epidermal cells, hair follicles and sweat glands (Figure 4.9a). Little or no immunostaining for PCNA was seen in interstitial fibroblast-like cells or microvessels. In two dcSSc samples, PCNA immunostaining was detected in dermal fibroblast-like cells (Figure 4.9b) and in microvessels (Figure 4.9c). These two dcSSc samples also contained myofibroblasts and increased ED-A FN expression. Double immunofluorescence labelling demonstrated colocalisation between PCNA and α-SMA immunofluorescence indicating pericyte proliferation (Figure 4.9d and 4.9e). Colocalisation between PAL-E and PCNA was also seen (Figure 4.9f). Serial dcSSc sections stained with PCNA and PAL-E revealed that PCNA immunostaining was present in 14% of PAL-E positive microvessels compared with 3% of normal sections ($p<0.05$).

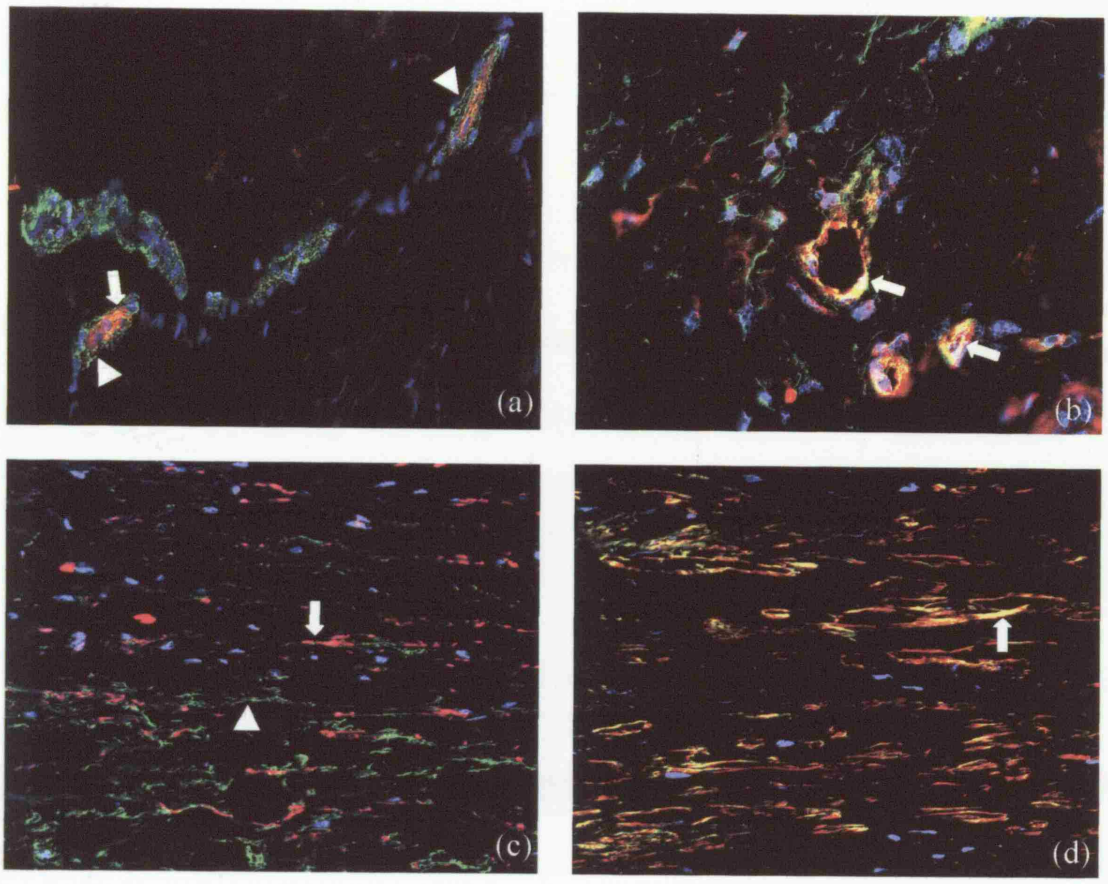


**Figure 4.8.**

**Cellular localisation of LOX using double immunofluorescence labelling.**

Cryosections from dcSSc skin were labelled with antibodies against LOX, α-SMA, PAL-E and Thy-1. Immunofluorescence for α-SMA (arrowhead, green colour, **a**) did not colocalise with immunofluorescence for LOX within microvessels (arrow, red colour, **a**). However, immunofluorescence for LOX (green colour) and PAL-E (red colour) did show some colocalisation within the vessel wall (arrows, yellow colour, **b**). In the interstitium, LOX immunofluorescence (arrow, red colour, **c**) did not colocalise with α-SMA immunofluorescence (arrowhead, green colour, **c**). Colocalisation between LOX and Thy-1 was observed in interstitial cells (arrow, yellow colour, **d**). Original magnification **a,b** x40, **c,d** x20.

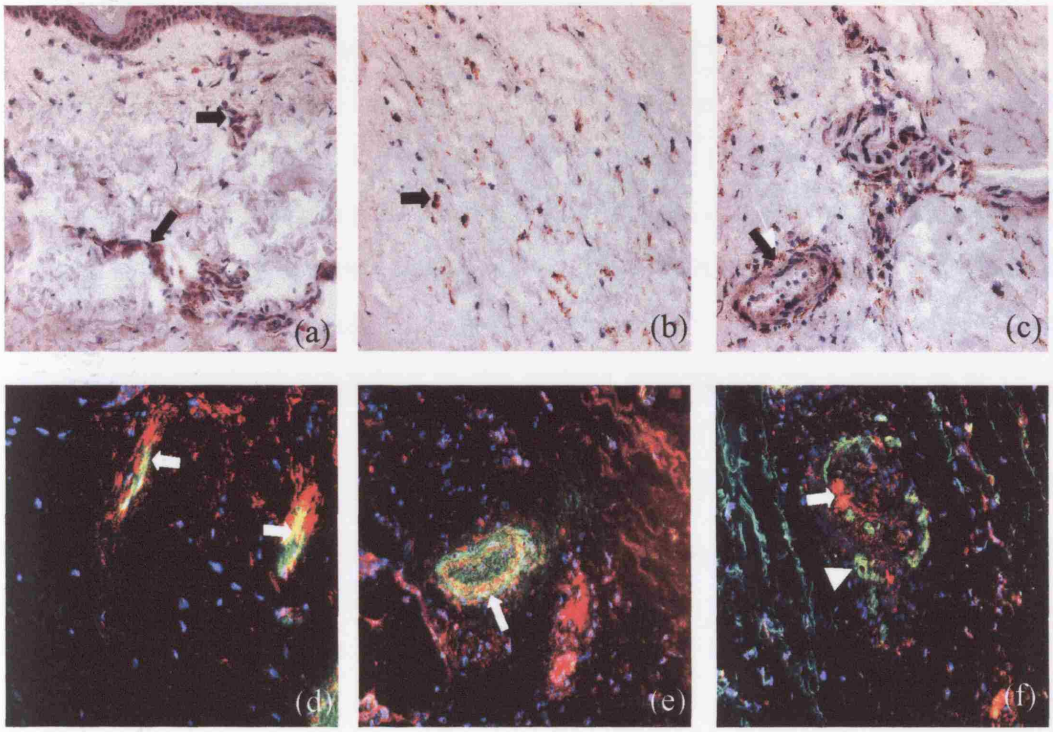


**Figure 4.9.**

**Distribution of proliferating cells in normal and dcSSc skin.**

Cryosections from normal (**a**) and dcSSc (**b and c**) were stained with an anti-PCNA antibody. In normal skin, PCNA immunostaining was restricted to cells within the epidermis and sweat glands (arrows, **a**). In two out of ten dcSSc samples, PCNA was detected in fibroblastic cells (arrows, **b**) and in microvessels (arrows, **c**). Cryosections were double-stained with combination of antibodies against PCNA and α-SMA (**d and e**) or PCNA and PAL-E (**f**). PCNA is labelled with Texas Red (red colour) while α-SMA and PAL-E are labelled with FITC (green colour). Colocalisation was detected with PCNA and α-SMA antibodies within the microvasculature (arrows, yellow colour, **d and e**). When used in combination with PAL-E, PCNA-labelled cells (arrows, **f**) were predominantly located adjacent and abluminal to endothelial cells (arrowheads, **f**). Original magnification x20.

### 4.3.6 Correlation of immunohistochemistry with clinical findings

After assessment of the immunohistochemical findings (Table 4.3), dcSSc patient samples could be divided in the following way:

(i) Evidence of myofibroblasts and ED-A FN

(ii) Evidence of collagen synthesis only

(iii) Evidence of myofibroblasts/ED-A FN and collagen synthesis

(iv) No evidence of either myofibroblasts/ED-A FN or collagen synthesis.

The mean disease duration and skin score of each group was then compared using an ANOVA analysis in order to determine whether these parameters could be associated with the immunohistochemical findings. No significant association was found between either mean disease duration ($p=0.11$) or skin score ($p=0.97$) and any of the immunohistochemical groups. The pattern of capillary damage in eight of ten dcSSc patients was assessed according to the criteria established by Cutolo et al (92). Of these eight patients, three had an active pattern of capillary damage while five displayed a late pattern of damage (Figure 4.10). However, no significant association could be found between patterns of capillary damage and our immunohistochemical groups ($p=0.33$).

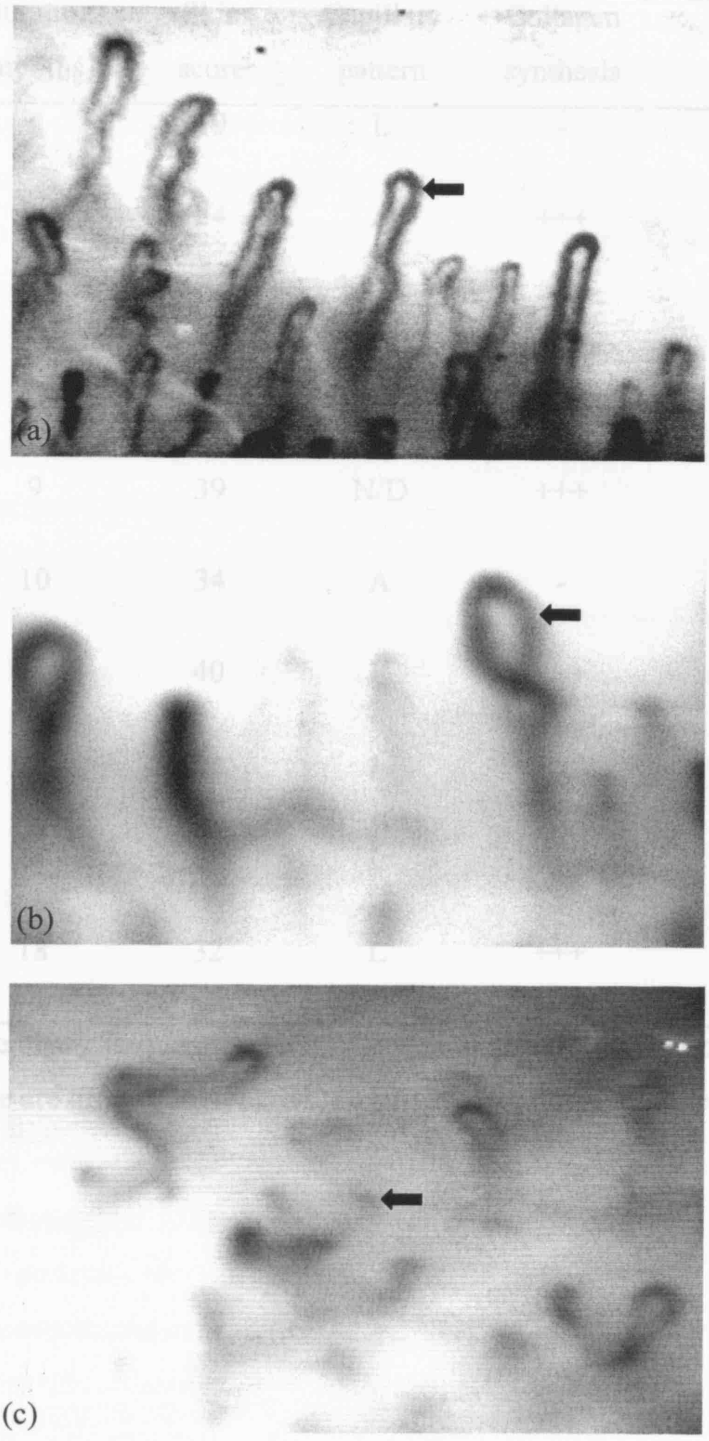


**Figure 4.10.**

**Nailfold capillaroscopy of normal and dcSSc patients.**

In normal tissue, nailfold capillaries are numerous (arrow, **a**). In dcSSc, the active pattern of capillary damage is characterised by the presence of frequent giant capillaries (arrow, **b**) accompanied by moderate capillary loss and disorganisation of capillary architecture. Late disease pattern was characterised by severe capillary disorganisation (arrow, **c**) with loss of capillaries. Magnification x150.

**Table 4.3: Correlation of immunohistochemical and clinical data**

| | Duration (months) | Skin score | Capillary pattern | Collagen synthesis | Myofibroblasts /ED-A FN |
|---|---|---|---|---|---|
| Patient 1 | 4 | 19 | L | - | +++ |
| Patient 2 | 6 | 24 | A | +++ | + |
| Patient 3 | 7 | 41 | A | - | +++ |
| Patient 4 | 9 | 38 | N/D | - | +++ |
| Patient 5 | 9 | 39 | N/D | +++ | +++ |
| Patient 6 | 10 | 34 | A | - | +++ |
| Patient 7 | 11 | 40 | L | +++ | - |
| Patient 8 | 14 | 36 | L | - | - |
| Patient 9 | 18 | 32 | L | - | - |
| Patient 10 | 18 | 32 | L | +++ | +++ |

Immunohistochemistry is quantified as; -, absent, +, weak, +++, strong. Patterns of capillary damage are graded as A, active, L, late or N/D, not determined.

## 4.4 KEY FINDINGS AND CONCLUSIONS

### Myofibroblasts and pericytes express ED-A FN in dcSSc

The data presented in this chapter confirms that ED-A FN expressing myofibroblasts are present in dcSSc but not in normal skin. Six of ten dcSSc samples contained both myofibroblasts and ED-A FN and in five of these samples, expression of both markers was detected exclusively in the lower reticular dermis. This finding is discussed in further detail in chapter 7. Increased expression of ED-A FN was detected only in those dcSSc samples containing myofibroblasts. This is the first report of ED-A FN expression by myofibroblasts in dcSSc skin. Double immunofluorescence labelling experiments confirmed the expression of ED-A FN by interstitial myofibroblasts and microvascular pericytes. ED-A FN is essential for myofibroblast formation (200), therefore, the expression of ED-A FN by pericytes may be significant in the differentiation of perivascular fibroblasts and pericytes into myofibroblasts. No colocalisation between ED-A FN and endothelial cells was observed. Myofibroblasts and ED-A FN were not detected in skin taken from patients with atrophic dcSSc, indicating that as the disease progresses from the fibrotic to atrophic stage, myofibroblasts do not persist in the dermis.

### Myofibroblasts are not the principle collagen-synthesising cell in dcSSc

Increased collagen synthesis as determined by LOX immunostaining was detected in four dcSSc samples where it was restricted to interstitial fibroblasts. Although some LOX expression was detected within the microvascular wall, double-labelling analysis demonstrated that LOX immunoreactivity did not colocalise with α-SMA, suggesting that pericytes do not express LOX in dcSSc skin. LOX expression colocalised with endothelial cells in agreement with previous findings (249) although its endothelial-specific function is unclear. In the two dcSSc samples that were positive for both LOX expression and the presence of myofibroblasts, little or no colocalisation between either marker was detected, indicating that in these two samples, myofibroblasts were not the predominant collagen-synthesising cells.

### Pericytes and myofibroblasts express Thy-1 in dcSSc

The analysis of Thy-1 immunostaining revealed the presence of two Thy-$1^{+ve}$ cell populations in normal skin. One population was identified as α-SMA expressing pericytes within the microvascular wall, the second population, which was α-$SMA^{-ve}$

and located interstitially, was identified as perivascular fibroblasts. In all dcSSc samples, interstitial expression of Thy-1 was increased as determined by immunohistochemistry. Western blot analysis of cultured fibroblasts showed that Thy-1 expression was not increased on dcSSc fibroblasts when compared to normal fibroblasts, suggesting that apparent interstitial increase *in vivo* is attributable to a redistribution of Thy-1 expressing cells. Using double immunofluorescence labelling with α-SMA and ED-A FN antibodies, a proportion of interstitial Thy-$1^{+ve}$ cells was identified as myofibroblasts within the reticular dermis. LOX expression was also found to localise to Thy-$1^{+ve}$ cells indicating that a proportion of Thy-$1^{+ve}$ population are collagen-synthesising fibroblasts. This is supported by the finding that Thy-$1^{+ve}$ fibroblasts produce 2- to 3-fold more collagen than Thy-$1^{-ve}$ fibroblasts (103).

**Increased pericyte proliferation in dcSSc**

Evidence of pericyte proliferation was detected in two dcSSc samples that contained myofibroblasts. Increased pericyte proliferation and an increased pericyte to endothelial cell ratio have been recently reported in dcSSc (195) and keloid skin (443).

Correlation of the immunohistochemical findings and clinical data revealed that the presence of myofibroblasts showed no significant association with either disease duration ($p=0.11$) or skin score ($p=0.97$). Additionally, no association was observed between the presence of myofibroblasts and either late or active capillary damage ($p=0.33$). While these preliminary findings are based on a relatively small cohort of patients, they suggest that further studies with a larger cohort, specifically designed to correlate immunohistochemical findings with clinical data on a patient by patient basis, may be highly informative.

In conclusion, these findings confirm that both microvascular pericytes and myofibroblasts express ED-A FN and Thy-1 in dcSSc skin. Moreover, there is evidence to suggest that myofibroblasts are not the principal collagen-synthesising cell in dcSSc skin. The data also shows that in dcSSc skin there is a significant re-distribution of Thy-$1^{+ve}$ and α-$SMA^{+ve}$ cells from the perivascular region to the interstitium possibly as a result of microvascular activation.

# CHAPTER 5: THE DIFFERENTIATION OF PERICYTES TO MYOFIBROBLASTS *IN VITRO*

## 5.1 INTRODUCTION

Evidence from a number of studies supports the hypothesis that the differentiation of pericytes into other mesenchymal cell types is a significant pathological mechanism in a number of human disorders (485). For example, the differentiation of pericytes into osteoblasts is thought to be a key mechanism in the initiation of vascular calcification, a common complication of many diseases including atherosclerosis, diabetes, end stage renal disease and calciphylaxis (62;86). Similarly, the differentiation of pericytes is believed to play a key role during the progression of fibrosis. In excessive dermal scarring, the differentiation of pericytes to fibroblasts occurs (439), while pericyte to myofibroblast differentiation has been reported in fibrotic liver (66;391) and kidney (186). It is unclear whether this type of cellular plasticity can be considered as transdifferentiation between completely different cell types or whether a common mesenchymal cell may function in different roles with small yet significant phenotypic modulation. It has been shown that pericytes express the cell surface protein STRO-1, a marker of bone marrow-derived stem cells with pluripotent capacity. This has led to the hypothesis that the microvasculature represents an adult stem cell niche (114;402).

The majority of studies investigating pericyte differentiation are based upon immunohistochemical analyses of changing phenotypic markers in tissue (66;186;391;439). Due to the technical difficulties associated with culturing pericytes, *in vitro* analyses of pericyte differentiation are limited. The majority of these studies have used bovine retinal pericytes (BRP) (135). It has been shown that under varying culturing conditions, BRP can differentiate into adipocytes, (135), chondrocytes (135) or smooth muscle cells (107). However, the use BRP as an *in vitro* model to study human pericyte behaviour is controversial. Moreover, the range of recombinant proteins and antibodies that cross-react with bovine material is limited. Ivarrson *et al.* successfully isolated human pericytes from highly vascularised placental tissue (214) and subsequently showed that these cells acquire a fibroblast-like morphology and synthesise collagen mRNA (214;439). However, little is known regarding these fibroblast-like cells with regards to their phenotype and function.

Data from the previous chapters show that pericytes in dcSSc skin share the same phenotype as pericytes in wound repair tissue and excessive scarring (439;440). Furthermore, pericytes and myofibroblasts express α-SMA, Thy-1 and ED-A FN in dcSSc skin, supporting the hypothesis that pericytes are progenitors for myofibroblasts in dcSSc. The aim of the experiments discussed in this chapter was to further characterise the phenotype and function of differentiated placental pericytes *in vitro*.

## 5.2 EXPERIMENTAL DESIGN

In order to investigate the differentiation of pericytes *in vitro*, cultured pericytes were grown *in vitro* and phenotypically assessed for evidence of myofibroblast differentiation. Furthermore, functional assays were carried out to compare the ability of pericytes and myofibroblasts to contract uniaxially tethered collagen lattices. Finally, the role of PDGFRβ signalling in the differentiation of pericytes was assessed.

## 5.3 RESULTS

### 5.3.1 Characterisation of microvascular pericytes

Microvascular fragments were isolated from human placenta and cultured in DMEM containing 10% FCS as described in section 2.2.2. After 5 to 7 days, significant numbers of pericytes had emerged from the microvascular fragments (Figure 5.1a and 5.1b). Pericytes appeared as large stellate-shaped cells and after a further period of 4 to 6 days, these cells had reached near confluence (Figure 5.1c). These cells are referred to as early passage pericytes. Cells were then trypsinised and sub-cultured. After a further 5 to 7 days, the cells appeared more elongated and spindle-like in appearance (Figure 5.1d), closely resembling cultured fibroblasts (Figure 5.1e). These cells are referred to as late passage pericytes. The cells were investigated further by immunofluorescence analysis. Cells were initially stained with the 3G5 antibody which has been previously used to identify cultured pericytes (135;315). Characteristic punctuate immunostaining for 3G5 was detected in early passage pericytes (Figure 5.2a), whilst no 3G5 immunostaining was seen in late passage pericytes or fibroblasts (Figure 5.2b and 5.2c).

Expression of α-SMA was also used to identify pericytes (416). α-SMA immunostaining revealed that 50% of early and late passage pericytes contained

prominent α-SMA-containing stress fibres (Figures 5.3a, 5.3b and 5.3e). By comparison, α-SMA stress fibres were detected in less than 10% of cultured fibroblasts (Figure 5.3c and 5.3e). Treatment of cultured fibroblasts with 2ng/ml TGF-β for 4 consecutive days to generate myofibroblasts (199) resulted in a substantial increase in α-SMA expression (Figure 5.3d and 5.3e). Analysis of whole cell lysates by Western blotting confirmed that α-SMA expression remained constant in pericyte cultures from early to late passage as they acquired a myofibroblastic phenotype (Figure 5.4).

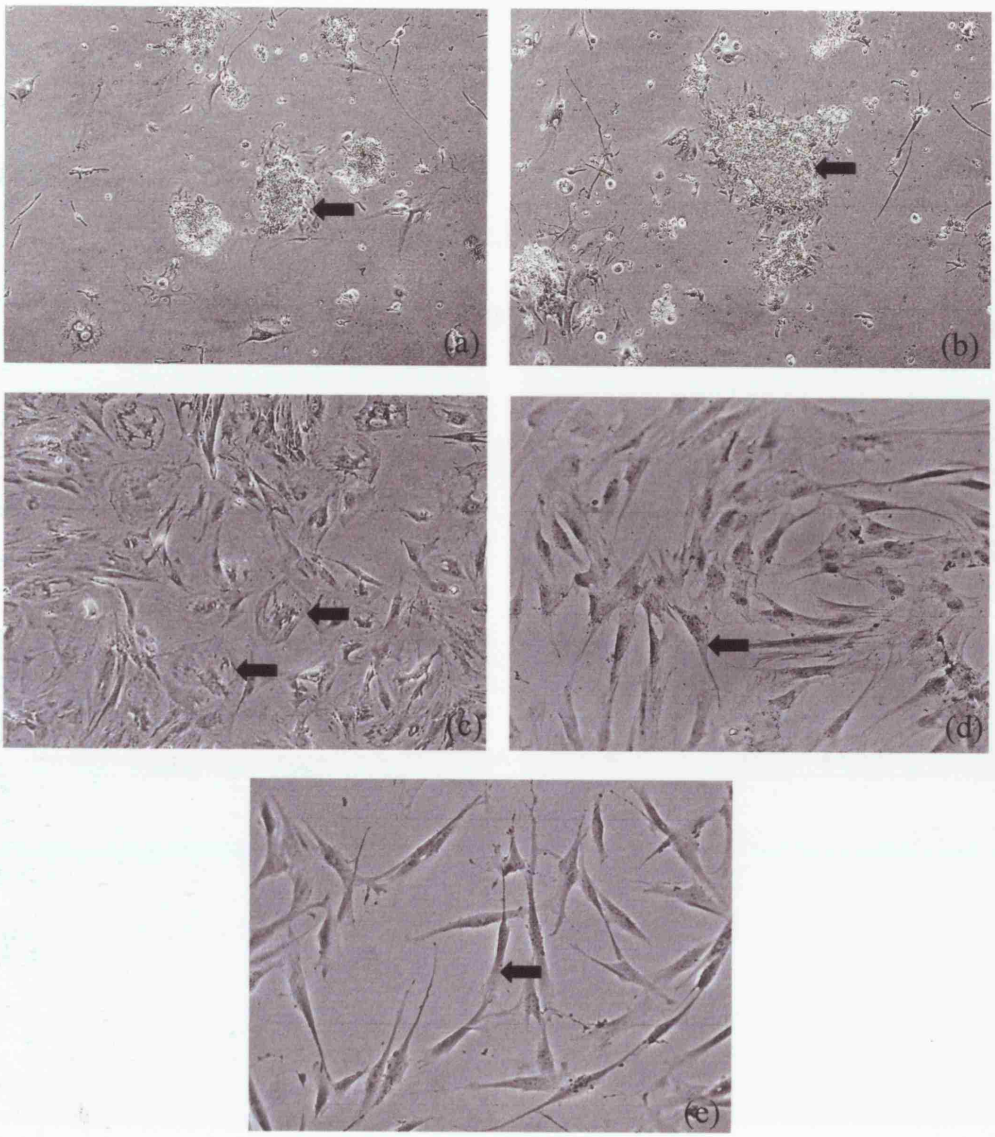


**Figure 5.1.**

**Isolation of cultured pericytes from microvascular fragments.**

Microvascular fragments (arrows, **a** and **b)** were isolated and cultured in DMEM containing 10% FCS. After 5-7 days, stellate shaped pericytes were detected growing from the fragments (arrows, **c**). After sub-culturing the pericytes appeared more elongated and spindle-like (arrows, **d**) morphologically similar to fibroblasts (arrow, **e**). Original magnification **a-e** x10.

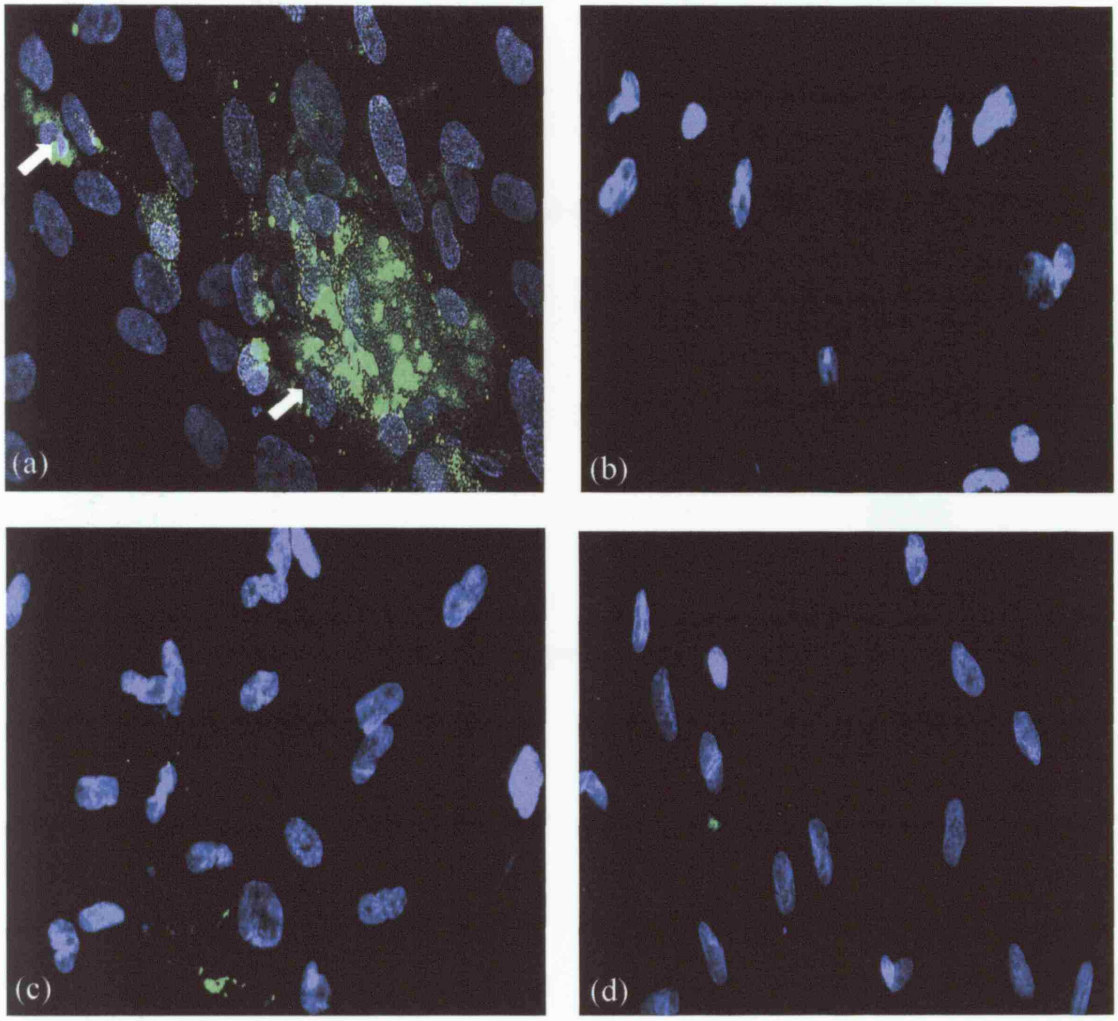


**Figure 5.2.**

**Expression of 3G5 by cultured pericytes.**

Cells growing from microvascular fragments stained positively for the pericyte marker 3G5 (arrows, **a**). After sub-culturing, 3G5 staining was not detectable in late passage pericytes (**b**). 3G5 staining was not detected in fibroblasts (**c**). Control staining with mouse IgG (**d**). Original magnification **a-d** x40.

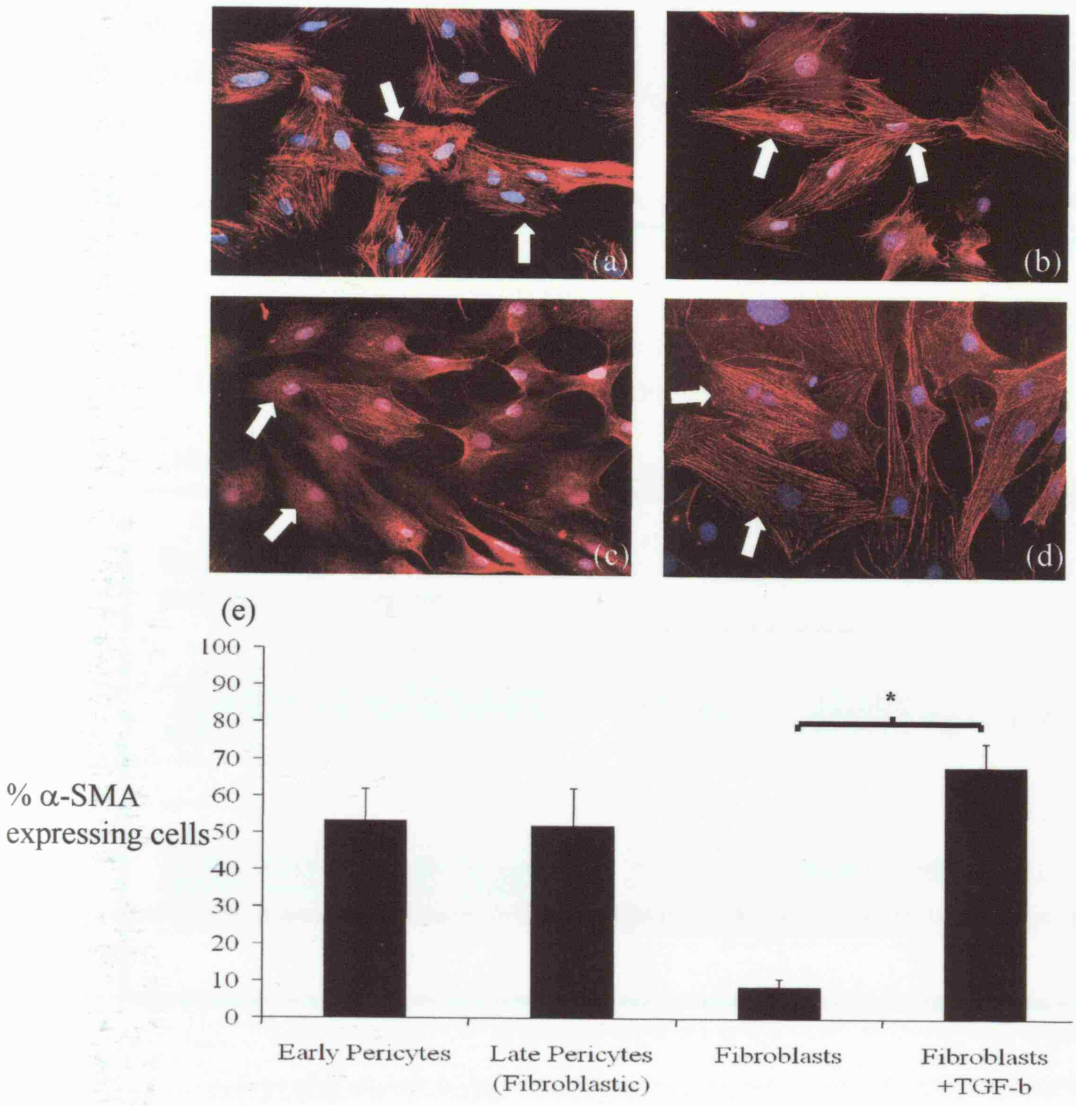


**Figure 5.3.**

**Persistence of α-SMA expression by immunofluorescence in sub-cultured pericytes.**

Cultured pericytes and fibroblasts were stained with an anti-α-SMA antibody. α-SMA+ve stress fibres were prominent in both early passage pericytes (arrows, **a**) and late passage pericytes that had acquired a fibroblastic morphology (arrows, **b**). The majority of cultured fibroblasts did not express α-SMA+ve stress fibres (arrows, **c**). Treatment of fibroblasts with 2ng/ml TGF-β for 4 days resulted in the formation of α-SMA expressing myofibroblasts, (arrows, **d**). Quantification of cell numbers revealed that over 50% of early and late passage pericytes and myofibroblasts express α-SMA compared with <10% of fibroblasts (**e**). *= $p<0.05$. Original magnification **a-d** x10.

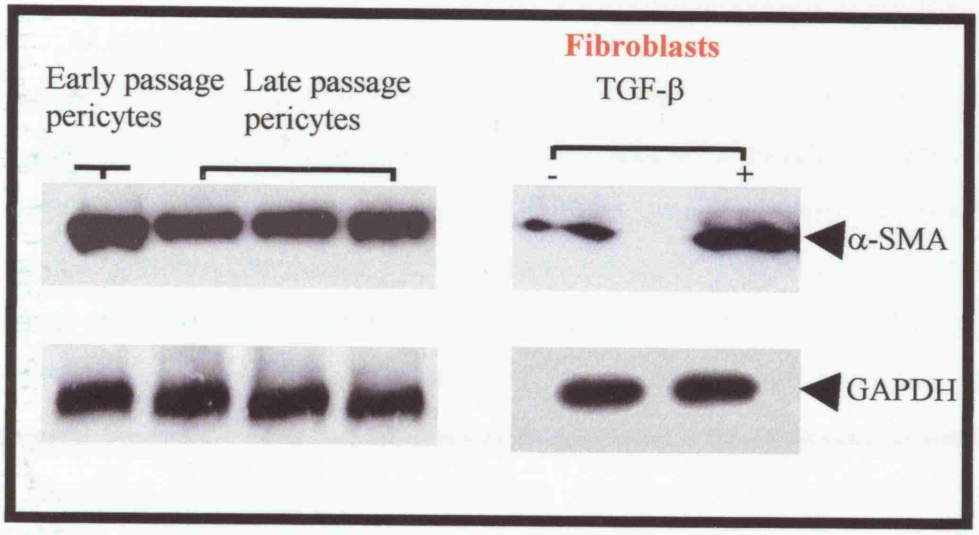


**Figure 5.4.**

**Persistence of α-SMA expression by Western blotting in sub-cultured pericytes.** Western blot analysis confirmed that α-SMA is expressed in early pericytes and late passage pericytes with a fibroblastic morphology. By comparison, cultured fibroblasts express reduced α-SMA, however, addition of TGF-β (2ng/ml) to cultured fibroblasts results in the formation of myofibroblasts and an increase in α-SMA expression. Equal protein loading was confirmed by probing the blots with an antibody against GAPDH.

### 5.3.2 Expression of ED-A FN and vinculin by cultured pericytes

Based upon the fibroblastic morphology of late passage pericytes, the expression of α-SMA and the loss of 3G5 staining it was hypothesised that pericytes had undergone a phenotypic transition to myofibroblasts. To investigate this further, the expression of ED-A FN and vinculin was assessed. Elevated expression of ED-A FN and vinculin has previously been used to distinguish myofibroblasts from fibroblasts *in vitro* (121;455). ED-A FN expression was detected in both early and late passage pericytes. Expression was localised both within the cell cytoplasm and in the intracellular space (Figure 5.5a and 5.5b). In agreement with previous studies, cultured fibroblasts displayed low baseline levels of ED-A FN expression (Figure 5.5c) (199). To promote myofibroblast differentiation, fibroblasts were treated with 2ng/ml TGF-β for 4 days as previously described (199). After TGF-β treatment, a marked elevation in ED-A FN expression by myofibroblasts was detected by immunofluorescence (Figure 5.5d). Analysis of whole cell lysates by Western blot analysis confirmed that early and late passage pericytes and myofibroblasts express elevated levels of ED-A FN compared to fibroblasts (Figure 5.4e). α-SMA+ve stress fibres terminate at a specialised adhesion complex called the fibronexus in myofibroblasts. Fibronexus junctions can be identified by increased incorporation of vinculin into adhesion complexes (121;455). In cultured fibroblasts, vinculin expression was confined to small adhesion complexes located at the cell periphery (Figure 5.6c). After treatment with TGF-β, fibronexus adhesion complexes in myofibroblasts were found to be considerably larger and more extensive (Figure 5.6d). In early and late passage pericytes, large adhesion complexes similar to those observed in myofibroblasts were detected (Figure 5.6a and 5.6b).

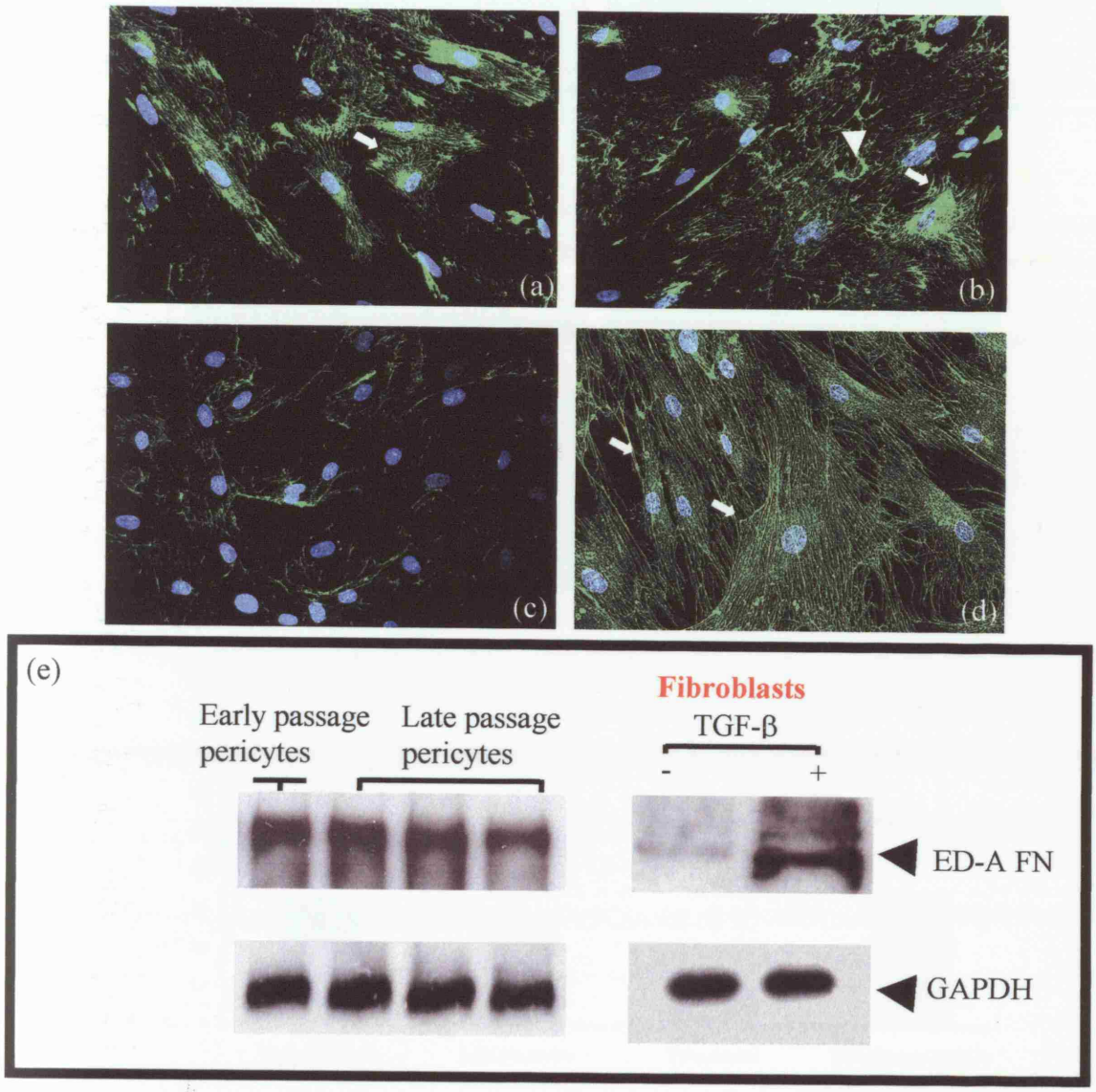


**Figure 5.5.**

**Cultured pericytes express ED-A FN.**

Cultured pericytes were stained with a monoclonal antibody against ED-A FN. Cytoplasmic ED-A FN staining was detected in both early and late passage pericytes (arrows, **a** and **b**). ED-A FN was also detected in the intracellular space (arrowhead, **b**). Fibroblasts expressed low levels of ED-A FN (**c**), however, a significant increase in ED-A FN expression was observed in fibroblasts after 4 days of treatment with TGF-β (2ng/ml) (arrow, **d**). Western blot analysis of cell lysates confirmed that ED-A FN was expressed by early and late passage pericytes and myofibroblasts only at lo levels in fibroblasts **(e)**. Equal protein loading was confirmed by probing the blots with an antibody against GAPDH.

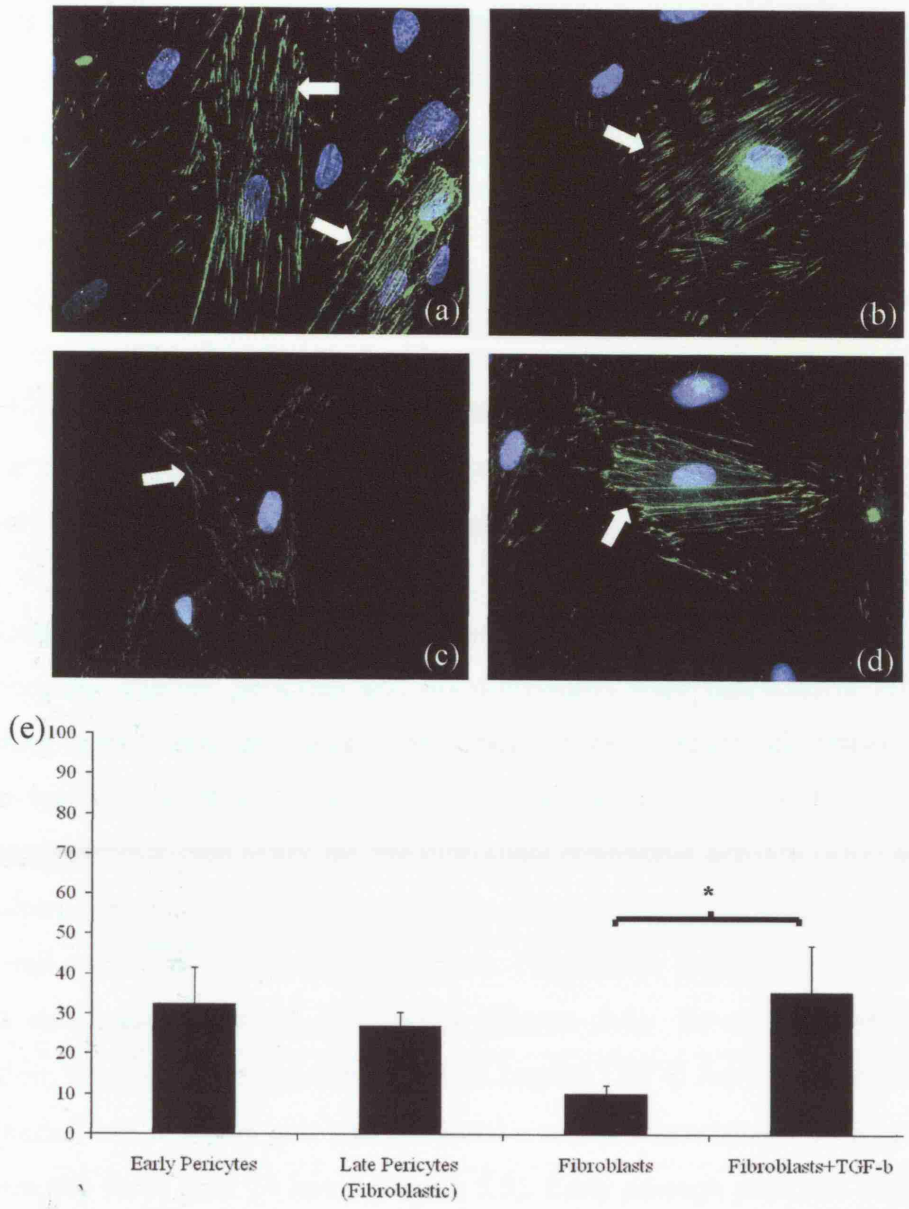


**Figure 5.6.**

**Cultured pericytes exhibit fibronexus adhesion complexes.**

To examine the distribution of fibronexus cell-adhesion complexes, pericytes and fibroblasts were stained with an anti-vinculin antibody. Cells with fibronexus complexes were detected in early (arrows, **a**) and late passage pericytes (arrow, **b**). By comparison, fibroblasts contained small adhesion complexes (arrow, **c**). Addition of TGF-β (2ng/ml) to fibroblasts for 4 days resulted in the formation of myofibroblasts and the presence of fibronexus complexes similar to those observed in pericytes (arrow, **d**). Quantification of the number of cells containing fibronexus complexes confirmed that early and late passage pericytes and myofibroblasts contained an increased number of cells with fibronexus complexes when compared with fibroblasts (**e**). Original magnification **a-d** x20.

Quantification of cell numbers demonstrated that 30% of early and late passage pericytes and myofibroblasts contained fibronexus adhesion complexes compared to 10% of fibroblasts ($p<0.05$) (Figure 5.6e). Increased vinculin in the fibronexus complex in myofibroblasts is thought to be due to increased incorporation of cytosolic vinculin into the cytoskeleton (199). To analyse this in pericytes, Western blotting of fractionated cell lysates was carried out. In control fibroblasts, vinculin expression was predominantly restricted to the cytosolic fraction with little expression in the cytoskeletal fraction. In agreement with previous findings, TGF-β treatment promoted the incorporation of vinculin into the cytoskeleton (Figure 5.7) (199). In both early and late passage pericytes and similarly in myofibroblasts, vinculin was detected in both the cytosolic and cytoskeletal fractions (Figure 5.7).

### 5.3.3 Collagen gel contraction by cultured pericytes

To determine whether pericytes and myofibroblasts were functionally homologous, the ability of early and late passage pericytes to contract uniaxially tethered collagen lattices was compared with that of fibroblasts and myofibroblasts. This is a well characterised functional assay for myofibroblast contractile activity (455) and the use of a culture force monitor (CFM) allows the force generated by contractile cells to be monitored over time and quantified (124). Fibroblasts contracted collagen lattices with a maximum force of 200 dynes (Figure 5.8). To promote myofibroblast formation, fibroblasts were pre-treated with 2ng/ml TGF-β for 4 days. Myofibroblasts were seeded into collagen gels and produced a robust contraction, exerting 750 dynes of contractile force after 24 hours (Figure 5.8). Early passage pericytes were found to potently contract collagen lattices, generating 500 dynes of contractile force after 24 hours (Figure 5.9). Late passage pericytes contracted collagen gels with a contractile force of 650 dynes ($p<0.05$). TGF-β did not increase the contractile force of early or late passage pericytes (Figure 5.9).

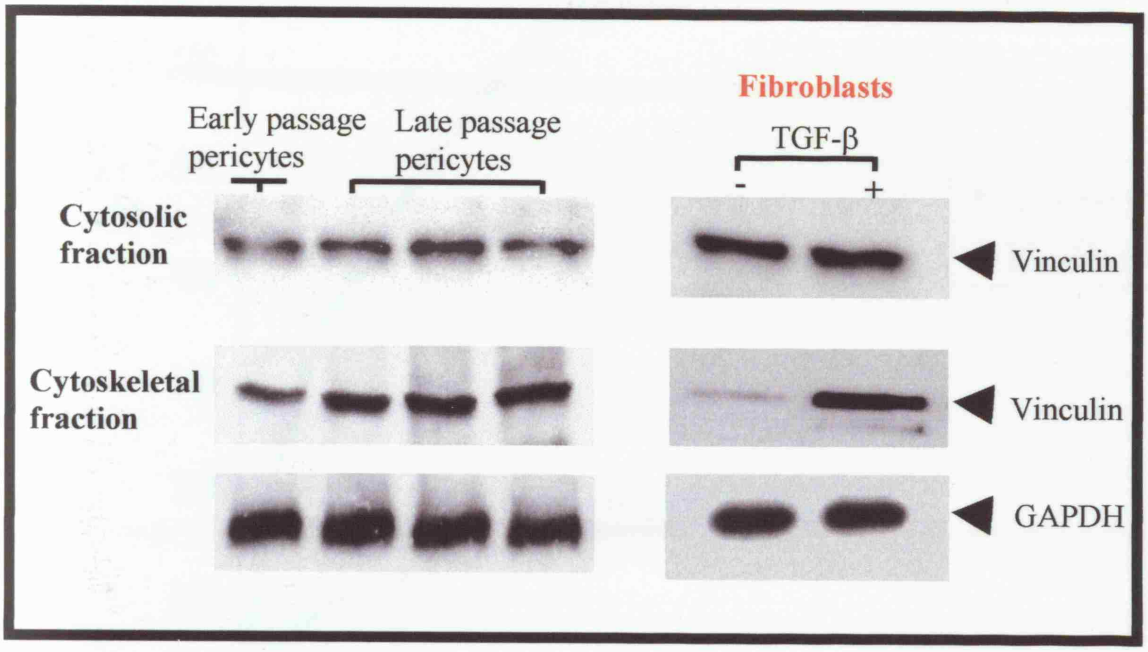


**Figure 5.7.**

**Expression of vinculin in the cytoskeletal fraction of cultured pericytes.**

Western blot analysis showed that following treatment with TGF-β (2ng/ml), that vinculin is incorporated into the cytoskeleton of fibroblasts. In early and late passage pericytes, vinculin expression in the cytoskeleton is maintained at elevated levels within fibronexus complexes. Equal protein loading was confirmed by probing the blots with an antibody against GAPDH.

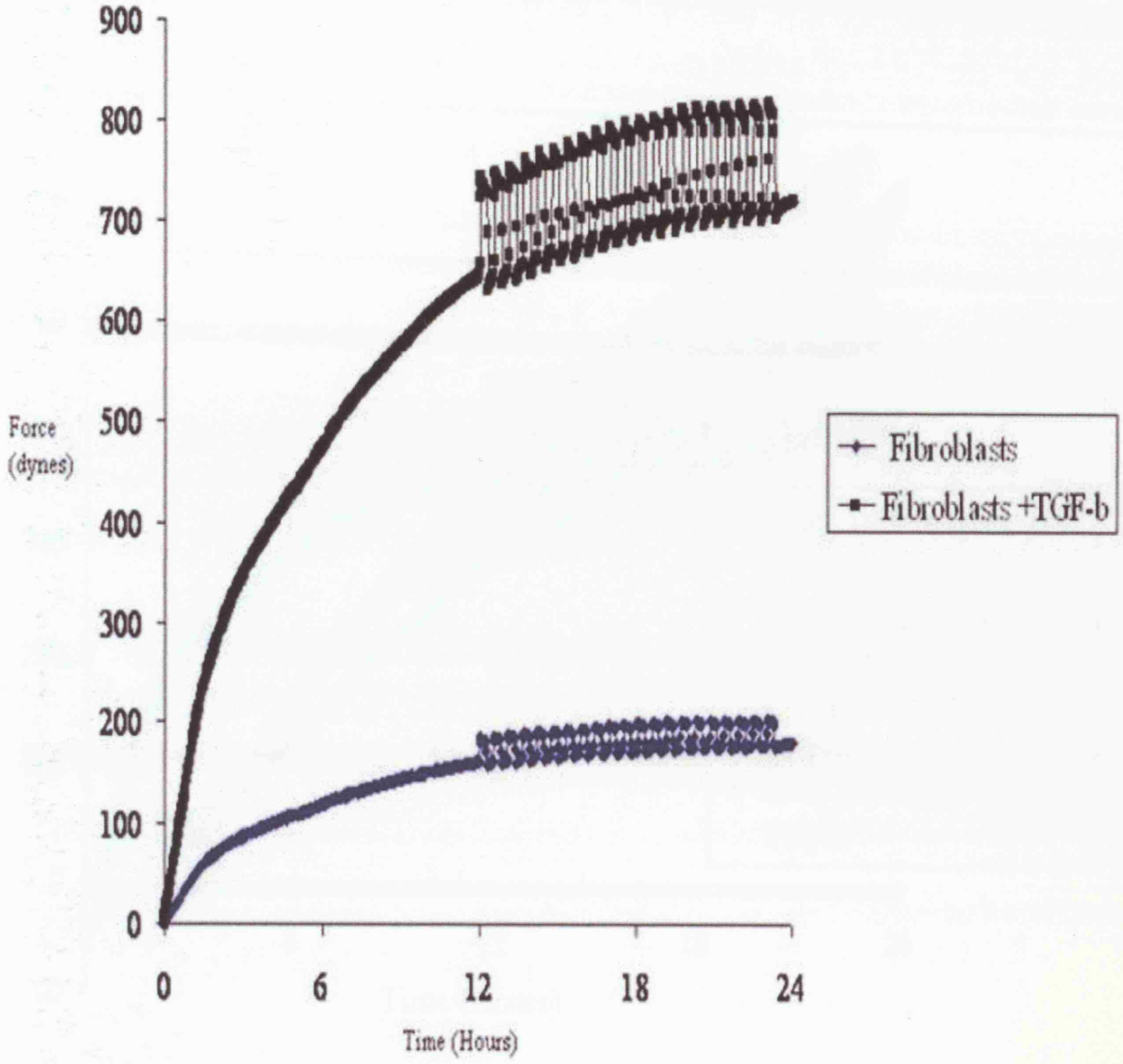


**Figure 5.8.**

**TGF-β promotes collagen gel contraction by fibroblasts.**

In order to compare the contractile ability of myofibroblasts and fibroblasts, the force generated by both cell types when contracting uniaxially tethered collagen gels was measured using a culture force monitor (CFM). Fibroblasts contracted collagen gels with a contractile force of approximately 200 dynes. Myofibroblasts, which were generated by addition of TGF-β (2ng/ml) to fibroblast, contracted collagen gels with a contractile force exceeding 700 dynes.

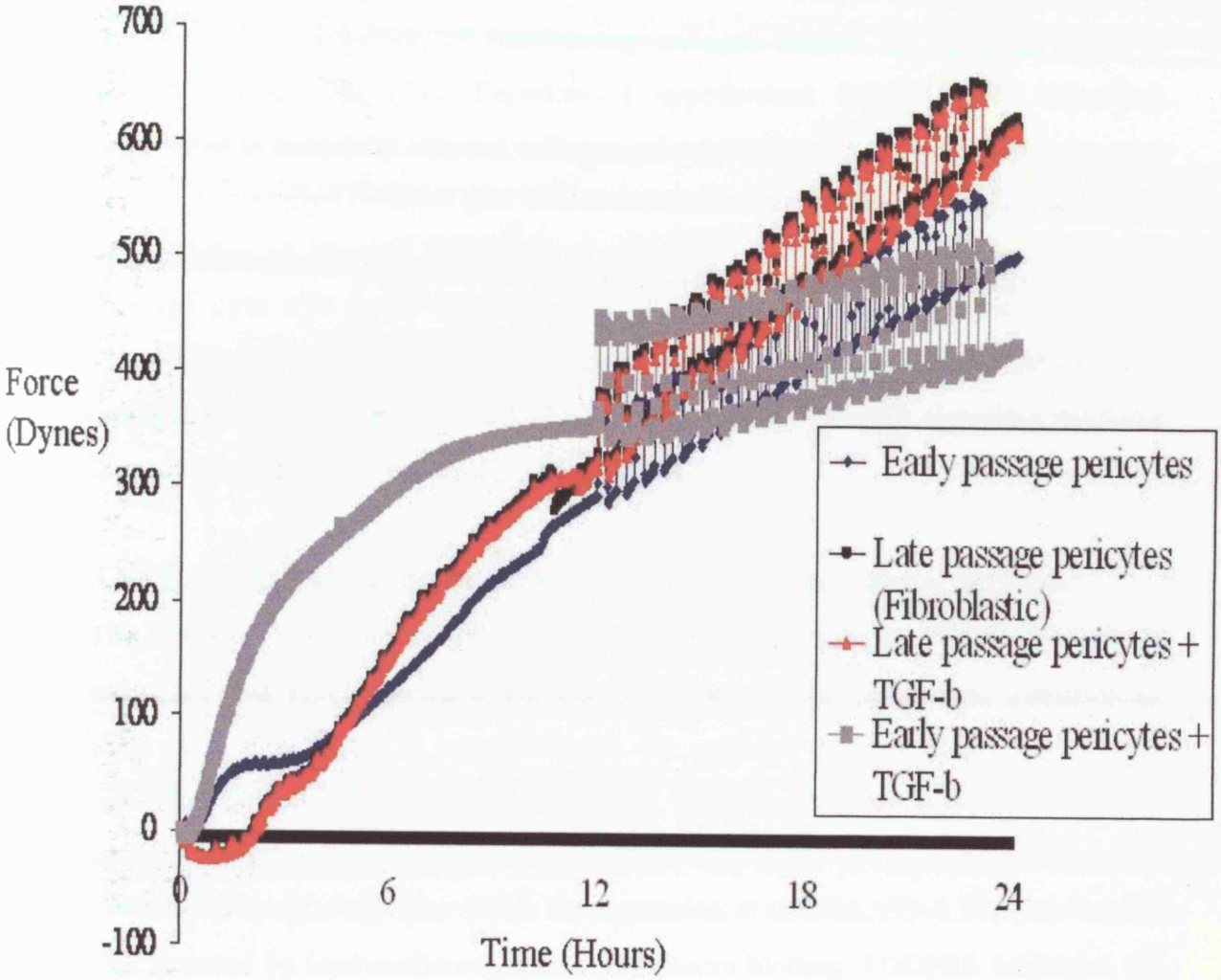


**Figure 5.9.**

**Cultured pericytes display similar contractile properties to myofibroblasts.**

Early and late passage pericytes were seeded into uniaxially tethered collagen lattices. Early passage pericytes generated 500 dynes of contractile force while late passage pericytes generated 650 dynes of contractile force. The addition of TGF-β (2ng/ml) to early and late passage pericytes did not significantly alter their ability to contract collagen gels.

### 5.3.4 PDGFRβ blockade inhibits collagen gel contraction

Previous studies have established that PDGF-BB is a potent stimulator of tethered collagen contraction by proto-myofibroblasts (2). Moreover, PDGFRβ signalling is thought to play a key role in pericyte differentiation *in vivo* (439) and PDGF-BB stimulates the contraction of free-floating collagen lattices by pericytes (426) or smooth muscle cells (71). Therefore, I hypothesised that PDGFRβ signalling contributed to uniaxially tethered collagen gel contraction by pericytes. Early passage pericytes contracted collagen gels with a contractile force of 500 dynes (Figure 5.10). The addition of 10ng/ml PDGF-BB to pericytes resulted in gel contraction with a force of over 650 dynes ($p<0.05$) (Figure 5.10). In contrast, treatment with the PDGFRβ inhibitor imatinib mesylate inhibited both baseline and PDGF-BB induced collagen gel contraction (Figure 5.10), confirming that PDGFRβ signalling mediates the ability of pericytes to contract collagen gels.

### 5.3.5 PDGFRβ blockade does not inhibit phenotypic transition of pericytes

The inhibition of pericyte-mediated collagen gel contraction by PDGFRβ blockade suggested that PDGFRβ signalling may contribute to the phenotypic transition of early passage pericytes to myofibroblasts. To examine this, the effect of PDGFRβ inhibition on this transition was determined. Imatinib mesylate was added to early pericyte cultures immediately after isolation and prior to the acquisition of a fibroblastic morphology after which the expression of α-SMA, ED-A FN and vinculin was assessed by immunofluorescence and Western blotting. PDGFRβ inhibition did not prevent early pericytes from acquiring a fibroblastic morphology after 5 days of sub-culturing. Furthermore, the expression of α-SMA stress fibres (Figure 5.11), ED-A FN (Figure 5.12) or vinculin within fibronexus junctions was not impaired (Figure 5.13). These results suggest that the phenotypic transition of pericytes to myofibroblasts is not dependent on PDGFRβ signalling.

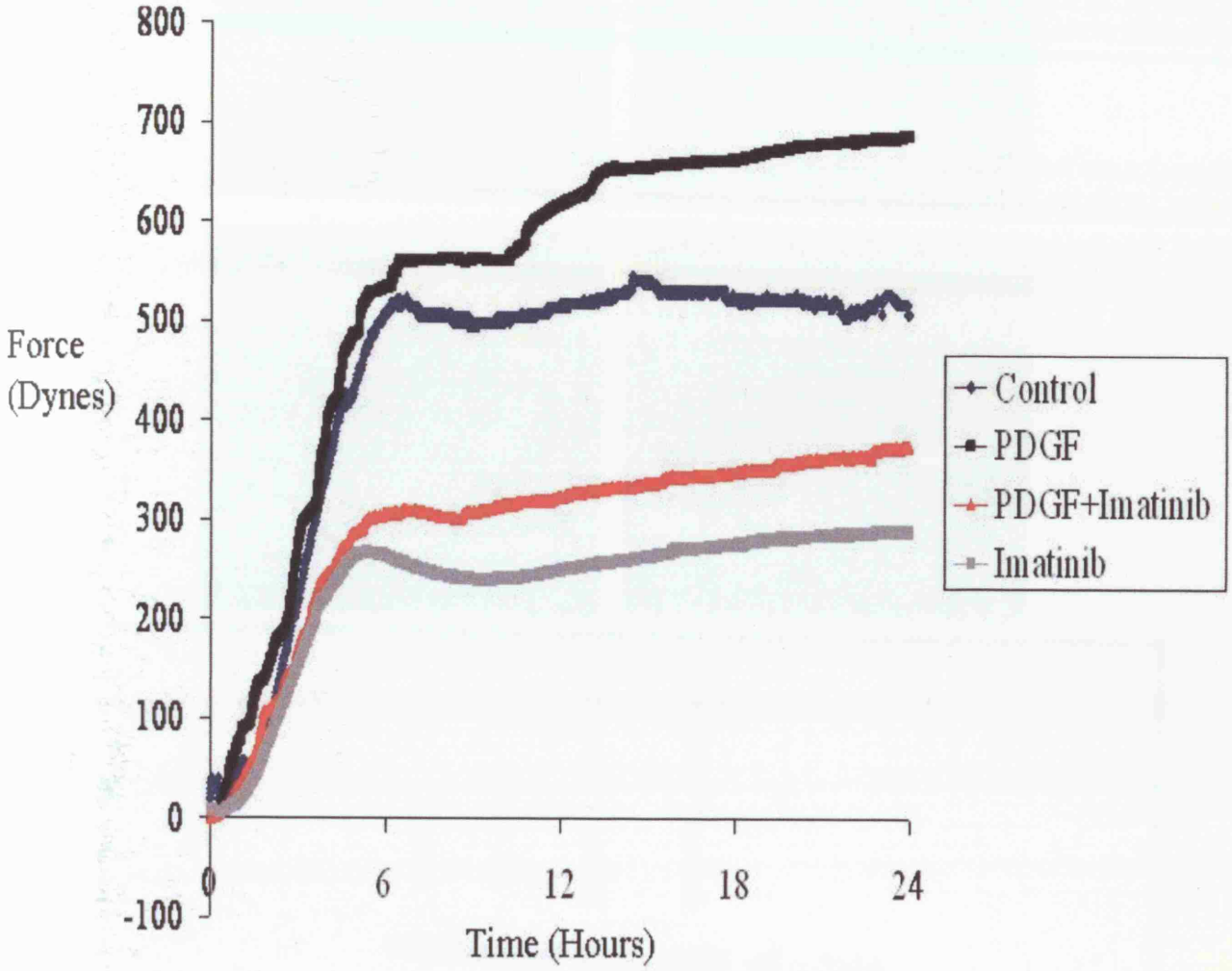


**Figure 5.10.**

**The contractile ability of pericytes is impaired by PDGFRβ inhibition.**

Early passage pericytes were seeded into uniaxially tethered collagen lattices. Addition of PDGF-BB (10ng/ml) significantly increased gel contraction by pericytes. However, both baseline and PDGF-BB stimulated gel contraction was inhibited by addition of imatinib mesylate (2μm).

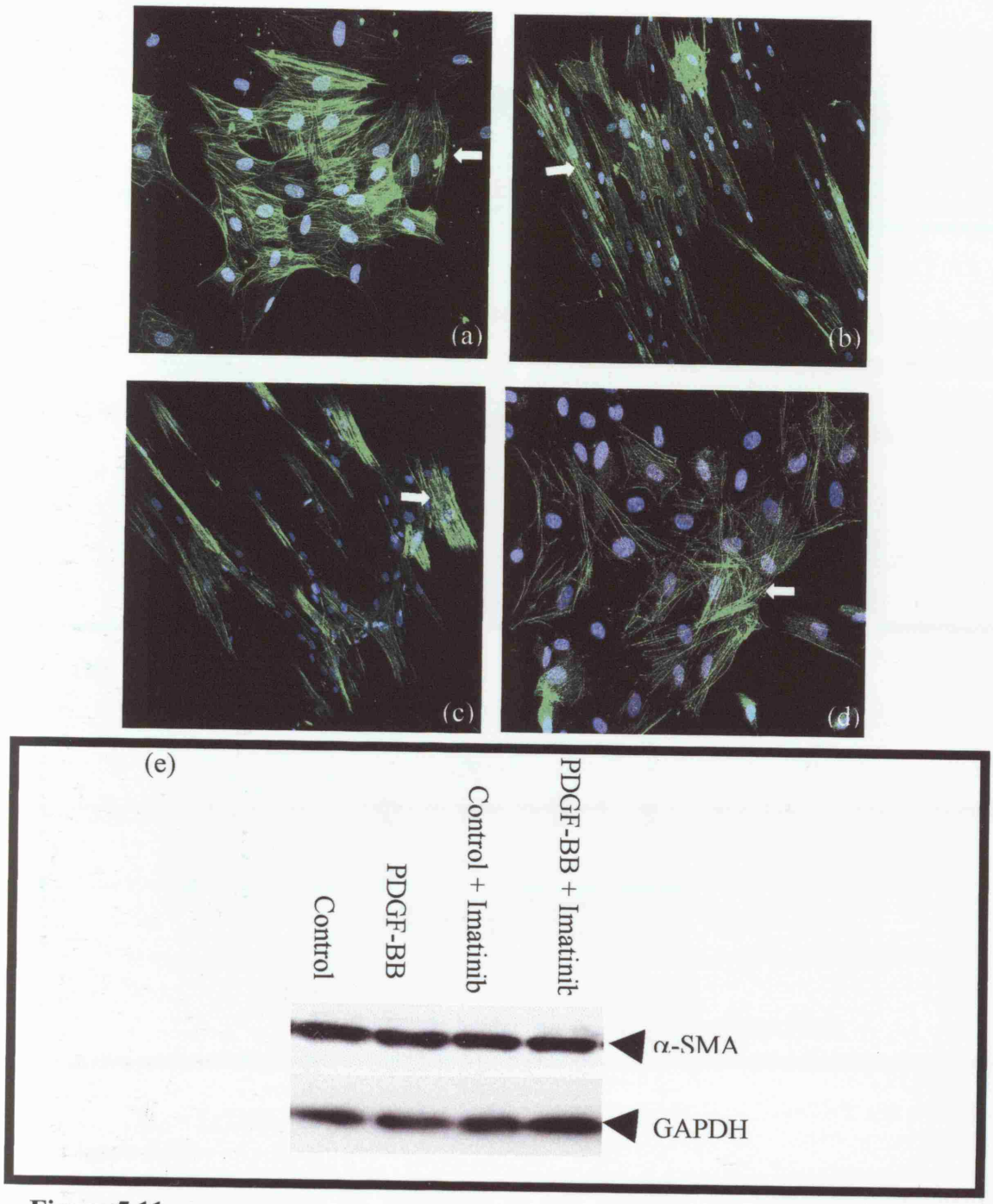


**Figure 5.11.**

**α-SMA expression by pericytes is not affected by PDGFRβ inhibition.** Immunofluorescence staining showing that α-SMA expression does not change in response to PDGF-BB (**b**), imatinib alone (**c**) and imatinib and PDGF-BB together (**d**) when compared to control cells (**a**). Western blot analysis confirming that ED-A FN expression is unaffected by imatinib treatment (**e**). Original magnification **a-d** x20. Equal protein loading was confirmed by probing the blots with an antibody against GAPDH.

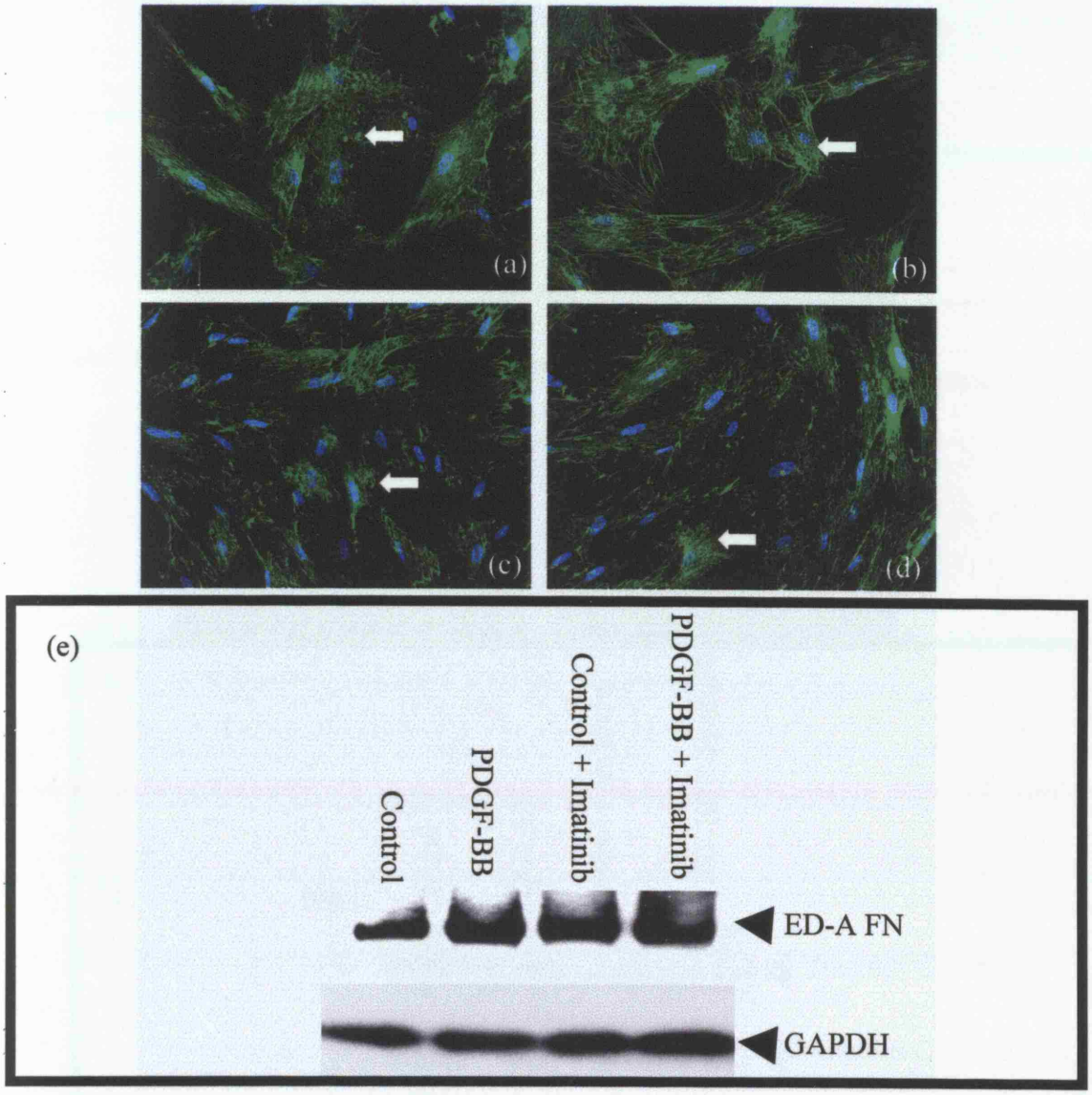


**Figure 5.12.**

**ED-A FN expression by pericytes is not affected by PDGFRβ inhibition.** Immunofluorescence staining showing that ED-A FN expression does not change in response to PDGF-BB (**b**), imatinib alone (**c**) and imatinib and PDGF-BB together (**d**) when compared to control cells (**a**). Western blot analysis confirming that ED-A FN expression is unaffected by imatinib treatment (**e**). Original magnification **a-d** x20. Equal protein loading was confirmed by probing the blots with an antibody against GAPDH.

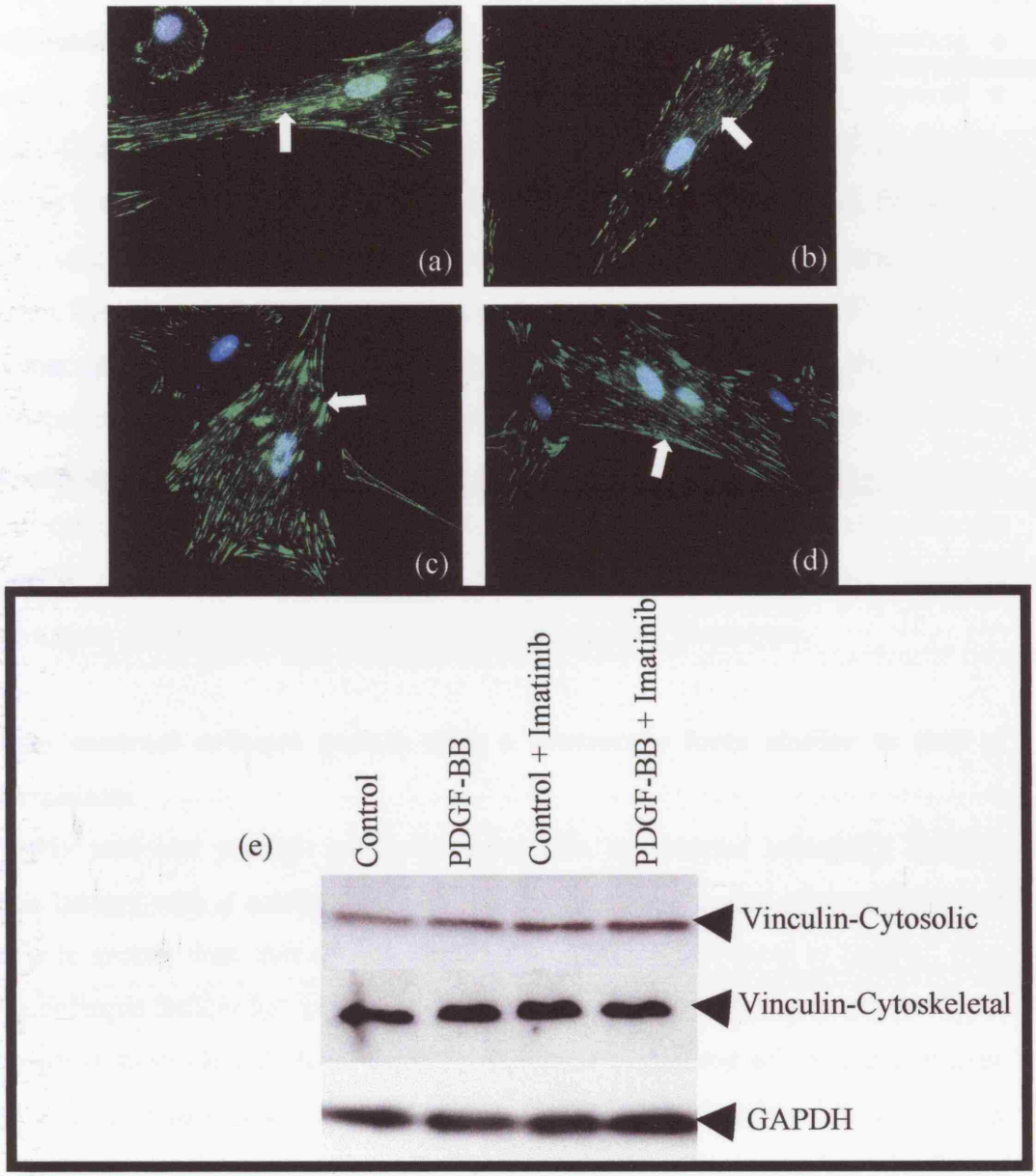


**Figure 5.13.**

**Vinculin expression by pericytes is not affected by PDGFRβ inhibition.** Immunofluorescence staining showing that vinculin expression does not change in response to PDGF-BB (**b**), imatinib alone (**c**) and imatinib and PDGF-BB together (**d**) when compared to control cells (**a**). Western blot analysis confirming that vinculin expression is unaffected by imatinib treatment in both cytosolic and cytoskeletal fractions (**e**). Original magnification **a-d** x20. Equal protein loading was confirmed by probing the blots with an antibody against GAPDH.

## 5.4 KEY FINDINGS AND CONCLUSIONS

### Pericytes differentiate into myofibroblasts *in vitro*

The data presented in this chapter demonstrate that cultured pericytes undergo a phenotypic transition to myofibroblasts *in vitro*. Moreover, cultured pericytes clearly demonstrated the capacity to contract tethered collagen lattices generating a contractile force comparable to myofibroblasts. Cultured pericytes acquired a fibroblast-like morphology and lost expression of the pericyte marker 3G5. Moreover, they were found to maintain the expression of α-SMA, ED-A FN and fibronexus adhesion junctions, which are considered to be typical myofibroblast characteristics. This is the first time that pericytes have been shown to exhibit elevated ED-A FN and fibronexus adhesion junctions *in vitro*, which supports the findings in the previous chapter that pericytes were found to express ED-A FN *in vivo*. It is noteworthy that unlike fibroblasts, early passage pericytes express known markers of myofibroblasts without stimulation by TGF-β. There are no reports of ED-A FN expression by pericytes in normal placenta, suggesting that culturing pericytes *in vitro* triggers a differentiation process that results in a myofibroblastic cell phenotype.

### Pericytes contract collagen lattices with a contractile force similar to that of myofibroblasts

Both early and late passage pericytes were able to contract uniaxially tethered collagen lattices with a similar degree of contractile force to that of myofibroblasts and a force greater than that of fibroblasts. The ability of pericytes to contract free-floating collagen lattices has previously been demonstrated (239), however, this is the first time that the contractile force has been measured in tethered gels and shown to be similar to that of specialised contractile cells such as myofibroblasts. In the current study, the addition of TGF-β did not significantly augment the contraction of collagen lattices by pericytes. *In vivo,* the differentiation of myofibroblasts from fibroblasts is thought to be primarily stimulated by the actions of TGF-β (154;455). It is also known that the addition of TGF-β to myofibroblasts *in vitro* increases their ability to contract tethered collagen lattices (466) in a SMAD-dependent mechanism (250). The reasons for the difference in responsiveness to TGF-β between myofibroblasts derived from fibroblasts and pericytes is unclear, however, it may represent functional heterogeneity between myofibroblasts derived from different cell types.

**PDGF-BB promotes pericyte-mediated gel contraction but not their differentiation to myofibroblasts**

The addition of PDGF-BB to pericytes significantly promoted collagen gel contraction. PDGF-BB stimulates contraction of tethered collagen lattices by myofibroblasts (175) and promotes the contraction of untethered collagen gels by kidney pericytes (226), however, untethered gels are not considered to be appropriate models for myofibroblast function as they lack inherent mechanical tension. PDGF-BB is thought to stimulate cell contraction by activating the RhoA GTPase to phosphorylate the myosin light chain kinase (178). This in turn directly phosphorylates myosin light chain resulting in fibre contraction (11;80). Although PDGF-BB did increase the contractile ability of pericytes it did not enhance the synthesis of ED-A FN and fibronexus adhesion complexes. Addition of the PDGFRβ inhibitor imatinib mesylate inhibited both baseline and PDGF-BB induced contraction by pericytes yet did not effect the expression of α-SMA, ED-A FN and fibronexus complexes. These data indicate that the mechanism of PDGF-BB induced gel contraction by pericytes is not related to an increase in the α-SMA or ED-A FN expression.

In summary, these findings suggest that pericytes spontaneously undergo a transition to a myofibroblast-like cell *in vitro*. These cells display all the characteristics of myofibroblasts, namely, elevated α-SMA, ED-A FN expression and the presence of fibronexus like adhesion complexes. Moreover, early and late passage pericytes can contract tethered collagen lattices with a contractile force comparable to that of myofibroblasts and significantly greater than fibroblasts.

# CHAPTER 6: THE EFFECTS OF PDGFRβ BLOCKADE ON TISSUE REPAIR: *IN VIVO* AND *IN VITRO* ANALYSIS.

## 6.1 INTRODUCTION

The expression of PDGFRβ by pericytes has been demonstrated in a number of conditions associated with increased matrix biosynthesis, including dcSSc (354), excessive dermal scarring (439) and wound healing (440). The data presented in the previous chapters demonstrates that pericytes show a strong phenotypic convergence with myofibroblasts in fibrotic tissue and that expression of PDGFRβ by pericytes is a key feature of fibrotic dcSSc lesions. Therefore, there is evidence to suggest that pericytes play a pivotal role during tissue fibrosis and scarring. Moreover, PDGFRβ is likely to be an important mediator in this process. However, due to the embryonic lethality of PDGFRβ knockout mice, little is currently known about the mechanism(s) by which PDGFRβ signalling modulates tissue repair and fibrosis *in vivo* (422).

Predominantly, *in vitro* studies have highlighted the potential role of PDGFRβ signalling in functions that are important for tissue repair and fibrosis (191). PDGF-BB is a potent mitogen and motogen for fibroblasts and pericytes (93;192) while cultured dermal fibroblasts lacking PDGFRβ show impaired mitosis and complete inhibition of migration (159). Addition of exogenous PDGF-BB *in vivo* increases both fibroblast proliferation and migration into excisional wounds, leading to both increased ECM production and enhanced wound tensile strength (342;343). Wound healing in mice (174) and humans (247) and granulation tissue formation in subcutaneous implants (267) are accelerated by the addition of PDGF-BB. Although these studies demonstrated that exogenous PDGF can enhance tissue repair, they shed no light on the mechanism(s) by which increased expression of endogenous PDGFRβ may contribute to tissue repair and fibrosis. Therefore, much is yet to be appreciated about the role of PDGFRβ during adult tissue repair.

To gain an insight into the contribution of PDGFRβ signalling to tissue repair and scarring *in vivo*, the impact of selective PDGFRβ inhibition on excisional wound healing was assessed. Particular emphasis was placed on how PDGFRβ signalling contributes to pericyte function in tissue repair and matrix remodelling.

## 6.2 EXPERIMENTAL DESIGN

The PDGFRβ inhibitor, imatinib mesylate was used to selectively inhibit PDGFRβ-mediated signalling. Imatinib binds to the ATP binding site of the PDGFRβ and completely abrogates PDGFRβ derived signalling *in vitro* and *in vivo* (52;313). Excisional wound repair in mice was chosen as a model system in which to assess the contribution of PDGFRβ signalling in tissue repair and fibrosis. Excisional wound healing is a tissue repair process that is characterised by the formation of highly vascularised granulation tissue followed by the increased synthesis of ECM components including fibrillar collagens and ED-A FN (296). Imatinib was administered at the onset of wound healing (75mgs/kg/day, described in 2.6.1) and the effects on wound closure, cell proliferation and migration, angiogenesis, pericyte recruitment and ECM biosynthesis was assessed.

## 6.3 RESULTS

### 6.3.1 The effect of imatinib treatment on wound repair *in vivo*

Excisional wounds ($4mm^3$) were made on the back of 6 to 8 week old collagen 1α2 transgenic reporter mice (Figure 6.1a). After 3 days, the wound diameter of control mice was reduced by 40% of the original size and by 70% after 7 days (Figure 6.1b and 6.1c). In contrast, imatinib-treated wounds were reduced by 20% after 3 days and 50 % after 7 days (Figure 6.1d and 6.1e). These differences were statistically significant between 3 and 7 days post-wounding ($p<0.01$) (Figure 6.1h). By day 10, the differences in wound diameters were no longer significant and by day 14, the wounds were completely closed and no longer visible. Histological analysis of sections stained with haematoxylin and eosin 7 days post-wounding confirmed impaired wound closure following imatinib treatment compared to control wounds (Figure 6.1f and 6.1g).

Overall wound morphology was assessed by massons trichrome staining. After 3 days a provisional granulation tissue had formed in control mice, which was highly cellular and punctuated with microvessels, indicating areas of angiogenesis (Figure 6.2a). In contrast, the granulation tissue in treated mice was poorly defined, comparatively hypocellular and characterised by the presence of large dilated microvessels (Figure 6.2b). At day 7 post-wounding, control wounds showed extensive cellular infiltration of monocytes and recruitment of fibroblasts, and evidence of ECM biosynthesis (Figure 6.2c). In contrast, imatinib-treated wounds were characterised by reduced cell density, dilated microvessels and little or no evidence of ECM deposition (Figure

6.2d). After 14 days, control wounds were characterised by scar tissue rich in ECM (Figure 6.2e). Scar tissue had also formed in treated wounds, however, with reduced ECM content (Figure 6.2f).

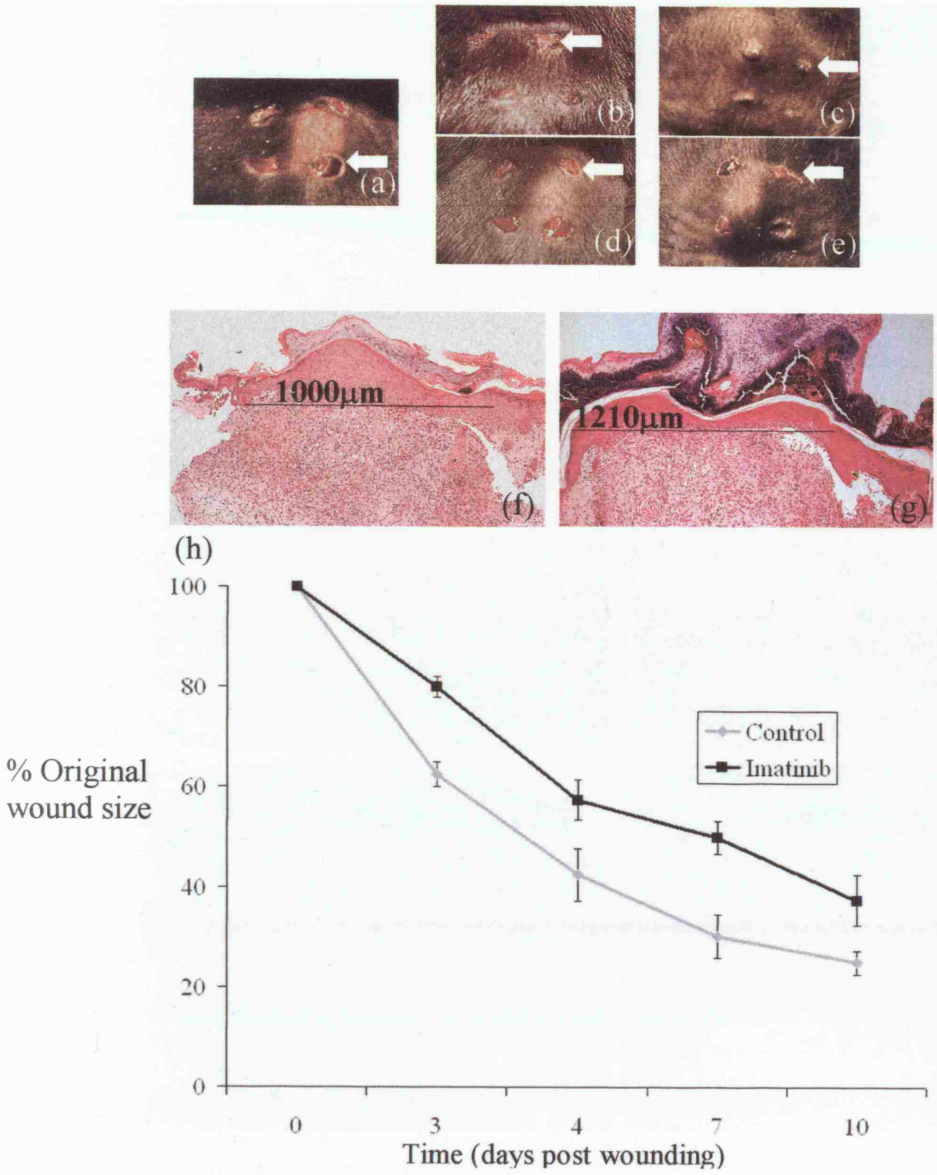


**Figure 6.1.**

**Wound closure is impaired in mice treated with imatinib.**

Four $mm^3$ punch wounds were made on the back of anaesthetized mice (arrows, **a**). After 3 days, wound diameters were noticeably smaller in control animals (arrows, **b**) in comparison to imatinib-treated animals (arrows, **d**). After 7 days, wound diameters in control wounds (arrows, **c**) were clearly reduced compared to imatinib-treated wounds (arrows, **e**). Analysis of sections stained with haematoxylin and eosin confirmed that after 7 days wound size were reduced in control animals (**f**) compared with imatinib-treated animals (**g**). Quantification of wound diameter over 10 days after injury. Results represent the mean $\pm$ s.e.m (**h**). Between 3 and 7 days post-wounding, the difference in wound diameter was significant ($p<0.05$). Original magnification **f,g** x10.

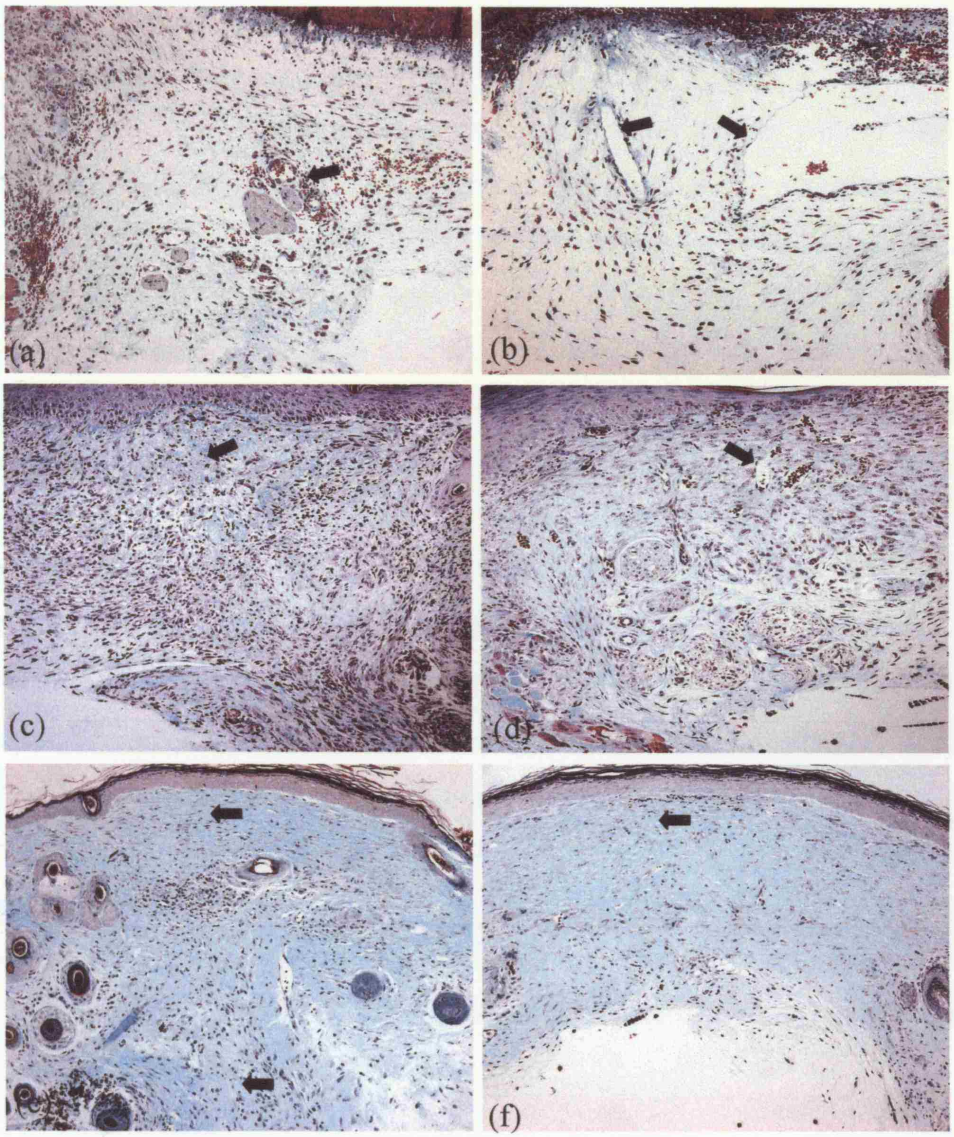


**Figure 6.2.**

**Imatinib treatment results in impaired wound healing.**

Massons trichrome staining after 3 days reveals granulation tissue forming in control mice (arrow, **a**). By contrast, imatinib-treated wounds are relatively hypocellular with large dilated microvessels (arrows, **b**). At 7 days post-wounding, newly deposited ECM is evident in control wounds (green colour, arrow, **c**) while imatinib-treated wounds show diminished matrix synthesis and abnormally distended microvessels (arrow, **d**). After 14 days, control wounds were characterised by extensive matrix throughout the resolving scar tissue (green colour, arrows, **e**). By comparison, ECM synthesis in imatinib-treated wounds is less extensive (arrow, **f**). Original magnification **a-f** x10.

### 6.3.2 The effect of imatinib treatment on fibroblasts and pericyte proliferation *in vitro* and during wound repair *in vivo*

The effect of imatinib treatment on cell proliferation during wound healing was assessed by BRDU incorporation. Immunohistochemical analysis of BRDU incorporation was carried out to identify proliferating cells. In control animals, 3 days post-wounding, BRDU immunostaining was evident in specific areas of the granulation tissue. The majority of BRDU-labelled cells were located at the wound margins, in the basal keratinocyte layer and in microvascular cells (Figure 6.3a). BRDU immunostaining was detected in both luminal endothelial cells and pericytes (Figure 6.3c). The addition of imatinib resulted in a substantial decrease in BRDU incorporation at the wound margins and basal keratinocyte layer after 3 days (Figure 6.3b). BRDU immunostaining of microvessels was also reduced as a result of imatinib treatment (Figure 6.3d). After 7 days, in control animals, BRDU-labelled cells were more uniformly distributed throughout the granulation tissue (Figure 6.3e). Seven days post-wounding, BRDU-labelled cells were more evident than after 3 days and were located throughout the wound tissue, however, overall numbers were still reduced in comparison to control tissue (Figure 6.3f). Quantification of the number of positively stained cells using image analysis confirmed that the reduction in BRDU incorporation after 3 and 7 days in treated tissues was statistically significant ($p<0.005$), (Figure 6.3g).

The principal PDGF-BB responsive cells in the dermis are fibroblasts and pericytes (191). Therefore, an *in vitro* approach was used to confirm that fibroblast and pericyte proliferation was inhibited by imatinib treatment. Increasing concentrations (1-100ng/ml) of PDGF-BB produced a marked increase in pericyte and fibroblast proliferation after a 48 hour incubation period in a dose-dependent manner up to 10ng/ml (Figure 6.4a). PDGF-BB at a concentration of 10ng/ml induced a robust mitogenic response in both cultured pericytes and fibroblasts after 48 hours treatment (Figure 6.4b and 6.4c). This response was significantly reduced by imatinib treatment ($p<0.005$), (Figure 6.4b and 6.4c). Serum-induced mitogenesis of pericytes and fibroblasts was also reduced by imatinib treatment (Figure 6.4b and 6.4c).

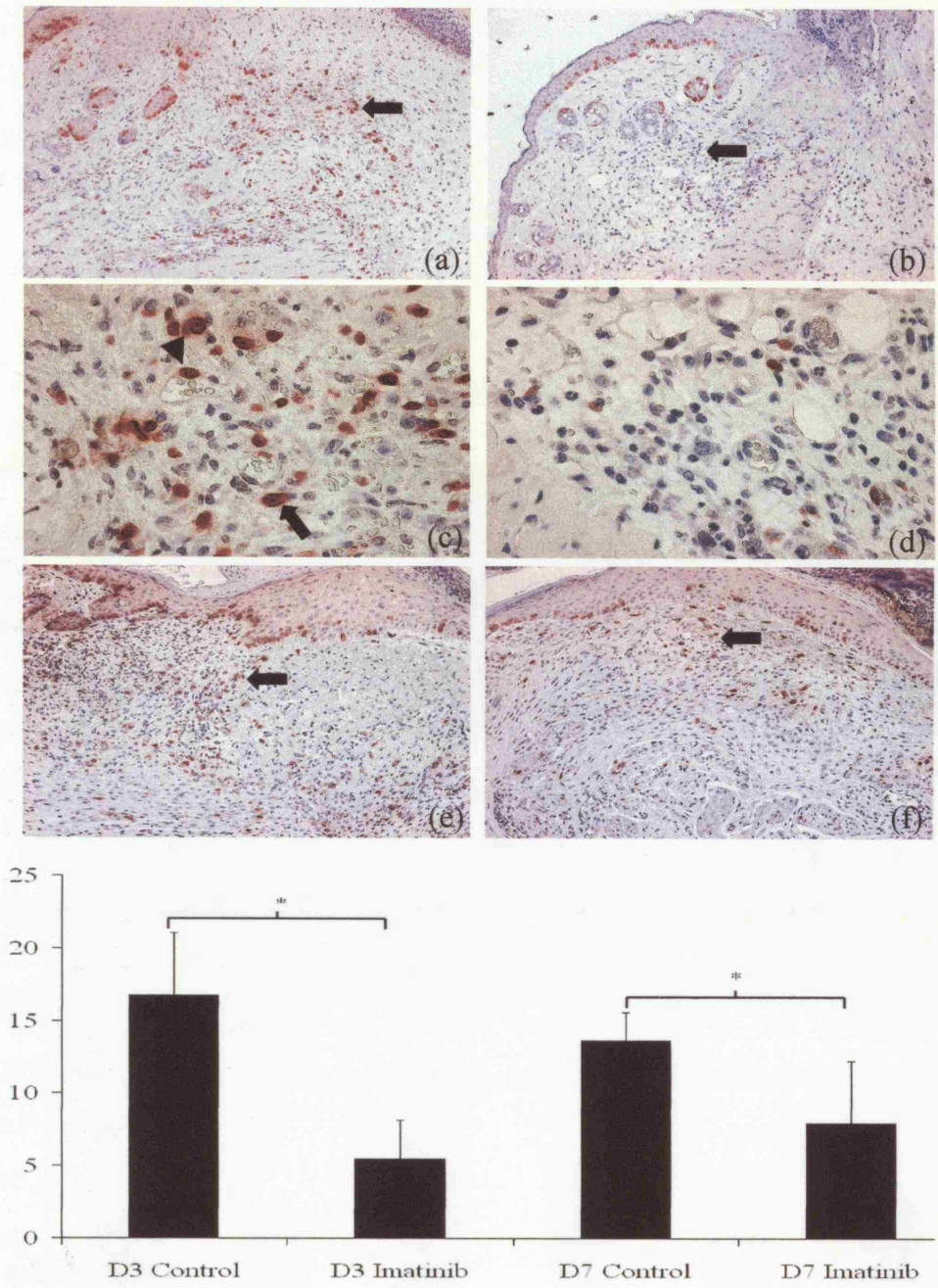


**Figure 6.3.**

**Cell proliferation is inhibited in imatinib-treated mice.**

Three days after injury, BRDU immunostaining, which was predominant at the wound margins in control animals (arrows, **a**) was significantly reduced in imatinib-treated animals (arrows, **b**). In control animals, BRDU immunostaining present in abluminal (arrows, **c**) and luminal microvascular cells (arrowhead, **c**) was reduced in imatinib-treated animals (**d**). After 7 days, BRDU immunostaining was present in the granulation tissue of both control and imatinib-treated animals (arrows, **e** and **f**). Quantification of BRDU stained cells confirmed that imatinib treatment produced a significant reduction in cell proliferation after 3 and 7 days (**g**). Results represent the mean $\pm$ s.d. *= $p<0.005$. Original magnification **a,b,e,f** x10 and **c,d** x40.

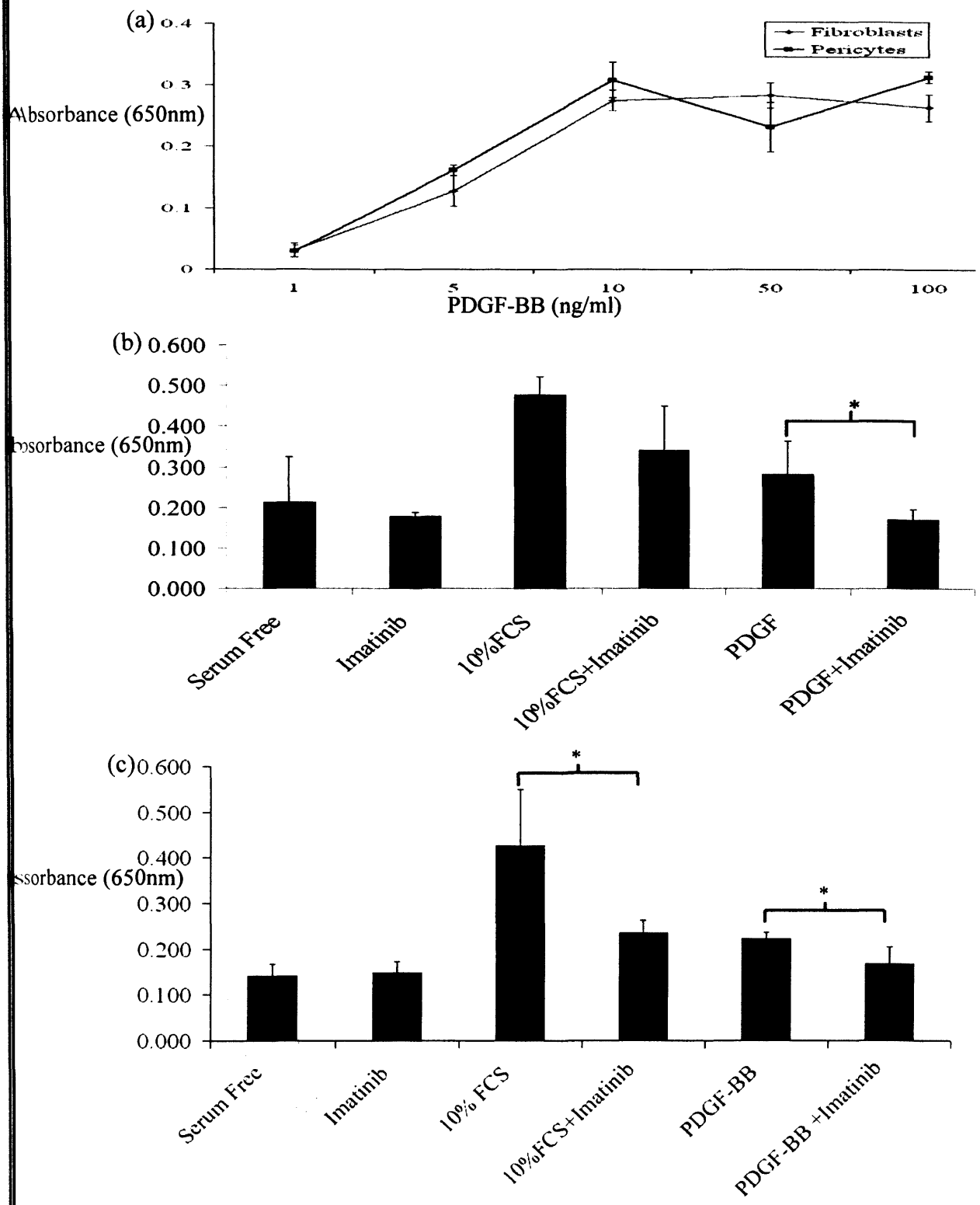


**Figure 6.4.**

**Inhibition of pericyte and fibroblast proliferation by imatinib *in vitro*.**

PDGF-BB produced a marked elevation of pericyte and fibroblast proliferation in a dose dependent manner up to 10ng/ml (**a**). Both 10% FCS and PDGF-BB (10ng/ml) induced stimulation of pericyte (**b**) and fibroblast (**c**) proliferation, was inhibited by treatment with imatinib. Results represent the mean $\pm$ s.d.;*= $p<0.05$.

### 6.3.3 Imatinib treatment does not affect apoptosis *in vivo* and *in vitro*

Imatinib treatment resulted in reduced cellularity in the granulation tissue. Therefore, the role of imatinib on apoptotic cell death was investigated in order to establish whether increased apoptotic cell death was responsible for the hypocellularity of imatinib-treated wounds. Analysis of day 7 wound sections by TUNEL staining demonstrated that apoptotic nuclei were evenly distributed throughout control and imatinib-treated wounds (Figure 6.5). Counting of apoptotic cell nuclei revealed no significant difference between control and imatinib-treated wounds (Figure 6.5e). The effect of imatinib on apoptosis on cultured fibroblasts and pericytes was also assessed *in vitro.* To induce apoptosis, fibroblasts and pericytes were treated with 100μM etoposide as previously described (302). TUNEL staining revealed extensive apoptosis in fibroblast (Figure 6.6b) and pericyte cultures (Figure 6.6d) with over 60% of cells showing evidence of apoptosis (Figure 6.6i). In comparison, little or no evidence of apoptosis was detected after the cells were treated with imatinib for 48 hours (Figure 6.6f and 6.6h).

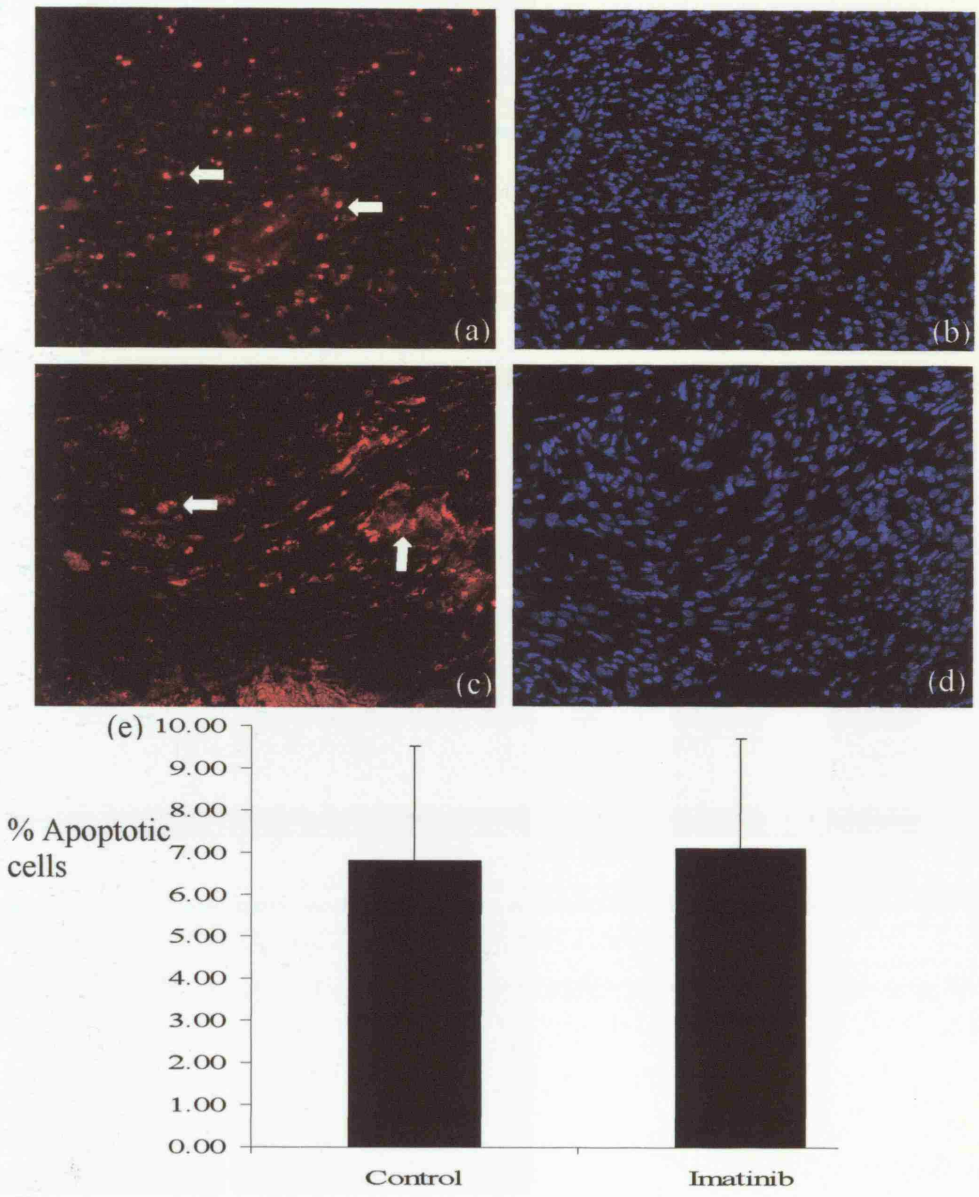


**Figure 6.5.**

**Imatinib treatment does not affect apoptotic cell death *in vivo.***

Apoptotic cell death in day 7 wounds was assessed by TUNEL staining. Apoptotic nuclei (arrows, red colour) were detected in both control (**a**) and imatinib-treated wounds (**c**). Cell nuclei were counterstained with DAPI (**b, d**). Analysis of the percentage of apoptotic cell nuclei in control and imatinib-treated sections revealed no significant difference (**e**) ($p=0.8$). Data shown is mean $\pm$ s.d. Original magnification **a-d** x10.

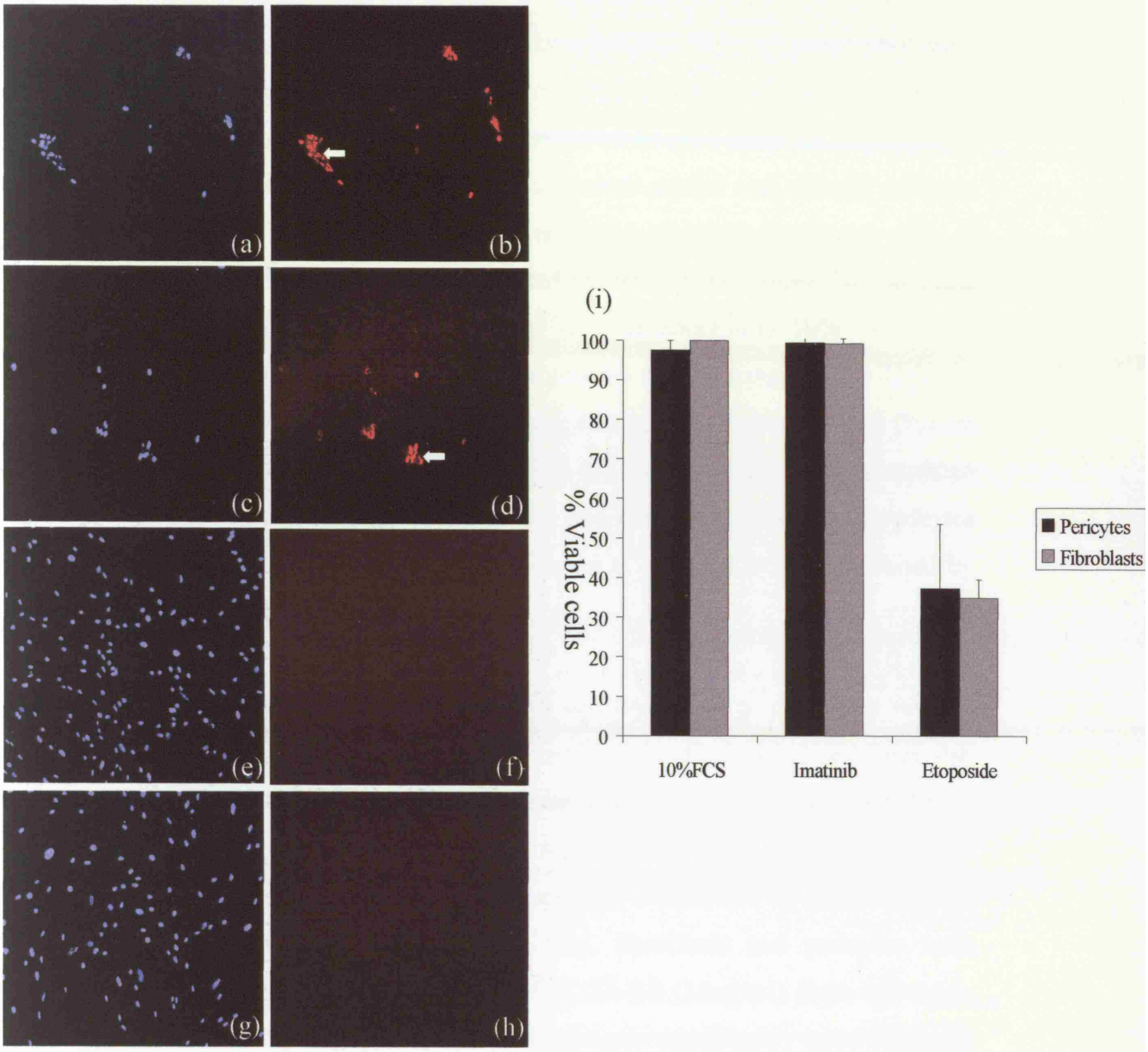


**Figure 6.6.**

**Imatinib does not induce apoptosis in fibroblasts and pericytes *in vitro*.**

Apoptotic cells were detected by TUNEL staining in both fibroblasts (red colour, arrow, **b**) and pericytes (red colour, arrow, **d**) after treatment with 100μM etoposide for 48 hours. Treatment with imatinib (2μM) for 48 hours did not induce apoptosis in either fibroblasts (**f**) or pericytes (**h**). DAPI counterstaining is shown **a,c,e,g**. The number of viable cells was counted in x20 field of view (n=5). No significant difference was recorded in the number of viable cells between imatinib treatment and control treatment (10% FCS) (i). Original magnification **a-h** x10.

### 6.3.4 The effect of imatinib on fibroblast and pericyte migration *in vitro*

PDGF-BB is known to promote the motility of fibroblasts (410) and pericytes (93) *in vitro*. Therefore, it was hypothesised that the hypocellularity of imatinib-treated wounds could in part be caused by an inhibition of PDGF-BB mediated migration of fibroblasts and pericytes. To confirm this, a series of *in vitro* analyses investigating fibroblast and pericyte migration using scratch wound assays and relaxed collagen gels was carried out. The cell-mediated contraction of relaxed collagen gels is dependent on the small tractional forces exerted by cells as they spread and migrate on collagen fibres (455). In the presence of DMEM containing 10% FCS, both fibroblasts and pericytes had completely closed *in vitro* scratch wounds after 72 hours (Figure 6.7b and 6.8b). In the absence of serum, cell migration was reduced (Figure 6.7a and 6.8a). Addition of imatinib resulted in the inhibition of serum stimulated pericyte and fibroblast migration (Figure 6.7e and 6.8e). Fibroblast and pericytes migration was stimulated by the PDGF-BB (Figure 6.7c and 6.8c) and inhibited by imatinib treatment (Figure 6.7f and 6.8f).

The ability of PDGF-BB to stimulate pericytes and fibroblasts to contract a relaxed collagen gel, a process dependent on the tractional forces of migrating cells was also assessed. Both fibroblasts and pericytes contracted collagen gels when incubated with DMEM containing 10% FCS compared with serum-free DMEM (Figure 6.9a,c and 6.10a,c). Addition of imatinib resulted in reduced gel contraction by fibroblasts and pericytes (Figure 6.9b,d and 6.10b,d). Similarly, fibroblasts and pericytes were incubated for 24h in the presence or absence of PDGF-BB (10ng/ml). Both cell types, when incubated with PDGF-BB contracted collagen gels significantly more than cells incubated with vehicle alone (Figure 6.9a,e and 6.10a,e). PDGF-BB induced gel contraction by both cell types was significantly inhibited by imatinib treatment (Figure 6.9f and 6.10f). Recording the gel weight before and after treatment confirmed that the addition of imatinib provoked a significant inhibition of contraction by both fibroblasts and pericytes in response to 10% FCS and PDGF-BB (Figure 6.9g and 6.10g).

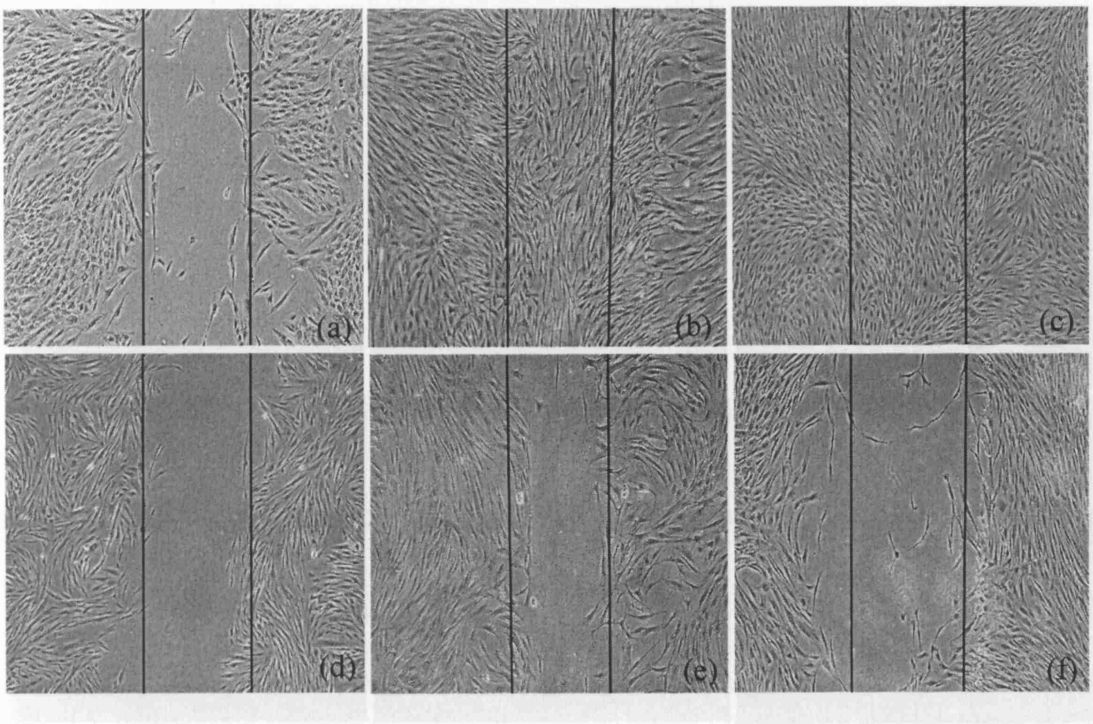


**Figure 6.7.**

**Imatinib treatment impairs migration of fibroblasts in scratch wounds.**

Scratch wounds were made in confluent fibroblast monolayers. Both 10% FCS (**b**) or 10ng/ml PDGF-BB (**c**), induced fibroblasts to fill the scratch wound after 72 hours in comparison to serum-free DMEM (**a**). Addition of imatinib (2μm) abrogated migration induced by both 10% FCS (**e**) and PDGF-BB in fibroblasts (**f**). Treatment with imatinib in serum-free medium had no effect (**d**).

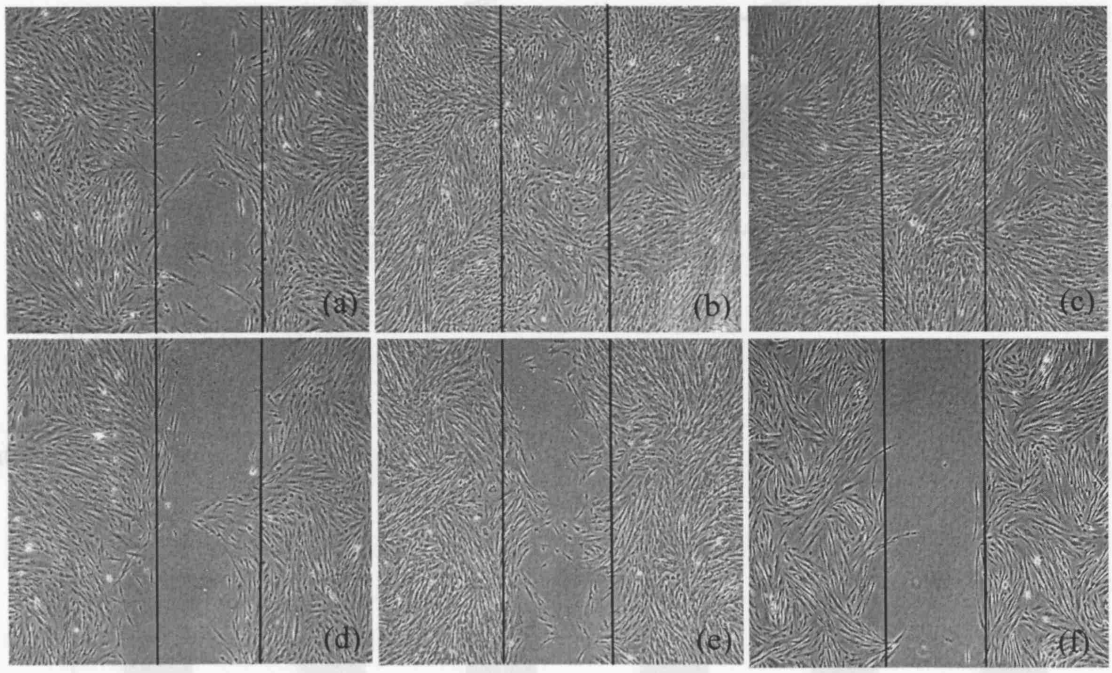


**Figure 6.8.**

**Imatinib treatment impairs migration of pericytes in scratch wounds.**

Scratch wounds were made in confluent pericyte monolayers. In response to both 10% FCS (**b**) or10ng/ml PDGF-BB (**c**), pericytes filled a scratch wound after 72 hours in comparison to serum-free DMEM (**a**). Addition of imatinib (2μm) inhibited pericyte migration induced by both 10% FCS (**e**) and PDGF-BB (**f**). Treatment with imatinib in serum-free medium had no effect (**d**).

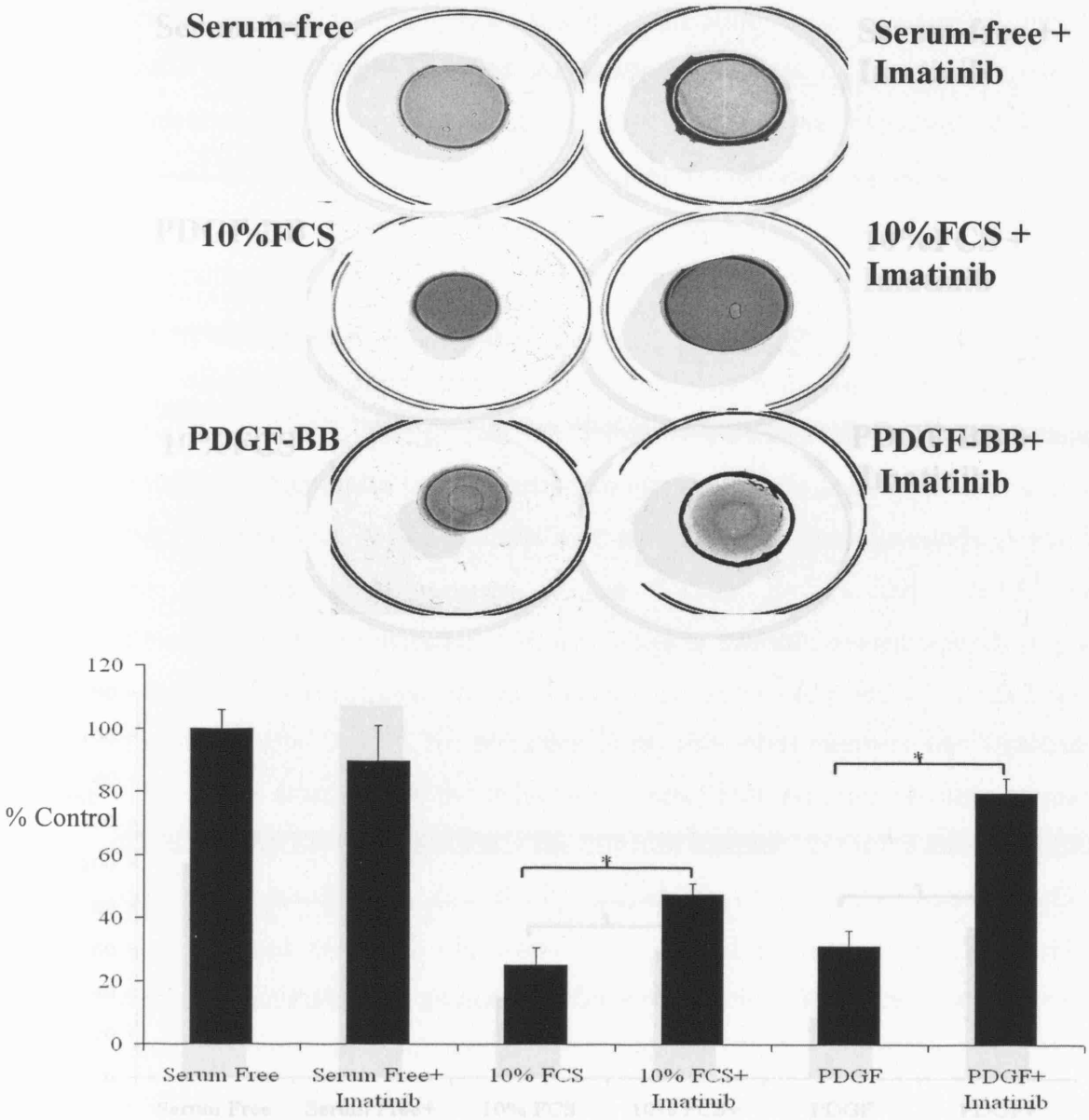


**Figure 6.9.**

**Impairment of fibroblast migration in free-floating collagen matrices**

Fibroblasts were seeded into a collagen gel matrix, and allowed to contract over a 24 hour period. Treatment with DMEM containing 10% FCS and PDGF-BB (10ng/ml) stimulated gel contraction in contrast to serum-free DMEM. Serum and PDGF-BB induced contraction was inhibited by treatment with 2 μm imatinib. Treatment with imatinib alone had no effect on contraction. Measurement of gel weight confirmed that imatinib treatment produced a significant reduction of fibroblast mediated gel contraction induced by serum and PDGF-BB. Results represent the mean $\pm$ s.d; *=$p<0.05$.

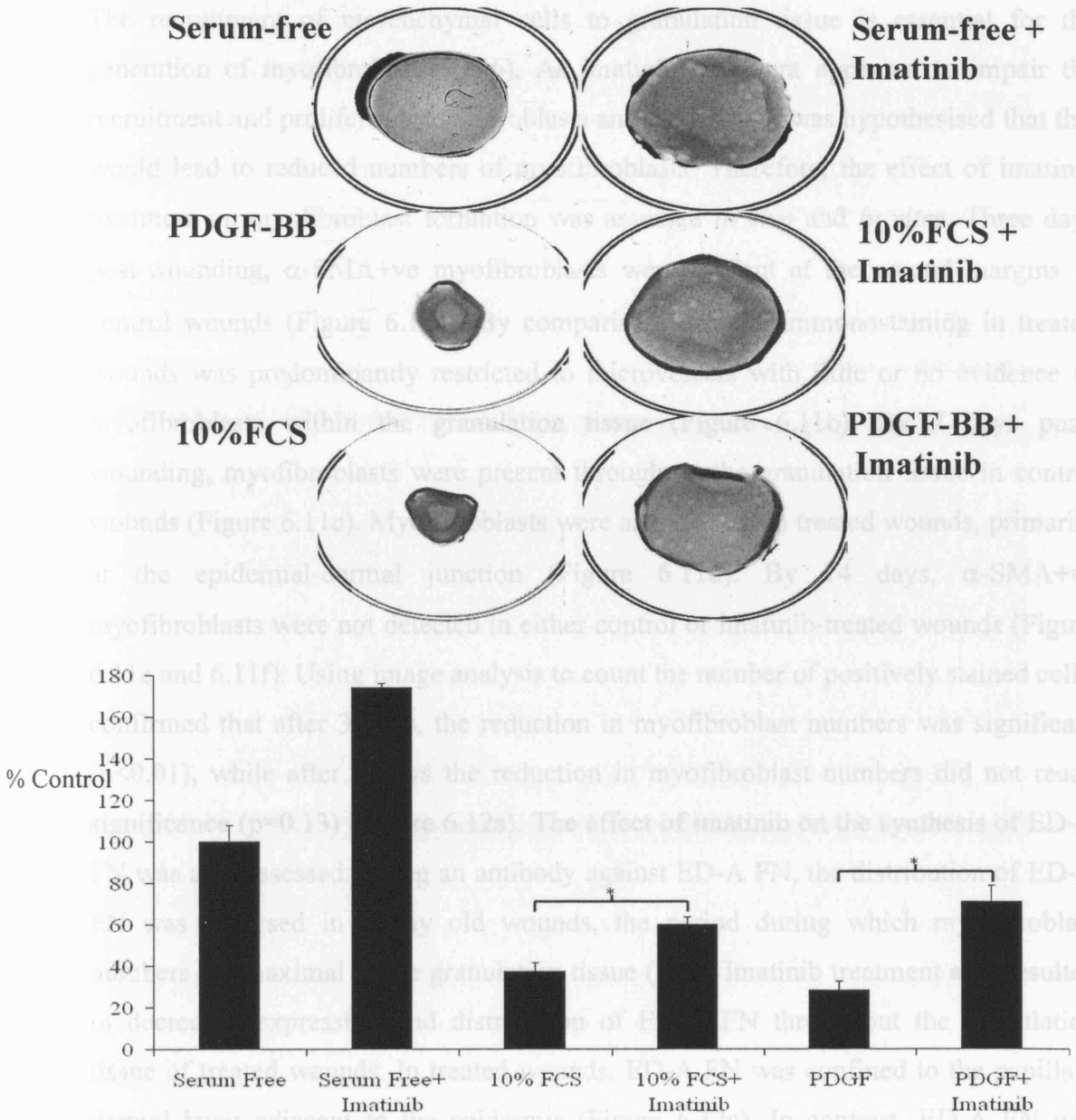


**Figure 6.10.**

**Impairment of pericyte migration in free-floating collagen matrices**

Treatment with DMEM containing 10% FCS and PDGF-BB (10ng/ml) induced pronounced gel contraction in contrast to DMEM alone. Contraction that was induced by serum or PDGF-BB was inhibited following treatment with 2μm imatinib. Treatment with imatinib alone had no significant effect on contraction. Measurement of gel weight confirmed that imatinib treatment produced a significant impairment of pericyte mediated gel contraction induced by serum and PDGF-BB. Results represent the mean $\pm$ s.d. *=$p<0.05$.

### 6.3.5 The effect of imatinib on myofibroblast formation *in vivo* and *in vitro*

The recruitment of mesenchymal cells to granulation tissue is essential for the generation of myofibroblasts (296). As imatinib treatment appeared to impair the recruitment and proliferation of fibroblasts and pericytes, it was hypothesised that this would lead to reduced numbers of myofibroblasts. Therefore, the effect of imatinib treatment on myofibroblast formation was assessed *in vivo* and *in vitro*. Three days post-wounding, α-SMA+ve myofibroblasts were evident at the wound margins in control wounds (Figure 6.11a). By comparison, α-SMA immunostaining in treated wounds was predominantly restricted to microvessels with little or no evidence of myofibroblasts within the granulation tissue (Figure 6.11b). By 7 days post-wounding, myofibroblasts were present throughout the granulation tissue in control wounds (Figure 6.11c). Myofibroblasts were also present in treated wounds, primarily at the epidermal-dermal junction (Figure 6.11d). By 14 days, α-SMA+ve myofibroblasts were not detected in either control or imatinib-treated wounds (Figure 6.11e and 6.11f). Using image analysis to count the number of positively stained cells, confirmed that after 3 days, the reduction in myofibroblast numbers was significant ($p<0.01$), while after 7 days the reduction in myofibroblast numbers did not reach significance ($p=0.13$) (Figure 6.12a). The effect of imatinib on the synthesis of ED-A FN was also assessed. Using an antibody against ED-A FN, the distribution of ED-A FN was analysed in 7 day old wounds, the period during which myofibroblast numbers are maximal in the granulation tissue (200). Imatinib treatment also resulted in decreased expression and distribution of ED-A FN throughout the granulation tissue of treated wounds. In treated wounds, ED-A FN was confined to the papillary dermal layer adjacent to the epidermis (Figure 6.12c). In contrast, ED-A FN was distributed throughout the granulation tissue in control wounds (Figure 6.12b).

In order to investigate the potential mechanism by which imatinib treatment resulted in reduced numbers of myofibroblasts, dermal fibroblasts were treated *in vitro* with 2 ng/ml TGF-β for 4 days to promote myofibroblast differentiation. After 4 days treatment with TGF-β, 72% of the fibroblasts contained α-SMA+ve stress fibres (Figure 6.13c and 6.13e), compared with 4% of fibroblasts treated with vehicle alone (Figure 6.13a and 6.13e). After the addition of imatinib in combination with TGF-β, 64% of fibroblasts were α-SMA+ve (Figure 6.13d and 6.13e). This difference was not statistically significant ($p=0.14$). Imatinib treatment alone resulted in 3% of fibroblasts displaying α-SMA+ve fibres (Figure 6.13b and 6.13e).

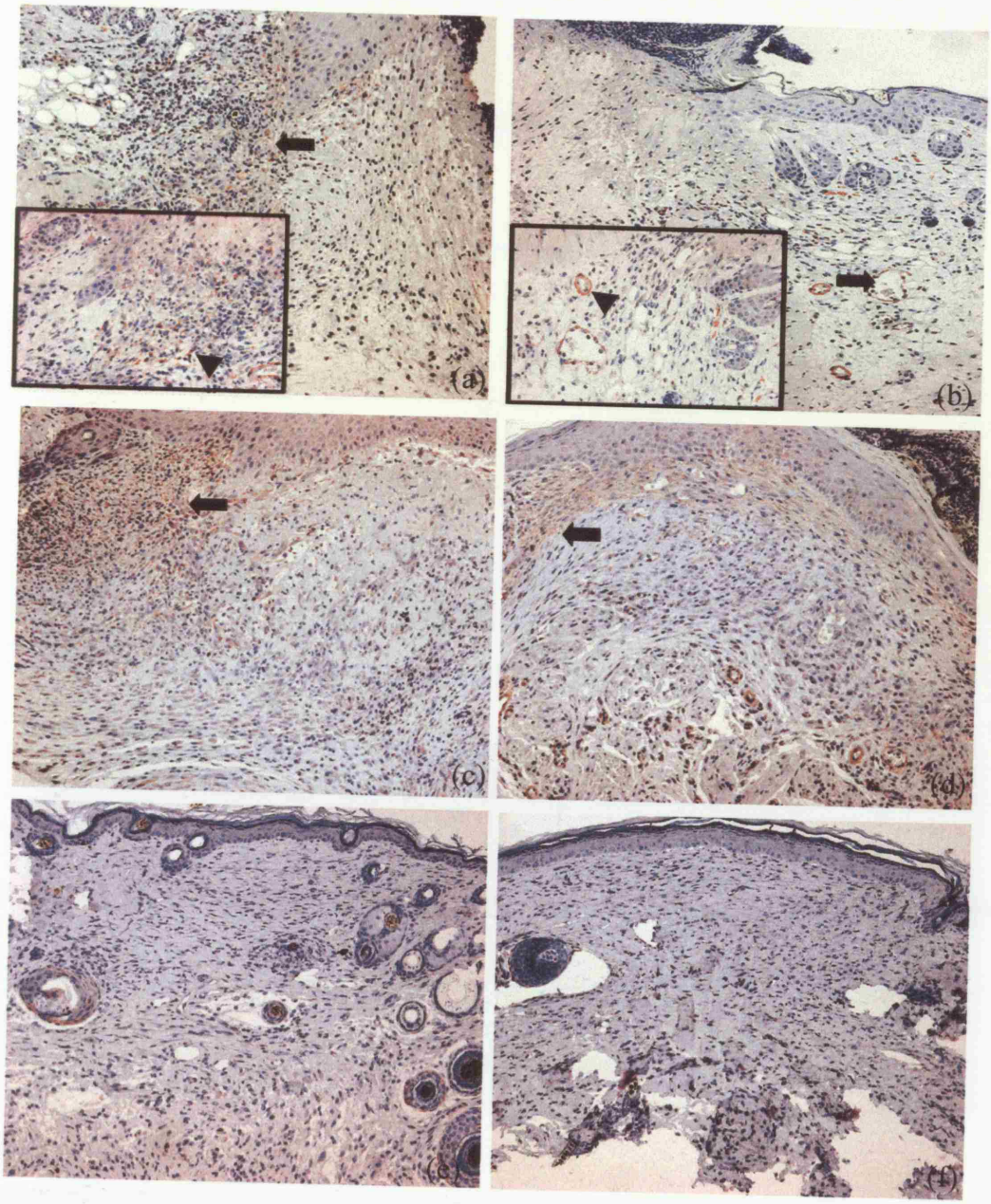


**Figure 6.11.**

**Imatinib treatment reduces the number of myofibroblasts in wound tissue.**

Three days after injury, α-SMA expressing myofibroblasts are present in the wound margins of control animals (arrow, **a,** arrowhead, inset, **a**), however, not in the granulation tissue of imatinib-treated animals where α-SMA immunostaining was restricted to microvessels (arrow, **b,** arrowhead inset, **b**). After 7 days, myofibroblasts were present throughout the granulation tissue of control wounds (arrows, **c**) and in imatinib-treated wounds, particularly at the epidermal/dermal junction (arrow, **d**). After 14 days, myofibroblasts were absent from both control (**e**) and treated wounds (**f**). Original magnification **a-f** x10, inset **a,b** x40

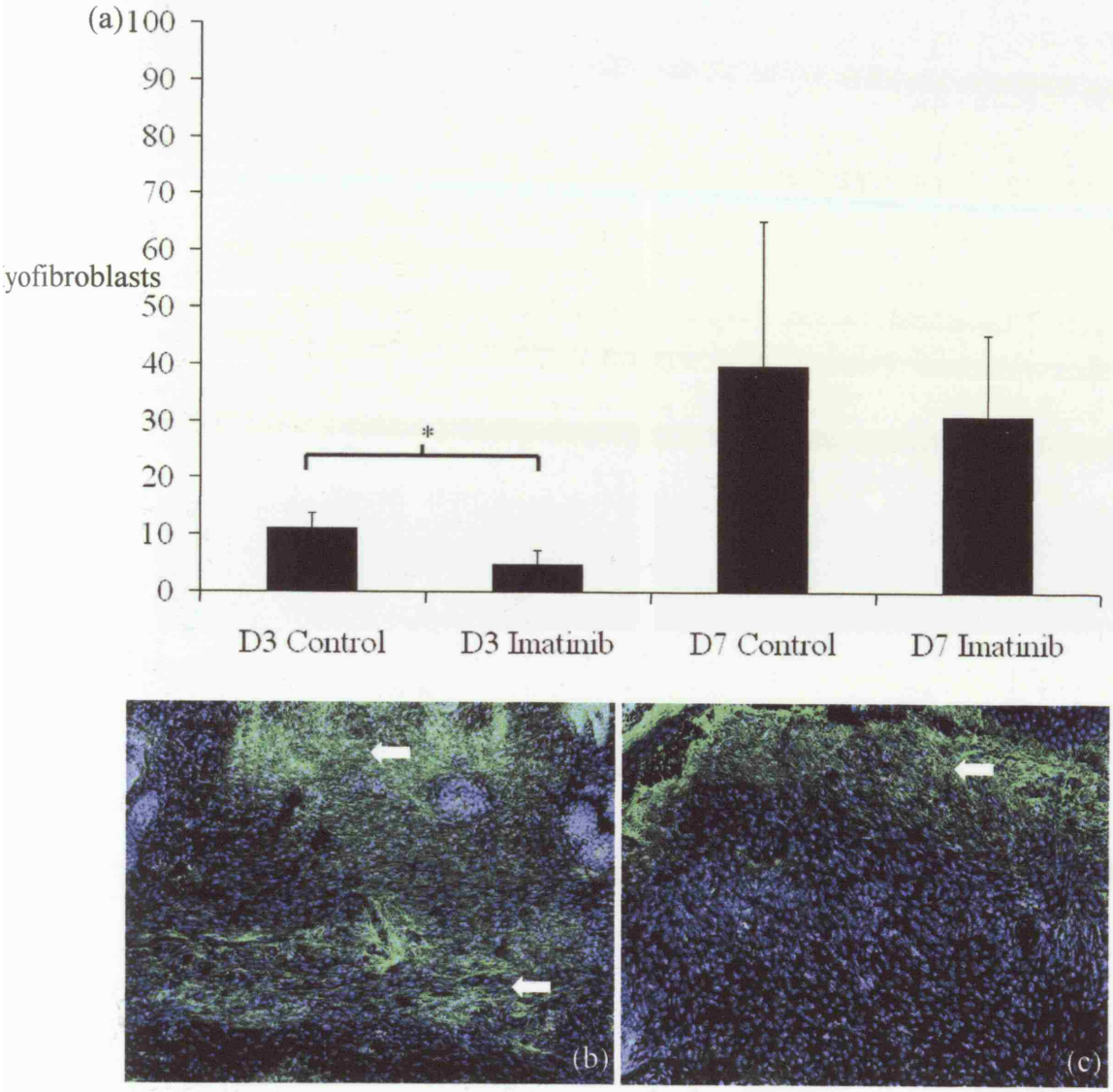


**Figure 6.12.**

**Imatinib treatment reduces myofibroblast numbers and ED-A FN expression in wound tissue.**

Quantification of the number α-SMA+ve cells by image analysis confirmed a significant reduction in myofibroblasts in imatinib-treated animals 3 days after injury. After 7 days, myofibroblast numbers were still lower in imatinib-treated animals, however, the difference was not statistically significant (**a**). Results represent the mean ± s.d.; *= $p<0.01$. Expression of ED-A FN was also reduced as a result of imatinib treatment (arrow, **c**) compared to control tissue (arrows, **b**). Original magnification **b,c** x10

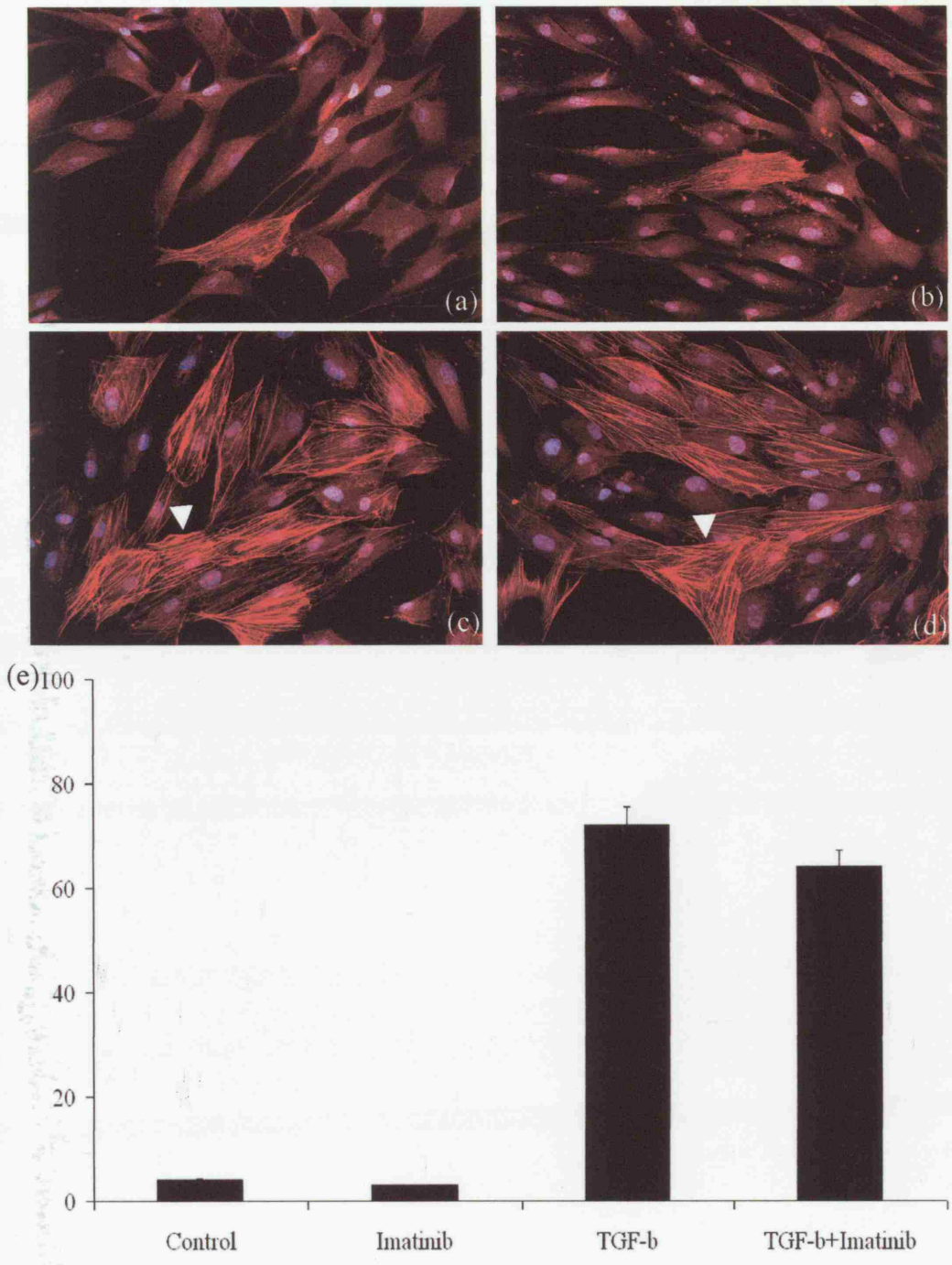


**Figure 6.13.**

**Imatinib treatment does not inhibit myofibroblast formation *in vitro*.**

Treatment with either serum-free DMEM (**a**) or imatinib alone (**b**) had no effect on α-SMA fibre formation. Addition of TGF-β (2ng/ml) to cultured fibroblasts produced prominent α-SMA stress fibres (arrowhead, **c**), which was not inhibited by imatinib treatment (arrowhead, **d**). Quantification of myofibroblast numbers after TGF-β and imatinib treatment demonstrated that imatinib treatment did not inhibit myofibroblast formation *in vitro* (**e**). Results represent the mean ± s.d. Original magnification **a-d** x20.

### 6.3.6 The effect of imatinib on collagen biosynthesis during wound repair

To determine whether collagen type I biosynthesis was affected by blockade of PDGFRβ signalling, a transgenic mouse harbouring a 17kb fragment of the collagen 1α2 upstream enhancer and minimal promoter fused to a β-galactosidase (Lac-Z) reporter gene was used. Initial experiments were carried out to confirm the expression of the transgene in excisional wound healing. Analysis of transgene activity over a 28 day period post wounding revealed that the β-galactosidase activity remained at baseline until 5 days post wounding, at which point the expression of the transgene was significantly increased ($p<0.001$). Increased transgene expression was maintained until 14 days post wounding after which expression returned to baseline levels (Figure 6.14a and 6.14b). The effect of imatinib on collagen transgene expression was then assessed. After 3 days, transgene expression in both control and imatinib-treated wounds remained at baseline levels (Figure 6.14c). After 7 days however, transgene expression, while significantly elevated in control wounds, remained at baseline levels in treated wounds ($p<0.01$). Fourteen days post wounding, increased transgene expression had been maintained in control wounds, however, it was still significantly diminished in treated wounds ($p<0.01$), (Figure 6.14c).

Transgene expression in whole wounds was assessed macroscopically. Figure 6.15 demonstrates that after 7 and 14 days respectively, imatinib treatment resulted in significantly reduced transgene expression as depicted by the distribution of blue X-gal staining. Immunohistochemical analysis of transgene distribution days revealed that transgene-expressing cells in control samples were located throughout the granulation tissue 7 and 14 days post-wounding (Figure 6.16a and 6.16c). By contrast, in imatinib-treated wounds, transgene expression was noticeably less pronounced and was restricted to a small number of cells in the wound margins (Figure 6.16b and 6.16d). To confirm the reduction in collagen protein, day 14 wound sections were probed with an antibody against collagen type I. After 14 days, the expression of collagen type I protein was reduced in imatinib-treated wounds (Figure 6.16f) compared to control wounds (Figure 6.16e), mirroring the reduced expression of the collagen transgene.

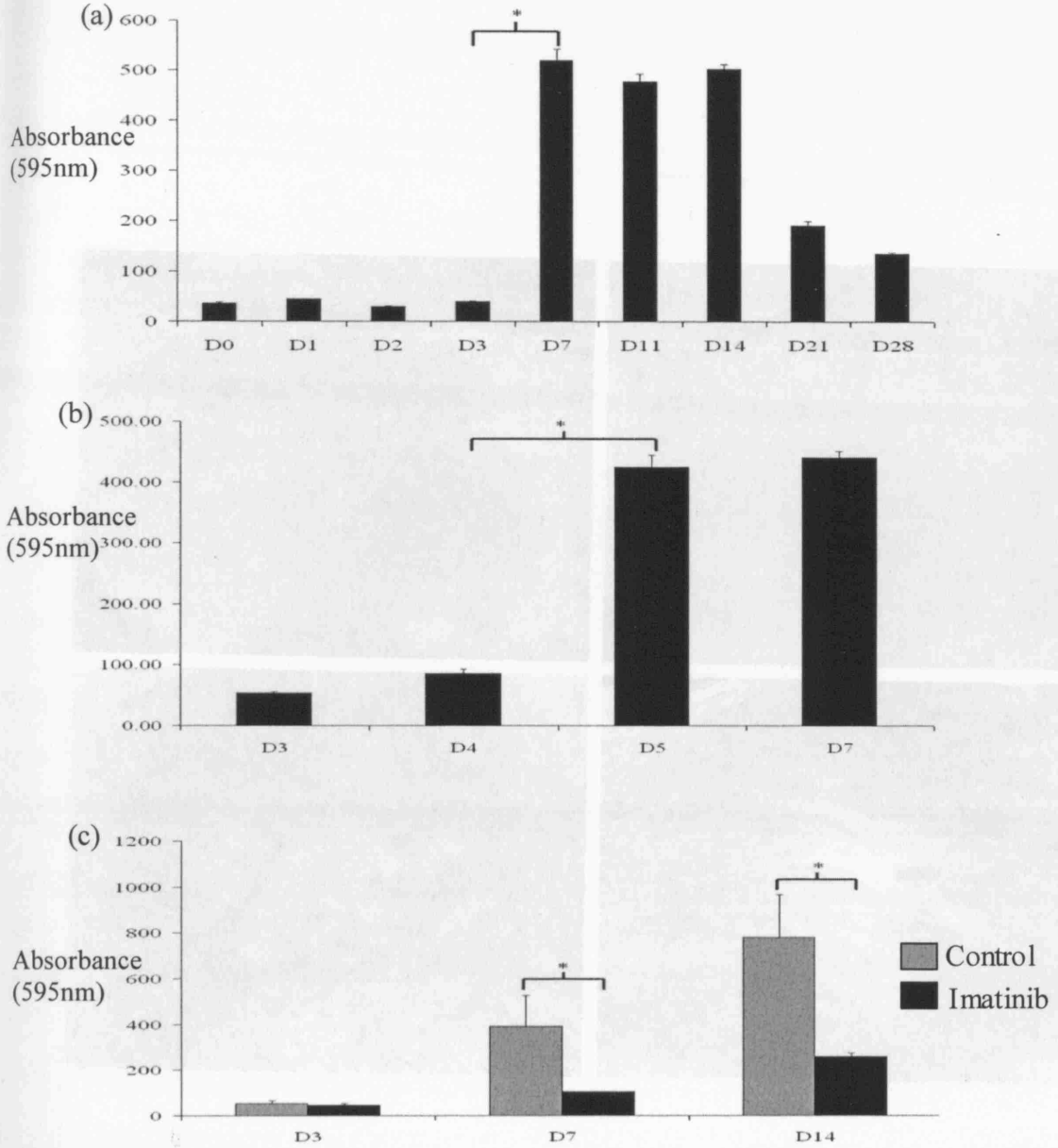


**Figure 6.14.**

**Collagen type I gene promoter activity is reduced in imatinib-treated wounds.**

Wounds were excised from mice at specific time points and collagen type I gene promoter activity was assessed by measuring β-galactosidase activity. Over a 28 day period, transgene activity was maximal between days 7 and 14 (**a**) with activity rising from baseline levels at day 5 (**b**). Treatment with imatinib resulted in a significant decrease in transgene activity at days 7 and 14 (**c**). Results represent the mean ± s.d.; *=$p<0.01$.

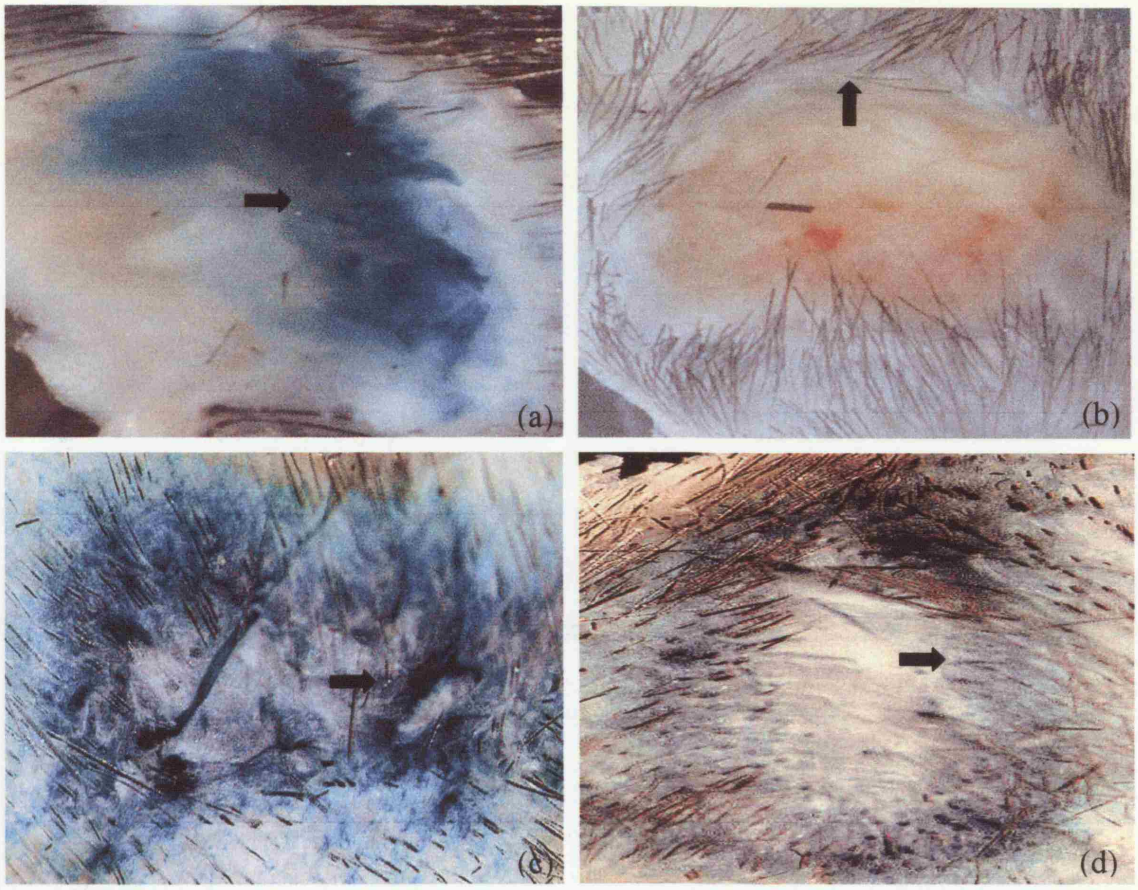


**Figure 6.15.**

**The distribution of collagen-synthesising cells in control and imatinib-treated whole wounds.**

Wounds were excised from mice at day 7 and 14 and stained with 1 mg/ml 5-bromo-4-chloro-3-indolyo-B-D-galactoside solution (X-gal). After 7 and 14 days, control wounds showed uniformly intense X-gal staining (arrow, **a,c**) while staining in tissue from imatinib-treated mice was significantly weaker and confined to the wound margins (arrow, **b,d**).

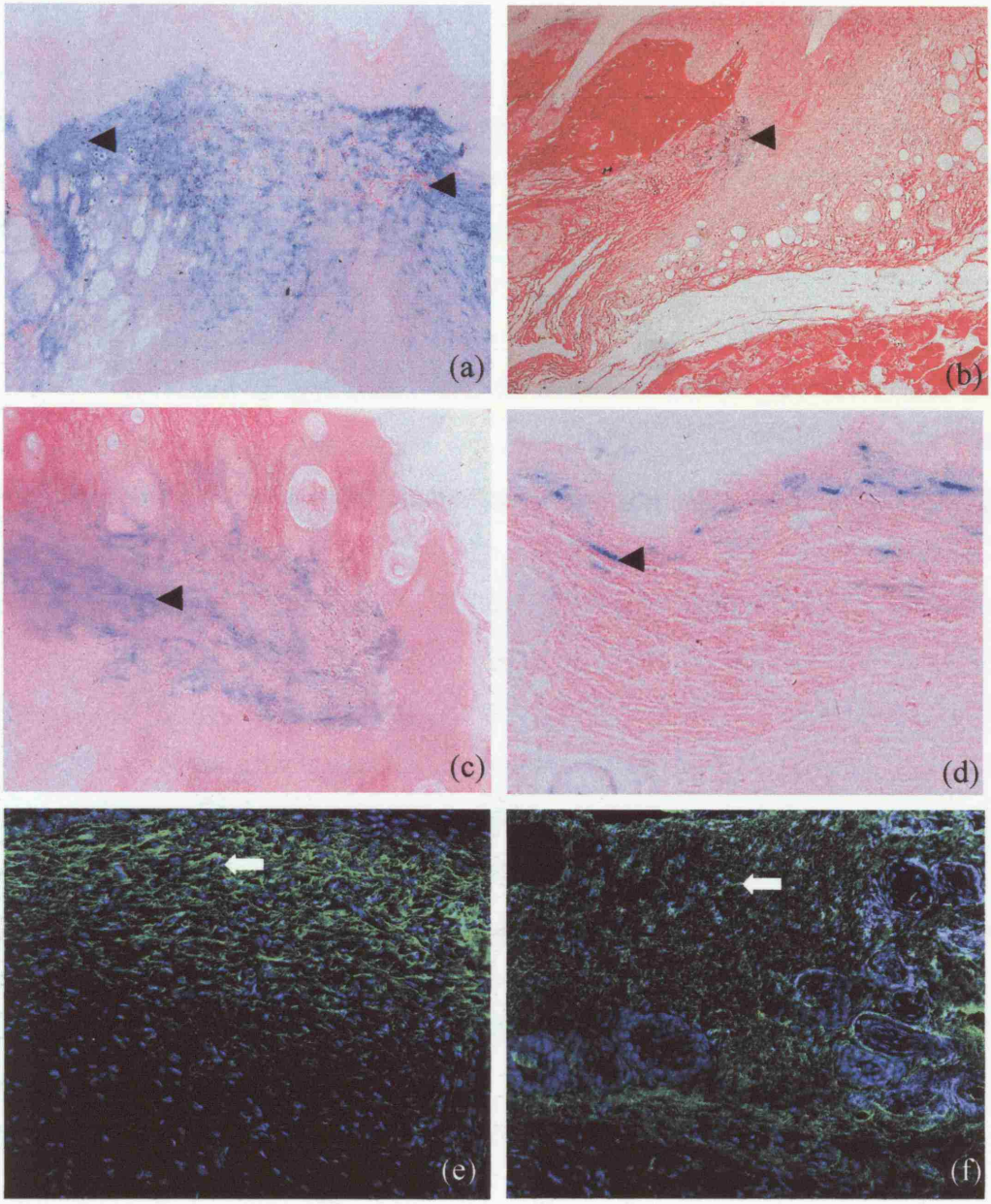


**Figure 6.16.**

**The distribution of collagen-synthesising cells in tissue sections of control and imatinib-treated wounds.**

Wounds were stained with 1 mg/ml X-gal. After 7 and 14 days in control tissue, X-gal staining could be observed in fibroblastic cells in the granulation tissue (arrowheads, **a,c**). By comparison, sections from imatinib-treated animals revealed reduced X-gal staining with blue cells being confined to the wound margins (arrowhead, **b,d**). Immunofluorescence staining of 14 day old wounds with an anti-collagen type I antibody confirmed that expression of collagen protein was concordantly reduced in imatinib-treated wounds (arrow, **f**) relative to control tissue (arrow, **e**). Original magnification, **a-f** x10.

### 6.3.7 The effect of imatinib treatment on microvessel formation during wound repair *in vivo*

The effect of imatinib treatment on neovascularisation was assessed. Massons trichrome staining of 3 and 7 day post-wound sections demonstrated abnormal microvascular morphology as a result of imatinib treatment. In control tissue after 3 and 7 days, areas of granulation tissue rich in microvessels were readily detected (Figure 6.17a and 6.17c). In contrast, microvessels in imatinib-treated wounds were abnormally distended in appearance and fewer in number (Figure 6.17b and 6.17d). Microvascular density was quantified by immunostaining for CD31. Control tissue 7 and 14 days post-wounding displayed extensive immunostaining for CD31 throughout the granulation tissue (Figure 6.18a and 6.18c). By comparison, CD31 immunostaining was less extensive in imatinib-treated wounds after 7 and 14 days respectively (Figure 6.18b and 6.18d). Quantification of the number of CD31+ve microvessels demonstrated that imatinib treatment resulted in a significant reduction in the number of microvessels 7 days post-wounding ($p<0.05$) (Figure 6.18e). After 14 days, while fewer vessels were detected in imatinib-treated tissue compared with controls, the difference was not statistically significant ($p=0.06$) (Figure 6.18e). Pericyte coverage as determined by NG2 immunostaining (333) was readily detected in day 7 control tissue (Figure 6.19a), however, was significantly reduced in treated tissue ($p<0.05$) (Figure 6.19b). After 14 days pericyte coverage was still reduced in treated tissue (Figure 6.19c) compared to controls (Figure 6.19d), however, the difference was no longer significant ($p=0.08$).

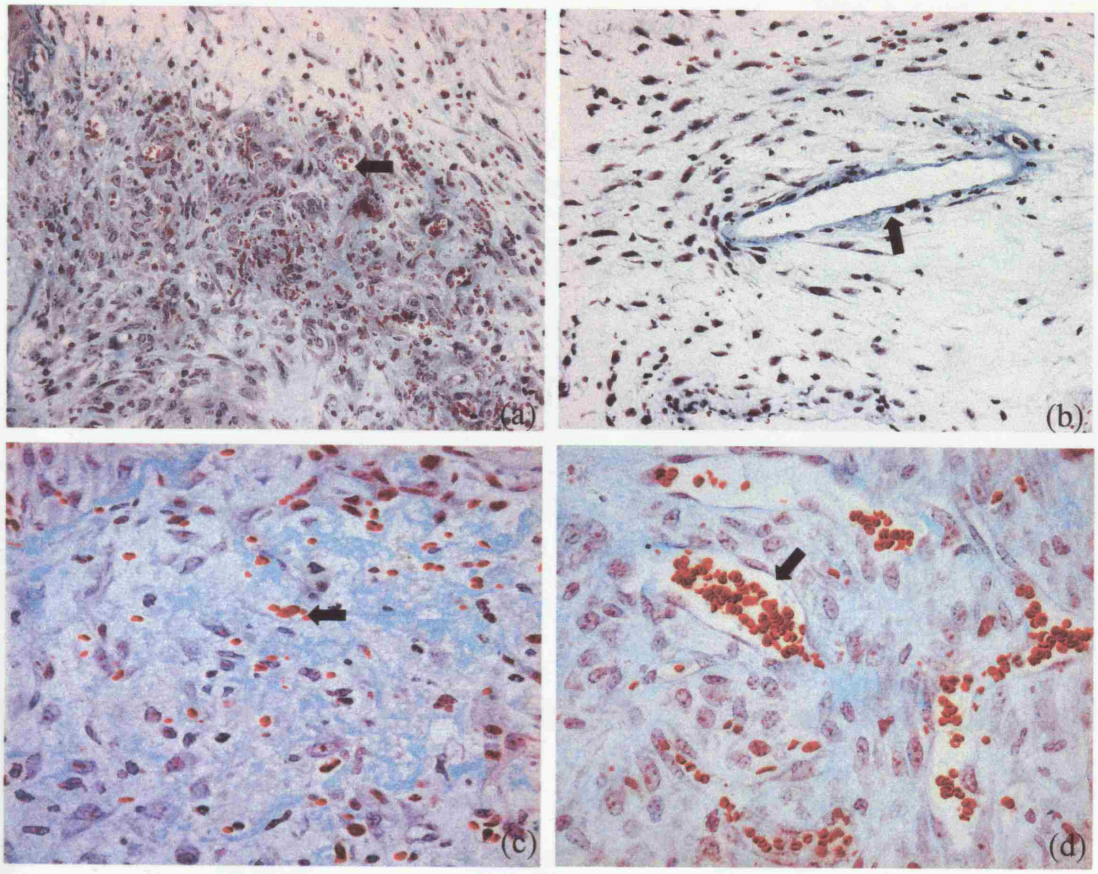


**Figure 6.17.**

**Imatinib treatment results in impaired microvascular formation in wound tissue.** Massons trichrome staining demonstrates microvessel formation in control wounds after 3 (arrows, **a**) and 7 days respectively (arrows, **c**). In imatinib-treated wounds, however, microvascular formation is severely impaired with vessels appearing abnormally large distended after 3 (arrows, **b**) and 7 days (arrows, **d**). Original magnification **a-d** x20.

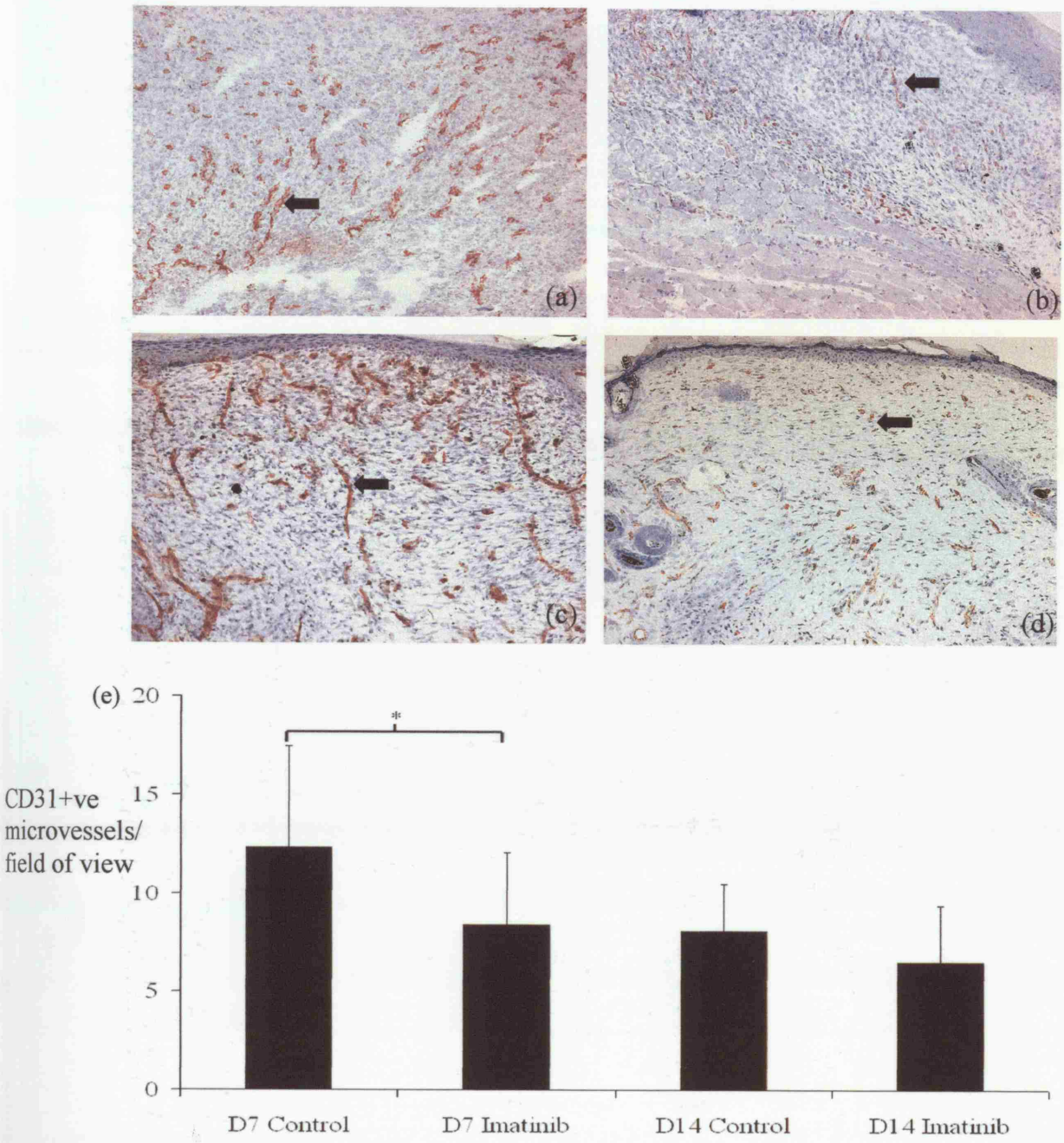


**Figure 6.18.**

**Imatinib treatment results in reduced CD31 expression in wound tissue.**

Control and imatinib-treated tissue were stained with antibodies recognising endothelial cells (CD31). In control wounds, 7 and 14 days after injury, CD31 immunostaining was prominent in the granulation tissue (arrows, **a,c**) while in imatinib-treated wounds, CD31 staining was reduced (arrows, **b,d**). Quantification of CD31 stained cells confirmed that imatinib treatment produced a significant reduction in microvascular density after 7 days (**e**). Results represent the mean $\pm$ s.d.; *= $p<0.05$. Original magnification, **a-d** x10.

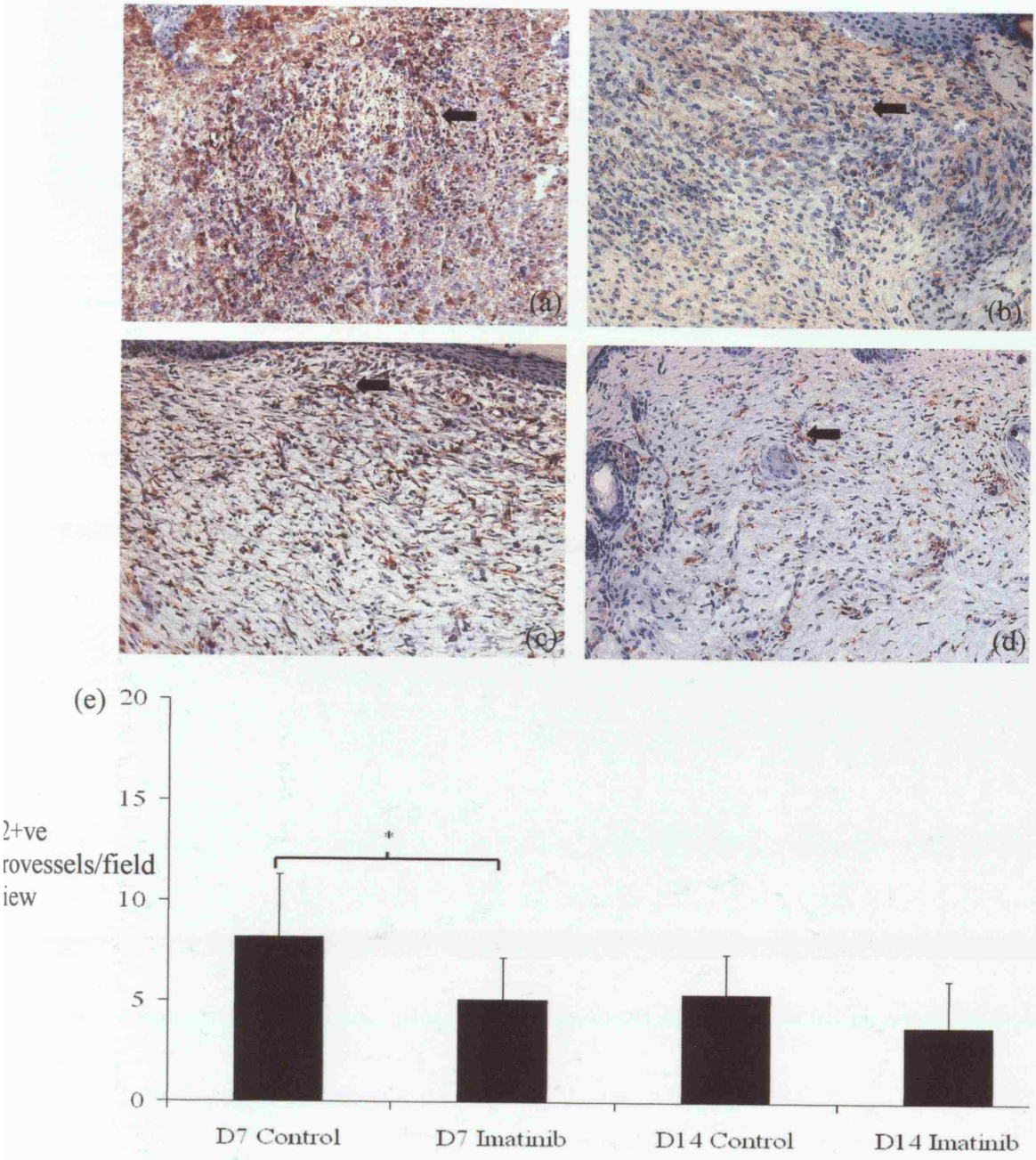


**Figure 6.19.**

**Imatinib treatment results in reduced NG2 expression in wound tissue.**

Cryosections from control and imatinib-treated wounds were stained with antibodies against the pericyte marker NG2. In control wounds, 7 and 14 days after injury, immunostaining for NG2 was prominent throughout the granulation tissue (arrows, **a,c**) while in imatinib-treated wounds, NG2 staining was comparatively reduced (arrows, **b,d**). Original magnification, **a-d** x10. Quantification of NG2 stained cells confirming that imatinib treatment produced a significant reduction in pericyte coverage after 7 days (**e**). Results represent the mean $\pm$ s.d.; *= $p<0.05$.

## 6.4 KEY FINDINGS AND CONCLUSIONS

### Inhibition of PDGFRβ impairs dermal wound healing

The data presented in this chapter demonstrate that blockade of PDGFRβ *in vivo* impairs the progression of cutaneous wound healing. Blockade of PDGFRβ signalling by imatinib appears to inhibit mesenchymal (specifically fibroblast and pericyte) recruitment by inhibiting cell proliferation and migration. Cell proliferation as assessed by BRDU incorporation was significantly reduced in the granulation tissue of imatinib-treated wounds compared to control tissue. *In vitro,* serum and PDGF-BB induced fibroblast and pericyte proliferation was blocked by imatinib treatment.

Imatinib-treated wounds had the same number of apoptotic nuclei as control wounds and imatinib did not induce apoptosis *in vitro*, therefore, the hypocellularity of imatinib-treated wounds cannot be attributed to increased apoptosis. A study of synovial fibroblasts similarly showed that while imatinib inhibited proliferation, it had no discernable effect on apoptosis (376). Imatinib treatment resulted in reduced wound closure after 7 days. Early wound closure is a result of tractional forces generated by cells migrating into the wound (455). Taken together, these findings indicate that PDGFRβ blockade resulted in diminished cell migration into the wound. This was supported by two independent *in vitro* assays; using scratch wounds and relaxed collagen gels, PDGF-BB and serum induced migration in fibroblasts and pericytes was inhibited by imatinib.

### PDGFRβ inhibition results in reduced myofibroblast numbers

Three days post-wounding, imatinib treatment resulted in significantly reduced numbers of myofibroblasts in the granulation tissue. After seven days, the reduction in myofibroblast numbers was no longer significant. Interestingly, imatinib treatment had no effect on the TGF-β mediated differentiation of myofibroblasts *in vitro,* suggesting that PDGFRβ signalling does not directly stimulate the formation of myofibroblasts but rather promotes the recruitment of cells that become myofibroblasts in response to TGF-β and mechanical tension. The difference in myofibroblast numbers was less pronounced at 7 days than at 3 days, suggesting that alternative mechanisms of myofibroblast generation such as recruitment from the bone marrow may compensate for a reduced pool of fibroblasts and pericytes resulting from PDGFRβ inhibition (111;147).

**PDGFRβ inhibition results in abnormal microvascular formation**

Microvascular density was reduced in imatinib-treated wounds with microvessels that appeared abnormally dilated and distended in appearance. These microaneurysms have been observed in PDGFRβ and PDGF-B chain knockout embryos (277;422). Subsequent studies showed that they were caused primarily by a failure to adequately recruit pericytes during angiogenesis (194). Using an antibody against NG2, a marker for pericytes (333), it was confirmed that imatinib treatment resulted in reduced numbers of microvessels containing NG2-expressing pericytes. Furthermore, using an *in vitro* approach, imatinib treatment was shown to significantly impair the migration and proliferation of cultured pericytes in response to both PDGF-BB and serum. These findings indicate that PDGFRβ signalling plays a critical role in recruiting pericytes to nascent capillaries during embryonic and post-natal angiogenesis.

**PDGFRβ inhibition results in diminished ECM biosynthesis and deposition**

Histological analysis revealed that PDGFRβ inhibition resulted in reduced ECM deposition during wound healing. The principal fibrillar collagen laid down during dermal tissue repair is collagen type I (296). Using a collagen 1α2 transgenic reporter mouse, collagen gene activity was significantly reduced as a result of imatinib treatment. Furthermore, expression of collagen type I protein was also reduced as assessed by immunofluorescence. *In vitro*, PDGF-BB does not stimulate collagen biosynthesis in fibroblasts (82), therefore, the effects on collagen expression induced by imatinib treatment may be an indirect result of reduced fibroblast and pericyte recruitment into the wound. Similarly, the expression of ED-A FN was also reduced as a result of imatinib treatment yet PDGF-BB had no effect on ED-A FN expression by fibroblasts (455). Again, this is likely to reflect the impaired recruitment of fibroblasts and pericytes to the wound tissue.

In summary, the data presented in this chapter confirm that *in vivo,* PDGFRβ activation is an essential component in promoting fibroblast and pericyte activation and recruitment during tissue repair. The subsequent reduction in myofibroblast numbers, diminished collagen and ED-A FN expression suggest that targeting the PDGFRβ should be considered as a therapeutic strategy in the treatment of fibrotic disorders.

# CHAPTER 7: DISCUSSION

The overall aim of this study was to determine the potential contribution of microvascular pericytes to the pathogenesis of dcSSc and fibrosis. In this chapter, the results presented are discussed and a rationale for the role of pericytes in fibroproliferative disorders is proposed.

## 7.1 Expression of PDGFRβ by activated pericytes in systemic sclerosis

### 7.1.1 Microvascular pericytes express PDGFRβ across the SSc disease spectrum

Activated pericytes expressing PDGFRβ play a key role in the pathogenesis and progression of a number of fibrotic disorders, including dermal scarring (439) and renal fibrosis (332). However, the phenotype and contribution of pericytes to the pathogenesis of SSc is unknown. Therefore, the focus of my initial studies was to establish whether pericytes were activated and whether they expressed PDGFRβ in dcSSc. Using an immunohistochemical approach, I was able to show for the first time that pericytes express the activation marker HMW-MAA and PDGFRβ in both ARP and dcSSc skin. A key consideration of these experiments was the specificity of the monoclonal anti-HMW-MAA antibody used to detect activated pericytes. Immunohistochemical analyses using this antibody have revealed that HMW-MAA is expressed at very low levels in microvessels of normal tissue (389;390;440). However, in diverse conditions associated with an activation of the microvasculature such as tumours, inflammatory synovitis and the granulation tissue of healing wounds, HMW-MAA expression is significantly increased (389;390;440). Transmission and double immunofluorescence labelling studies confirmed that HMW-MAA expression localised to pericytes (389;440). In agreement with previous studies, HMW-MAA expression did not localise to endothelial cells or fibroblasts (363;390), confirming the specificity of the antibody. Therefore, the evidence that HMW-MAA is expressed by pericytes in activated tissue is compelling.

Elevated PDGFRβ expression has been previously reported in dcSSc tissue (246), however, the cell types expressing PDGFRβ were not identified and the pattern of receptor expression across disease subsets remained unknown.

In the current study, increased PDGFRβ expression was found not only in fibrotic dcSSc tissue but also in non-fibrotic ARP tissue. ARP often represents a 'pre-scleroderma' state (34) and the finding that pericytes are activated and express

PDGFRβ in ARP is of potential significance in linking early microvascular abnormalities with subsequent fibrosis. As discussed in section 1.3.1, 10-15% of patients with ARP will develop a connective tissue disorder (425). Autoimmune Raynaud's is characterised by circulating autoantibodies and is associated with irreversible tissue damage with ulceration, scarring and structural change within the microvasculature (350). By contrast, in PRP, episodic ischaemia in response to stimuli is reversible and the absence of tissue damage is a defining feature (230). The expression of HMW-MAA and PDGFRβ in ARP, but not in PRP, is the first report of differences at the molecular level between these two conditions. The elevated expression of PDGFRβ by perivascular cells is a key component of pathological remodelling following vascular injury and damage (56) and in experimental models of PAH, vascular remodelling and hypertension can be reversed by PDGFRβ blockade (324;387). A recently published case report describes an impressive improvement in PAH in response to PDGFRβ inhibition (164). Therefore, anti-PDGFRβ therapy in SSc patients with early or pre-clinical disease in which PDGFRβ-driven vascular remodelling may play a major pathogenic role merits further investigation.

Pericyte activation and PDGFRβ expression were not detected in atrophic dcSSc skin. During the atrophic phase of SSc, the disease is no longer progressive and cutaneous involvement in diffuse patients has by this stage begun to regress (34). The MRSS of patients in the atrophic phase of the disease often shows a significant reduction which may be partially explained by the finding that fibroblasts isolated from atrophic dcSSc skin no longer display elevated collagen biosynthesis (517).

### 7.1.2 The significance of pericyte activation in fibrotic tissue

The expression of HMW-MAA by microvascular pericytes has been reported in tissues with an associated fibrotic component such as tumour stroma, wound healing and excessive dermal scarring (214;389;439). The expression of HMW-MAA and PDGFRβ by pericytes in SSc and ARP confirms that in this respect, the microvasculature in SSc and ARP is similar to that of wound healing and tumour stroma (440). Recent studies in dermal scarring have shown that *in vivo,* microvascular pericytes, which express both HMW-MAA and PDGFRβ, can migrate from the microvasculature and differentiate into collagen-synthesising fibroblasts, a phenomenon also seen in microvascular fragments isolated *in vitro* (439). The synthesis of fibrillar collagens by pericytes has also been observed in fibrotic liver (248) and kidney (145). Interestingly, targeted PDGF-B depletion using specific aptamers prevents renal scarring *in vivo* by blocking kidney pericyte proliferation and synthesis of collagen (332). Therefore, in SSc it is plausible to hypothesise that the activation of PDGFRβ may stimulate a similar differentiation of pericytes into collagen-synthesising cells. This model would provide a mechanism by which initial microvascular damage gives rise to fibrosis in dcSSc. While direct evidence of a pericyte to fibroblast transition is currently lacking in SSc, the theory is partially supported by data showing that high collagen-producing fibroblasts are located in predominantly perivascular regions in SSc tissue (386).

### 7.1.3 Expression of the PDGF AB/BB ligand across the SSc disease spectrum

The staining for PDGFRβ in both dcSSc and ARP skin was granular in appearance, which has previously been shown in cultured fibroblasts to be a characteristic of ligand activation. It has been suggested that these granules represent receptor-ligand complexes (423;453). Therefore, the distribution of the activating ligand PDGF AB/BB was investigated. In ARP, PDGF-B ligand localised to pericytes, however, this was not the case in dcSSc skin, in which dermal macrophages were the primary source of the ligand. This suggests that autocrine and paracrine PDGF pathways are active in ARP and dcSSc skin respectively. The localisation of the PDGF-B ligand to pericytes in ARP may reflect the predominantly vascular nature of the condition. The lack of PDGF AB/BB expression by pericytes in dcSSc may reflect transition of the disease from the vascular to fibrotic phase. The expression of PDGF AB/BB by dermal macrophages at sites of ECM biosynthesis has been previously reported *in*

*vivo* (279;358;366). However, it was recently shown that macrophage-derived PDGF-B is not necessary for the formation of granulation tissue and that its absence during wound healing increases angiogenesis (55). PDGF-AB/BB expression was not detected in endothelial cells corroborating similar findings in dermal wound healing tissue (440).

In summary, I have shown that increased expression of PDGFRβ by activated pericytes is a characteristic of ARP and early dcSSc skin. Moreover, the distribution of the activating PDGF-B ligand shifts from pericytes to macrophages as the disease moves from its vascular to fibrotic phase.

## 7.2 The spatial relationship between pericytes, fibroblasts and myofibroblasts in dcSSc

### 7.2.1 The distribution of myofibroblasts and ED-A FN in dcSSc

A key function of pericytes is their role as progenitor cells for other mesenchymal cell types, including osteoblasts (115), chondrocytes and adipocytes (135). On the basis of immunohistochemical data, it has also been argued that pericytes differentiate into fibroblasts during the development of fibrosis (106;115;361;439). The data presented in chapter 3 confirm that pericytes express an activated phenotype that has previously been associated with their differentiation during fibrosis (439). Therefore, in SSc, which consists of a microvascular and fibrotic component, the potential differentiation of pericytes merits investigation.

Pericytes have also been shown to differentiate into myofibroblasts during fibrosis (186;391). The myofibroblast plays a central role in connective tissue remodelling during wound healing and fibrosis. Myofibroblasts are known to be present in dcSSc skin (219;377), however, their ontogeny and role in the disease pathophysiology remains unknown. The results presented in chapter 4 confirm that myofibroblasts are present in dcSSc skin. They also show for the first time show that that ED-A FN is synthesised by myofibroblasts and pericytes in dcSSc skin.

Fibronectins play key roles in the adhesive and migratory behaviour of cells related to fundamental processes such as embryogenesis, malignancy, hemostasis, wound healing, host defense and maintenance of tissue integrity (137). Fibronectins are a

mixture of several protein types that differ in both their primary structure and post-translational modifications. The amino acid sequence variations are the consequence of the alternative processing of a single primary transcript at three sites: extra domain B (ED-B), extra domain A (ED-A) and type III homologies connecting segment (IIICS) (137). The ED-A splice variant of fibronectin is singularly essential in the differentiation of myofibroblasts from fibroblasts (455). The expression of the ED-A FN splice variant of fibronectin is high in embryonic tissue and thereafter declines and is hardly present in normal tissue (340). However, as previously discussed in section 1.6.3.4, ED-A FN expression increases dramatically during tissue repair and fibrosis (200;217), where it is essential for myofibroblast formation (394). Hence, the expression of ED-A FN by pericytes in dcSSc may play a major role in the differentiation of perivascular fibroblasts and pericytes into myofibroblasts. This may represent a critical step in the transition from the vascular to fibrotic phase in SSc pathophysiology.

An interesting observation was the localisation of ED-A FN and myofibroblasts to the lower reticular dermal layers. A similar distribution of total fibronectin has also been observed in dcSSc skin (87). The significance of the predominantly reticular distribution is unclear, however, it may reflect microenvironmental differences between the papillary and reticular dermis. It has been previously reported that reticular dermal fibroblasts are more contractile in collagen matrices when compared to papillary dermal fibroblasts (424). The absence of myofibroblasts from dermal layers lacking ED-A FN confirms the critical nature of ED-A FN for myofibroblast formation.

It is perhaps noteworthy that myofibroblasts were not present in atrophic dcSSc skin. As previously discussed, the atrophic phase of the disease is often accompanied by improvement in dermal fibrosis and skin tightness (34) and I and others have shown that vascular activation does not persist into atrophic tissue (63;354). It plausible to hypothesise that the improvement in MRSS reported in atrophic skin (100) is associated with the loss of myofibroblasts from lesional skin. In the current study, no association between the presence of myofibroblasts and disease parameters, including skin score, disease duration and capillary damage was detected. However, given the relatively small sample size, the relationship between skin fibrosis and tightening in dcSSc and myofibroblasts merits further study.

### 7.2.2 Myofibroblasts and collagen biosynthesis in dcSSc skin

The expression of LOX was used to identify collagen-synthesising fibroblasts. LOX is responsible for catalysing lysine-associated crosslinks in collagen and has been previously shown to be significantly increased in fibrotic tissue and coordinately expressed by collagen-synthesising cells (99;242). Increased LOX immunostaining was detected in four of the ten dcSSc samples analysed. While this may appear low it is in close agreement with a previous study in which 50% of dcSSc samples showed evidence of elevated collagen biosynthesis (219). Only two samples contained both myofibroblasts and collagen-synthesising cells, indicating that these two cell populations may appear in distinct phases of the disease. Double-labelling analysis of samples that contained both myofibroblasts and LOX immunoreactivity revealed no spatial colocalisation, suggesting that myofibroblasts are not the principle collagen-synthesising cell in dcSSc. The relationship between myofibroblasts and excessive collagen deposition during fibrosis remains unclear. Previous studies using double-labelling analysis of collagen type I mRNA and α-SMA protein appeared to indicate that myofibroblasts are major producers of collagen in fibrotic tissue (134;507). However, more recent studies using transgenic technology have demonstrated that in certain circumstances collagen-producing cells are not myofibroblasts (183;215). Moreover, during murine wound healing, myofibroblasts are no longer present in the granulation tissue after 12 days (200), yet collagen biosynthesis continues well after this point (415). Interestingly, previous analyses of dcSSc skin also demonstrated that there was no correlation between the presence of myofibroblasts and α1(I) procollagen mRNA (219). Other studies have identified fibrocytes (75), bone marrow-derived fibroblasts (183;263) and pericytes (439) as sources of collagen biosynthesis. Therefore, further studies aimed at identifying collagen-synthesising cells and their origins are essential.

### 7.2.3 Myofibroblasts and pericytes converge phenotypically in dcSSc

Double-labelling studies confirmed the expression of Thy-1 by myofibroblasts and pericytes, providing further support for the differentiation of pericytes into myofibroblasts. It had previously been suggested that Thy-1 expression was specific to fibroblasts (371) and more recently, Koumas and colleagues reported that only fibroblasts expressing Thy-1 have the potential to become myofibroblasts (252). Moreover, Thy-1-expressing fibroblasts have been shown to synthesise and bind

higher levels of CTGF (176), which is now considered a key autocrine mediator in the activation of fibroblasts during fibrosis (406). Interestingly a marked increase in interstitial Thy-1 immunostaining was detected in dcSSc skin compared to normal tissue. The reasons for this are unclear as Western blot analysis demonstrated that cultured dcSSc fibroblasts do not express increased levels of Thy-1 compared to control fibroblasts. Therefore, the apparent increase in Thy-1 immunostaining may be caused by a migration of Thy-$1^{+ve}$ cells from the microvascular wall to the interstitium. This is supported by the finding of reduced perivascular staining of Thy-1 in dcSSc skin in comparison to normal skin and supports the hypothesis that Thy-$1^{+ve}$ pericytes undergo a phenotypic transition to interstitial myofibroblasts in dcSSc. Thy-1 immunostaining was elevated throughout all layers of the dermis, however, myofibroblasts were only detected in the reticular dermal layers where ED-A FN was expressed. Therefore, while Thy-1 may play a role in myofibroblast differentiation, in areas of the skin lacking ED-A FN, Thy-$1^{+ve}$ cells do not appear to acquire a myofibroblastic phenotype.

### 7.2.4 Increased proliferation of pericytes in dcSSc skin

The finding of increased pericyte proliferation corroborates similar data from a recently published study of dcSSc skin, in which increased pericyte proliferation was observed without a corresponding rise in microvascular density (195). Pericyte proliferation is normally associated with angiogenesis and increased microvascular density (161), however, SSc is characterised by a failed angiogenic response and reduced microvascular density (112). Increased pericyte proliferation without an increase in capillary density has also been demonstrated in an *in vivo* model of tumour formation and was found to be mediated by PDGFRβ (153). This data supports the idea that in dcSSc skin, the proliferation of pericytes, which may be mediated by increased signalling through elevated levels of PDGFRβ, creates a pool of myofibroblast progenitor cells. These Thy-$1^{+ve}$ cells then migrate from the microvascular wall and differentiate into myofibroblasts through the actions of ED-A FN and other factors (Figure 7.1).

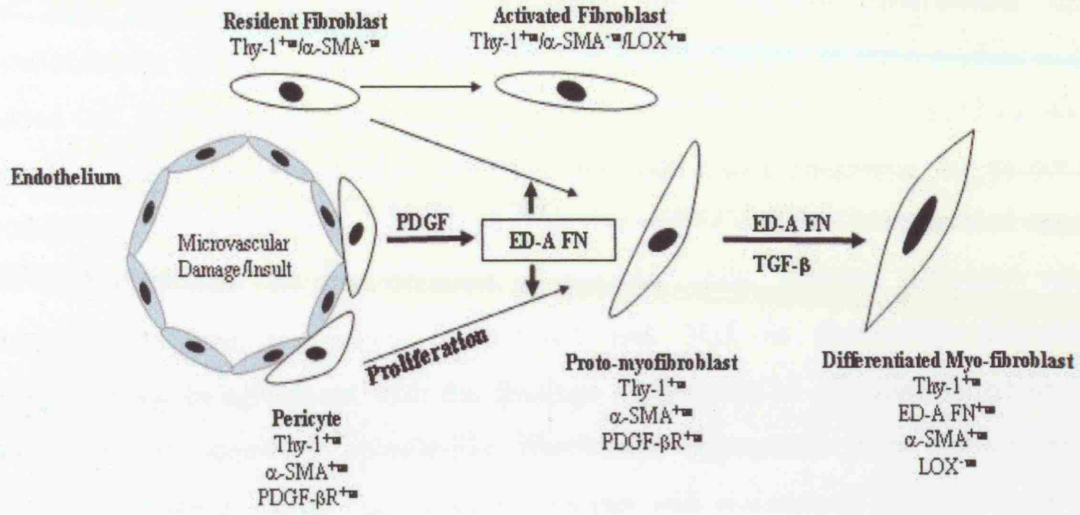


**Figure 7.1.**

**Convergence of microvascular pericytes and resident fibroblasts to a myofibroblast lineage in SSc.**

Two pathways potentially contribute to the fibrogenic response in dcSSc. In this model, microvascular pericytes (Thy-$1^{+ve}$/α-$SMA^{+ve}$) become activated as a result of microvascular damage and produce the ED-A splice variant of fibronectin, a protein known to induce the myofibroblast phenotype. The microvascular-derived ED-A FN in concert with the actions of TGF-β may also act upon resident perivascular fibroblasts (Thy-$1^{+ve}$/α-$SMA^{-ve}$) stimulating their differentiation into myofibroblasts. Proliferation of both pericytes and fibroblasts may help to create a pool of potential myofibroblasts.

## 7.3 The differentiation of pericytes into myofibroblasts *in vitro*

### 7.3.1 Pericytes undergo a phenotypic transition to myofibroblasts *in vitro*

The data presented in chapter 4 suggested that pericytes differentiate into myofibroblasts in dcSSc skin. To test this hypothesis further, *in vitro* studies were carried out. It has not yet been possible to isolate pericytes from mammalian skin, therefore, pericytes were established from placental tissue following the protocol established by Ivarrson *et al.* (214;439). The placenta is a highly vascularised organ and highly suitable for the isolation of vascular cells. Isolated pericytes were identified by their expression of α-SMA and 3G5 as previously described (214;315;439). In agreement with the findings of Ivarrson *et al.,* cultured pericytes were found to acquire a spindle-like fibroblastic appearance after sub-culturing (214;439). However, these late passage pericytes still maintained high levels of α-SMA incorporated into stress fibres, suggesting that they were not fibroblasts as previously reported, but myofibroblasts (214;439). In support of this, early and late passage pericytes were also found to express ED-A FN and increased levels of vinculin within fibronexus type adhesion junctions, two key markers of myofibroblasts (121;455). The fibronexus is a specialised adhesion complex that uses transmembrane integrins to link intracellular actin with extracellular fibronectin. Functionally, this provides a bi-directional mechano-transduction system that allows force that is generated by stress fibres to be transmitted to the surrounding ECM and extracellular mechanical signals to be transmitted to the cell (59). In agreement with previous findings, fibroblasts did not express ED-A FN and did not possess fibronexus adhesion complexes (120;121;199). However, treatment of fibroblasts with TGF-β to generate myofibroblasts resulted in the synthesis of α-SMA, ED-A FN and the presence of fibronexus complexes, confirming earlier findings (121;199).

Previous studies investigating the differentiation of pericytes *in vitro* had used bovine retinal pericytes (BRP). The earliest studies described their differentiation into osteoblasts, capable of synthesising a calcified matrix *in vitro* and *in vivo* (115;392). Subsequent analysis revealed that BRP can also differentiate into chondrocytes, adipocytes when grown with specific growth media (135). The differentiation of BRP into myofibroblasts or fibroblasts has not been previously reported. Recently, pericytes isolated from the central nervous system (CNS) were shown to selectively differentiate into glial cells *in vitro* (118), while *in vivo,* CNS pericytes are known to migrate from the microvascular wall after injury, possibly as a prelude to

differentiation (119). Therefore, the ultimate phenotype of pericytes appears to be largely dependent on their tissue of origin and to a lesser extent the conditions under which they are cultured. Interestingly, pericytes also express STRO-1, a marker of bone marrow-derived mesenchymal stem cells (32), which has led to the hypothesis that the pericytes represent an adult stem-cell niche within the microvasculature (32).

### 7.3.2 Pericytes are highly contractile cells

Pericytes were investigated for their ability to contract tethered collagen lattices, which is a well characterised assay for myofibroblast function (455). Both early and late passage pericytes were found to be highly contractile, generating a force similar to that of myofibroblasts and significantly greater than that of fibroblasts. Pericyte contractility has been previously demonstrated in free-floating collagen matrices (426). However, the reduction in diameter of these lattices is caused by small tractional forces generated by non-directional migration of cultured cells (125) and therefore, unrestrained gels are poor models for mechanically regulated processes such as tissue contraction. In a living organism, almost all tissues are tethered in such a way that cell contraction will inevitably increase stress in the surrounding matrix. This feedback mechanical signal is missing in floating collagen lattices (175).

The finding that pericytes are almost as contractile as myofibroblasts is potentially significant. It has been suggested that pericyte contractility is the basis for controlling vessel diameter and blood flow in small capillaries (426). However, in an earlier study using inert silicone matrices as a model for contraction, retinal pericytes were found to be significantly more contractile than aortic vSMCs (239). The contractile forces required to regulate capillary diameter are considerably less than that to contract large vessels, suggesting that pericytes carry out additional functions for which an enhanced contractile ability is required.

### 7.3.3 Pericyte contraction is induced by PDGF

The addition of TGF-β did not promote gel contraction by pericytes. The contractile properties of TGF-β with regard to fibroblasts and myofibroblasts are well established (455), however, the effects of TGF-β on cultured pericytes are less clear. D'Amore *et al.* have shown that TGF-β can induce migration, albeit weakly in cultured retinal pericytes (93). TGF-β induces the expression of contractile proteins such as α-SMA in undifferentiated 10T1/2 mesenchymal cells (202) and in brain pericytes that lack α-SMA (472). However, in pericytes expressing α-SMA, TGF-β induces growth arrest (409). The repertoire of TGF-β receptors and TGF-β isoforms is highly heterogeneous between pericytes from different tissue beds. Therefore, the effects of TGF-β on pericytes can be variable (15;295).

In my experiments, the addition of PDGF-BB increased the contractile force exerted by pericytes, while serum induced contraction by pericytes was partially blocked by PDGFRβ inhibition. It has previously been shown that PDGF-BB and TGF-β do not stimulate the contraction of free-floating matrices by liver pericytes (362), however, the effect of PDGF-BB on pericytes in tethered gels was previously unknown. PDGF-BB promotes fibroblast contractility in collagen lattices in a Rho-kinase dependent mechanism (2). Interestingly, neither PDGF-BB treatment nor PDGFRβ blockade affected the expression of contractile proteins such as α-SMA and ED-A FN in pericytes, suggesting that PDGF-induced contraction is not dependent on the increased synthesis of contractile proteins. Rather PDGF-BB is thought to induce contraction in cells expressing α-SMA by promoting an increase in the intracellular $Ca^{2+}$ concentration, leading to the subsequent phosphorylation of the myosin light chain (MLC) catalysed by $Ca^{2+}$/calmodulin-dependent MLC kinase (MLCK), which induces contraction (231;372). The finding that PDGF-BB induces pericyte contraction of tethered collagen gels further supports the hypothesis that PDGF-BB is central to pericyte function during fibrosis. However, PDGFRβ blockade did not inhibit pericyte to myofibroblast differentiation. Further studies are required to unravel the molecular mechanisms underlying pericyte differentiation.

## 7.4 The effects of PDGFRβ blockade on tissue repair: *In vivo* and *in vitro* analysis

### 7.4.1 PDGFβ receptor activation promotes fibroblast and pericyte recruitment during cutaneous wound healing

In the previous chapters, I have established that pericytes become activated and express PDGFRβ in dcSSc tissue. Additionally, *in vivo* and *in vitro* data supports the hypothesis that pericytes can differentiate into myofibroblasts in fibrotic tissue and that PDGF-BB may play an important role in the function of these differentiated myofibroblasts. In the final chapter I focus on the function of PDGFRβ signalling during extracellular matrix deposition *in vivo.*

Due to the embryonic lethality of PDGFRβ knockout mice, our understanding of the role of PDGFRβ in tissue repair and fibrosis has predominantly stemmed from *in vitro* studies and immunohistochemical analyses (191). Comparatively little is known about how PDGFRβ signalling contributes to fibrosis and scarring *in vivo*. To address this, I have employed the selective PDGFRβ inhibitor imatinib mesylate and assessed its affects on cutaneous wound healing *in vivo*. Besides the PDGFRβ, imatinib is also known to inhibit the c-abl and c-kit tyrosine kinases (52). Therefore, the possibility that inhibition of these kinases contribute to the impairment of wound healing and collagen biosynthesis cannot be ruled out. However, while c-abl was recently identified as a potential mediator of TGF-β activity (94), in the current study, imatinib was found to have no effect on the TGF-β induced formation of myofibroblasts *in vitro*, nor were any previously reported characteristics of impaired TGF-β signalling during wound healing such as accelerated re-epithelialisation detected (20). Furthermore, there is no published evidence that c-kit is involved in wound healing or directly mediates fibroblast and pericyte proliferation and migration, which taken together support the hypothesis that the effect of imatinib on these cells is attributable to PDGFRβ blockade.

The data suggest that *in vivo,* PDGFRβ is a key mitogen and motogen for both fibroblasts and pericytes during tissue repair in vivo. Between 3 and 7 days post-wounding, cell proliferation was significantly reduced in the granulation tissue of imatinib-treated wounds. In control tissue after 3 days, proliferating cells were located predominantly in the wound margins and in the basal epidermis. Reduced cell proliferation in imatinib-treated wounds was also associated with interstitial

fibroblasts and microvascular cells. Using an *in vitro* approach, imatinib treatment was shown to significantly impair the migration and proliferation of cultured fibroblasts and pericytes in response to both PDGF-BB and serum. In agreement with a recently published study, imatinib did not induce apoptosis *in vivo* or *in vitro* (376), suggesting that inhibition of proliferation and migration are the principle mechanisms by which imatinib impairs wound healing. A further aspect of imatinib treatment was a significant reduction in wound closure. Wound closure is thought to be initiated by tractional forces generated by fibroblasts migrating into newly forming granulation tissue (455). As the wound closes, mechanical tension develops, which combined with the actions of TGF-β and ED-A FN induces the formation of myofibroblasts, which then contract the wound (200). As the granulation tissue of imatinib-treated wounds was generally hypocellular compared to controls, it is plausible that the failure to initiate wound closure stems from the inhibition of PDGFβR-mediated recruitment of fibroblasts into the wound. The subsequent reduction in tractional force generation could conceivably result in reduced wound closure.

### 7.4.2 PDGFRβ inhibition results in reduced myofibroblast numbers

The impairment of fibroblast recruitment would also account for the delay in the appearance of myofibroblasts in imatinib-treated wounds. Imatinib treatment resulted in a reduction in the number of α-SMA expressing myofibroblasts and reduced expression of ED-A FN, which is crucial for myofibroblast formation (394). After 3 days, α-SMA immunostaining, denoting the presence of myofibroblasts, was present in control tissue but absent in treated tissue. By 7 days, the number of myofibroblasts in treated wounds was still reduced, however, the difference was no longer statistically significant. During wound healing the differentiation of myofibroblasts from fibroblasts is stimulated by mechanical tension generated as wound margins are re-approximated (200;455). Therefore, a reduction in cell migration and recruitment would result in a smaller pool of cells from which myofibroblasts could be formed and loss of tractional forces would delay the generation of mechanical tension which is an essential requirement for myofibroblast formation. Imatinib treatment had no effect on the TGF-β-mediated differentiation of myofibroblasts *in vitro,* supporting the idea that the reduction in myofibroblasts seen in treated animals is a secondary repercussion of impaired fibroblast migration and proliferation. Interestingly, it has been proposed that imatinib attenuates the fibrotic response by inhibiting TGF-β mediated signalling via a novel non-Smad dependent pathway (94;476). While further

studies are required to confirm this, my data demonstrate that the induction of the myofibroblast phenotype by TGF-β *in vitro* is not affected by imatinib treatment.

### 7.4.3 PDGFRβ signalling promotes collagen biosynthesis during tissue repair *in vivo*

Distribution and quantification of collagen type I biosynthesis was analysed using a collagen transgenic reporter mouse harbouring 17kb of the far upstream collagen enhancer fused to luciferase and β-galactosidase reporter genes (42). The transgene has been previously shown to be activated during tissue repair and mirror endogenous collagen mRNA expression and distribution (347). PDGFRβ blockade resulted in a significant reduction in collagen gene activation and protein expression. Addition of exogenous PDGF-BB has been shown to increase the synthesis of matrix components such as fibronectin and collagen during excisional wound healing (344). Moreover, the forced over-expression of PDGF-B chain in the lung produces a pronounced fibrotic response and increased collagen biosynthesis (498). However, PDGF-B has been shown to have no direct stimulatory affect on type I collagen gene transcription in cultured fibroblasts (82). Therefore, the observed pro-fibrotic effects of PDGF-B are likely to stem from its capacity to promote fibroblast proliferation and recruitment rather than a direct activation of ECM gene transcription. Thus, the reduction in collagen biosynthesis brought about by imatinib treatment is a consequence of reduced fibroblast and pericyte proliferation and recruitment.

### 7.4.4 PDGFRβ signalling is required for microvascular formation during tissue repair

The data demonstrate that during tissue repair endogenous PDGFRβ plays a key role in mediating fibroblast and pericyte proliferation *in vivo*. A prominent characteristic of imatinib-treated granulation tissue in my experiments was the appearance of abnormally distended microvessels. These so-called micro-aneurysms have been well documented in the tissue of PDGFRβ and PDGF-B chain knockout embryos. Subsequent studies demonstrated that during development, endothelial-derived PDGF-B acts as a potent chemotactic and mitogenic agent for PDGFRβ expressing pericytes as they migrate along nascent capillaries (194). Therefore, disruption to the PDGFRβ signalling pathway leads to a failure to recruit pericytes during new vessel development and results in micro-aneurysm formation. Using an *in vitro* approach,

imatinib treatment was shown to impair the migration and proliferation of cultured pericytes in response to both PDGF-BB and serum. These findings are in agreement with studies showing impaired microvascular formation in response to PDGFRβ inhibition in the vasculature of tumours (29;399). It was recently demonstrated that during tumour formation, the differentiation of pericytes from bone marrow-derived progenitor cells is PDGFRβ-dependent (420). While this mechanism of pericyte recruitment has yet to be demonstrated in wound healing, it is clear that PDGFRβ signalling is central to the expansion and recruitment of resident pericytes in the adult. PDGFRβ was found to have no effect on fibroblast and pericytes apoptosis *in vivo* and *in vitro* in agreement with previous findings (376).

## 7.5 OVERALL CONCLUSIONS

These studies have demonstrated that pericytes become activated and express PDGFRβ in SSc tissue. *In vivo* and *in vitro* evidence suggesting that pericytes are precursor cells for myofibroblasts in fibrotic tissue is proposed. Finally, *in vivo* analyses suggest that PDGFRβ is a critical factor in mediating fibroblast and pericyte recruitment in tissue repair and scarring. These findings suggest that PDGFRβ signalling plays a key role in the pathogenesis of SSc by driving pericyte activation identifying the PDGFRβ as a therapeutic target.

## 7.6 FUTURE STUDIES

A multi-centre phase I clinical trial of imatinib in SSc is currently ongoing and the initial results are keenly awaited. PDGFRβ blockade has also been successful in treating experimental PAH (387). Further studies should be carried out in SSc, exploring the capacity of PDGFRβ blockade to act as a dual therapeutic agent, simultaneously targeting fibrosis and PAH.

It has become apparent that the view of the fibroblast as the principal 'fibrotic' cell is out-dated. The discovery of fibrocytes and bone marrow-derived fibroblasts has added extra dimensions of complexity and discovering how these cells are recruited, become activated and interact in fibrotic tissue will be essential in our understanding of fibrotic conditions such as SSc.

Gene array studies of pericytes are beginning to yield information on the molecular cues that drive pericyte differentiation. Further studies incorporating in vivo analyses of gene expression using laser dissection techniques will clarify our understanding of the mechanisms that regulate pericyte differentiation.

Due to the lethality of the PDGFRβ knockout mice, there is still much to appreciate about the *in vivo* roles of PDGFRβ signalling. The generation of a conditional 'floxed' PDGFRβ knockout mouse (159) will go some way to address this shortfall in our knowledge and will potentially clarify the role of PDGFRβ signalling in many adult pathologies.

Reference List


1. Preliminary criteria for the classification of systemic sclerosis (scleroderma). Subcommittee for scleroderma criteria of the American Rheumatism Association Diagnostic and Therapeutic Criteria Committee. Arthritis Rheum 1980, 23: 581-590

2. Abe M, Ho CH, Kamm KE, and Grinnell F: Different molecular motors mediate platelet-derived growth factor and lysophosphatidic acid-stimulated floating collagen matrix contraction. J Biol Chem 2003, 278: 47707-47712

3. Abe R, Donnelly SC, Peng T, Bucala R, and Metz CN: Peripheral blood fibrocytes: differentiation pathway and migration to wound sites. J Immunol 2001, 166: 7556-7562

4. Abraham D, Ponticos M, and Nagase H: Connective tissue remodeling: cross-talk between endothelins and matrix metalloproteinases. Curr Vasc Pharmacol 2005, 3: 369-379

5. Abraham DJ, Vancheeswaran R, Dashwood MR, Rajkumar VS, Pantelides P, Xu SW, du Bois RM, and Black CM: Increased levels of endothelin-1 and differential endothelin type A and B receptor expression in scleroderma-associated fibrotic lung disease. Am J Pathol 1997, 151: 831-841

6. Abraham DJ and Varga J: Scleroderma: from cell and molecular mechanisms to disease models. Trends Immunol 2005, 26: 587-595

7. Adamson IY and Bowden DH: The pathogenesis of bloemycin-induced pulmonary fibrosis in mice. Am J Pathol 1974, 77: 185-197

8. Akagi A, Tajima S, Ishibashi A, Yamaguchi N, and Nagai Y: Expression of type XVI collagen in human skin fibroblasts: enhanced expression in fibrotic skin diseases. J Invest Dermatol 1999, 113: 246-250

9. Allanore Y, Borderie D, Lemarechal H, Ekindjian OG, and Kahan A: Lack of association of eNOS (G894T) and p22phox NADPH oxidase subunit (C242T) polymorphisms with systemic sclerosis in a cohort of French Caucasian patients. Clin Chim Acta 2004, 350: 51-55

10. Allcock RJ, Forrest I, Corris PA, Crook PR, and Griffiths ID: A study of the prevalence of systemic sclerosis in northeast England. Rheumatology (Oxford) 2004, 43: 596-602

11. Amano M, Ito M, Kimura K, Fukata Y, Chihara K, Nakano T, Matsuura Y, and Kaibuchi K: Phosphorylation and activation of myosin by Rho-associated kinase (Rho-kinase). J Biol Chem 1996, 271: 20246-20249

12. Andersen GN, Caidahl K, Kazzam E, Petersson AS, Waldenstrom A, Mincheva-Nilsson L, and Rantapaa-Dahlqvist S: Correlation between increased nitric oxide production and markers of endothelial activation in systemic sclerosis: findings with the soluble adhesion molecules E-selectin, intercellular adhesion molecule 1, and vascular cell adhesion molecule 1. Arthritis Rheum 2000, 43: 1085-1093

13. Anderson ME, Moore TL, Hollis S, Clark S, Jayson MI, and Herrick AL: Endothelial-dependent vasodilation is impaired in patients with systemic sclerosis, as assessed by low dose iontophoresis. Clin Exp Rheumatol 2003, 21: 403

14. Antonelli-Orlidge A, Saunders KB, Smith SR, and D'Amore PA: An activated form of transforming growth factor beta is produced by cocultures of endothelial cells and pericytes. Proc Natl Acad Sci U S A 1989, 86: 4544-4548

15. Armulik A, Abramsson A, and Betsholtz C: Endothelial/pericyte interactions. Circ Res 2005, 97: 512-523

16. Arnett FC, Cho M, Chatterjee S, Aguilar MB, Reveille JD, and Mayes MD: Familial occurrence frequencies and relative risks for systemic sclerosis (scleroderma) in three United States cohorts. Arthritis Rheum 2001, 44: 1359-1362

17. Arnett FC, Howard RF, Tan F, Moulds JM, Bias WB, Durban E, Cameron HD, Paxton G, Hodge TJ, Weathers PE, and Reveille JD: Increased prevalence of systemic sclerosis in a Native American tribe in Oklahoma. Association with an Amerindian HLA haplotype. Arthritis Rheum 1996, 39: 1362-1370

18. Asano Y, Ihn H, Yamane K, Jinnin M, Mimura Y, and Tamaki K: Phosphatidylinositol 3-kinase is involved in alpha2(I) collagen gene expression in normal and scleroderma fibroblasts. J Immunol 2004, 172: 7123-7135

19. Asano Y, Ihn H, Yamane K, Kubo M, and Tamaki K: Impaired Smad7-Smurf-mediated negative regulation of TGF-beta signaling in scleroderma fibroblasts. J Clin Invest 2004, 113: 253-264

20. Ashcroft GS, Yang X, Glick AB, Weinstein M, Letterio JL, Mizel DE, Anzano M, Greenwell-Wild T, Wahl SM, Deng C, and Roberts AB: Mice lacking Smad3 show accelerated wound healing and an impaired local inflammatory response. Nat Cell Biol 1999, 1: 260-266

21. Atamas SP, Luzina IG, Choi J, Tsymbalyuk N, Carbonetti NH, Singh IS, Trojanowska M, Jimenez SA, and White B: Pulmonary and activation-regulated chemokine stimulates collagen production in lung fibroblasts. Am J Respir Cell Mol Biol 2003, 29: 743-749

22. Atamas SP and White B: Cytokine regulation of pulmonary fibrosis in scleroderma. Cytokine Growth Factor Rev 2003, 14: 537-550

23. Atamas SP, Yurovsky VV, Wise R, Wigley FM, Goter Robinson CJ, Henry P, Alms WJ, and White B: Production of type 2 cytokines by CD8+ lung cells is associated with greater decline in pulmonary function in patients with systemic sclerosis. Arthritis Rheum 1999, 42: 1168-1178

24. Ausprunk DH and Folkman J: Migration and proliferation of endothelial cells in preformed and newly formed blood vessels during tumor angiogenesis. Microvasc Res 1977, 14: 53-65

25. Avila JJ, Lympany PA, Pantelidis P, Welsh KI, Black CM, and du Bois RM: Fibronectin gene polymorphisms associated with fibrosing alveolitis in systemic sclerosis. Am J Respir Cell Mol Biol 1999, 20: 106-112

26. Basu D and Reveille JD: Anti-scl-70. Autoimmunity 2005, 38: 65-72

27. Bedossa P, Houglum K, Trautwein C, Holstege A, and Chojkier M: Stimulation of collagen alpha 1(I) gene expression is associated with lipid peroxidation in hepatocellular injury: a link to tissue fibrosis? Hepatology 1994, 19: 1262-1271

28. Bell S, Krieg T, and Meurer M: Antibodies to Ro/SSA detected by ELISA: correlation with clinical features in systemic scleroderma. Br J Dermatol 1989, 121: 35-41

29. Bergers G, Song S, Meyer-Morse N, Bergsland E, and Hanahan D: Benefits of targeting both pericytes and endothelial cells in the tumor vasculature with kinase inhibitors. J Clin Invest 2003, 111: 1287-1295

30. Betsholtz C: Insight into the physiological functions of PDGF through genetic studies in mice. Cytokine Growth Factor Rev 2004, 15: 215-228

31. Betsholtz C, Lindblom P, and Gerhardt H: Role of pericytes in vascular morphogenesis. EXS 2005, 115-125

32. Bianco P, Riminucci M, Gronthos S, and Robey PG: Bone marrow stromal stem cells: nature, biology, and potential applications. Stem Cells 2001, 19: 180-192

33. Bjarnegard M, Enge M, Norlin J, Gustafsdottir S, Fredriksson S, Abramsson A, Takemoto M, Gustafsson E, Fassler R, and Betsholtz C: Endothelium-specific ablation of PDGFB leads to pericyte loss and glomerular, cardiac and placental abnormalities. Development 2004, 131: 1847-1857

34. Black CM: The aetiopathogenesis of systemic sclerosis: thick skin--thin hypotheses. The Parkes Weber Lecture 1994. J R Coll Physicians Lond 1995, 29: 119-130

35. Black CM and Denton CP: Scleroderma and related disorders in adults and children. Oxford Textbook of Rheumatology. Edited by Maddison P, Isenberg DA, Woo P, and Glass DN. Oxford University Press, 1998, pp. 1217-1247

36. Bolster MB, Ludwicka A, Sutherland SE, Strange C, and Silver RM: Cytokine concentrations in bronchoalveolar lavage fluid of patients with systemic sclerosis. Arthritis Rheum 1997, 40: 743-751

37. Bolster MB and Silver RM: Assessment and management of scleroderma lung disease. Curr Opin Rheumatol 1999, 11: 508-513

38. Bombardieri S, Medsger TA, Jr., Silman AJ, and Valentini G: The assessment of the patient with systemic sclerosis. Introduction. Clin Exp Rheumatol 2003, 21: S2-S4

39. Bordron A, Dueymes M, Levy Y, Jamin C, Leroy JP, Piette JC, Shoenfeld Y, and Youinou PY: The binding of some human antiendothelial cell antibodies induces endothelial cell apoptosis. J Clin Invest 1998, 101: 2029-2035

40. Borkham-Kamphorst E, Herrmann J, Stoll D, Treptau J, Gressner AM, and Weiskirchen R: Dominant-negative soluble PDGF-beta receptor inhibits

hepatic stellate cell activation and attenuates liver fibrosis. Lab Invest 2004, 84: 766-777

41. Borrello MA and Phipps RP: Differential Thy-1 expression by splenic fibroblasts defines functionally distinct subsets. Cell Immunol 1996, 173: 198-206

42. Bou-Gharios G, Garrett LA, Rossert J, Niederreither K, Eberspaecher H, Smith C, Black C, and Crombrugghe B: A potent far-upstream enhancer in the mouse pro alpha 2(I) collagen gene regulates expression of reporter genes in transgenic mice. J Cell Biol 1996, 134: 1333-1344

43. Bou-Gharios G, Osman J, Black C, and Olsen I: Excess matrix accumulation in scleroderma is caused partly by differential regulation of stromelysin and TIMP-1 synthesis. Clin Chim Acta 1994, 231: 69-78

44. Boulanger CM, Tanner FC, Bea ML, Hahn AW, Werner A, and Luscher TF: Oxidized low density lipoproteins induce mRNA expression and release of endothelin from human and porcine endothelium. Circ Res 1992, 70: 1191-1197

45. Bouros D, Wells AU, Nicholson AG, Colby TV, Polychronopoulos V, Pantelidis P, Haslam PL, Vassilakis DA, Black CM, and du Bois RM: Histopathologic subsets of fibrosing alveolitis in patients with systemic sclerosis and their relationship to outcome. Am J Respir Crit Care Med 2002, 165: 1581-1586

46. Brachvogel B, Moch H, Pausch F, Schlotzer-Schrehardt U, Hofmann C, Hallmann R, von der MK, Winkler T, and Poschl E: Perivascular cells expressing annexin A5 define a novel mesenchymal stem cell-like population with the capacity to differentiate into multiple mesenchymal lineages. Development 2005, 132: 2657-2668

47. Bradham DM, Igarashi A, Potter RL, and Grotendorst GR: Connective tissue growth factor: a cysteine-rich mitogen secreted by human vascular endothelial cells is related to the SRC-induced immediate early gene product CEF-10. J Cell Biol 1991, 114: 1285-1294

48. Brentnall TJ, Kenneally D, Barnett AJ, de Aizpurua HJ, Lolait SJ, Ashcroft R, and Toh BH: Autoantibodies to fibroblasts in scleroderma. J Clin Lab Immunol 1982, 8: 9-12

49. Brew K, Dinakarpandian D, and Nagase H: Tissue inhibitors of metalloproteinases: evolution, structure and function. Biochim Biophys Acta 2000, 1477: 267-283

50. Brouwer R, Vree Egberts WT, Hengstman GJ, Raijmakers R, van Engelen BG, Seelig HP, Renz M, Mierau R, Genth E, Pruijn GJ, and van Venrooij WJ: Autoantibodies directed to novel components of the PM/Scl complex, the human exosome. Arthritis Res 2002, 4: 134-138

51. Bruckdorfer KR, Hillary JB, Bunce T, Vancheeswaran R, and Black CM: Increased susceptibility to oxidation of low-density lipoproteins isolated from patients with systemic sclerosis. Arthritis Rheum 1995, 38: 1060-1067

52. Buchdunger E, Cioffi CL, Law N, Stover D, Ohno-Jones S, Druker BJ, and Lydon NB: Abl protein-tyrosine kinase inhibitor STI571 inhibits in vitro signal transduction mediated by c-kit and platelet-derived growth factor receptors. J Pharmacol Exp Ther 2000, 295: 139-145

53. Buchdunger E, O'Reilly T, and Wood J: Pharmacology of imatinib (STI571). Eur J Cancer 2002, 38 Suppl 5: S28-S36

54. Buckingham RB, Prince RK, and Rodnan GP: Progressive systemic sclerosis (PSS, scleroderma) dermal fibroblasts synthesize increased amounts of glycosaminoglycan. J Lab Clin Med 1983, 101: 659-669

55. Buetow BS, Crosby JR, Kaminski WE, Ramachandran RK, Lindahl P, Martin P, Betsholtz C, Seifert RA, Raines EW, and Bowen-Pope DF: Platelet-derived growth factor B-chain of hematopoietic origin is not necessary for granulation tissue formation and its absence enhances vascularization. Am J Pathol 2001, 159: 1869-1876

56. Buetow BS, Tappan KA, Crosby JR, Seifert RA, and Bowen-Pope DF: Chimera analysis supports a predominant role of PDGFRbeta in promoting smooth-muscle cell chemotaxis after arterial injury. Am J Pathol 2003, 163: 979-984

57. Bunn CC, Denton CP, Shi-wen X, Knight C, and Black CM: Anti-RNA polymerases and other autoantibody specificities in systemic sclerosis. Br J Rheumatol 1998, 37: 15-20

58. Bunn, C. C. and Tormey, V. J. Antinuclear antibodies in systemic sclerosis. CPD BulletinImmunology and Allergy 1, 78-81. 2000.
Ref Type: Generic

59. Burridge K and Chrzanowska-Wodnicka M: Focal adhesions, contractility, and signaling. Annu Rev Cell Dev Biol 1996, 12: 463-518

60. Calamia KT, Scolapio JS, and Viggiano TR: Endoscopic YAG laser treatment of watermelon stomach (gastric antral vascular ectasia) in patients with systemic sclerosis. Clin Exp Rheumatol 2000, 18: 605-608

61. Campbell PM and LeRoy EC: Pathogenesis of systemic sclerosis: a vascular hypothesis. Semin Arthritis Rheum 1975, 4: 351-368

62. Canfield AE, Doherty MJ, Wood AC, Farrington C, Ashton B, Begum N, Harvey B, Poole A, Grant ME, and Boot-Handford RP: Role of pericytes in vascular calcification: a review. Z Kardiol 2000, 89 Suppl 2:20-7: 20-27

63. Carulli MT, Ong VH, Ponticos M, Shiwen X, Abraham DJ, Black CM, and Denton CP: Chemokine receptor CCR2 expression by systemic sclerosis fibroblasts: evidence for autocrine regulation of myofibroblast differentiation. Arthritis Rheum 2005, 52: 3772-3782

64. Carvalho D, Savage CO, Black CM, and Pearson JD: IgG antiendothelial cell autoantibodies from scleroderma patients induce leukocyte adhesion to human vascular endothelial cells in vitro. Induction of adhesion molecule expression and involvement of endothelium-derived cytokines. J Clin Invest 1996, 97: 111-119

65. Casciola-Rosen L, Wigley F, and Rosen A: Scleroderma autoantigens are uniquely fragmented by metal-catalyzed oxidation reactions: implications for pathogenesis. J Exp Med 1997, 185: 71-79

66. Cassiman D, Libbrecht L, Desmet V, Denef C, and Roskams T: Hepatic stellate cell/myofibroblast subpopulations in fibrotic human and rat livers. J Hepatol 2002, 36: 200-209

67. Chambers RC, Leoni P, Kaminski N, Laurent GJ, and Heller RA: Global expression profiling of fibroblast responses to transforming growth factor-beta1 reveals the induction of inhibitor of differentiation-1 and provides evidence of smooth muscle cell phenotypic switching. Am J Pathol 2003, 162: 533-546

68. Chan LS, Vanderlugt CJ, Hashimoto T, Nishikawa T, Zone JJ, Black MM, Wojnarowska F, Stevens SR, Chen M, Fairley JA, Woodley DT, Miller SD, and Gordon KB: Epitope spreading: lessons from autoimmune skin diseases. J Invest Dermatol 1998, 110: 103-109

69. Chanez P, Lacoste JY, Guillot B, Giron J, Barneon G, Enander I, Godard P, Michel FB, and Bousquet J: Mast cells' contribution to the fibrosing alveolitis of the scleroderma lung. Am Rev Respir Dis 1993, 147: 1497-1502

70. Charo IF and Ransohoff RM: The many roles of chemokines and chemokine receptors in inflammation. N Engl J Med 2006, 354: 610-621

71. Chen JK, Haimes HB, and Weinberg CB: Role of growth factors in the contraction and maintenance of collagen lattices made with arterial smooth muscle cells. J Cell Physiol 1991, 146: 110-116

72. Chen Y, Shi-wen X, van Beek J, Kennedy L, McLeod M, Renzoni EA, Bou-Gharios G, Wilcox-Adelman S, Goetinck PF, Eastwood M, Black CM, Abraham DJ, and Leask A: Matrix Contraction by Dermal Fibroblasts Requires Transforming Growth Factor-{beta}/Activin-Linked Kinase 5, Heparan Sulfate-Containing Proteoglycans, and MEK/ERK: Insights into Pathological Scarring in Chronic Fibrotic Disease. Am J Pathol 2005, 167: 1699-1711

73. Chesney J and Bucala R: Peripheral blood fibrocytes: novel fibroblast-like cells that present antigen and mediate tissue repair. Biochem Soc Trans 1997, 25: 520-524

74. Chesney J and Bucala R: Peripheral blood fibrocytes: mesenchymal precursor cells and the pathogenesis of fibrosis. Curr Rheumatol Rep 2000, 2: 501-505

75. Chesney J, Metz C, Stavitsky AB, Bacher M, and Bucala R: Regulated production of type I collagen and inflammatory cytokines by peripheral blood fibrocytes. J Immunol 1998, 160: 419-425

76. Chizzolini C, Parel Y, Scheja A, and Dayer JM: Polarized subsets of human T-helper cells induce distinct patterns of chemokine production by normal and systemic sclerosis dermal fibroblasts. Arthritis Res Ther 2005, 8: R10

77. Chizzolini C, Raschi E, Rezzonico R, Testoni C, Mallone R, Gabrielli A, Facchini A, Del Papa N, Borghi MO, Dayer JM, and Meroni PL: Autoantibodies to fibroblasts induce a proadhesive and proinflammatory fibroblast phenotype in patients with systemic sclerosis. Arthritis Rheum 2002, 46: 1602-1613

78. Chizzolini C, Rezzonico R, Ribbens C, Burger D, Wollheim FA, and Dayer JM: Inhibition of type I collagen production by dermal fibroblasts upon contact with activated T cells: different sensitivity to inhibition between systemic sclerosis and control fibroblasts. Arthritis Rheum 1998, 41: 2039-2047

79. Cho H, Kozasa T, Bondjers C, Betsholtz C, and Kehrl JH: Pericyte-specific expression of Rgs5: implications for PDGF and EDG receptor signaling during vascular maturation. FASEB J 2003, 17: 440-442

80. Chrzanowska-Wodnicka M and Burridge K: Rho-stimulated contractility drives the formation of stress fibers and focal adhesions. J Cell Biol 1996, 133: 1403-1415

81. Chvapil M, McCarthy DW, Misiorowski RL, Madden JW, and Peacock EE, Jr.: Activity and extractability of lysyl oxidase and collagen proteins in developing granuloma tissue. Proc Soc Exp Biol Med 1974, 146: 688-693

82. Clark JG, Madtes DK, and Raghu G: Effects of platelet-derived growth factor isoforms on human lung fibroblast proliferation and procollagen gene expression. Exp Lung Res 1993, 19: 327-344

83. Clements P, Lachenbruch P, Siebold J, White B, Weiner S, Martin R, Weinstein A, Weisman M, Mayes M, Collier D, and .: Inter and intraobserver variability of total skin thickness score (modified Rodnan TSS) in systemic sclerosis. J Rheumatol 1995, 22: 1281-1285

84. Coghlan JG and Mukerjee D: The heart and pulmonary vasculature in scleroderma: clinical features and pathobiology. Curr Opin Rheumatol 2001, 13: 495-499

85. Cohen MP, Frank RN, and Khalifa AA: Collagen production by cultured retinal capillary pericytes. Invest Ophthalmol Vis Sci 1980, 19: 90-94

86. Collett GD and Canfield AE: Angiogenesis and pericytes in the initiation of ectopic calcification. Circ Res 2005, 96: 930-938

87. Cooper SM, Keyser AJ, Beaulieu AD, Ruoslahti E, Nimni ME, and Quismorio FP, Jr.: Increase in fibronectin in the deep dermis of involved skin in progressive systemic sclerosis. Arthritis Rheum 1979, 22: 983-987

88. Cox D, Earle L, Jimenez SA, Leiferman KM, Gleich GJ, and Varga J: Elevated levels of eosinophil major basic protein in the sera of patients with systemic sclerosis. Arthritis Rheum 1995, 38: 939-945

89. Crilly A, Hamilton J, Clark CJ, Jardine A, and Madhok R: Analysis of transforming growth factor beta1 gene polymorphisms in patients with systemic sclerosis. Ann Rheum Dis 2002, 61: 678-681

90. Crocker DJ, Murad TM, and Geer JC: Role of the pericyte in wound healing. An ultrastructural study. Exp Mol Pathol 1970, 13: 51-65

91. Cutolo M, Pizzorni C, Tuccio M, Burroni A, Craviotto C, Basso M, Seriolo B, and Sulli A: Nailfold videocapillaroscopic patterns and serum autoantibodies in systemic sclerosis. Rheumatology (Oxford) 2004, 43: 719-726

92. Cutolo M, Sulli A, Pizzorni C, and Accardo S: Nailfold videocapillaroscopy assessment of microvascular damage in systemic sclerosis. J Rheumatol 2000, 27: 155-160

93. D'Amore PA and Smith SR: Growth factor effects on cells of the vascular wall: a survey. Growth Factors 1993, 8: 61-75

94. Daniels CE, Wilkes MC, Edens M, Kottom TJ, Murphy SJ, Limper AH, and Leof EB: Imatinib mesylate inhibits the profibrogenic activity of TGF-beta and prevents bleomycin-mediated lung fibrosis. J Clin Invest 2004, 114: 1308-1316

95. Daniil ZD, Gilchrist FC, Nicholson AG, Hansell DM, Harris J, Colby TV, and du Bois RM: A histologic pattern of nonspecific interstitial pneumonia is associated with a better prognosis than usual interstitial pneumonia in patients with cryptogenic fibrosing alveolitis. Am J Respir Crit Care Med 1999, 160: 899-905

96. Darby I, Skalli O, and Gabbiani G: Alpha-smooth muscle actin is transiently expressed by myofibroblasts during experimental wound healing. Lab Invest 1990, 63: 21-29

97. Davis EC, Blattel SA, and Mecham RP: Remodeling of elastic fiber components in scleroderma skin. Connect Tissue Res 1999, 40: 113-121

98. De Keyser F, Peene I, Joos R, Naeyaert JM, Messiaen L, and Veys EM: Occurrence of scleroderma in monozygotic twins. J Rheumatol 2000, 27: 2267-2269

99. Decitre M, Gleyzal C, Raccurt M, Peyrol S, Aubert-Foucher E, Csiszar K, and Sommer P: Lysyl oxidase-like protein localizes to sites of de novo fibrinogenesis in fibrosis and in the early stromal reaction of ductal breast carcinomas. Lab Invest 1998, 78: 143-151

100. Denton CP and Black CM: Scleroderma--clinical and pathological advances. Best Pract Res Clin Rheumatol 2004, 18: 271-290

101. Denton CP, Cailes JB, Phillips GD, Wells AU, Black CM, and Bois RM: Comparison of Doppler echocardiography and right heart catheterization to assess

pulmonary hypertension in systemic sclerosis. Br J Rheumatol 1997, 36: 239-243

102. Denton CP, Lindahl GE, Khan K, Shiwen X, Ong VH, Gaspar NJ, Lazaridis K, Edwards DR, Leask A, Eastwood M, Leoni P, Renzoni EA, Bou GG, Abraham DJ, and Black CM: Activation of key profibrotic mechanisms in transgenic fibroblasts expressing kinase-deficient type II Transforming growth factor-{beta} receptor (T{beta}RII{delta}k). J Biol Chem 2005, 280: 16053-16065

103. Derdak S, Penney DP, Keng P, Felch ME, Brown D, and Phipps RP: Differential collagen and fibronectin production by Thy 1+ and Thy 1- lung fibroblast subpopulations. Am J Physiol 1992, 263: L283-L290

104. Desmouliere A, Chaponnier C, and Gabbiani G: Tissue repair, contraction, and the myofibroblast. Wound Repair Regen 2005, 13: 7-12

105. Desmouliere A, Redard M, Darby I, and Gabbiani G: Apoptosis mediates the decrease in cellularity during the transition between granulation tissue and scar. Am J Pathol 1995, 146: 56-66

106. Diaz-Flores L, Gutierrez R, and Varela H: Behavior of postcapillary venule pericytes during postnatal angiogenesis. J Morphol 1992, 213: 33-45

107. Diaz-Flores L, Gutierrez R, Varela H, Rancel N, and Valladares F: Microvascular pericytes: a review of their morphological and functional characteristics. Histol Histopathol 1991, 6: 269-286

108. Diaz-Flores L, Valladares F, Gutierrez R, and Varela H: The role of the pericytes of the adventitial microcirculation in the arterial intimal thickening. Histol Histopathol 1990, 5: 145-153

109. Ding H, Wu X, Bostrom H, Kim I, Wong N, Tsoi B, O'Rourke M, Koh GY, Soriano P, Betsholtz C, Hart TC, Marazita ML, Field LL, Tam PP, and Nagy A: A specific requirement for PDGF-C in palate formation and PDGFR-alpha signaling. Nat Genet 2004, 36: 1111-1116

110. Diot E, Giraudeau B, Diot P, Degenne D, Ritz L, Guilmot JL, and Lemarie E: Is anti-topoisomerase I a serum marker of pulmonary involvement in systemic sclerosis? Chest 1999, 116: 715-720

111. Direkze NC, Hodivala-Dilke K, Jeffery R, Hunt T, Poulsom R, Oukrif D, Alison MR, and Wright NA: Bone marrow contribution to tumor-associated myofibroblasts and fibroblasts. Cancer Res 2004, 64: 8492-8495

112. Distler O, Distler JH, Scheid A, Acker T, Hirth A, Rethage J, Michel BA, Gay RE, Muller-Ladner U, Matucci-Cerinic M, Plate KH, Gassmann M, and Gay S: Uncontrolled expression of vascular endothelial growth factor and its receptors leads to insufficient skin angiogenesis in patients with systemic sclerosis. Circ Res 2004, 95: 109-116

113. Distler O, Pap T, Kowal-Bielecka O, Meyringer R, Guiducci S, Landthaler M, Scholmerich J, Michel BA, Gay RE, Matucci-Cerinic M, Gay S, and Muller-Ladner U: Overexpression of monocyte chemoattractant protein 1 in systemic sclerosis: role of platelet-derived growth factor and effects on monocyte chemotaxis and collagen synthesis. Arthritis Rheum 2001, 44: 2665-2678

114. Doherty M, Boot-Handford RP, Grant ME, and Canfield AE: Identification of genes expressed during the osteogenic differentiation of vascular pericytes in vitro [In Process Citation]. Biochem Soc Trans 1998, 26: S4

115. Doherty MJ, Ashton BA, Walsh S, Beresford JN, Grant ME, and Canfield AE: Vascular pericytes express osteogenic potential in vitro and in vivo. J Bone Miner Res 1998, 13: 828-838

116. Doherty MJ and Canfield AE: Gene expression during vascular pericyte differentiation. Crit Rev Eukaryot Gene Expr 1999, 9: 1-17

117. Dong C, Zhu S, Wang T, Yoon W, Li Z, Alvarez RJ, ten Dijke P, White B, Wigley FM, and Goldschmidt-Clermont PJ: Deficient Smad7 expression: a putative molecular defect in scleroderma. Proc Natl Acad Sci U S A 2002, 99: 3908-3913

118. Dore-Duffy P, Katychev A, Wang X, and Van BE: CNS microvascular pericytes exhibit multipotential stem cell activity. J Cereb Blood Flow Metab 2006, 26: 613-624

119. Dore-Duffy P, Owen C, Balabanov R, Murphy S, Beaumont T, and Rafols JA: Pericyte migration from the vascular wall in response to traumatic brain injury [In Process Citation]. Microvasc Res 2000, 60: 55-69

120. Dugina V, Alexandrova A, Chaponnier C, Vasiliev J, and Gabbiani G: Rat fibroblasts cultured from various organs exhibit differences in alpha-smooth muscle actin expression, cytoskeletal pattern, and adhesive structure organization. Exp Cell Res 1998, 238: 481-490

121. Dugina V, Fontao L, Chaponnier C, Vasiliev J, and Gabbiani G: Focal adhesion features during myofibroblastic differentiation are controlled by intracellular and extracellular factors. J Cell Sci 2001, 114: 3285-3296

122. Dziadzio M, Usinger W, Leask A, Abraham D, Black CM, Denton C, and Stratton R: N-terminal connective tissue growth factor is a marker of the fibrotic phenotype in scleroderma. QJM 2005, 98: 485-492

123. Dziankowska-Bartkowiak B, Waszczykowska E, Zalewska A, and Sysa-Jedrzejowska A: Correlation of Endostatin and Tissue Inhibitor of Metalloproteinases 2

(TIMP2) Serum Levels With Cardiovascular Involvement in Systemic Sclerosis Patients. Mediators Inflamm 2005, 2005: 144-149

124. Eastwood M, Porter R, Khan U, McGrouther G, and Brown R: Quantitative analysis of collagen gel contractile forces generated by dermal fibroblasts and the relationship to cell morphology. J Cell Physiol 1996, 166: 33-42

125. Ehrlich HP and Rajaratnam JB: Cell locomotion forces versus cell contraction forces for collagen lattice contraction: an in vitro model of wound contraction. Tissue Cell 1990, 22: 407-417

126. Enge M, Bjarnegard M, Gerhardt H, Gustafsson E, Kalen M, Asker N, Hammes HP, Shani M, Fassler R, and Betsholtz C: Endothelium-specific platelet-derived growth factor-B ablation mimics diabetic retinopathy. EMBO J 2002, 21: 4307-4316

127. Englert H, Small-McMahon J, Chambers P, O'Connor H, Davis K, Manolios N, White R, Dracos G, and Brooks P: Familial risk estimation in systemic sclerosis. Aust N Z J Med 1999, 29: 36-41

128. Eriksson A, Siegbahn A, Westermark B, Heldin CH, and Claesson-Welsh L: PDGF alpha- and beta-receptors activate unique and common signal transduction pathways. EMBO J 1992, 11: 543-550

129. Fadok VA, Bratton DL, Konowal A, Freed PW, Westcott JY, and Henson PM: Macrophages that have ingested apoptotic cells in vitro inhibit proinflammatory cytokine production through autocrine/paracrine mechanisms involving TGF-beta, PGE2, and PAF. J Clin Invest 1998, 101: 890-898

130. Falanga V, Soter NA, Altman RD, and Kerdel FA: Elevated plasma histamine levels in systemic sclerosis (scleroderma). Arch Dermatol 1990, 126: 336-338

131. Falkner D, Wilson J, Fertig N, Clawson K, Medsger TA, Jr., and Morel PA: Studies of HLA-DR and DQ alleles in systemic sclerosis patients with autoantibodies to RNA polymerases and U3-RNP (fibrillarin). J Rheumatol 2000, 27: 1196-1202

132. Falkner D, Wilson J, Medsger TA, Jr., and Morel PA: HLA and clinical associations in systemic sclerosis patients with anti-Th/To antibodies. Arthritis Rheum 1998, 41: 74-80

133. Fanning GC, Welsh KI, Bunn C, Du BR, and Black CM: HLA associations in three mutually exclusive autoantibody subgroups in UK systemic sclerosis patients. Br J Rheumatol 1998, 37: 201-207

134. Faouzi S, Le Bail B, Neaud V, Boussarie L, Saric J, Bioulac-Sage P, Balabaud C, and Rosenbaum J: Myofibroblasts are responsible for collagen synthesis in the stroma of human hepatocellular carcinoma: an in vivo and in vitro study. J Hepatol 1999, 30: 275-284

135. Farrington-Rock C, Crofts NJ, Doherty MJ, Ashton BA, Griffin-Jones C, and Canfield AE: Chondrogenic and adipogenic potential of microvascular pericytes. Circulation 2004, 110: 2226-2232

136. Fatini C, Gensini F, Sticchi E, Battaglini B, Angotti C, Conforti ML, Generini S, Pignone A, Abbate R, and Matucci-Cerinic M: High prevalence of polymorphisms of angiotensin-converting enzyme (I/D) and endothelial nitric oxide synthase (Glu298Asp) in patients with systemic sclerosis. Am J Med 2002, 112: 540-544

137. Ffrench-Constant C: Alternative splicing of fibronectin--many different proteins but few different functions. Exp Cell Res 1995, 221: 261-271

138. Flanders KC, Sullivan CD, Fujii M, Sowers A, Anzano MA, Arabshahi A, Major C, Deng C, Russo A, Mitchell JB, and Roberts AB: Mice lacking Smad3 are protected against cutaneous injury induced by ionizing radiation. Am J Pathol 2002, 160: 1057-1068

139. Fleischmajer R, Dessau W, Timpl R, Krieg T, Luderschmidt C, and Wiestner M: Immunofluorescence analysis of collagen, fibronectin, and basement membrane protein in scleroderma skin. J Invest Dermatol 1980, 75: 270-274

140. Fleischmajer R, Gay S, Meigel WN, and Perlish JS: Collagen in the cellular and fibrotic stages of scleroderma. Arthritis Rheum 1978, 21: 418-428

141. Fleischmajer R, Jacobs L, Schwartz E, and Sakai LY: Extracellular microfibrils are increased in localized and systemic scleroderma skin. Lab Invest 1991, 64: 791-798

142. Fleischmajer R and Perlish JS: Glycosaminoglycans in scleroderma and scleredema. J Invest Dermatol 1972, 58: 129-132

143. Fleischmajer R and Perlish JS: Capillary alterations in scleroderma. J Am Acad Dermatol 1980, 2: 161-170

144. Fleischmajer R, Perlish JS, and Reeves JR: Cellular infiltrates in scleroderma skin. Arthritis Rheum 1977, 20: 975-984

145. Floege J, Eng E, Young BA, Alpers CE, Barrett TB, Bowen-Pope DF, and Johnson RJ: Infusion of platelet-derived growth factor or basic fibroblast growth factor induces selective glomerular mesangial cell proliferation and matrix accumulation in rats. J Clin Invest 1993, 92: 2952-2962

146. Folkman J and D'Amore PA: Blood vessel formation: what is its molecular basis? [comment]. Cell 1996, 87: 1153-1155

147. Forbes SJ, Russo FP, Rey V, Burra P, Rugge M, Wright NA, and Alison MR: A significant proportion of myofibroblasts are of bone marrow origin in human liver fibrosis. Gastroenterology 2004, 126: 955-963

148. Franceschini F, Cavazzana I, Generali D, Quinzanini M, Viardi L, Ghirardello A, Doria A, and Cattaneo R: Anti-Ku antibodies in connective tissue diseases: clinical and serological evaluation of 14 patients. J Rheumatol 2002, 29: 1393-1397

149. Frank S, Madlener M, and Werner S: Transforming growth factors beta1, beta2, and beta3 and their receptors are differentially regulated during normal and impaired wound healing. J Biol Chem 1996, 271: 10188-10193

150. Fredriksson L, Li H, and Eriksson U: The PDGF family: four gene products form five dimeric isoforms. Cytokine Growth Factor Rev 2004, 15: 197-204

151. French LE, Lessin SR, Addya K, Denardo B, Margolis DJ, Leonard DG, and Rook AH: Identification of clonal T cells in the blood of patients with systemic sclerosis: positive correlation with response to photopheresis. Arch Dermatol 2001, 137: 1309-1313

152. Fujimoto M, Shimozuma M, Yazawa N, Kubo M, Ihn H, Sato S, Tamaki T, Kikuchi K, and Tamaki K: Prevalence and clinical relevance of 52-kDa and 60-kDa Ro/SS-A autoantibodies in Japanese patients with systemic sclerosis. Ann Rheum Dis 1997, 56: 667-670

153. Furuhashi M, Sjoblom T, Abramsson A, Ellingsen J, Micke P, Li H, Bergsten-Folestad E, Eriksson U, Heuchel R, Betsholtz C, Heldin CH, and Ostman A: Platelet-derived growth factor production by B16 melanoma cells leads to increased pericyte abundance in tumors and an associated increase in tumor growth rate. Cancer Res 2004, 64: 2725-2733

154. Gabbiani G: The myofibroblast in wound healing and fibrocontractive diseases. J Pathol 2003, 200: 500-503

155. Gabbiani G, Ryan GB, and Majne G: Presence of modified fibroblasts in granulation tissue and their possible role in wound contraction. Experientia 1971, 27: 549-550

156. Gabrielli A, Di Loreto C, Taborro R, Candela M, Sambo P, Nitti C, Danieli MG, DeLustro F, Dasch JR, and Danieli G: Immunohistochemical localization of intracellular and extracellular associated TGF beta in the skin of patients with systemic sclerosis (scleroderma) and primary Raynaud's phenomenon. Clin Immunol Immunopathol 1993, 68: 340-349

157. Gailit J, Marchese MJ, Kew RR, and Gruber BL: The differentiation and function of myofibroblasts is regulated by mast cell mediators. J Invest Dermatol 2001, 117: 1113-1119

158. Galindo M, Santiago B, Rivero M, Rullas J, Alcami J, and Pablos JL: Chemokine expression by systemic sclerosis fibroblasts: abnormal regulation of monocyte chemoattractant protein 1 expression. Arthritis Rheum 2001, 44: 1382-1386

159. Gao Z, Sasaoka T, Fujimori T, Oya T, Ishii Y, Sabit H, Kawaguchi M, Kurotaki Y, Naito M, Wada T, Ishizawa S, Kobayashi M, Nabeshima Y, and Sasahara M: Deletion of the PDGFR-beta gene affects key fibroblast functions important for wound healing. J Biol Chem 2005, 280: 9375-9389

160. Gay S, Jones RE, Jr., Huang GQ, and Gay RE: Immunohistologic demonstration of platelet-derived growth factor (PDGF) and sis-oncogene expression in scleroderma. J Invest Dermatol 1989, 92: 301-303

161. Gerhardt H and Betsholtz C: Endothelial-pericyte interactions in angiogenesis. Cell Tissue Res 2003, 314: 15-23

162. Gershwin ME, Abplanalp H, Castles JJ, Ikeda RM, van der WJ, Eklund J, and Haynes D: Characterization of a spontaneous disease of white leghorn chickens resembling progressive systemic sclerosis (scleroderma). J Exp Med 1981, 153: 1640-1659

163. Gharaee-Kermani M, Denholm EM, and Phan SH: Costimulation of fibroblast collagen and transforming growth factor beta1 gene expression by monocyte chemoattractant protein-1 via specific receptors. J Biol Chem 1996, 271: 17779-17784

164. Ghofrani HA, Seeger W, and Grimminger F: Imatinib for the treatment of pulmonary arterial hypertension. N Engl J Med 2005, 353: 1412-1413

165. Giacomelli R, Cipriani P, Fulminis A, Barattelli G, Matucci-Cerinic M, D'Alo S, Cifone G, and Tonietti G: Circulating gamma/delta T lymphocytes from systemic sclerosis (SSc) patients display a T helper (Th) 1 polarization. Clin Exp Immunol 2001, 125: 310-315

166. Giacomelli R, Matucci-Cerinic M, Cipriani P, Ghersetich I, Lattanzio R, Pavan A, Pignone A, Cagnoni ML, Lotti T, and Tonietti G: Circulating Vdelta1+ T cells are activated and accumulate in the skin of systemic sclerosis patients. Arthritis Rheum 1998, 41: 327-334

167. Giaid A, Yanagisawa M, Langleben D, Michel RP, Levy R, Shennib H, Kimura S, Masaki T, Duguid WP, and Stewart DJ: Expression of endothelin-1 in the lungs of patients with pulmonary hypertension. N Engl J Med 1993, 328: 1732-1739

168. Ginis I, Mentzer SJ, and Faller DV: Oxygen tension regulates neutrophil adhesion to human endothelial cells via an LFA-1-dependent mechanism. J Cell Physiol 1993, 157: 569-578

169. Goerdt S, Politz O, Schledzewski K, Birk R, Gratchev A, Guillot P, Hakiy N, Klemke CD, Dippel E, Kodelja V, and Orfanos CE: Alternative versus classical activation of macrophages. Pathobiology 1999, 67: 222-226

170. Goffin JM, Pittet P, Csucs G, Lussi JW, Meister JJ, and Hinz B: Focal adhesion size controls tension-dependent recruitment of {alpha}-smooth muscle actin to stress fibers. J Cell Biol 2006, 172: 259-268

171. Goldblatt F, Gordon TP, and Waterman SA: Antibody-mediated gastrointestinal dysmotility in scleroderma. Gastroenterology 2002, 123: 1144-1150

172. Grassi W, Core P, Carlino G, and Cervini C: Effects of peripheral cold exposure on microvascular dynamics in systemic sclerosis. Arthritis Rheum 1994, 37: 384-390

173. Green MC, Sweet HO, and Bunker LE: Tight-skin, a new mutation of the mouse causing excessive growth of connective tissue and skeleton. Am J Pathol 1976, 82: 493-512

174. Greenhalgh DG, Sprugel KH, Murray MJ, and Ross R: PDGF and FGF stimulate wound healing in the genetically diabetic mouse. Am J Pathol 1990, 136: 1235-1246

175. Grinnell F, Ho CH, Lin YC, and Skuta G: Differences in the regulation of fibroblast contraction of floating versus stressed collagen matrices. J Biol Chem 1999, 274: 918-923

176. Hagood JS, Lasky JA, Nesbitt JE, and Segarini P: Differential expression, surface binding, and response to connective tissue growth factor in lung fibroblast subpopulations. Chest 2001, 120: 64S-66S

177. Han G, Lu SL, Li AG, He W, Corless CL, Kulesz-Martin M, and Wang XJ: Distinct mechanisms of TGF-beta1-mediated epithelial-to-mesenchymal transition and metastasis during skin carcinogenesis. J Clin Invest 2005, 115: 1714-1723

178. Han YP, Nien YD, and Garner WL: Recombinant human platelet-derived growth factor and transforming growth factor-beta mediated contraction of human dermal fibroblast populated lattices is inhibited by Rho/GTPase inhibitor but does not require phosphatidylinositol-3' kinase. Wound Repair Regen 2002, 10: 169-176

179. Harrison NK, Myers AR, Corrin B, Soosay G, Dewar A, Black CM, du Bois RM, and Turner-Warwick M: Structural features of interstitial lung disease in systemic sclerosis. Am Rev Respir Dis 1991, 144: 706-713

180. Hasegawa M, Sato S, Echigo T, Hamaguchi Y, Yasui M, and Takehara K: Up regulated expression of fractalkine/CX3CL1 and CX3CR1 in patients with systemic sclerosis. Ann Rheum Dis 2005, 64: 21-28

181. Hasegawa M, Sato S, and Takehara K: Augmented production of chemokines (monocyte chemotactic protein-1 (MCP-1), macrophage inflammatory protein-1alpha (MIP-1alpha) and MIP-1beta) in patients with systemic sclerosis: MCP-1 and MIP-1alpha may be involved in the development of pulmonary fibrosis. Clin Exp Immunol 1999, 117: 159-165

182. Hasegawa M, Sato S, and Takehara K: Augmented production of transforming growth factor-beta by cultured peripheral blood mononuclear cells from patients with systemic sclerosis. Arch Dermatol Res 2004, 296: 89-93

183. Hashimoto N, Jin H, Liu T, Chensue SW, and Phan SH: Bone marrow-derived progenitor cells in pulmonary fibrosis. J Clin Invest 2004, 113: 243-252

184. Hata R, Akai J, Kimura A, Ishikawa O, Kuwana M, and Shinkai H: Association of functional microsatellites in the human type I collagen alpha2 chain (COL1A2) gene with systemic sclerosis. Biochem Biophys Res Commun 2000, 272: 36-40

185. Hatamochi A, Ueki H, Mauch C, and Krieg T: Effect of histamine on collagen and collagen m-RNA production in human skin fibroblasts. J Dermatol Sci 1991, 2: 407-412

186. Hattori M, Horita S, Yoshioka T, Yamaguchi Y, Kawaguchi H, and Ito K: Mesangial phenotypic changes associated with cellular lesions in primary focal segmental glomerulosclerosis. Am J Kidney Dis 1997, 30: 632-638

187. Hayashi K, Fong KS, Mercier F, Boyd CD, Csiszar K, and Hayashi M: Comparative immunocytochemical localization of lysyl oxidase (LOX) and the lysyl oxidase-like (LOXL) proteins: changes in the expression of LOXL during development and growth of mouse tissues. J Mol Histol 2004, 35: 845-855

188. Hayes RL and Rodnan GP: The ultrastructure of skin in progressive systemic sclerosis (scleroderma). I. Dermal collagen fibers. Am J Pathol 1971, 63: 433-442

189. Hein S, Yamamoto SY, Okazaki K, Jourdan-LeSaux C, Csiszar K, and Bryant-Greenwood GD: Lysyl oxidases: expression in the fetal membranes and placenta. Placenta 2001, 22: 49-57

190. Heldin CH, Backstrom G, Ostman A, Hammacher A, Ronnstrand L, Rubin K, Nister M, and Westermark B: Binding of different dimeric forms of PDGF to human

fibroblasts: evidence for two separate receptor types. EMBO J 1988, 7: 1387-1393

191. Heldin CH and Westermark B: Mechanism of action and in vivo role of platelet-derived growth factor. Physiol Rev 1999, 79: 1283-1316

192. Heldin CH, Westermark B, and Wasteson A: Platelet-derived growth factor: purification and partial characterization. Proc Natl Acad Sci U S A 1979, 76: 3722-3726

193. Hellstrom M, Gerhardt H, Kalen M, Li X, Eriksson U, Wolburg H, and Betsholtz C: Lack of pericytes leads to endothelial hyperplasia and abnormal vascular morphogenesis. J Cell Biol 2001, 153: 543-553

194. Hellstrom M, Kal n M, Lindahl P, Abramsson A, and Betsholtz C: Role of PDGF-B and PDGFR-beta in recruitment of vascular smooth muscle cells and pericytes during embryonic blood vessel formation in the mouse. Development 1999, 126: 3047-3055

195. Helmbold P, Fiedler E, Fischer M, and Marsch WC: Hyperplasia of dermal microvascular pericytes in scleroderma*. J Cutan Pathol 2004, 31: 431-440

196. Herman IM, Newcomb PM, Coughlin JE, and Jacobson S: Characterization of microvascular cell cultures from normotensive and hypertensive rat brains: pericyte-endothelial cell interactions in vitro. Tissue Cell 1987, 19: 197-206

197. Herrick AL and Clark S: Quantifying digital vascular disease in patients with primary Raynaud's phenomenon and systemic sclerosis. Ann Rheum Dis 1998, 57: 70-78

198. Hill MB, Phipps JL, Cartwright RJ, Milford WA, Greaves M, and Hughes P: Antibodies to membranes of endothelial cells and fibroblasts in scleroderma. Clin Exp Immunol 1996, 106: 491-497

199. Hinz B, Dugina V, Ballestrem C, Wehrle-Haller B, and Chaponnier C: Alpha-smooth muscle actin is crucial for focal adhesion maturation in myofibroblasts. Mol Biol Cell 2003, 14: 2508-2519

200. Hinz B, Mastrangelo D, Iselin CE, Chaponnier C, and Gabbiani G: Mechanical tension controls granulation tissue contractile activity and myofibroblast differentiation. Am J Pathol 2001, 159: 1009-1020

201. Hirschi KK and D'Amore PA: Pericytes in the microvasculature. Cardiovasc Res 1996, 32: 687-698

202. Hirschi KK, Rohovsky SA, and D'Amore PA: PDGF, TGF-beta, and heterotypic cell-cell interactions mediate endothelial cell-induced recruitment of 10T1/2 cells and their differentiation to a smooth muscle fate. J Cell Biol 1998, 141: 805-814

203. Ho M, Veale D, Eastmond C, Nuki G, and Belch J: Macrovascular disease and systemic sclerosis. Ann Rheum Dis 2000, 59: 39-43

204. Hoch RV and Soriano P: Roles of PDGF in animal development. Development 2003, 130: 4769-4784

205. Hochberg MC, Perlmutter DL, Medsger TA, Jr., Nguyen K, Steen V, Weisman MH, White B, and Wigley FM: Lack of association between augmentation mammoplasty and systemic sclerosis (scleroderma). Arthritis Rheum 1996, 39: 1125-1131

206. Hudson LL, Rocca KM, Kuwana M, and Pandey JP: Interleukin-10 genotypes are associated with systemic sclerosis and influence disease-associated autoimmune responses. Genes Immun 2005, 6: 274-278

207. Igarashi A, Nashiro K, Kikuchi K, Sato S, Ihn H, Fujimoto M, Grotendorst GR, and Takehara K: Connective tissue growth factor gene expression in tissue

sections from localized scleroderma, keloid, and other fibrotic skin disorders. J Invest Dermatol 1996, 106: 729-733

208. Ihn H, Sato S, Fujimoto M, Igarashi A, Yazawa N, Kubo M, Kikuchi K, Takehara K, and Tamaki K: Characterization of autoantibodies to endothelial cells in systemic sclerosis (SSc): association with pulmonary fibrosis. Clin Exp Immunol 2000, 119: 203-209

209. Ihn H, Yamane K, Kubo M, and Tamaki K: Blockade of endogenous transforming growth factor beta signaling prevents up-regulated collagen synthesis in scleroderma fibroblasts: association with increased expression of transforming growth factor beta receptors. Arthritis Rheum 2001, 44: 474-480

210. Ihn H, Yamane K, Yazawa N, Kubo M, Fujimoto M, Sato S, Kikuchi K, and Tamaki K: Distribution and antigen specificity of anti-U1RNP antibodies in patients with systemic sclerosis. Clin Exp Immunol 1999, 117: 383-387

211. Ioannidis JP, Vlachoyiannopoulos PG, Haidich AB, Medsger TA, Jr., Lucas M, Michet CJ, Kuwana M, Yasuoka H, van den HF, Te BL, van Laar JM, Verbeet NL, Matucci-Cerinic M, Georgountzos A, and Moutsopoulos HM: Mortality in systemic sclerosis: an international meta-analysis of individual patient data. Am J Med 2005, 118: 2-10

212. Irani AM, Gruber BL, Kaufman LD, Kahaleh MB, and Schwartz LB: Mast cell changes in scleroderma. Presence of MCT cells in the skin and evidence of mast cell activation. Arthritis Rheum 1992, 35: 933-939

213. Irani K: Oxidant signaling in vascular cell growth, death, and survival : a review of the roles of reactive oxygen species in smooth muscle and endothelial cell mitogenic and apoptotic signaling. Circ Res 2000, 87: 179-183

214. Ivarsson M, Sundberg C, Farrokhnia N, Pertoft H, Rubin K, and Gerdin B: Recruitment of type I collagen producing cells from the microvasculature in vitro. Exp Cell Res 1996, 229: 336-349

215. Iwano M, Plieth D, Danoff TM, Xue C, Okada H, and Neilson EG: Evidence that fibroblasts derive from epithelium during tissue fibrosis. J Clin Invest 2002, 110: 341-350

216. Jacobsen S, Ullman S, Shen GQ, Wiik A, and Halberg P: Influence of clinical features, serum antinuclear antibodies, and lung function on survival of patients with systemic sclerosis. J Rheumatol 2001, 28: 2454-2459

217. Jarnagin WR, Rockey DC, Koteliansky VE, Wang SS, and Bissell DM: Expression of variant fibronectins in wound healing: cellular source and biological activity of the EIIIA segment in rat hepatic fibrogenesis. J Cell Biol 1994, 127: 2037-2048

218. Jelaska A, Arakawa M, Broketa G, and Korn JH: Heterogeneity of collagen synthesis in normal and systemic sclerosis skin fibroblasts. Increased proportion of high collagen-producing cells in systemic sclerosis fibroblasts. Arthritis Rheum 1996, 39: 1338-1346

219. Jelaska A and Korn JH: Role of apoptosis and transforming growth factor beta1 in fibroblast selection and activation in systemic sclerosis. Arthritis Rheum 2000, 43: 2230-2239

220. Jimenez SA and Artlett CM: Microchimerism and systemic sclerosis. Curr Opin Rheumatol 2005, 17: 86-90

221. Jimenez SA and Christner PJ: Murine animal models of systemic sclerosis. Curr Opin Rheumatol 2002, 14: 671-680

222. Jimenez SA, Feldman G, Bashey RI, Bienkowski R, and Rosenbloom J: Co-ordinate increase in the expression of type I and type III collagen genes in progressive systemic sclerosis fibroblasts. Biochem J 1986, 237: 837-843

223. Johnson RW, Tew MB, and Arnett FC: The genetics of systemic sclerosis. Curr Rheumatol Rep 2002, 4: 99-107

224. Jordana M, Schulman J, McSharry C, Irving LB, Newhouse MT, Jordana G, and Gauldie J: Heterogeneous proliferative characteristics of human adult lung fibroblast lines and clonally derived fibroblasts from control and fibrotic tissue. Am Rev Respir Dis 1988, 137: 579-584

225. Kadono T, Kikuchi K, Ihn H, Takehara K, and Tamaki K: Increased production of interleukin 6 and interleukin 8 in scleroderma fibroblasts. J Rheumatol 1998, 25: 296-301

226. Kagami S, Urushihara M, Kitamura A, Kondo S, Hisayama T, Kitamura M, Loster K, Reutter W, and Kuroda Y: PDGF-BB enhances alpha1beta1 integrin-mediated activation of the ERK/AP-1 pathway involved in collagen matrix remodeling by rat mesangial cells. J Cell Physiol 2004, 198: 470-478

227. Kahaleh MB: Endothelin, an endothelial-dependent vasoconstrictor in scleroderma. Enhanced production and profibrotic action. Arthritis Rheum 1991, 34: 978-983

228. Kahaleh MB, Fan PS, and Otsuka T: Gammadelta receptor bearing T cells in scleroderma: enhanced interaction with vascular endothelial cells in vitro. Clin Immunol 1999, 91: 188-195

229. Kahari VM, Sandberg M, Kalimo H, Vuorio T, and Vuorio E: Identification of fibroblasts responsible for increased collagen production in localized scleroderma by in situ hybridization. J Invest Dermatol 1988, 90: 664-670

230. Kallenberg CG: Raynaud's phenomenon as an early sign of connective tissue diseases. Vasa Suppl 1992, 34:25-8: 25-28

231. Kamm KE and Stull JT: The function of myosin and myosin light chain kinase phosphorylation in smooth muscle. Annu Rev Pharmacol Toxicol 1985, 25: 593-620

232. Kapanci Y, Ribaux C, Chaponnier C, and Gabbiani G: Cytoskeletal features of alveolar myofibroblasts and pericytes in normal human and rat lung. J Histochem Cytochem 1992, 40: 1955-1963

233. Karrer S, Bosserhoff AK, Weiderer P, Distler O, Landthaler M, Szeimies RM, Muller-Ladner U, Scholmerich J, and Hellerbrand C: The -2518 promotor polymorphism in the MCP-1 gene is associated with systemic sclerosis. J Invest Dermatol 2005, 124: 92-98

234. Kaufmann SH: gamma/delta and other unconventional T lymphocytes: what do they see and what do they do? Proc Natl Acad Sci U S A 1996, 93: 2272-2279

235. Kawaguchi Y, Suzuki K, Hara M, Hidaka T, Ishizuka T, Kawagoe M, and Nakamura H: Increased endothelin-1 production in fibroblasts derived from patients with systemic sclerosis. Ann Rheum Dis 1994, 53: 506-510

236. Kawakami T, Ihn H, Xu W, Smith E, LeRoy C, and Trojanowska M: Increased expression of TGF-beta receptors by scleroderma fibroblasts: evidence for contribution of autocrine TGF-beta signaling to scleroderma phenotype. J Invest Dermatol 1998, 110: 47-51

237. Kaye SA, Seifalian AM, Lim SG, Hamilton G, and Black CM: Ischaemia of the small intestine in patients with systemic sclerosis: Raynaud's phenomenon or chronic vasculopathy? QJM 1994, 87: 495-500

238. Keane MP, Arenberg DA, Lynch JP, III, Whyte RI, Iannettoni MD, Burdick MD, Wilke CA, Morris SB, Glass MC, DiGiovine B, Kunkel SL, and Strieter RM: The CXC chemokines, IL-8 and IP-10, regulate angiogenic activity in idiopathic pulmonary fibrosis. J Immunol 1997, 159: 1437-1443

239. Kelley C, D'Amore P, Hechtman HB, and Shepro D: Microvascular pericyte contractility in vitro: comparison with other cells of the vascular wall. J Cell Biol 1987, 104: 483-490

240. Kelman Z: PCNA: structure, functions and interactions. Oncogene 1997, 14: 629-640

241. Kielty CM, Raghunath M, Siracusa LD, Sherratt MJ, Peters R, Shuttleworth CA, and Jimenez SA: The Tight skin mouse: demonstration of mutant fibrillin-1 production and assembly into abnormal microfibrils. J Cell Biol 1998, 140: 1159-1166

242. Kim Y, Peyrol S, So CK, Boyd CD, and Csiszar K: Coexpression of the lysyl oxidase-like gene (LOXL) and the gene encoding type III procollagen in induced liver fibrosis. J Cell Biochem 1999, 72: 181-188

243. Kinbara T, Shirasaki F, Kawara S, Inagaki Y, de Crombrugghe B, and Takehara K: Transforming growth factor-beta isoforms differently stimulate proalpha2 (I) collagen gene expression during wound healing process in transgenic mice. J Cell Physiol 2002, 190: 375-381

244. Kirk TZ, Mark ME, Chua CC, Chua BH, and Mayes MD: Myofibroblasts from scleroderma skin synthesize elevated levels of collagen and tissue inhibitor of metalloproteinase (TIMP-1) with two forms of TIMP-1. J Biol Chem 1995, 270: 3423-3428

245. Kischer CW, Pindur J, Krasovitch P, and Kischer E: Characteristics of granulation tissue which promote hypertrophic scarring. Scanning Microsc 1990, 4: 877-887

246. Klareskog L, Gustafsson R, Scheynius A, and Hallgren R: Increased expression of platelet-derived growth factor type B receptors in the skin of patients with systemic sclerosis. Arthritis Rheum 1990, 33: 1534-1541

247. Knighton DR, Ciresi KF, Fiegel VD, Austin LL, and Butler EL: Classification and treatment of chronic nonhealing wounds. Successful treatment with autologous platelet-derived wound healing factors (PDWHF). Ann Surg 1986, 204: 322-330

248. Knittel T, Schuppan D, Meyer zum Buschenfelde KH, and Ramadori G: Differential expression of collagen types I, III, and IV by fat-storing (Ito) cells in vitro [see comments]. Gastroenterology 1992, 102: 1724-1735

249. Kobayashi H, Ishii M, Chanoki M, Yashiro N, Fushida H, Fukai K, Kono T, Hamada T, Wakasaki H, and Ooshima A: Immunohistochemical localization of lysyl oxidase in normal human skin. Br J Dermatol 1994, 131: 325-330

250. Kobayashi T, Liu X, Wen FQ, Kohyama T, Shen L, Wang XQ, Hashimoto M, Mao L, Togo S, Kawasaki S, Sugiura H, Kamio K, and Rennard SI: Smad3 mediates TGF-beta1-induced collagen gel contraction by human lung fibroblasts. Biochem Biophys Res Commun 2006, 339: 290-295

251. Koch AE, Kronfeld-Harrington LB, Szekanecz Z, Cho MM, Haines GK, Harlow LA, Strieter RM, Kunkel SL, Massa MC, Barr WG, and .: In situ expression of cytokines and cellular adhesion molecules in the skin of patients with systemic sclerosis. Their role in early and late disease. Pathobiology 1993, 61: 239-246

252. Koumas L, Smith TJ, Feldon S, Blumberg N, and Phipps RP: Thy-1 expression in human fibroblast subsets defines myofibroblastic or lipofibroblastic phenotypes. Am J Pathol 2003, 163: 1291-1300

253. Kourembanas S, Hannan RL, and Faller DV: Oxygen tension regulates the expression of the platelet-derived growth factor-B chain gene in human endothelial cells. J Clin Invest 1990, 86: 670-674

254. Kourembanas S, Marsden PA, McQuillan LP, and Faller DV: Hypoxia induces endothelin gene expression and secretion in cultured human endothelium. J Clin Invest 1991, 88: 1054-1057

255. Kreis TE and Birchmeier W: Stress fiber sarcomeres of fibroblasts are contractile. Cell 1980, 22: 555-561

256. Kundra V, Escobedo JA, Kazlauskas A, Kim HK, Rhee SG, Williams LT, and Zetter BR: Regulation of chemotaxis by the platelet-derived growth factor receptor-beta. Nature 1994, 367: 474-476

257. Kuryliszyn-Moskal A, Klimiuk PA, and Sierakowski S: Soluble adhesion molecules (sVCAM-1, sE-selectin), vascular endothelial growth factor (VEGF) and endothelin-1 in patients with systemic sclerosis: relationship to organ systemic involvement. Clin Rheumatol 2005, 24: 111-116

258. Kuwana M, Feghali CA, Medsger TA, Jr., and Wright TM: Autoreactive T cells to topoisomerase I in monozygotic twins discordant for systemic sclerosis. Arthritis Rheum 2001, 44: 1654-1659

259. Kuwana M, Inoko H, Kameda H, Nojima T, Sato S, Nakamura K, Ogasawara T, Hirakata M, Ohosone Y, Kaburaki J, Okano Y, and Mimori T: Association of human leukocyte antigen class II genes with autoantibody profiles, but not

with disease susceptibility in Japanese patients with systemic sclerosis. Intern Med 1999, 38: 336-344

260. Kuwana M, Kaburaki J, Mimori T, Kawakami Y, and Tojo T: Longitudinal analysis of autoantibody response to topoisomerase I in systemic sclerosis. Arthritis Rheum 2000, 43: 1074-1084

261. Kuwana M, Kaburaki J, Okano Y, Tojo T, and Homma M: Clinical and prognostic associations based on serum antinuclear antibodies in Japanese patients with systemic sclerosis. Arthritis Rheum 1994, 37: 75-83

262. Lagan AL, Pantelidis P, Renzoni EA, Fonseca C, Beirne P, Taegtmeyer AB, Denton CP, Black CM, Wells AU, du Bois RM, and Welsh KI: Single-nucleotide polymorphisms in the SPARC gene are not associated with susceptibility to scleroderma. Rheumatology (Oxford) 2005, 44: 197-201

263. Lawson WE, Polosukhin VV, Zoia O, Stathopoulos GT, Han W, Plieth D, Loyd JE, Neilson EG, and Blackwell TS: Characterization of fibroblast-specific protein 1 in pulmonary fibrosis. Am J Respir Crit Care Med 2005, 171: 899-907

264. Leask A and Abraham DJ: TGF-beta signaling and the fibrotic response. FASEB J 2004, 18: 816-827

265. Leask A, Abraham DJ, Finlay DR, Holmes A, Pennington D, Shi-wen X, Chen Y, Venstrom K, Dou X, Ponticos M, Black C, Bernabeu C, Jackman JK, Findell PR, and Connolly MK: Dysregulation of transforming growth factor beta signaling in scleroderma: overexpression of endoglin in cutaneous scleroderma fibroblasts. Arthritis Rheum 2002, 46: 1857-1865

266. Leask A, Holmes A, and Abraham DJ: Connective tissue growth factor: a new and important player in the pathogenesis of fibrosis. Curr Rheumatol Rep 2002, 4: 136-142

267. Lepisto J, Laato M, Niinikoski J, Lundberg C, Gerdin B, and Heldin CH: Effects of homodimeric isoforms of platelet-derived growth factor (PDGF-AA and PDGF-BB) on wound healing in rat. J Surg Res 1992, 53: 596-601

268. LeRoy EC: Systemic sclerosis. A vascular perspective. Rheum Dis Clin North Am 1996, 22: 675-694

269. LeRoy EC: Increased collagen synthesis by scleroderma skin fibroblasts in vitro: a possible defect in the regulation or activation of the scleroderma fibroblast. J Clin Invest 1974, 54: 880-889

270. LeRoy EC, Black C, Fleischmajer R, Jablonska S, Krieg T, Medsger TA, Jr., Rowell N, and Wollheim F: Scleroderma (systemic sclerosis): classification, subsets and pathogenesis. J Rheumatol 1988, 15: 202-205

271. LeRoy EC and Medsger TA, Jr.: Raynaud's phenomenon: a proposal for classification. Clin Exp Rheumatol 1992, 10: 485-488

272. LeRoy EC and Medsger TA, Jr.: Criteria for the classification of early systemic sclerosis. J Rheumatol 2001, 28: 1573-1576

273. Leveen P, Pekny M, Gebre-Medhin S, Swolin B, Larsson E, and Betsholtz C: Mice deficient for PDGF B show renal, cardiovascular, and hematological abnormalities. Genes Dev 1994, 8: 1875-1887

274. Levi-Schaffer F, Garbuzenko E, Rubin A, Reich R, Pickholz D, Gillery P, Emonard H, Nagler A, and Maquart FA: Human eosinophils regulate human lung- and skin-derived fibroblast properties in vitro: a role for transforming growth factor beta (TGF-beta). Proc Natl Acad Sci U S A 1999, 96: 9660-9665

275. Levin ER: Endothelins. N Engl J Med 1995, 333: 356-363

276. Li JH, Zhu HJ, Huang XR, Lai KN, Johnson RJ, and Lan HY: Smad7 inhibits fibrotic effect of TGF-Beta on renal tubular epithelial cells by blocking Smad2 activation. J Am Soc Nephrol 2002, 13: 1464-1472

277. Lindahl P, Johansson BR, Leveen P, and Betsholtz C: Pericyte loss and microaneurysm formation in PDGF-B-deficient mice. Science 1997, 277: 242-245

278. Lindblom P, Gerhardt H, Liebner S, Abramsson A, Enge M, Hellstrom M, Backstrom G, Fredriksson S, Landegren U, Nystrom HC, Bergstrom G, Dejana E, Ostman A, Lindahl P, and Betsholtz C: Endothelial PDGF-B retention is required for proper investment of pericytes in the microvessel wall. Genes Dev 2003, 17: 1835-1840

279. Lindmark G, Sundberg C, Glimelius B, Pahlman L, Rubin K, and Gerdin B: Stromal expression of platelet-derived growth factor beta-receptor and platelet-derived growth factor B-chain in colorectal cancer. Lab Invest 1993, 69: 682-689

280. Liu T, Dhanasekaran SM, Jin H, Hu B, Tomlins SA, Chinnaiyan AM, and Phan SH: FIZZ1 stimulation of myofibroblast differentiation. Am J Pathol 2004, 164: 1315-1326

281. Lloyd CM, Minto AW, Dorf ME, Proudfoot A, Wells TN, Salant DJ, and Gutierrez-Ramos JC: RANTES and monocyte chemoattractant protein-1 (MCP-1) play an important role in the inflammatory phase of crescentic nephritis, but only MCP-1 is involved in crescent formation and interstitial fibrosis. J Exp Med 1997, 185: 1371-1380

282. Lovell CR, Nicholls AC, Duance VC, and Bailey AJ: Characterization of dermal collagen in systemic sclerosis. Br J Dermatol 1979, 100: 359-369

283. Lunardi C, Bason C, Navone R, Millo E, Damonte G, Corrocher R, and Puccetti A: Systemic sclerosis immunoglobulin G autoantibodies bind the human cytomegalovirus late protein UL94 and induce apoptosis in human endothelial cells [In Process Citation]. Nat Med 2000, 6: 1183-1186

284. Lunardi C, Dolcino M, Peterlana D, Bason C, Navone R, Tamassia N, Beri R, Corrocher R, and Puccetti A: Antibodies against Human Cytomegalovirus in the Pathogenesis of Systemic Sclerosis: A Gene Array Approach. PLoS Med 2005, 3: e2

285. Luzina IG, Atamas SP, Wise R, Wigley FM, Xiao HQ, and White B: Gene expression in bronchoalveolar lavage cells from scleroderma patients. Am J Respir Cell Mol Biol 2002, 26: 549-557

286. MacGregor AJ, Canavan R, Knight C, Denton CP, Davar J, Coghlan J, and Black CM: Pulmonary hypertension in systemic sclerosis: risk factors for progression and consequences for survival. Rheumatology (Oxford) 2001, 40: 453-459

287. Maisonpierre PC, Suri C, Jones PF, Bartunkova S, Wiegand SJ, Radziejewski C, Compton D, McClain J, Aldrich TH, Papadopoulos N, Daly TJ, Davis S, Sato TN, and Yancopoulos GD: Angiopoietin-2, a natural antagonist for Tie2 that disrupts in vivo angiogenesis [see comments]. Science 1997, 277: 55-60

288. Maitre A, Hours M, Bonneterre V, Arnaud J, Arslan MT, Carpentier P, Bergeret A, and de Gaudemaris R: Systemic sclerosis and occupational risk factors: role of solvents and cleaning products. J Rheumatol 2004, 31: 2395-2401

289. Majumdar S, Li D, Ansari T, Pantelidis P, Black CM, Gizycki M, du Bois RM, and Jeffery PK: Different cytokine profiles in cryptogenic fibrosing alveolitis and fibrosing alveolitis associated with systemic sclerosis: a quantitative study of open lung biopsies. Eur Respir J 1999, 14: 251-257

290. Marasini B, Cugno M, Bassani C, Stanzani M, Bottasso B, and Agostoni A: Tissue-type plasminogen activator and von Willebrand factor plasma levels as markers of endothelial involvement in patients with Raynaud's phenomenon [published erratum appears in Int J Microcirc Clin Exp 1993 Apr;12(2):223]. Int J Microcirc Clin Exp 1992, 11: 375-382

291. Marguerie C, Bunn CC, Copier J, Bernstein RM, Gilroy JM, Black CM, So AK, and Walport MJ: The clinical and immunogenetic features of patients with autoantibodies to the nucleolar antigen PM-Scl. Medicine (Baltimore) 1992, 71: 327-336

292. Maricq HR and Maize JC: Nailfold capillary abnormalities. Clin Rheum Dis 1982, 8: 455-478

293. Maricq HR, Weinrich MC, Keil JE, Smith EA, Harper FE, Nussbaum AI, LeRoy EC, McGregor AR, Diat F, and Rosal EJ: Prevalence of scleroderma spectrum disorders in the general population of South Carolina. Arthritis Rheum 1989, 32: 998-1006

294. Marie I, Cordel N, Lenormand B, Hellot MF, Levesque H, Courtois H, and Joly P: Clonal T cells in the blood of patients with systemic sclerosis. Arch Dermatol 2005, 141: 88-89

295. Marra F, Bonewald LF, Park-Snyder S, Park IS, Woodruff KA, and Abboud HE: Characterization and regulation of the latent transforming growth factor-beta complex secreted by vascular pericytes. J Cell Physiol 1996, 166: 537-546

296. Martin P: Wound healing--aiming for perfect skin regeneration. Science 1997, 276: 75-81

297. Martin P, D'Souza D, Martin J, Grose R, Cooper L, Maki R, and McKercher SR: Wound healing in the PU.1 null mouse--tissue repair is not dependent on inflammatory cells. Curr Biol 2003, 13: 1122-1128

298. Martin P, Dickson MC, Millan FA, and Akhurst RJ: Rapid induction and clearance of TGF beta 1 is an early response to wounding in the mouse embryo. Dev Genet 1993, 14: 225-238

299. Masuda H, Fukumoto M, Hirayoshi K, and Nagata K: Coexpression of the collagen-binding stress protein HSP47 gene and the alpha 1(I) and alpha 1(III) collagen genes in carbon tetrachloride-induced rat liver fibrosis. J Clin Invest 1994, 94: 2481-2488

300. Mattila L, Airola K, Ahonen M, Hietarinta M, Black C, Saarialho-Kere U, and Kahari VM: Activation of tissue inhibitor of metalloproteinases-3 (TIMP-3) mRNA expression in scleroderma skin fibroblasts. J Invest Dermatol 1998, 110: 416-421

301. Mavalia C, Scaletti C, Romagnani P, Carossino AM, Pignone A, Emmi L, Pupilli C, Pizzolo G, Maggi E, and Romagnani S: Type 2 helper T-cell predominance and high CD30 expression in systemic sclerosis. Am J Pathol 1997, 151: 1751-1758

302. Mayorga M, Bahi N, Ballester M, Comella JX, and Sanchis D: Bcl-2 is a key factor for cardiac fibroblast resistance to programmed cell death. J Biol Chem 2004, 279: 34882-34889

303. McCarty GAVDWFMJ: Antinuclear Antibodies. Contempary techniques and clinical applications to connective tissue diseases. New York Oxford University Press, 1984

304. McGaha T, Saito S, Phelps RG, Gordon R, Noben-Trauth N, Paul WE, and Bona C: Lack of skin fibrosis in tight skin (TSK) mice with targeted mutation in the interleukin-4R alpha and transforming growth factor-beta genes. J Invest Dermatol 2001, 116: 136-143

305. McHugh NJ, Harvey GR, Whyte J, and Dorsey JK: Segregation of autoantibodies with disease in monozygotic twin pairs discordant for systemic sclerosis. Three further cases. Arthritis Rheum 1995, 38: 1845-1850

306. Micklem K, Rigney E, Cordell J, Simmons D, Stross P, Turley H, Seed B, and Mason D: A human macrophage-associated antigen (CD68) detected by six different monoclonal antibodies. Br J Haematol 1989, 73: 6-11

307. Milhoan KA, Lane TA, and Bloor CM: Hypoxia induces endothelial cells to increase their adherence for neutrophils: role of PAF. Am J Physiol 1992, 263: H956-H962

308. Mori T, Kawara S, Shinozaki M, Hayashi N, Kakinuma T, Igarashi A, Takigawa M, Nakanishi T, and Takehara K: Role and interaction of connective tissue growth factor with transforming growth factor-beta in persistent fibrosis: A mouse fibrosis model. J Cell Physiol 1999, 181: 153-159

309. Mori Y, Chen SJ, and Varga J: Modulation of endogenous Smad expression in normal skin fibroblasts by transforming growth factor-beta. Exp Cell Res 2000, 258: 374-383

310. Mori Y, Chen SJ, and Varga J: Expression and regulation of intracellular SMAD signaling in scleroderma skin fibroblasts. Arthritis Rheum 2003, 48: 1964-1978

311. Mukerjee D, St George D, Coleiro B, Knight C, Denton CP, Davar J, Black CM, and Coghlan JG: Prevalence and outcome in systemic sclerosis associated

pulmonary arterial hypertension: application of a registry approach. Ann Rheum Dis 2003, 62: 1088-1093

312. Muryoi T, Kasturi KN, Kafina MJ, Cram DS, Harrison LC, Sasaki T, and Bona CA: Antitopoisomerase I monoclonal autoantibodies from scleroderma patients and tight skin mouse interact with similar epitopes. J Exp Med 1992, 175: 1103-1109

313. Myllarniemi M, Frosen J, Calderon Ramirez LG, Buchdunger E, Lemstrom K, and Hayry P: Selective tyrosine kinase inhibitor for the platelet-derived growth factor receptor in vitro inhibits smooth muscle cell proliferation after reinjury of arterial intima in vivo. Cardiovasc Drugs Ther 1999, 13: 159-168

314. Namiki A, Brogi E, Kearney M, Kim EA, Wu T, Couffinhal T, Varticovski L, and Isner JM: Hypoxia induces vascular endothelial growth factor in cultured human endothelial cells. J Biol Chem 1995, 270: 31189-31195

315. Nayak RC, Berman AB, George KL, Eisenbarth GS, and King GL: A monoclonal antibody (3G5)-defined ganglioside antigen is expressed on the cell surface of microvascular pericytes. J Exp Med 1988, 167: 1003-1015

316. Nehls V and Drenckhahn D: Heterogeneity of microvascular pericytes for smooth muscle type alpha-actin. J Cell Biol 1991, 113: 147-154

317. Nehls V and Drenckhahn D: The versatility of microvascular pericytes: from mesenchyme to smooth muscle? Histochemistry 1993, 99: 1-12

318. Neidhart M, Kuchen S, Distler O, Bruhlmann P, Michel BA, Gay RE, and Gay S: Increased serum levels of antibodies against human cytomegalovirus and prevalence of autoantibodies in systemic sclerosis. Arthritis Rheum 1999, 42: 389-392

319. Nguyen VA, Sgonc R, Dietrich H, and Wick G: Endothelial injury in internal organs of University of California at Davis line 200 (UCD 200) chickens, an animal model for systemic sclerosis (Scleroderma). J Autoimmun 2000, 14: 143-149

320. Nicholson AG, Colby TV, du Bois RM, Hansell DM, and Wells AU: The prognostic significance of the histologic pattern of interstitial pneumonia in patients presenting with the clinical entity of cryptogenic fibrosing alveolitis. Am J Respir Crit Care Med 2000, 162: 2213-2217

321. Nietert PJ and Silver RM: Systemic sclerosis: environmental and occupational risk factors. Curr Opin Rheumatol 2000, 12: 520-526

322. Nietert PJ, Silver RM, Mitchell HC, Shaftman SR, and Tilley BC: Demographic and clinical factors associated with in-hospital death among patients with systemic sclerosis. J Rheumatol 2005, 32: 1888-1892

323. Nishijima C, Hayakawa I, Matsushita T, Komura K, Hasegawa M, Takehara K, and Sato S: Autoantibody against matrix metalloproteinase-3 in patients with systemic sclerosis. Clin Exp Immunol 2004, 138: 357-363

324. Noiseux N, Boucher CH, Cartier R, and Sirois MG: Bolus endovascular PDGFR-beta antisense treatment suppressed intimal hyperplasia in a rat carotid injury model. Circulation 2000, 102: 1330-1336

325. Nomura M, Yamagishi S, Harada S, Hayashi Y, Yamashima T, Yamashita J, and Yamamoto H: Possible participation of autocrine and paracrine vascular endothelial growth factors in hypoxia-induced proliferation of endothelial cells and pericytes. J Biol Chem 1995, 270: 28316-28324

326. O'Kane S and Ferguson MW: Transforming growth factor beta s and wound healing. Int J Biochem Cell Biol 1997, 29: 63-78

327. Oddis CV, Okano Y, Rudert WA, Trucco M, Duquesnoy RJ, and Medsger TA, Jr.: Serum autoantibody to the nucleolar antigen PM-Scl. Clinical and immunogenetic associations. Arthritis Rheum 1992, 35: 1211-1217

328. Odenthal M, Neubauer K, Meyer zum Buschenfelde KH, and Ramadori G: Localization and mRNA steady-state level of cellular fibronectin in rat liver undergoing a CCl4-induced acute damage or fibrosis. Biochim Biophys Acta 1993, 1181: 266-272

329. Ohtsuka T, Yamakage A, and Yamazaki S: The polymorphism of transforming growth factor-beta1 gene in Japanese patients with systemic sclerosis. Br J Dermatol 2002, 147: 458-463

330. Okano Y and Medsger TA, Jr.: Autoantibody to Th ribonucleoprotein (nucleolar 7-2 RNA protein particle) in patients with systemic sclerosis. Arthritis Rheum 1990, 33: 1822-1828

331. Oliver MH, Harrison NK, Bishop JE, Cole PJ, and Laurent GJ: A rapid and convenient assay for counting cells cultured in microwell plates: application for assessment of growth factors. J Cell Sci 1989, 92 ( Pt 3): 513-518

332. Ostendorf T, Kunter U, Grone HJ, Bahlmann F, Kawachi H, Shimizu F, Koch KM, Janjic N, and Floege J: Specific antagonism of PDGF prevents renal scarring in experimental glomerulonephritis. J Am Soc Nephrol 2001, 12: 909-918

333. Ozerdem U, Monosov E, and Stallcup WB: NG2 proteoglycan expression by pericytes in pathological microvasculature. Microvasc Res 2002, 63: 129-134

334. Pandey JP and Takeuchi F: TNF-alpha and TNF-beta gene polymorphisms in systemic sclerosis. Hum Immunol 1999, 60: 1128-1130

335. Pannu J, Gore-Hyer E, Yamanaka M, Smith EA, Rubinchik S, Dong JY, Jablonska S, Blaszczyk M, and Trojanowska M: An increased transforming growth factor

beta receptor type I:type II ratio contributes to elevated collagen protein synthesis that is resistant to inhibition via a kinase-deficient transforming growth factor beta receptor type II in scleroderma. Arthritis Rheum 2004, 50: 1566-1577

336. Pantelidis P, McGrath DS, Southcott AM, Black CM, and du Bois RM: Tumour necrosis factor-alpha production in fibrosing alveolitis is macrophage subset specific. Respir Res 2001, 2: 365-372

337. Pantelidis P, Southcott AM, Black CM, and du Bois RM: Up-regulation of IL-8 secretion by alveolar macrophages from patients with fibrosing alveolitis: a subpopulation analysis. Clin Exp Immunol 1997, 108: 95-104

338. Paroli M, Schiaffella E, Di Rosa F, and Barnaba V: Persisting viruses and autoimmunity. J Neuroimmunol 2000, 107: 201-204

339. Perbal B: CCN proteins: multifunctional signalling regulators. Lancet 2004, 363: 62-64

340. Peters JH and Hynes RO: Fibronectin isoform distribution in the mouse. I. The alternatively spliced EIIIB, EIIIA, and V segments show widespread codistribution in the developing mouse embryo. Cell Adhes Commun 1996, 4: 103-125

341. Peters T, Sindrilaru A, Hinz B, Hinrichs R, Menke A, Al Azzeh EA, Holzwarth K, Oreshkova T, Wang H, Kess D, Walzog B, Sulyok S, Sunderkotter C, Friedrich W, Wlaschek M, Krieg T, and Scharffetter-Kochanek K: Wound-healing defect of CD18(-/-) mice due to a decrease in TGF-beta1 and myofibroblast differentiation. EMBO J 2005, 24: 3400-3410

342. Pierce GF, Mustoe TA, Lingelbach J, Masakowski VR, Griffin GL, Senior RM, and Deuel TF: Platelet-derived growth factor and transforming growth factor-beta

enhance tissue repair activities by unique mechanisms. J Cell Biol 1989, 109: 429-440

343. Pierce GF, Mustoe TA, Senior RM, Reed J, Griffin GL, Thomason A, and Deuel TF: In vivo incisional wound healing augmented by platelet-derived growth factor and recombinant c-sis gene homodimeric proteins. J Exp Med 1988, 167: 974-987

344. Pierce GF, Vande BJ, Rudolph R, Tarpley J, and Mustoe TA: Platelet-derived growth factor-BB and transforming growth factor beta 1 selectively modulate glycosaminoglycans, collagen, and myofibroblasts in excisional wounds. Am J Pathol 1991, 138: 629-646

345. Pignone A, Scaletti C, Matucci-Cerinic M, Vazquez-Abad D, Meroni PL, Del Papa N, Falcini F, Generini S, Rothfield N, and Cagnoni M: Anti-endothelial cell antibodies in systemic sclerosis: significant association with vascular involvement and alveolo-capillary impairment. Clin Exp Rheumatol 1998, 16: 527-532

346. Pilling D, Buckley CD, Salmon M, and Gomer RH: Inhibition of fibrocyte differentiation by serum amyloid P. J Immunol 2003, 171: 5537-5546

347. Ponticos M, Abraham D, Alexakis C, Lu QL, Black C, Partridge T, and Bou-Gharios G: Col1a2 enhancer regulates collagen activity during development and in adult tissue repair. Matrix Biol 2004, 22: 619-628

348. Postlethwaite AE, Raghow R, Stricklin GP, Poppleton H, Seyer JM, and Kang AH: Modulation of fibroblast functions by interleukin 1: increased steady-state accumulation of type I procollagen messenger RNAs and stimulation of other functions but not chemotaxis by human recombinant interleukin 1 alpha and beta. J Cell Biol 1988, 106: 311-318

349. Postlethwaite AE, Shigemitsu H, and Kanangat S: Cellular origins of fibroblasts: possible implications for organ fibrosis in systemic sclerosis. Curr Opin Rheumatol 2004, 16: 733-738

350. Prescott RJ, Freemont AJ, Jones CJ, Hoyland J, and Fielding P: Sequential dermal microvascular and perivascular changes in the development of scleroderma. J Pathol 1992, 166: 255-263

351. Quaglino D, Jr., Bergamini G, Boraldi F, Manzini E, Davidson JM, and Pasquali R, I: Connective tissue in skin biopsies from patients suffering systemic sclerosis. J Submicrosc Cytol Pathol 1996, 28: 287-296

352. Querfeld C, Eckes B, Huerkamp C, Krieg T, and Sollberg S: Expression of TGF-beta 1, -beta 2 and -beta 3 in localized and systemic scleroderma. J Dermatol Sci 1999, 21: 13-22

353. Rajkumar, V. S., Howell, K, Csiszar, K., Denton, C. P., Black, C. M., and Abraham, D. J. Shared expression of phenotypic markers in systemic sclerosis indicates a convergence of pericytes and fibroblasts to a myofibroblast lineage in fibrosis. Arthritis Res Ther. 1113-1123. 2005.
Ref Type: Generic

354. Rajkumar VS, Sundberg C, Abraham DJ, Rubin K, and Black CM: Activation of microvascular pericytes in autoimmune Raynaud's phenomenon and systemic sclerosis. Arthritis Rheum 1999, 42: 930-941

355. Ranieri E, Gesualdo L, Grandaliano G, Maiorano E, and Schena FP: The role of alpha-smooth muscle actin and platelet-derived growth factor-beta receptor in the progression of renal damage in human IgA nephropathy. J Nephrol 2001, 14: 253-262

356. Renzoni E, Lympany P, Sestini P, Pantelidis P, Wells A, Black C, Welsh K, Bunn C, Knight C, Foley P, and du Bois RM: Distribution of novel polymorphisms of the interleukin-8 and CXC receptor 1 and 2 genes in systemic sclerosis and cryptogenic fibrosing alveolitis. Arthritis Rheum 2000, 43: 1633-1640

357. Reuter R and Luhrmann R: Immunization of mice with purified U1 small nuclear ribonucleoprotein (RNP) induces a pattern of antibody specificities characteristic of the anti-Sm and anti-RNP autoimmune response of patients with lupus erythematosus, as measured by monoclonal antibodies. Proc Natl Acad Sci U S A 1986, 83: 8689-8693

358. Reuterdahl C, Sundberg C, Rubin K, Funa K, and Gerdin B: Tissue localization of beta receptors for platelet-derived growth factor and platelet-derived growth factor B chain during wound repair in humans. J Clin Invest 1993, 91: 2065-2075

359. Rhodin JA: Ultrastructure of mammalian venous capillaries, venules, and small collecting veins. J Ultrastruct Res 1968, 25: 452-500

360. Rhodin JA and Fujita H: Capillary growth in the mesentery of normal young rats. Intravital video and electron microscope analyses. J Submicrosc Cytol Pathol 1989, 21: 1-34

361. Richardson RL, Hausman GJ, and Campion DR: Response of pericytes to thermal lesion in the inguinal fat pad of 10-day-old rats. Acta Anat (Basel) 1982, 114: 41-57

362. Rockey DC, Housset CN, and Friedman SL: Activation-dependent contractility of rat hepatic lipocytes in culture and in vivo. J Clin Invest 1993, 92: 1795-1804

363. Ronnov-Jessen L, Petersen OW, Koteliansky VE, and Bissell MJ: The origin of the myofibroblasts in breast cancer. Recapitulation of tumor environment in

culture unravels diversity and implicates converted fibroblasts and recruited smooth muscle cells. J Clin Invest 1995, 95: 859-873

364. Ronnstrand L, Terracio L, Claesson-Welsh L, Heldin CH, and Rubin K: Characterization of two monoclonal antibodies reactive with the external domain of the platelet-derived growth factor receptor. J Biol Chem 1988, 263: 10429-10435

365. Ross R, Glomset J, Kariya B, and Harker L: A platelet-dependent serum factor that stimulates the proliferation of arterial smooth muscle cells in vitro. Proc Natl Acad Sci U S A 1974, 71: 1207-1210

366. Ross R, Masuda J, Raines EW, Gown AM, Katsuda S, Sasahara M, Malden LT, Masuko H, and Sato H: Localization of PDGF-B protein in macrophages in all phases of atherogenesis. Science 1990, 248: 1009-1012

367. Rubin K, Tingstrom A, Hansson GK, Larsson E, Ronnstrand L, Klareskog L, Claesson-Welsh L, Heldin CH, Fellstrom B, and Terracio L: Induction of B-type receptors for platelet-derived growth factor in vascular inflammation: possible implications for development of vascular proliferative lesions. Lancet 1988, 1: 1353-1356

368. Rubin LJ, Badesch DB, Barst RJ, Galie N, Black CM, Keogh A, Pulido T, Frost A, Roux S, Leconte I, Landzberg M, and Simonneau G: Bosentan therapy for pulmonary arterial hypertension. N Engl J Med 2002, 346: 896-903

369. Rudnicka L, Varga J, Christiano AM, Iozzo RV, Jimenez SA, and Uitto J: Elevated expression of type VII collagen in the skin of patients with systemic sclerosis. Regulation by transforming growth factor-beta. J Clin Invest 1994, 93: 1709-1715

370. Saalbach A, Aneregg U, Bruns M, Schnabel E, Herrmann K, and Haustein UF: Novel fibroblast-specific monoclonal antibodies: properties and specificities. J Invest Dermatol 1996, 106: 1314-1319

371. Saalbach A, Aust G, Haustein UF, Herrmann K, and Anderegg U: The fibroblast-specific MAb AS02: a novel tool for detection and elimination of human fibroblasts. Cell Tissue Res 1997, 290: 593-599

372. Sachinidis A, Locher R, Hoppe J, and Vetter W: The platelet-derived growth factor isomers, PDGF-AA, PDGF-AB and PDGF-BB, induce contraction of vascular smooth muscle cells by different intracellular mechanisms. FEBS Lett 1990, 275: 95-98

373. Sacks DG, Okano Y, Steen VD, Curtiss E, Shapiro LS, and Medsger TA, Jr.: Isolated pulmonary hypertension in systemic sclerosis with diffuse cutaneous involvement: association with serum anti-U3RNP antibody. J Rheumatol 1996, 23: 639-642

374. Saito E, Fujimoto M, Hasegawa M, Komura K, Hamaguchi Y, Kaburagi Y, Nagaoka T, Takehara K, Tedder TF, and Sato S: CD19-dependent B lymphocyte signaling thresholds influence skin fibrosis and autoimmunity in the tight-skin mouse. J Clin Invest 2002, 109: 1453-1462

375. Sambo P, Jannino L, Candela M, Salvi A, Donini M, Dusi S, Luchetti MM, and Gabrielli A: Monocytes of patients with systemic sclerosis (scleroderma) spontaneously release in vitro increased amounts of superoxide anion. J Invest Dermatol 1999, 112: 78-84

376. Sandler C, Joutsiniemi S, Lindstedt KA, Juutilainen T, Kovanen PT, and Eklund KK: Imatinib mesylate inhibits platelet derived growth factor stimulated proliferation of rheumatoid synovial fibroblasts. Biochem Biophys Res Commun 2006, 347: 31-35

377. Sappino AP, Masouye I, Saurat JH, and Gabbiani G: Smooth muscle differentiation in scleroderma fibroblastic cells. Am J Pathol 1990, 137: 585-591

378. Sato H, Lagan AL, Alexopoulou C, Vassilakis DA, Ahmad T, Pantelidis P, Veeraraghavan S, Renzoni E, Denton C, Black C, Wells AU, du Bois RM, and Welsh KI: The TNF-863A allele strongly associates with anticentromere antibody positivity in scleroderma. Arthritis Rheum 2004, 50: 558-564

379. Sato M, Muragaki Y, Saika S, Roberts AB, and Ooshima A: Targeted disruption of TGF-beta1/Smad3 signaling protects against renal tubulointerstitial fibrosis induced by unilateral ureteral obstruction. J Clin Invest 2003, 112: 1486-1494

380. Sato S, Hasegawa M, Fujimoto M, Tedder TF, and Takehara K: Quantitative genetic variation in CD19 expression correlates with autoimmunity. J Immunol 2000, 165: 6635-6643

381. Sato S, Hayakawa I, Hasegawa M, Fujimoto M, and Takehara K: Function blocking autoantibodies against matrix metalloproteinase-1 in patients with systemic sclerosis. J Invest Dermatol 2003, 120: 542-547

382. Sato S, Nagaoka T, Hasegawa M, Tamatani T, Nakanishi T, Takigawa M, and Takehara K: Serum levels of connective tissue growth factor are elevated in patients with systemic sclerosis: association with extent of skin sclerosis and severity of pulmonary fibrosis. J Rheumatol 2000, 27: 149-154

383. Satoh M, Ajmani AK, Ogasawara T, Langdon JJ, Hirakata M, Wang J, and Reeves WH: Autoantibodies to RNA polymerase II are common in systemic lupus erythematosus and overlap syndrome. Specific recognition of the phosphorylated (IIO) form by a subset of human sera. J Clin Invest 1994, 94: 1981-1989

384. Satoh M, Kuwana M, Ogasawara T, Ajmani AK, Langdon JJ, Kimpel D, Wang J, and Reeves WH: Association of autoantibodies to topoisomerase I and the phosphorylated (IIO) form of RNA polymerase II in Japanese scleroderma patients. J Immunol 1994, 153: 5838-5848

385. Scala E, Pallotta S, Frezzolini A, Abeni D, Barbieri C, Sampogna F, De Pita O, Puddu P, Paganelli R, and Russo G: Cytokine and chemokine levels in systemic sclerosis: relationship with cutaneous and internal organ involvement. Clin Exp Immunol 2004, 138: 540-546

386. Scharffetter K, Lankat-Buttgereit B, and Krieg T: Localization of collagen mRNA in normal and scleroderma skin by in-situ hybridization. Eur J Clin Invest 1988, 18: 9-17

387. Schermuly RT, Dony E, Ghofrani HA, Pullamsetti S, Savai R, Roth M, Sydykov A, Lai YJ, Weissmann N, Seeger W, and Grimminger F: Reversal of experimental pulmonary hypertension by PDGF inhibition. J Clin Invest 2005, 115: 2811-2821

388. Schlingemann RO, Dingjan GM, Emeis JJ, Blok J, Warnaar SO, and Ruiter DJ: Monoclonal antibody PAL-E specific for endothelium. Lab Invest 1985, 52: 71-76

389. Schlingemann RO, Rietveld FJ, de Waal RM, Ferrone S, and Ruiter DJ: Expression of the high molecular weight melanoma-associated antigen by pericytes during angiogenesis in tumors and in healing wounds. Am J Pathol 1990, 136: 1393-1405

390. Schlingemann RO, Rietveld FJ, Kwaspen F, van de Kerkhof PC, de Waal RM, and Ruiter DJ: Differential expression of markers for endothelial cells, pericytes, and basal lamina in the microvasculature of tumors and granulation tissue. Am J Pathol 1991, 138: 1335-1347

391. Schmitt-Graff A, Kruger S, Bochard F, Gabbiani G, and Denk H: Modulation of alpha smooth muscle actin and desmin expression in perisinusoidal cells of normal and diseased human livers. Am J Pathol 1991, 138: 1233-1242

392. Schor AM, Allen TD, Canfield AE, Sloan P, and Schor SL: Pericytes derived from the retinal microvasculature undergo calcification in vitro. J Cell Sci 1990, 97 ( Pt 3): 449-461

393. Seibold JR, Giorno RC, and Claman HN: Dermal mast cell degranulation in systemic sclerosis. Arthritis Rheum 1990, 33: 1702-1709

394. Serini G, Bochaton-Piallat ML, Ropraz P, Geinoz A, Borsi L, Zardi L, and Gabbiani G: The fibronectin domain ED-A is crucial for myofibroblastic phenotype induction by transforming growth factor-beta1. J Cell Biol 1998, 142: 873-881

395. Sgonc R: The vascular perspective of systemic sclerosis: of chickens, mice and men. Int Arch Allergy Immunol 1999, 120: 169-176

396. Sgonc R, Gruschwitz MS, Dietrich H, Recheis H, Gershwin ME, and Wick G: Endothelial cell apoptosis is a primary pathogenetic event underlying skin lesions in avian and human scleroderma. J Clin Invest 1996, 98: 785-792

397. Shah M, Foreman DM, and Ferguson MW: Control of scarring in adult wounds by neutralising antibody to transforming growth factor beta. Lancet 1992, 339: 213-214

398. Shah M, Foreman DM, and Ferguson MW: Neutralisation of TGF-beta 1 and TGF-beta 2 or exogenous addition of TGF-beta 3 to cutaneous rat wounds reduces scarring. J Cell Sci 1995, 108 ( Pt 3): 985-1002

399. Shaheen RM, Tseng WW, Davis DW, Liu W, Reinmuth N, Vellagas R, Wieczorek AA, Ogura Y, McConkey DJ, Drazan KE, Bucana CD, McMahon G, and

Ellis LM: Tyrosine kinase inhibition of multiple angiogenic growth factor receptors improves survival in mice bearing colon cancer liver metastases by inhibition of endothelial cell survival mechanisms. Cancer Res 2001, 61: 1464-1468

400. Sharp GC, Irvin WS, May CM, Holman HR, McDuffie FC, Hess EV, and Schmid FR: Association of antibodies to ribonucleoprotein and Sm antigens with mixed connective-tissue disease, systematic lupus erythematosus and other rheumatic diseases. N Engl J Med 1976, 295: 1149-1154

401. Shepro D and Morel NM: Pericyte physiology. FASEB J 1993, 7: 1031-1038

402. Shi S and Gronthos S: Perivascular niche of postnatal mesenchymal stem cells in human bone marrow and dental pulp. J Bone Miner Res 2003, 18: 696-704

403. Shi Y and Massague J: Mechanisms of TGF-beta signaling from cell membrane to the nucleus. Cell 2003, 113: 685-700

404. Shi-wen X, Chen Y, Denton CP, Eastwood M, Renzoni EA, Bou-Gharios G, Pearson JD, Dashwood M, du Bois RM, Black CM, Leask A, and Abraham DJ: Endothelin-1 promotes myofibroblast induction through the ETA receptor via a rac/phosphoinositide 3-kinase/Akt-dependent pathway and is essential for the enhanced contractile phenotype of fibrotic fibroblasts. Mol Biol Cell 2004, 15: 2707-2719

405. Shi-wen X, Denton CP, Dashwood MR, Holmes AM, Bou-Gharios G, Pearson JD, Black CM, and Abraham DJ: Fibroblast matrix gene expression and connective tissue remodeling: role of endothelin-1. J Invest Dermatol 2001, 116: 417-425

406. Shi-wen X, Pennington D, Holmes A, Leask A, Bradham D, Beauchamp JR, Fonseca C, du Bois RM, Martin GR, Black CM, and Abraham DJ: Autocrine

overexpression of CTGF maintains fibrosis: RDA analysis of fibrosis genes in systemic sclerosis. Exp Cell Res 2000, 259: 213-224

407. Shi-wen X, Stanton LA, Kennedy L, Pala D, Chen Y, Howat SL, Renzoni EA, Carter DE, Bou-Gharios G, Stratton RJ, Pearson JD, Beier F, Lyons KM, Black CM, Abraham DJ, and Leask A: CCN2 is necessary for adhesive responses to transforming growth factor-beta1 in embryonic fibroblasts. J Biol Chem 2006, 281: 10715-10726

408. Shiraishi T, Morimoto S, Itoh K, Sato H, Sugihara K, Onishi T, and Ogihara T: Radioimmunoassay of human platelet-derived growth factor using monoclonal antibody toward a synthetic 73-97 fragment of its B-chain. Clin Chim Acta 1989, 184: 65-74

409. Sieczkiewicz GJ and Herman IM: TGF-beta 1 signaling controls retinal pericyte contractile protein expression. Microvasc Res 2003, 66: 190-196

410. Siegbahn A, Hammacher A, Westermark B, and Heldin CH: Differential effects of the various isoforms of platelet-derived growth factor on chemotaxis of fibroblasts, monocytes, and granulocytes. J Clin Invest 1990, 85: 916-920

411. Silman AJ and Newman J: Epidemiology of systemic sclerosis. Curr Opin Rheumatol 1996, 8: 585-589

412. Silver R: Scleroderma and Pseudoscleroderma: Environmental Exposure. Systemic Sclerosis. Edited by Clements PJ and Furst DE. Williams & Wilkins, Baltimore, 1996, pp. 81-98

413. Silvera MR, Sempowski GD, and Phipps RP: Expression of TGF-beta isoforms by Thy-1+ and Thy-1- pulmonary fibroblast subsets: evidence for TGF-beta as a regulator of IL-1-dependent stimulation of IL-6. Lymphokine Cytokine Res 1994, 13: 277-285

414. Sims DE: Recent advances in pericyte biology--implications for health and disease. Can J Cardiol 1991, 7: 431-443

415. Singer AJ and Clark RA: Cutaneous wound healing. N Engl J Med 1999, 341: 738-746

416. Skalli O, Pelte MF, Peclet MC, Gabbiani G, Gugliotta P, Bussolati G, Ravazzola M, and Orci L: Alpha-smooth muscle actin, a differentiation marker of smooth muscle cells, is present in microfilamentous bundles of pericytes. J Histochem Cytochem 1989, 37: 315-321

417. Skalli O, Ropraz P, Trzeciak A, Benzonana G, Gillessen D, and Gabbiani G: A monoclonal antibody against alpha-smooth muscle actin: a new probe for smooth muscle differentiation. J Cell Biol 1986, 103: 2787-2796

418. Smith-Mungo LI and Kagan HM: Lysyl oxidase: properties, regulation and multiple functions in biology. Matrix Biol 1998, 16: 387-398

419. Song E, Ouyang N, Horbelt M, Antus B, Wang M, and Exton MS: Influence of alternatively and classically activated macrophages on fibrogenic activities of human fibroblasts. Cell Immunol 2000, 204: 19-28

420. Song S, Ewald AJ, Stallcup W, Werb Z, and Bergers G: PDGFRbeta(+) perivascular progenitor cells in tumours regulate pericyte differentiation and vascular survival. Nat Cell Biol 2005, 7: 870-879

421. Soriano P: The PDGF alpha receptor is required for neural crest cell development and for normal patterning of the somites. Development 1997, 124: 2691-2700

422. Soriano P: Abnormal kidney development and hematological disorders in PDGF beta-receptor mutant mice. Genes Dev 1994, 8: 1888-1896

423. Sorkin A, Westermark B, Heldin CH, and Claesson-Welsh L: Effect of receptor kinase inactivation on the rate of internalization and degradation of PDGF and the PDGF beta-receptor. J Cell Biol 1991, 112: 469-478

424. Sorrell JM, Baber BA, and Caplan AI: Construction of a bilayered dermal equivalent containing human papillary and reticular dermal fibroblasts: Use of fluorescent vital dyes. Tissue Engineering 1996, 2: 39-49

425. Spencer-Green G: Outcomes in primary Raynaud phenomenon: a meta-analysis of the frequency, rates, and predictors of transition to secondary diseases. Arch Intern Med 1998, 158: 595-600

426. Speyer CL, Steffes CP, and Ram JL: Effects of vasoactive mediators on the rat lung pericyte: quantitative analysis of contraction on collagen lattice matrices. Microvasc Res 1999, 57: 134-143

427. Stafford L, Englert H, Gover J, and Bertouch J: Distribution of macrovascular disease in scleroderma. Ann Rheum Dis 1998, 57: 476-479

428. Steen VD: Scleroderma renal crisis. Rheum Dis Clin North Am 1996, 22: 861-878

429. Steen VD, Conte C, Owens GR, and Medsger TA, Jr.: Severe restrictive lung disease in systemic sclerosis. Arthritis Rheum 1994, 37: 1283-1289

430. Steen VD and Medsger TA, Jr.: Epidemiology and natural history of systemic sclerosis. Rheum Dis Clin North Am 1990, 16: 1-10

431. Steen VD and Medsger TA, Jr.: Severe organ involvement in systemic sclerosis with diffuse scleroderma. Arthritis Rheum 2000, 43: 2437-2444

432. Stein M, Keshav S, Harris N, and Gordon S: Interleukin 4 potently enhances murine macrophage mannose receptor activity: a marker of alternative immunologic macrophage activation. J Exp Med 1992, 176: 287-292

433. Stone PJ, Korn JH, North H, Lally EV, Miller LC, Tucker LB, Strongwater S, Snider GL, and Franzblau C: Cross-linked elastin and collagen degradation products in the urine of patients with scleroderma. Arthritis Rheum 1995, 38: 517-524

434. Stratton R, Shiwen X, Martini G, Holmes A, Leask A, Haberberger T, Martin GR, Black CM, and Abraham D: Iloprost suppresses connective tissue growth factor production in fibroblasts and in the skin of scleroderma patients. J Clin Invest 2001, 108: 241-250

435. Stratton RJ, Coghlan JG, Pearson JD, Burns A, Sweny P, Abraham DJ, and Black CM: Different patterns of endothelial cell activation in renal and pulmonary vascular disease in scleroderma. QJM 1998, 91: 561-566

436. Strehlow D and Korn JH: Biology of the scleroderma fibroblast. Curr Opin Rheumatol 1998, 10: 572-578

437. Sugiura Y, Banno S, Matsumoto Y, Niimi T, Yoshinouchi T, Hayami Y, Naniwa T, and Ueda R: Transforming growth factor beta1 gene polymorphism in patients with systemic sclerosis. J Rheumatol 2003, 30: 1520-1523

438. Sundberg C, Branting M, Gerdin B, and Rubin K: Tumor cell and connective tissue cell interactions in human colorectal adenocarcinoma. Transfer of platelet-derived growth factor-AB/BB to stromal cells. Am J Pathol 1997, 151: 479-492

439. Sundberg C, Ivarsson M, Gerdin B, and Rubin K: Pericytes as collagen-producing cells in excessive dermal scarring. Lab Invest 1996, 74: 452-466

440. Sundberg C, Ljungstrom M, Lindmark G, Gerdin B, and Rubin K: Microvascular pericytes express platelet-derived growth factor-beta receptors in human healing wounds and colorectal adenocarcinoma. Am J Pathol 1993, 143: 1377-1388

441. Suri C, Jones PF, Patan S, Bartunkova S, Maisonpierre PC, Davis S, Sato TN, and Yancopoulos GD: Requisite role of angiopoietin-1, a ligand for the TIE2 receptor, during embryonic angiogenesis [see comments]. Cell 1996, 87: 1171-1180

442. Susol E, Rands AL, Herrick A, McHugh N, Barrett JH, Ollier WE, and Worthington J: Association of markers for TGFbeta3, TGFbeta2 and TIMP1 with systemic sclerosis. Rheumatology (Oxford) 2000, 39: 1332-1336

443. Szulgit G, Rudolph R, Wandel A, Tenenhaus M, Panos R, and Gardner H: Alterations in fibroblast alpha1beta1 integrin collagen receptor expression in keloids and hypertrophic scars. J Invest Dermatol 2002, 118: 409-415

444. Tachibana I, Bodorova J, Berditchevski F, Zutter MM, and Hemler ME: NAG-2, a novel transmembrane-4 superfamily (TM4SF) protein that complexes with integrins and other TM4SF proteins. J Biol Chem 1997, 272: 29181-29189

445. Takahashi K, Brooks RA, Kanse SM, Ghatei MA, Kohner EM, and Bloom SR: Production of endothelin 1 by cultured bovine retinal endothelial cells and presence of endothelin receptors on associated pericytes. Diabetes 1989, 38: 1200-1202

446. Takeuchi F, Nabeta H, Fussel M, Conrad K, and Frank KH: Association of the TNFa13 microsatellite with systemic sclerosis in Japanese patients. Ann Rheum Dis 2000, 59: 293-296

447. Tallquist M and Kazlauskas A: PDGF signaling in cells and mice. Cytokine Growth Factor Rev 2004, 15: 205-213

448. Tamby MC, Humbert M, Guilpain P, Servettaz A, Dupin N, Christner JJ, Simonneau G, Fermanian J, Weill B, Guillevin L, and Mouthon L: Antibodies to

fibroblasts in idiopathic and scleroderma associated pulmonary hypertension. Eur Respir J 2006,

449. Tan FK and Arnett FC: Genetic factors in the etiology of systemic sclerosis and Raynaud phenomenon. Curr Opin Rheumatol 2000, 12: 511-519

450. Tan FK, Arnett FC, Reveille JD, Ahn C, Antohi S, Sasaki T, Nishioka K, and Bona CA: Autoantibodies to fibrillin 1 in systemic sclerosis: ethnic differences in antigen recognition and lack of correlation with specific clinical features or HLA alleles. Arthritis Rheum 2000, 43: 2464-2471

451. Tan FK, Stivers DN, Foster MW, Chakraborty R, Howard RF, Milewicz DM, and Arnett FC: Association of microsatellite markers near the fibrillin 1 gene on human chromosome 15q with scleroderma in a Native American population. Arthritis Rheum 1998, 41: 1729-1737

452. Tan FK, Wang N, Kuwana M, Chakraborty R, Bona CA, Milewicz DM, and Arnett FC: Association of fibrillin 1 single-nucleotide polymorphism haplotypes with systemic sclerosis in Choctaw and Japanese populations. Arthritis Rheum 2001, 44: 893-901

453. Tingstrom A, Reuterdahl C, Lindahl P, Heldin CH, and Rubin K: Expression of platelet-derived growth factor-beta receptors on human fibroblasts. Regulation by recombinant platelet-derived growth factor-BB, IL-1, and tumor necrosis factor-alpha. J Immunol 1992, 148: 546-554

454. Tolusso B, Fabris M, Caporali R, Cuomo G, Isola M, Soldano F, Montecucco C, Valentini G, and Ferraccioli G: -238 and +489 TNF-alpha along with TNF-RII gene polymorphisms associate with the diffuse phenotype in patients with Systemic Sclerosis. Immunol Lett 2005, 96: 103-108

455. Tomasek JJ, Gabbiani G, Hinz B, Chaponnier C, and Brown RA: Myofibroblasts and mechano-regulation of connective tissue remodelling. Nat Rev Mol Cell Biol 2002, 3: 349-363

456. Tormey VJ, Bunn CC, Denton CP, and Black CM: Anti-fibrillarin antibodies in systemic sclerosis. Rheumatology (Oxford) 2001, 40: 1157-1162

457. Torry DJ, Richards CD, Podor TJ, and Gauldie J: Anchorage-independent colony growth of pulmonary fibroblasts derived from fibrotic human lung tissue. J Clin Invest 1994, 93: 1525-1532

458. Toubi E, Kessel A, Grushko G, Sabo E, Rozenbaum M, and Rosner I: The association of serum matrix metalloproteinases and their tissue inhibitor levels with scleroderma disease severity. Clin Exp Rheumatol 2002, 20: 221-224

459. Tsuji-Yamada J, Nakazawa M, Minami M, and Sasaki T: Increased frequency of interleukin 4 producing CD4+ and CD8+ cells in peripheral blood from patients with systemic sclerosis. J Rheumatol 2001, 28: 1252-1258

460. Valentini G, Baroni A, Esposito K, Naclerio C, Buommino E, Farzati A, Cuomo G, and Farzati B: Peripheral blood T lymphocytes from systemic sclerosis patients show both Th1 and Th2 activation. J Clin Immunol 2001, 21: 210-217

461. Valius M and Kazlauskas A: Phospholipase C-gamma 1 and phosphatidylinositol 3 kinase are the downstream mediators of the PDGF receptor's mitogenic signal. Cell 1993, 73: 321-334

462. van der Straaten HM, Canninga-van Dijk MR, Verdonck LF, Castigliego D, Borst HP, Aten J, and Fijnheer R: Extra-domain-A fibronectin: a new marker of fibrosis in cutaneous graft-versus-host disease. J Invest Dermatol 2004, 123: 1057-1062

463. Vancheeswaran R, Azam A, Black C, and Dashwood MR: Localization of endothelin-1 and its binding sites in scleroderma skin. J Rheumatol 1994, 21: 1268-1276

464. Vanderlaan M and Thomas CB: Characterization of monoclonal antibodies to bromodeoxyuridine. Cytometry 1985, 6: 501-505

465. Vanderlugt CL and Miller SD: Epitope spreading in immune-mediated diseases: implications for immunotherapy. Nat Rev Immunol 2002, 2: 85-95

466. Vaughan MB, Howard EW, and Tomasek JJ: Transforming growth factor-beta1 promotes the morphological and functional differentiation of the myofibroblast. Exp Cell Res 2000, 257: 180-189

467. Vayssairat M, Baudot N, Abuaf N, and Johanet C: Long-term follow-up study of 164 patients with definite systemic sclerosis: classification considerations. Clin Rheumatol 1992, 11: 356-363

468. Vazquez-Abad D, Russell CA, Cusick SM, Earnshaw WC, and Rothfield NF: Longitudinal study of anticentromere and antitopoisomerase-I isotypes. Clin Immunol Immunopathol 1995, 74: 257-270

469. Veale DJ, Collidge TA, and Belch JJ: Increased prevalence of symptomatic macrovascular disease in systemic sclerosis. Ann Rheum Dis 1995, 54: 853-855

470. Vecchi A, Garlanda C, Lampugnani MG, Resnati M, Matteucci C, Stoppacciaro A, Schnurch H, Risau W, Ruco L, Mantovani A, and .: Monoclonal antibodies specific for endothelial cells of mouse blood vessels. Their application in the identification of adult and embryonic endothelium. Eur J Cell Biol 1994, 63: 247-254

471. Veeraraghavan S, Renzoni EA, Jeal H, Jones M, Hammer J, Wells AU, Black CM, Welsh KI, and du Bois RM: Mapping of the immunodominant T cell epitopes of the protein topoisomerase I. Ann Rheum Dis 2004, 63: 982-987

472. Verbeek MM, Otte-Holler I, Wesseling P, Ruiter DJ, and de Waal RM: Induction of alpha-smooth muscle actin expression in cultured human brain pericytes by transforming growth factor-beta 1. Am J Pathol 1994, 144: 372-382

473. Visse R and Nagase H: Matrix metalloproteinases and tissue inhibitors of metalloproteinases: structure, function, and biochemistry. Circ Res 2003, 92: 827-839

474. von Bierbrauer A, Barth P, Willert J, Baerwald C, Mennel HD, and Schmidt JA: Electron microscopy and capillaroscopically guided nailfold biopsy in connective tissue diseases: detection of ultrastructural changes of the microcirculatory vessels. Br J Rheumatol 1998, 37: 1272-1278

475. Wallis DD, Tan FK, Kielty CM, Kimball MD, Arnett FC, and Milewicz DM: Abnormalities in fibrillin 1-containing microfibrils in dermal fibroblast cultures from patients with systemic sclerosis (scleroderma). Arthritis Rheum 2001, 44: 1855-1864

476. Wang S, Wilkes MC, Leof EB, and Hirschberg R: Imatinib mesylate blocks a non-Smad TGF-beta pathway and reduces renal fibrogenesis in vivo. FASEB J 2005, 19: 1-11

477. Watson M, Hally RJ, McCue PA, Varga J, and Jimenez SA: Gastric antral vascular ectasia (watermelon stomach) in patients with systemic sclerosis. Arthritis Rheum 1996, 39: 341-346

478. Westermark B and Wasteson A: A platelet factor stimulating human normal glial cells. Exp Cell Res 1976, 98: 170-174

479. Whitby DJ and Ferguson MW: The extracellular matrix of lip wounds in fetal, neonatal and adult mice. Development 1991, 112: 651-668

480. White B and Yurovsky VV: Oligoclonal expansion of V delta 1+ gamma/delta T-cells in systemic sclerosis patients. Ann N Y Acad Sci 1995, 756: 382-391

481. Wigley FM and Flavahan NA: Raynaud's phenomenon. Rheum Dis Clin North Am 1996, 22: 765-781

482. Wigley FM, Wise RA, Miller R, Needleman BW, and Spence RJ: Anticentromere antibody as a predictor of digital ischemic loss in patients with systemic sclerosis. Arthritis Rheum 1992, 35: 688-693

483. Worda M, Sgonc R, Dietrich H, Niederegger H, Sundick RS, Gershwin ME, and Wick G: In vivo analysis of the apoptosis-inducing effect of anti-endothelial cell antibodies in systemic sclerosis by the chorionallantoic membrane assay. Arthritis Rheum 2003, 48: 2605-2614

484. Xu SW, Denton CP, Dashwood MR, Abraham DJ, and Black CM: Endothelin-1 regulation of intercellular adhesion molecule-1 expression in normal and sclerodermal fibroblasts. J Cardiovasc Pharmacol 1998, 31 Suppl 1: S545-S547

485. Yamagishi S and Imaizumi T: Pericyte biology and diseases. Int J Tissue React 2005, 27: 125-135

486. Yamagishi S, Yonekura H, Yamamoto Y, Fujimori H, Sakurai S, Tanaka N, and Yamamoto H: Vascular endothelial growth factor acts as a pericyte mitogen under hypoxic conditions. Lab Invest 1999, 79: 501-509

487. Yamakage A, Kikuchi K, Smith EA, LeRoy EC, and Trojanowska M: Selective upregulation of platelet-derived growth factor alpha receptors by

transforming growth factor beta in scleroderma fibroblasts. J Exp Med 1992, 175: 1227-1234

488. Yamamoto T, Eckes B, Hartmann K, and Krieg T: Expression of monocyte chemoattractant protein-1 in the lesional skin of systemic sclerosis. J Dermatol Sci 2001, 26: 133-139

489. Yamamoto T, Hartmann K, Eckes B, and Krieg T: Role of stem cell factor and monocyte chemoattractant protein-1 in the interaction between fibroblasts and mast cells in fibrosis. J Dermatol Sci 2001, 26: 106-111

490. Yamamoto T, Takagawa S, Katayama I, Yamazaki K, Hamazaki Y, Shinkai H, and Nishioka K: Animal model of sclerotic skin. I: Local injections of bleomycin induce sclerotic skin mimicking scleroderma. J Invest Dermatol 1999, 112: 456-462

491. Yamane K, Ihn H, Asano Y, Yazawa N, Kubo M, Kikuchi K, Soma Y, and Tamaki K: Clinical and laboratory features of scleroderma patients with pulmonary hypertension. Rheumatology (Oxford) 2000, 39: 1269-1271

492. Yamane K, Ihn H, and Tamaki K: Epidermal growth factor up-regulates expression of transforming growth factor beta receptor type II in human dermal fibroblasts by phosphoinositide 3-kinase/Akt signaling pathway: Resistance to epidermal growth factor stimulation in scleroderma fibroblasts. Arthritis Rheum 2003, 48: 1652-1666

493. Yamane K, Kashiwagi H, Suzuki N, Miyauchi T, Yanagisawa M, Goto K, and Masaki T: Elevated plasma levels of endothelin-1 in systemic sclerosis. Arthritis Rheum 1991, 34: 243-244

494. Yamane K, Miyauchi T, Suzuki N, Yuhara T, Akama T, Suzuki H, and Kashiwagi H: Significance of plasma endothelin-1 levels in patients with systemic sclerosis. J Rheumatol 1992, 19: 1566-1571

495. Yang JM, Hildebrandt B, Luderschmidt C, and Pollard KM: Human scleroderma sera contain autoantibodies to protein components specific to the U3 small nucleolar RNP complex. Arthritis Rheum 2003, 48: 210-217

496. Yata Y, Gotwals P, Koteliansky V, and Rockey DC: Dose-dependent inhibition of hepatic fibrosis in mice by a TGF-beta soluble receptor: implications for antifibrotic therapy. Hepatology 2002, 35: 1022-1030

497. Yazawa N, Kikuchi K, Ihn H, Fujimoto M, Kubo M, Tamaki T, and Tamaki K: Serum levels of tissue inhibitor of metalloproteinases 2 in patients with systemic sclerosis. J Am Acad Dermatol 2000, 42: 70-75

498. Yi ES, Lee H, Yin S, Piguet P, Sarosi I, Kaufmann S, Tarpley J, Wang NS, and Ulich TR: Platelet-derived growth factor causes pulmonary cell proliferation and collagen deposition in vivo. Am J Pathol 1996, 149: 539-548

499. Yonekura H, Sakurai S, Liu X, Migita H, Wang H, Yamagishi S, Nomura M, Abedin MJ, Unoki H, Yamamoto Y, and Yamamoto H: Placenta growth factor and vascular endothelial growth factor B and C expression in microvascular endothelial cells and pericytes. Implication in autocrine and paracrine regulation of angiogenesis. J Biol Chem 1999, 274: 35172-35178

500. Yoshikai Y, Anatoniou D, Clark SP, Yanagi Y, Sangster R, Van den EP, Terhorst C, and Mak TW: Sequence and expression of transcripts of the human T-cell receptor beta-chain genes. Nature 1984, 312: 521-524

501. Young-Min SA, Beeton C, Laughton R, Plumpton T, Bartram S, Murphy G, Black C, and Cawston TE: Serum TIMP-1, TIMP-2, and MMP-1 in patients with

systemic sclerosis, primary Raynaud's phenomenon, and in normal controls. Ann Rheum Dis 2001, 60: 846-851

502. Yuan W and Varga J: Transforming growth factor-beta repression of matrix metalloproteinase-1 in dermal fibroblasts involves Smad3. J Biol Chem 2001, 276: 38502-38510

503. Yuan Y, Tan E, and Reddy R: The 40-kilodalton to autoantigen associates with nucleotides 21 to 64 of human mitochondrial RNA processing/7-2 RNA in vitro. Mol Cell Biol 1991, 11: 5266-5274

504. Yurovsky VV, Sutton PA, Schulze DH, Wigley FM, Wise RA, Howard RF, and White B: Expansion of selected V delta 1+ gamma delta T cells in systemic sclerosis patients. J Immunol 1994, 153: 881-891

505. Yurovsky VV, Wigley FM, Wise RA, and White B: Skewing of the CD8+ T-cell repertoire in the lungs of patients with systemic sclerosis. Hum Immunol 1996, 48: 84-97

506. Zeisberg M, Hanai J, Sugimoto H, Mammoto T, Charytan D, Strutz F, and Kalluri R: BMP-7 counteracts TGF-beta1-induced epithelial-to-mesenchymal transition and reverses chronic renal injury. Nat Med 2003, 9: 964-968

507. Zhang K, Rekhter MD, Gordon D, and Phan SH: Myofibroblasts and their role in lung collagen gene expression during pulmonary fibrosis. A combined immunohistochemical and in situ hybridization study. Am J Pathol 1994, 145: 114-125

508. Zhang Y and Gilliam AC: Animal models for scleroderma: an update. Curr Rheumatol Rep 2002, 4: 150-162

509. Zhang Y, McCormick LL, Desai SR, Wu C, and Gilliam AC: Murine sclerodermatous graft-versus-host disease, a model for human scleroderma:

cutaneous cytokines, chemokines, and immune cell activation. J Immunol 2002, 168: 3088-3098

510. Zhou X, Tan FK, Milewicz DM, Guo X, Bona CA, and Arnett FC: Autoantibodies to Fibrillin-1 Activate Normal Human Fibroblasts in Culture through the TGF-{beta} Pathway to Recapitulate the "Scleroderma Phenotype". J Immunol 2005, 175: 4555-4560

511. Zhou X, Tan FK, Reveille JD, Wallis D, Milewicz DM, Ahn C, Wang A, and Arnett FC: Association of novel polymorphisms with the expression of SPARC in normal fibroblasts and with susceptibility to scleroderma. Arthritis Rheum 2002, 46: 2990-2999

512. Zhou X, Tan FK, Stivers DN, and Arnett FC: Microsatellites and intragenic polymorphisms of transforming growth factor beta and platelet-derived growth factor and their receptor genes in Native Americans with systemic sclerosis (scleroderma): a preliminary analysis showing no genetic association. Arthritis Rheum 2000, 43: 1068-1073

513. Zhou X, Tan FK, Xiong M, Arnett FC, and Feghali-Bostwick CA: Monozygotic twins clinically discordant for scleroderma show concordance for fibroblast gene expression profiles. Arthritis Rheum 2005, 52: 3305-3314

514. Zhou Y, Hagood JS, and Murphy-Ullrich JE: Thy-1 expression regulates the ability of rat lung fibroblasts to activate transforming growth factor-beta in response to fibrogenic stimuli. Am J Pathol 2004, 165: 659-669

515. Ziai MR, Imberti L, Nicotra MR, Badaracco G, Segatto O, Natali PG, and Ferrone S: Analysis with monoclonal antibodies of the molecular and cellular heterogeneity of human high molecular weight melanoma associated antigen. Cancer Res 1987, 47: 2474-2480

516. Zimmerman, K. Der Peinere Bau der Blutcapillaren. A Anat Entwicklungsgesch 68, 29-109. 1-1-1923.

Ref Type: Generic

517. Zurita-Salinas CS, Krotzsch E, Diaz dL, and Alcocer-Varela J: Collagen turnover is diminished by different clones of skin fibroblasts from early- but not late-stage systemic sclerosis. Rheumatol Int 2004, 24: 283-290